Characterisation of Cellular Fibrinogen Phosphorylation and its Functional Implications in Clot Formation

Esther J. Cooke

Submitted in accordance with the requirements for the Degree of Doctor of Philosophy

The University of Leeds

School of Medicine

February 2015

The candidate confirms that the work submitted is her own, except where work which has formed part of jointly authored publications has been included. The contribution of the candidate and the other authors to this work has been explicitly indicated below. The candidate confirms that appropriate credit has been given within the thesis where reference has been made to the work of others.

The work in Chapters 2 and 3 of the thesis has appeared in publication as follows:

Smith, K.A., Pease, R.J., Avery, C.A., Brown, J.M., Adamson, P.J., **Cooke, E.J.**, Neergaard-Petersen, S., Cordell, P.A., Ariëns, R.A., Fishwick, C.W., Philippou, H., Grant, P.J. 2013. The activation peptide cleft exposed by thrombin cleavage of FXIII-A(2) contains a recognition site for the fibrinogen α chain. *Blood*, 121 (11), 2117-2126.

The candidate was responsible for the expression and purification of recombinant fibrinogen. The other authors contributed to study design, laboratory work, data analysis and writing of the manuscript.

Acknowledgements

I would first of all like to thank my supervisors Professor Peter Grant and Dr Kerrie Smith for the opportunity to undertake this PhD project, and for all the support and guidance you have given me over the last four years. In addition to your scientific ideas and contributions, you have advised and challenged me, and helped me to develop confidence and rigour in conducting independent research. I would particularly like to thank Kerrie for all that you have taught me, your patience and your encouragements.

Secondly, I wish to thank my fellow Grant group members. I owe a huge thank you to Paul for your ideas, knowledge and generosity; you have given up a great deal of time to help me and it is much appreciated. Richard, thank you for your input and the many words of wisdom, and Jane, your technical support has been invaluable. I would also like to thank Cora, May, Kingsley and Kathryn for your help and suggestions. You have all made my time here enjoyable and I will miss the eventful excursions.

There are many other people whom I have had the pleasure of working with in LIGHT. I would like to thank Ced for your CHO expertise and willingness to help me over the years. Thanks go to Katie, Emma, Amy, Fladia, Jess, Romana, Matt, Katy, Natalie, Fraser, Marco, Helen, Lewis, Carla, Nathan and Pooja for your advice and company in the lab, your friendship, and for Monday afternoon cake provision. I am also grateful to Gareth Howell for his assistance with the confocal microscope and image analysis.

Last but not least, I would like to thank my friends and family for your prayers and support, for all the fun times I've had in Leeds, for keeping me sane when experiments failed for the *n*th time and for looking out for me. I am especially thankful to my parents, who have believed in me, provided for me in many ways, and been a real encouragement. I could not have achieved this without your support, thank you.

Abstract

Fibrinogen is a vital component of coagulation; cleavage of fibrinogen yields fibrin monomers that polymerise to form a network of fibres, constituting the blood clot. Human fibrinogen is secreted from hepatocytes in its phosphorylated form, with 20-25 % of circulating fibrinogen phosphorylated exclusively at Aα chain Ser3 and Ser345. Phosphorylation of fibrinogen is elevated in acute phase conditions, venous thrombosis and ovarian cancer, but little is known about the regulation and effects of this modification. The aims of this PhD project were to characterise the cellular mechanism and functional role of fibrinogen phosphorylation *in vivo*.

Human hepatoma cells were incubated in the presence and absence of IL-6 and the phosphate content of secreted fibrinogen was analysed by western blotting. Interleukin-6 caused a 3.1-fold increase in fibrinogen phosphorylation, demonstrating for the first time that the up-regulation of this modification in acute phase conditions is regulated at the cellular level. Using real-time PCR, IL-6 was found to significantly enhance (6.0-fold) the expression of Golgi casein kinase Fam20A, whose recognition sequence matches the Ser3 and Ser345 phosphorylation sites. Expression of other potential fibrinogen kinases, including CK2, Fam20B and Fam20C, were unchanged. This finding suggests that Fam20A plays an important role in the hepatocellular response to acute phase conditions and may phosphorylate fibrinogen *in vivo*.

Chromatographic enrichment of phosphorylated human plasma fibrinogen was conducted for functional analyses. Binding and activity assays found no effect of fibrinogen phosphorylation on FXIII cross-linking of fibrin α and γ chains, plasmin(ogen) binding to fibrinogen, or α2-antiplasmin incorporation. Analysis by SDS-PAGE revealed a small decrease in the rate of fibrinogen degradation by plasmin with increasing phosphorylation, indicating a possible role in protection from fibrinolysis. Scanning electron microscopy and turbidimetric assays revealed thinner fibres and more extensive branching in clots with a higher phosphate content, which typically represents a pro-thrombotic structure.

This work highlights the importance of fibrinogen phosphorylation in maintaining the balance between clot formation and lysis. Investigations have shown that increased intracellular kinase activity leads to elevated fibrinogen phosphorylation in acute phase conditions. The observed alterations to clot phenotype with elevated fibrinogen

phosphorylation suggest this modification may help to stem bleeding following trauma. Furthermore, it may have important implications in the development of thrombosis, which would make it a valuable target for therapeutic intervention in associated pathologies.

Table of Contents

List of Figures

List of Tables

List of Abbreviations

2D-PAGE	Two-dimensional polyacrylamide gel electrophoresis
α2-AP	α2-antiplasmin
αC	C-terminus of the Aα chain
α_E	Fibrinogen Aα chain C-terminal extension in Fib420
γ’	Fibrinogen gamma prime
γA	Normal fibrinogen γ chain
Å	Angstrom
AGDV	Ala-Gly-Asp-Val
AGE	Advanced glycation end product
Ala	Alanine
AMI	Acute myocardial infarction
AP-fibrinogen	Ammonium sulphate-precipitated fibrinogen
Arg	Arginine
Asn	Asparagine
ATP	Adenosine triphosphate
BFA	Brefeldin A
BHK	Baby hamster kidney
BiP	Immunoglobulin binding protein
BLAST	Basic Local Alignment Search Tool
BSA	Bovine serum albumin
Ca^{2+}	Calcium ions
$CaCl_2$	Calcium chloride
CAD	Coronary artery disease
$CaPO_4$	Calcium phosphate
cDNA	Complementary DNA
C/EBP	CCAAT box/enhancer-binding protein
CHO	Chinese hamster ovary
CK	Casein kinase

CO_2	Carbon dioxide
COS	Monkey kidney (CV-1) origin with SV40 genes
Ct	Cycle threshold value
CV	Column volume
Cys	Cysteine
DAPI	4',6-Diamidino-2-phenylindole
DEAE	Diethylaminoethanol
dH_2O	Distilled water
DMSO	Dimethyl sulfoxide
DNA	Deoxyribonucleic acid
dNTP	Deoxynucleotide triphosphate
DTT	Dithiothreitol
EDTA	Ethylenediamine tetraacetic acid
ELISA	Enzyme-linked immunosorbent assay
ER	Endoplasmic reticulum
FGF23	Fibroblast growth factor 23
Fp	Fibrinopeptide
FSG	Fish skin gelatin
F(X)	Coagulation factor (X)
F(Xa)	Activated coagulation factor (X)
FXIII-A	FXIII A subunit
FXIII-a	Active FXIII-A2
FXIII-A2	Dimeric FXIII A subunits
FXIII-A2B2	FXIII zymogen
FXIII-B2	Dimeric FXIII B subunits
GAPDH	Glyceraldehyde 3-phosphate dehydrogenase
G-CK	Golgi casein kinase
Gln	Glutamine
Glu	Glutamic acid
Gly	Glycine
GST	Glutathione S-transferase
HCl	Tris-hydrochloride

HeBS	Hepes-buffered saline
HEK	Human embryonic kidney
HepG2	Human hepatoma
HMW	High molecular weight
HMWK	High molecular weight kininogen
HPLC	High performance liquid chromatography
HRP	Horseradish peroxidase
IGFBP	Insulin-like growth factor binding protein
IL-6	Interleukin 6
IMAC	Immobilised metal affinity chromatography
IRES	Internal ribosome entry sites
ITS	Insulin transferrin selenium
JAK-STAT	Janus kinase/signal transducers and activators of transcription
kb	Kilobases
kDa	Kilodalton
K_d	Dissociation constant
KH_2PO_4	Potassium dihydrogen phosphate
K_m	Michaelis constant
LB	Lysogeny broth
LC-MS/MS	Liquid chromatography-tandem mass spectrometry
LDS	Lithium dodecyl sulphate
LMW	Low molecular weight
LSCM	Laser scanning confocal microscopy
Lys	Lysine
$Lys50_{MA}$	Time to 50 % lysis
mA	Milliampere
MALDI-TOF/TOF	Matrix assisted laser desorption ionisation-time of flight/time of flight mass spectrometry
MaxAbs	Maximum absorbance
MES	2-(*N*-morpholino)ethanesulfonic acid
Met	Methionine
$MgCl_2$	Magnesium chloride

MOAC	Metal oxide/hydroxide affinity chromatography
MOPS	3-(N-morpholino)propanesulfonic acid
M-PER	Mammalian-Protein Extraction Reagent
mRNA	Mature messenger RNA
MWCO	Molecular weight cut off
NaCl	Sodium chloride
OPD	O-phenylenediamine dihydrochloride
PAD	Peripheral arterial disease
PAI	Plasminogen activator inhibitor
PBS	Phosphate-buffered saline
PCR	Polymerase chain reaction
PCSK9	Proprotein convertase subtilisin/kexin type 9
PDI	Protein disulphide isomerase
pI	Isoelectric point
P_i	Inorganic phosphate
PK	Protein kinase
PLA	Proximity ligation assay
pmC	pmaxCloning
PMSF	Phenylmethylsulfonyl fluoride
pNA	pNitroaniline
PNPP	P-nitrophenol phosphate
PPII	Poly-L-proline type II
Pro	Proline
PTM	Post translational modification
PVDF	Polyvinylidene-difluoride
rFXIII-A	Recombinant FXIII-A
RGD	Arg-Gly-Asp
RNA	Ribonulceic acid
RT-PCR	Reverse transcription-PCR
SDS	Sodium dodecyl sulphate
SDS-PAGE	Sodium dodecyl sulphate polyacrylamide gel electrophoresis
SEM	Scanning electron microscopy

Ser	Serine
siRNA	Small interfering RNA
SLE	Systemic lupus erythematous
SPR	Surface plasmon resonance
STSP	Staurosporine
TAE	Tris-acetate EDTA
TAFI	Thrombin-activatable fibrinolysis inhibitor
TBS	Tris-buffered saline
TF	Tissue factor
TFPI	Tissue factor pathway inhibitor
TGN46	*Trans*-Golgi network 46
Thr	Threonine
T_m	Melting temperature
TNF	Tumour necrosis factor
tPA	Tissue plasminogen activator
Tyr	Tyrosine
uPA	Urokinase
UV	Ultraviolet
Val	Valine
VTE	Venous thromboembolism
vWF	von Willebrand factor
WT	Wild-type
YL→DS	Y-ladder-to-double-stranded

Chapter 1

Introduction

Haemostasis refers to the vital physiological mechanisms that limit blood loss after vessel injury. These mechanisms must be tightly regulated as defects can lead to undesired bleeding or thrombus formation. Fibrinogen is a key player in the final stage of the coagulation cascade – an essential component of haemostasis – whereby cleavage of fibrinogen triggers the formation of a fibrin clot to repair the vascular defect. During synthesis, fibrinogen is phosphorylated at serine (Ser) 3 and Ser345 within its Aα chain, but the functional significance of this is yet to be characterised. Phosphorylation at these sites has been shown to affect clot structure and there is evidence to suggest this modification may be associated with thrombosis. Therefore, it is important to advance understanding of fibrinogen phosphorylation, including the process, its physiological purpose and its contribution to disease.

1.1. Haemostasis and coagulation

Haemostasis comprises several complex responses to vascular injury. Damage to the blood vessel results in the release of various cytokines, chemokines and proteins from endothelial cells, triggering localised pro-inflammatory and pro-coagulant activities. Vasoconstriction occurs to minimise blood loss, while platelets aggregate at the site of injury via adhesive von Willebrand factor (vWF) and fibrinogen, in order to seal the vessel wall. Simultaneously, coagulation factors are activated on the surface of tissue factor (TF)-bearing cells and activated platelets, ultimately leading to formation of an insoluble fibrin network to stabilise the platelet plug. The known coagulation factors (F) include TF, FVII, FXII, FXI, FIX, FVIII, FV, FX, prothrombin, fibrinogen and FXIII. Activation of coagulation factors occurs in a sequential manner and includes feedback mechanisms. Anticoagulation occurs at the appropriate time to prevent excessive coagulation, and is mediated by the activities of protein C, protein S, tissue factor pathway inhibitor (TFPI) and antithrombin III. There are two proposed models of coagulation: the classic coagulation cascade with intrinsic and extrinsic pathways leading to a common pathway, and a more recently established cell-based model of

coagulation involving initiation, amplification and propagation steps on TF-bearing cells and activated platelets (Hoffman and Monroe, 2001).

1.1.1. The coagulation cascade

Early reports described coagulation as a 'waterfall sequence' or 'cascade of proenzyme-enzyme transformations' (Davie and Ratnoff, 1964, Macfarlane, 1964). This led to refinement of the cascade model, involving sequential activation of serine proteases within separate intrinsic and extrinsic pathways, converging on a common pathway (Brandt, 1985). The extrinsic pathway is also known as the TF-pathway as it is triggered by exposure of sub-endothelial TF upon vessel injury. Tissue factor binds circulating FVII, which is activated to FVIIa, initiating the cascade. The contact activation (intrinsic) pathway involves binding of FXII to a negative surface, causing autoactivation of FXII and setting in motion a series of coagulation factor activations. These pathways both finish via a common route which ultimately leads to fibrin clot formation. Figure 1 illustrates this classic cascade model of coagulation.

1.1.1.1. Tissue factor pathway

The TF-pathway is the predominant contributor to coagulation. Tissue factor is a glycoprotein which is anchored to endothelial cells via a transmembrane domain. Vessel injury exposes TF, enabling interaction with circulating FVII. Tissue factor acts as a cofactor for FVII by accelerating its activation to FVIIa and increasing its enzymatic activity towards its substrates (Nemerson and Repke, 1985, Bjoern et al., 1991). The TF/FVIIa complex is the extrinsic tenase complex which feeds into the common pathway by activating FX. Activated FVII (FVIIa) also activates FIX, which can complex with FVIIIa on a cell surface for FX activation.

1.1.1.2. Contact activation pathway

Autoactivation of FXII occurs when it comes into contact with a negatively charged surface, such as sub-endothelial collagen, polyphosphate anions released from activated platelets, or lipopolysaccharides in bacterial cell walls (Kawamoto and Kaibara, 1990, Renne et al., 2005, Morrison and Cochrane, 1974, Smith et al., 2006). Surface-bound high molecular weight kininogen (HMWK) brings prekallikrein and FXI into proximity, leading to formation of a complex involving FXIIa, HMWK, prekallikrein (PK), and FXI (Schmaier et al., 1987). Prekallikrein is converted to kallikrein and activation of FXI in turn activates FIX, leading to formation of the intrinsic tenase complex involving FIXa and FVIIIa.

1.1.1.3. Common pathway

The common pathway of the coagulation cascade is responsible for thrombin generation and fibrin clot formation. Tenase complexes from the tissue factor and contact activation pathways activate FX, which binds to FVa in the presence of phospholipids and calcium ions to form a prothrombinase complex (Suttie and Jackson, 1977). Incorporation of FXa into the prothrombinase complex accelerates prothrombin cleavage by five orders of magnitude, compared to the activity of FXa alone (Nesheim et al., 1979). Production of active thrombin by prothrombinase leads to cleavage of N-terminal peptides from fibrinogen to initiate fibrin polymerisation (Blomback et al., 1966). Thrombin also activates transglutaminase FXIII, which forms covalent cross-links between adjacent fibrin molecules to stabilise the clot.

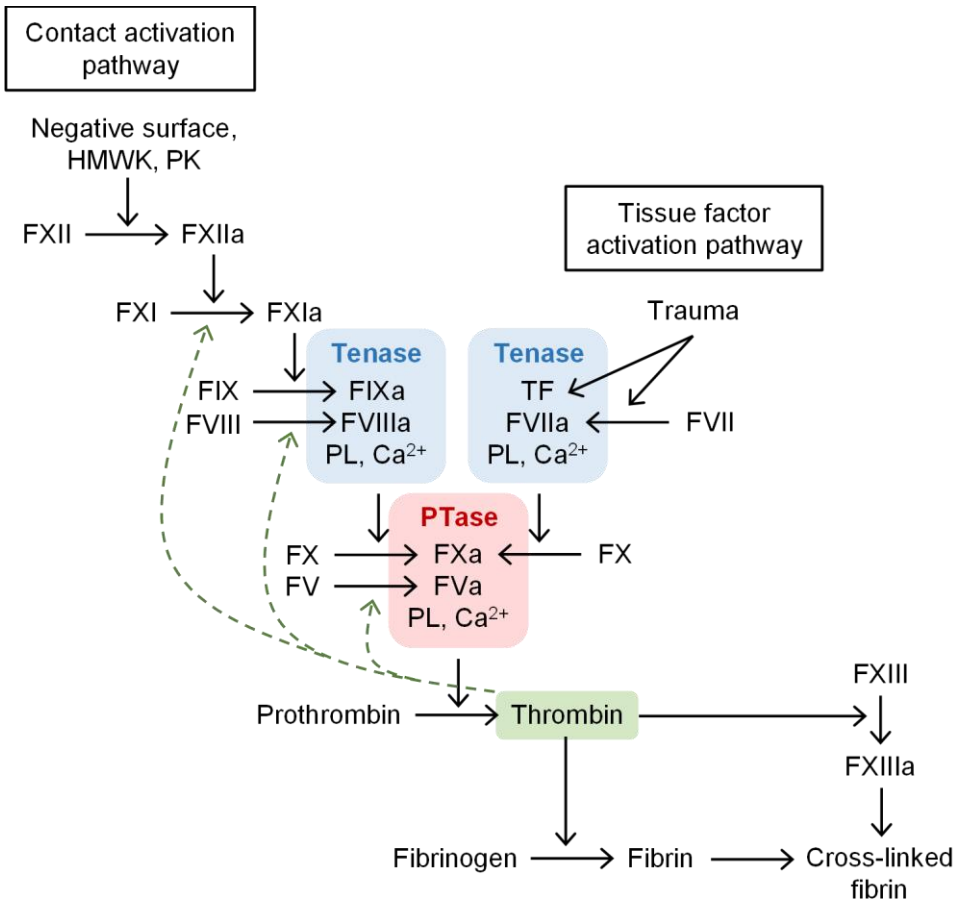

Figure 1. The coagulation cascade. The contact activation pathway and tissue factor pathway both result in the formation of a tenase complex (blue) in the presence of phospholipids (PL) and Ca^{2+} ions, leading to a common pathway. A prothrombinase complex (PTase) (pink) activates thrombin (green), whose generation is further enhanced by positive feedback mechanisms (green arrows). Thrombin cleaves fibrinogen, yielding fibrin monomers which polymerise to form a fibrin clot. The fibrin clot is stabilised by FXIII cross-linking.

1.1.2. The cell-based model of haemostasis

Although the cascade model of haemostasis appears to work well *in vitro*, it is inconsistent with the nature of certain haemostatic pathologies. For example, activation of FX by the extrinsic tenase (TF/FVIIa) would be expected to compensate for FVIII or FIX deficiencies in haemophiliacs if the two pathways were distinct. In addition, the cascade model does not explain the cross-activation of coagulation factors within different pathways, such as activation of FIX by extrinsic tenase, and activation of FXI by thrombin (Osterud and Rapaport, 1977, Gailani and Broze, 1993). Hence, the notion of separate intrinsic and extrinsic pathways has come under scrutiny (Gailani and Broze, 1991, Broze, 1992a, Broze, 1992b, Roberts et al., 1998), and has since been replaced by a cell-based model of haemostasis (Hoffman and Monroe, 2001). This model acknowledges the interrelation of various coagulation reactions and is more compatible with the *in vivo* condition.

The cell-based model of haemostasis consists of three overlapping phases – initiation, amplification and propagation – occurring on different cell surfaces. The initiation phase is localised to TF-bearing cells, while amplification occurs during transition to activated platelet surfaces – the site of propagation (figure 2). Haemostatic mechanisms are triggered when TF is exposed to flowing blood following vascular endothelium perforation or activation by inflammatory mediators. Factor IXa, FXa and small quantities of thrombin are produced on TF-bearing cells. If these exceed a threshold level, coagulation is initiated. During amplification, platelets adhere to the damaged endothelium and become partially activated. The thrombin produced during initiation completes platelet activation and also activates FVIII, FV and FXI. Coagulation factors localise to the activated platelet membrane, setting the scene for the propagation phase. During propagation, activated proteases combine with their co-factors to form tenase and prothrombinase complexes. Activated FXI provides additional FIXa for tenase complex formation, enhancing thrombin generation. Prothrombinase catalyses the proteolysis of two peptide bonds within the inactive zymogen, prothrombin, releasing active thrombin plus two fragments (Nesheim et al., 1979). The resulting surge of thrombin is sufficient to clot fibrinogen.

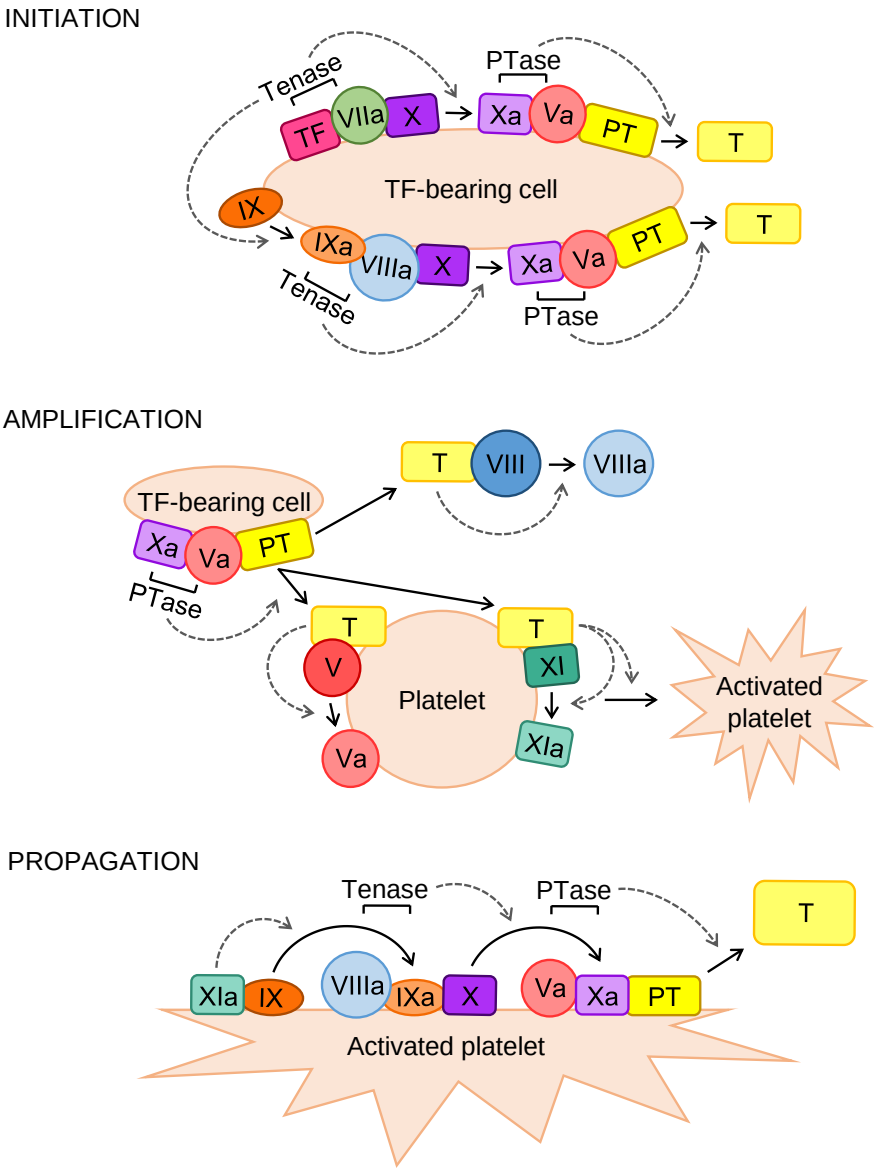

Figure 2. The cell-based model of haemostasis. Initiation of coagulation occurs on TF-bearing cells. Tenase complexes activate FX, leading to prothrombinase (PTase) formation and low levels of thrombin (T) generation from prothrombin (PT). During amplification, thrombin activates FVIII, as well as FV and FXI on the platelet surface. Platelets adhere to the extravascular matrix and are also activated by thrombin. Localisation of coagulation factors on the surface of activated platelets results in a burst of thrombin generation in the propagation phase. Solid arrows represent zymogen cleavage; dashed arrows represent activation.

1.1.3. Anticoagulant pathways

Coagulation processes are tightly regulated to maintain an appropriate balance between pro- and anti-coagulant activities. Tissue factor pathway inhibitor is the principal inhibitor of the extrinsic pathway, inhibiting FXa directly, as well as indirectly by forming a quaternary complex with the extrinsic tenase (TF/FVIIa) and FXa (Broze

et al., 1991, Sanders et al., 1985). Protein C is a coagulation factor zymogen that is activated by low levels of thrombin *in vivo* (Comp et al., 1982). Activated protein C inhibits FVIIIa and FVa which contribute to tenase and prothrombinase complexes respectively. Protein S functions as a cofactor for both protein C activation and the down-regulation of FXa activity by TFPI. Antithrombin III is a serine protease inhibitor which acts on several enzymes in the coagulation system, trapping them in an inactive complex via its reactive peptide bond at arginine (Arg) 393-Ser394 (Bjork et al., 1982). Its primary target is thrombin, but can also inhibit FXa, FXIa, FIXa, FXIIa, FVIIa, plasmin and kallikrein, although these inhibitions may not be physiologically relevant (Travis and Salvesen, 1983, Damus et al., 1973, Sanchez et al., 1998, Lawson et al., 1993, Bjork et al., 1982). Together, the various anticoagulant proteins ensure clotting only occurs above a threshold level of activation, and prevent excessive fibrin formation.

1.1.4. The fibrinolytic system

Following vascular repair, fibrin clots must be broken down and solubilised to prevent clot embolisation or thrombosis. This process is known as fibrinolysis. Figure 3 displays a simplified diagram of the fibrinolytic system. In brief, cleavage of plasminogen yields active plasmin – a serine protease which digests fibrin into fibrin degradation products.

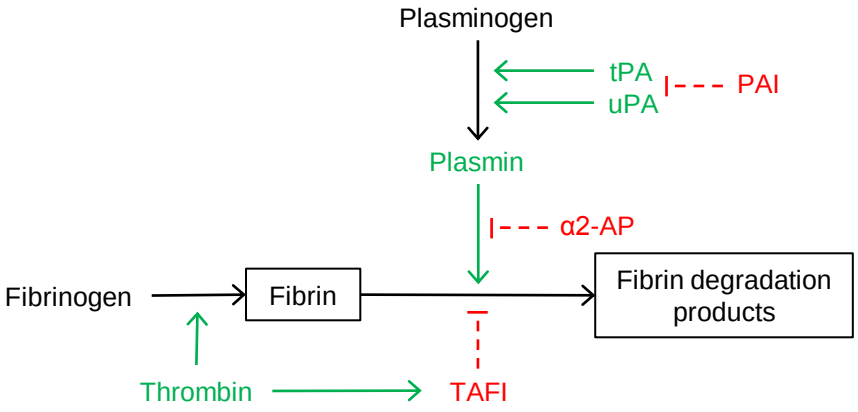

Figure 3. The fibrinolytic system. Fibrin clots are degraded by the enzyme plasmin, yielding fibrin degradation products. Plasmin is formed by cleavage of plasminogen by tissue plasminogen activator (tPA) or urokinase (uPA) and is inhibited by α2-antiplasmin (α2-AP). The plasminogen activators are inhibited by plasminogen activator inhibitor (PAI), and degradation of fibrin is inhibited by thrombin-activatable fibrinolysis inhibitor (TAFI). Green lines represent activation; red lines represent inhibition.

1.1.4.1. Plasminogen and its activators

Plasminogen is a 90 kilodalton (kDa) glycoprotein existing as two N-terminal variants: glutamic acid (Glu)-plasminogen and lysine (Lys)-plasminogen. The N-terminal peptide domain of Glu-plasminogen is removed by cleavage at Lys77-Lys78, releasing Lys-plasminogen. Lys-plasminogen is more readily activated, with a Michaelis constant (K_m) of 19 µM compared to 65 µM for Glu-plasminogen (Hoylaerts et al., 1982). Glu-plasminogen is converted to Lys-plasminogen on the endothelial cell surface for optimal activation of plasminogen (Gong et al., 2001). Lys-plasminogen also has higher affinity for fibrin due to altered conformation (Lucas et al., 1983). For activation, plasminogen is cleaved at the Arg561-valine (Val)562 peptide bond by tissue plasminogen activator (tPA) or urokinase (uPA) (Robbins et al., 1967). Tissue plasminogen activator is a 72 kDa glycoprotein released from endothelial cells to initiate fibrinolysis. It is the major intravascular activator of plasminogen, leading to the dissolution of fibrin clots in plasma. Urokinase is a 54 kDa glycoprotein which predominantly functions in pericellular proteolysis, enhancing activation of cell-bound plasminogen (Blasi, 1993).

Fibrin facilitates its own degradation by binding plasminogen and tPA, creating a localised pool of plasmin. This binding enhances plasminogen activation, which has a lower K_m in the presence of fibrin (Hoylaerts et al., 1982). Unlike tPA, uPA does not bind fibrin, yet does increase Glu-plasminogen activation in the presence of fibrin, possibly due to a conformational change in fibrin-bound plasminogen (Cesarman-Maus and Hajjar, 2005). Both plasminogen and tPA bind to the αC region of fibrinogen with high affinity (dissociation constants (K_d) of 32 nM and 33 nM respectively) at sites that are cryptic in fibrinogen but exposed in fibrin (Tsurupa and Medved, 2001a, Tsurupa and Medved, 2001b). Plasminogen and tPA bind to additional sites in fibrinogen D and E regions that are also only exposed in fibrin (Varadi and Patthy, 1983, Varadi and Patthy, 1984, Lucas et al., 1983), including Aα148-160, and γ312-324 in the case of tPA (Nieuwenhuizen, 1994). Plasminogen and tPA binding sites become exposed during fibrin assembly when D and E regions interact, disrupting interaction of the β- and γ-nodules with the coiled-coil region and Aα148-160 respectively (Yakovlev et al., 2000). Plasmin generation leads to proteolysis of fibrin into soluble fragments.

1.1.4.2. Plasmin digestion of fibrin(ogen)

Plasmin digests both native fibrinogen and polymerised fibrin clots. Evidence suggests that fibrinogen evolved from a single polypeptide chain, encoded by a single gene prior to duplication (Henschen et al., 1983, Crabtree et al., 1985). Thus, plasmin cleaves

sites at similar positions within the Aα, Bβ and γ chains of fibrinogen. Plasmin attacks fibrinogen from its C-terminal end, with the Aα chain being most susceptible to proteolysis. Sequential plasmin digestion of fibrinogen generates multiple fibrinogen degradation products, known as fragment X, fragment Y, fragments D1-D3 and fragment E (figure 4). The compositions and molecular weights of these degradation products are well characterised (Nussenzweig et al., 1961, Ferguson et al., 1975, Gaffney, 1980). The three main steps in plasmin-mediated digestion of fibrinogen are as follows. Firstly, two 50 kDa peptides are cleaved from the C-terminal ends of the Aα chains (αC), yielding fragment X (240 kDa) and free αC degradation products. Secondly, unilateral cleavage of Bβ and γ chain C-termini in fragment X, as well as further processing of the Aα chain, generates fragment Y (145 kDa) and fragment D1 (92 kDa), whereby fragment D1 is the cleaved C-termini, still held together by disulphide bonds. Thirdly, the same pattern of digestion on the intact half of fragment Y creates fragment E (50 kDa) – a dimer containing disulphide bonded Aα, Bβ and γ chain N-termini – and fragment D1. Additional shortening of the γ chain from its C-terminal end in fragment D1 creates fragments D2 (86 kDa) and D3 (82 kDa) (Southan et al., 1985). *In vivo*, degradation of cross-linked fibrin also yields a D-D dimer, which is used clinically in the diagnosis of thrombosis and pulmonary embolism (Brill-Edwards and Lee, 1999). Cleavage of fibrin in this way is essential for clot lysis.

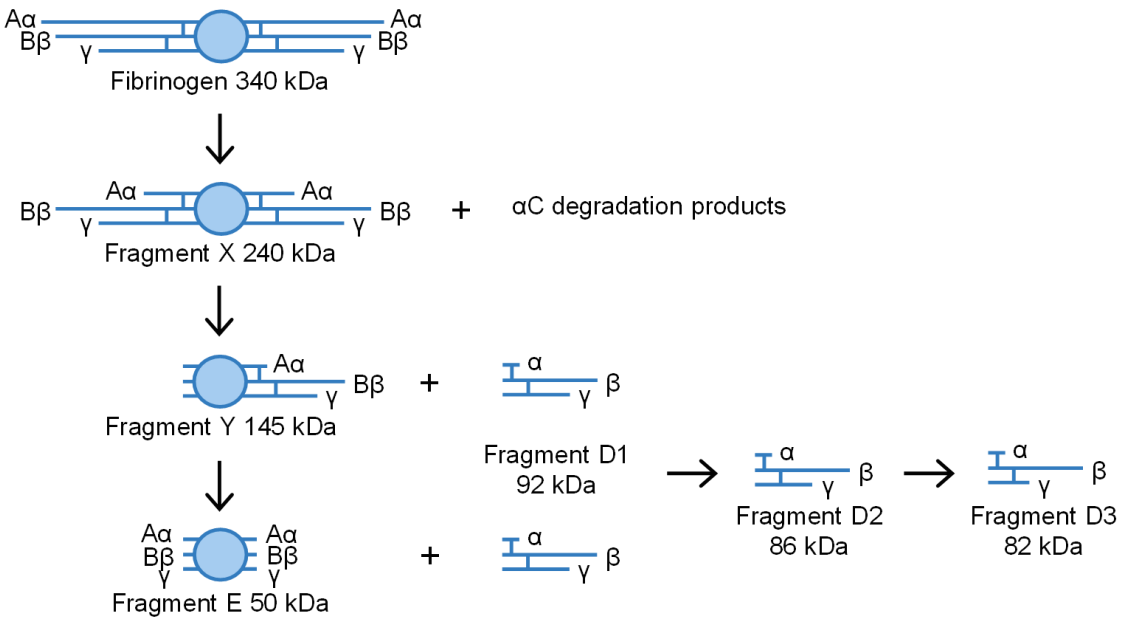

Figure 4. Plasmin digestion of fibrinogen. Carboxy-termini of fibrinogen Aα chains are digested by plasmin to generate fragment X and free αC degradation products. Asymmetric cleavage of the Aα, Bβ and γ chains of fragment X from their C-terminal ends yields fragment Y and fragment D1. Identical cleavage of the second monomer in fragment Y also yields fragment D1. The γ chain of fragment D1 is further digested to produce fragment D2 and fragment D3.

1.1.4.3. Fibrinolysis inhibitors

Fibrinolytic mechanisms must be constrained to prevent interference with vital clot formation. The key inhibitors of fibrinolysis include α2-antiplasmin (α2-AP), plasminogen activator inhibitor (PAI)-1, PAI-2, and thrombin-activatable fibrinolysis inhibitor (TAFI). The reactive site in the C-terminus of serine protease inhibitor α2-AP (Arg364) interacts covalently with the active site of plasmin to inhibit its proteolytic degradation of fibrin (Shieh and Travis, 1987, Lee et al., 1999). Alpha-2-antiplasmin also forms non-covalent, high affinity (K_d of 45-68 nM) interactions with fibrin D1 and D-D fragments, as well as the αC region, at sites that are cryptic in fibrinogen but exposed in fibrin (Tsurupa et al., 2010). This binding may orientate α2-AP to facilitate subsequent cross-linking of this inhibitor to fibrin by active FXIII. Plasminogen activator inhibitor-1 is the most important physiological inhibitor of tPA and uPA, while significant levels of PAI-2 in plasma are only detected in early pregnancy or pathological conditions (Cesarman-Maus and Hajjar, 2005). Free PAI-1 and PAI-2 complex with the active sites of tPA and uPA to prevent conversion of plasminogen to active plasmin. Fibrin-bound PAI-1 can also interact with tPA and uPA to prevent activation of plasminogen (Wagner et al., 1989). Thrombin-activatable fibrinolysis inhibitor is a 60kDa glycoprotein which, upon activation by thrombin, removes C-terminal lysine and arginine residues of fibrin degradation products, which normally provide additional tPA and plasminogen binding sites and induce a 2.5-fold increase in the rate of plasminogen activation (Wang et al., 1998). Hence, TAFI limits tPA and plasminogen binding to fibrin, thereby reducing plasmin generation and preventing further fibrinolysis.

1.2. Fibrin(ogen)

Fibrinogen was first isolated from horse plasma by Hammarsten in 1876, and from human plasma 70 years later (Cohn et al., 1946). Hammarsten discovered that fibrinogen plays a crucial role in coagulation as a precursor for fibrin upon exposure to thrombin. Indeed, the surge of thrombin activation during the propagation phase of haemostasis triggers fibrin polymerisation, creating a network of fibres to stabilise the platelet plug. Fibrinogen's structure and functions have been studied extensively since. Fibrinogen molecules are highly heterogeneous due to alternative mature messenger ribonucleic acid (mRNA) splicing and polymorphisms, described below, as well as post-translational modification (section 1.4), including Aα chain proteolysis.

1.2.1. Genetic regulation of fibrinogen

Fibrinogen Aα, Bβ and γ polypeptides are encoded by three genes – FGA, FGB and FGG, respectively – on the long arm of chromosome 4, region q23-32 (Henry et al., 1984). The location of all three genes on the same chromosome, as well as sequence homologies and similarities in 5' exon-intron domains, indicate divergence of FGA, FGB and FGG from a common ancestral gene. It is likely that the original gene duplicated to form FGA and a pre-FGB/FGG gene approximately 1 billion years ago, followed by subsequent duplication to form individual FGB and FGG genes some 500 million years ago (Crabtree et al., 1985). The genes are arranged in the order of FGG-FGA-FGB, with FGB in the opposite transcriptional orientation, which is a somewhat unexpected arrangement given the proposed evolutionary process (Kant et al., 1985). The three genes are of 5.4 (FGA), 8.2 (FGB) and 8.4 (FGG) kilobases (kb) in length and span a compact 50 kb cluster (Chung et al., 1990). The Aα chain gene consists of 5 exons, FGB of 8 exons, and FGG of 10 exons. Splicing of intron-exon junctions generates mRNA (Mount, 1982). Cloning of complementary deoxyribonucleic acid (cDNA) for fibrinogen chains enabled characterisation of the individual genes. The mRNA molecules coding for the fibrinogen Aα, Bβ and γ chains consist of 1,875, 1,900 and 1,600 coding nucleotides respectively, producing polypeptides of 625, 461 and 411 amino acids in length (Rixon et al., 1983, Chung et al., 1983, Haidaris et al., 1989).

1.2.1.1. Splice variants and polymorphisms

Francis et al. (1980) identified a larger variant of the fibrinogen γ chain, which was later isolated and established as γ' (Wolfenstein-Todel and Mosesson, 1980). This minor variant of the γ chain exists in 10% of fibrinogen molecules and typically forms a heterodimer with normal fibrinogen γ chain (γA) – γA/γ'. Fibrinogen γ' is a result of

alternative splicing, leading to replacement of the last four residues of γA with a 20-amino acid sequence (Chung and Davie, 1984). This extension carries a negative charge and is also sulphated at tyrosine (Tyr) residues 418 and 422, together impacting the functional properties of fibrinogen (Hortin, 1989, Meh et al., 2001). Lovely et al. (2003) reported a high affinity thrombin-binding site between residues 414 and 427 of the γ' extension. More recently, γ' has been shown to interfere with protofibril formation, producing clots with thinner fibres and mechanically weaker structures (Allan et al., 2012). This variant has been highlighted as a marker for thrombotic disease (Farrell, 2012).

An additional splice variant, Fib420, has a C-terminal extension of 236 amino acids on the Aα chain (α_E) which is homologous to the C-termini of the Bβ and γ chains and is encoded by exon 4 of the FGA gene (Fu and Grieninger, 1994). This sequence is N-glycosylated, giving α_E a higher than predicted molecular weight of 100 kDa. The α_E extension contains calcium binding sites that protect fibrinogen from proteolysis by plasmin (Applegate et al., 1998). However, no additional polymerisation or cross-linking sites were detected.

Several single nucleotide polymorphisms have been reported in fibrinogen. Two common polymorphisms include a threonine (Thr) to alanine (Ala) substitution at residue 312 in the Aα chain, and an arginine to lysine substitution at residue 448 in the Bβ chain (Baumann and Henschen, 1993). The fibrinogen Aα Thr312Ala polymorphism occurs in the αC region, which has an important functional role in FXIII cross-linking. This substitution influences the fibrin clot, leading to thicker fibres and increased α chain cross-linking – a proposed mechanism for its association with venous thrombosis and clot embolisation (Standeven et al., 2003, Carter et al., 2000). The fibrinogen Bβ Arg448Lys polymorphism also resides in the C-terminus, and has a frequency of 15 % in the Caucasian population (Baumann and Henschen, 1993). Clots composed of BβLys448 fibrinogen have thinner fibres, reduced porosity, increased stiffness and slower lysis times in plasma (Ajjan et al., 2008). This polymorphism is associated with thrombotic and coronary artery disease (Carter et al., 1997, Behague et al., 1996).

1.2.1.2. Dysfibrinogenemias

Dysfibrinogenemias are inherited mutations in one of the three fibrinogen genes, leading to fibrinogen abnormalities and defective fibrin clot formation. Such mutations may create a bleeding or thrombotic tendency depending on the location of the mutation. Certain mutations may also affect fibrinogen synthesis, leading to low levels

of circulating fibrinogen (hypodysfibrinogenemia). One of the more common dysfibrinogenemias is fibrinogen Dusart, characterised by a heterozygous base substitution causing an amino acid change at Aα Arg554 to a cysteine (Cys) residue (Soria et al., 1983). This causes a thrombophilic phenotype with abnormal clot properties. The Cys554 residue forms a disulphide bond with circulating albumin, which can hinder Aα chain interactions and lateral aggregation of protofibrils during clot formation, leading to thinner fibres (Koopman et al., 1993). Clots also have reduced porosity, increased branching, and increased resistance to fibrinolysis due to reduced plasminogen binding and activation by tPA (Collet et al., 1996). Another dysfibrinogenemia – fibrinogen Caracas – results from a base substitution and amino acid change from serine to N-glycosylated asparagine at position 434 of the Aα chain (Maekawa et al., 1991). Similar to fibrinogen Dusart, N-glycosylation of Asn434 impairs Aα chain interactions and lateral aggregation of protofibrils, producing clots with thinner fibres. In contrast, porosity was increased and clots were more susceptible to fibrinolysis (Woodhead et al., 1996). Additional abnormal fibrinogens result from replacement of Aα chain Arg16 with histidine or cysteine, as in fibrinogen Milano IV and fibrinogen Ledyard respectively (Lee et al., 1991, Bogli et al., 1992). These dysfibrinogenemias reduce the rate of cleavage of Aα chain N-terminal peptide fibrinopeptide A by thrombin to initiate polymerisation. Hence, clot formation is delayed and patients exhibit a bleeding phenotype. These hereditary diseases demonstrate how a minor genetic alteration can significantly alter the function of fibrinogen, with serious consequences.

1.2.2. Fibrinogen biosynthesis

Fibrinogen is predominantly synthesised in hepatocytes and secreted into plasma, circulating at an average concentration of 2.6 mg/ml (7.6 µM) (Forman and Barnhart, 1964, Butenas and Mann, 2002). Early studies with bovine, dog and rat fibrinogen revealed that the Aα, Bβ and γ chains are translated from separate mRNA transcripts and form a precursor molecule as fully assembled fibrinogen (Chung et al., 1980, Yu et al., 1980, Nickerson and Fuller, 1981). As is typical for secretory proteins, each chain also contains a signal peptide which is cleaved during co-translational translocation into the endoplasmic reticulum (ER). Kudryk et al. (1982) reported that synthesis and secretion of dog fibrinogen takes 15-20 minutes and that Aα, Bβ and γ chains are secreted to an equal extent. Disulphide bond formation between half molecules of dog fibrinogen took place in the ER, while phosphorylation and sulphation of fibrinogen occurred in a post-ER compartment. A study by Hartwig and Danishefsky (1991) using recombinant fibrinogen expression in monkey kidney (COS) cells provided early

evidence for fibrinogen intermediate complexes. Expression of Aα, Bβ and γ chains, either individually or as pairs, in baby hamster kidney (BHK) cells established a three-step model for fibrinogen biosynthesis: i) simultaneous formation of Aα-γ and Bβ-γ complexes, ii) addition of an Aα or Bβ chain to these intermediates to form a half molecule, and iii) assembly of mature, dimeric fibrinogen which is secreted from the cell (figure 5) (Huang et al., 1993b).

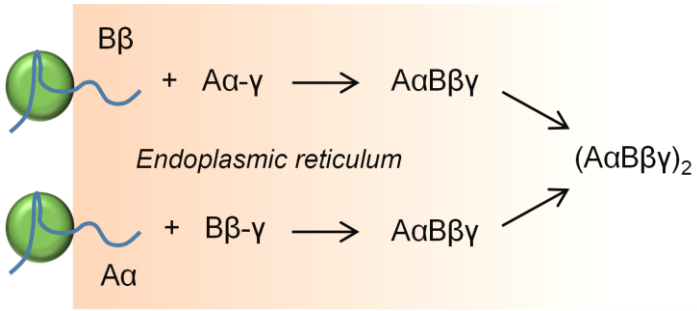

Figure 5. Fibrinogen assembly in the ER. Fibrinogen chains are translated on ribosomes (green) and translocated into the ER. Pools of intermediate Aα-γ and Bβ-γ complexes combine with newly synthesised Bβ or Aα chains respectively to form fibrinogen half molecules (AαBβγ). Two half molecules combine via N-terminal disulphide bonds to complete assembly of dimeric fibrinogen $(AαBβγ)_2$. Assembled fibrinogen undergoes further processing in the Golgi apparatus before secretion from the cell.

This model was supported by subsequent cell fusion experiments, fusing BHK cells expressing the Bβ and γ chains with those expressing only the Aα chain, and likewise fusing cells expressing the Aα and γ chains with those expressing only the Bβ chain (Huang et al., 1996). The predominant intermediate complex was dependent on the cellular level of individual chains, and incorporation of preformed Aα-γ and Bβ-γ complexes confirmed their role as functional intermediates in fibrinogen assembly. The presence of Aα-γ, Bβ-γ and AαBβγ intermediates was also demonstrated in human hepatoma (HepG2) cells, which synthesise and secrete fibrinogen naturally, but with much higher levels of the Aα-γ complex.

Surplus fibrinogen Aα and γ chains in HepG2 cells are due to different rates of synthesis and degradation. Yu et al. (1984) have demonstrated using pulse-chase experiments that Bβ chains are synthesised more slowly than Aα and γ chains, and combine with retained Aα and γ chains in the lumen of the ER whilst still being translated on the ribosome (figure 5). Retention of Aα and γ chains is mediated by lectin chaperones – calnexin and calreticulin – via monoglucosylated N-linked glycans

(Tamura et al., 2013). Lectin chaperones also provide the kinetic pause necessary for sequential hexamer formation from two trimers, rather than simultaneous combining of all six chains. The slower synthesis of the Bβ chain makes it the rate limiting step in fibrinogen assembly and secretion. The C-terminal of the Bβ chain also acts as a quality control for fibrinogen secretion. Truncation at Bβ Arg455, removing seven residues, inhibits fibrinogen secretion at a pre-Golgi compartment and permits secretion of individual chains and intermediate complexes (Vu et al., 2005). This suggests that the presence of the most C-terminal residues of the Bβ chain normally ensure that only fully assembled fibrinogen is secreted.

Degradation of fibrinogen chains in the ER is mediated by the ubiquitin-proteasome system (Xia and Redman, 1999). Differential degradation of chains also contributes to the existence of Aα and γ chain pools. Roy et al. (1992) discovered that lysosome inhibitors markedly block the degradation of free Aα chains and Aα-γ complexes, but have minimal effect on free γ chains and no effect on Bβ chains. Furthermore, only the Bβ chain bound to immunoglobulin binding protein (BiP) – a molecular chaperone involved in ER-associated degradation. These findings indicate that Bβ and γ chains are degraded in the ER, while Aα chains and Aα-γ complexes are degraded by lysosomes. Similarly, upon incubation with proteasome inhibitor MG132, Xia and Redman (2001) observed advanced accumulation of Bβ chains, ahead of Aα and γ, on translocon component Sec61, indicating unequal rates of retrotranslocation from the lumen of the ER for degradation. These mechanisms may be important in regulating the level of fibrinogen secretion.

Several pro-inflammatory stimuli and hormones are known to influence the level of fibrinogen secretion. Fibrinogen expression in hepatocytes is increased by conditioned media from (pre)adipocytes, and by hormones triiodothyronine, dexamethasone and prolonged exposure to insulin (Grieninger et al., 1983, Faber et al., 2012). Conversely, Ramackers et al. (2014) demonstrated that tumour necrosis factor (TNF)-α and interleukin-1β cause a down-regulation of fibrinogen production. It is well established that synthesis of fibrinogen increases in acute phase conditions in response to interleukin-6 (IL-6) (also known as hepatocyte stimulating factor). This has been demonstrated using cultured hepatocytes or hepatoma cells, as well as *in vivo* by injection of IL-6 into rats, eliciting a 3.4-fold increase in plasma fibrinogen concentration (Marinkovic et al., 1989, Faber et al., 2012, Nakata et al., 2012, Ramackers et al., 2014). Increased fibrinogen expression with IL-6 is mediated by IL-6 responsive elements and CCAAT box/enhancer-binding protein (C/EBP)-binding sites in the fibrinogen genes (Dalmon et al., 1993, Gervois et al., 2001). The ratio of chains inside the cell remains the same with IL-6 as all three genes are up-regulated. Interestingly,

pools of Aα and γ chains are also maintained during over-expression of the Bβ chain in HepG2 cells, induced by transfection of Bβ cDNA, as their expression is also up-regulated. Similarly, deficiency of Aα chain synthesis in hormone-deprived cells leads to concurrent degradation of surplus Bβ and γ chains (Plant and Grieninger, 1986). Although the mechanism is not clear, these co-ordinated responses highlight the importance of the correct ratio of individual polypeptides for fibrinogen biosynthesis.

1.2.3. Fibrinogen structure

Fibrinogen is a large 340kDa glycoprotein which circulates in blood plasma (Shulman 1953). It has a dimeric structure composed of two sets of three polypeptide chains – Aα, Bβ, and γ – consisting of 610, 461 and 411 amino acids respectively (Henschen et al., 1983). A low resolution structure of fibrinogen was first obtained by shadow-cast electron microscopy, revealing three nodules connected linearly by thin, thread-like strands (Hall and Slayter, 1959). Subsequent electron microscopy studies and low resolution X-ray crystallography confirmed that fibrinogen molecules are elongated, trinodular structures in which a central E region is linked by α-helical coiled-coils to two outer D regions (D-E-D) (figure 6) (Mosesson et al., 1981, Rao et al., 1991, Weisel et al., 1981). Recommended terminology for the structural domains of fibrinogen has been reviewed by Medved and Weisel (2009). The central E region of fibrinogen contains the N-termini of polypeptides from each monomer, which are held together by disulphide bonds (section 1.2.3.1). The N-termini of the Bβ chains form the BβN domains and, together with the Aα chain N-termini, constitute the funnel-shaped domain. Two small N-terminal peptides of the Aα and Bβ chains, termed fibrinopeptides (Fp) A and B, are cleaved sequentially by thrombin to release fibrin and initiate polymerisation. The N-termini of the γ chains meet in the central E region to form a single asymmetric γN domain, which is located on the opposite side of the molecule to FpA and FpB.

Weisel et al. (1985) discovered that the C-terminus of each chain is folded into an independent globular domain. The distal D nodules of fibrinogen contain the C-termini of the Bβ and γ chains, known as the β and γ nodules. Each of these nodules contains an A-, B-, and P- domain. The P-domains of β and γ nodules contain binding sites and pockets for fibrin polymerisation. Weisel et al. also characterised an additional fourth nodule of fibrinogen, which is non-covalently tethered to the E region and comprises the C-termini of the two Aα chains, known as the αC regions. Each αC region has two structurally distinct portions: i) the αC domains (residues ~Aα392-610) existing as folded, compact units and ii) the αC connectors (residues ~Aα221-391), connecting the

αC domains to the D regions (figure 6) (Medved et al., 1983, Tsurupa et al., 2002). Litvinov et al. (2007) provided the first direct evidence for intramolecular interactions involving αC domains, demonstrating that they interact homomerically with each other, as well as heteromerically with the central E region via FpB. The αC regions of fibrinogen have a wealth of functional importance with regards to fibrin polymerisation, cross-linking, fibrinolysis and interactions with other plasma proteins. The structure and function of the Aα chain is reviewed in detail in section 1.3.

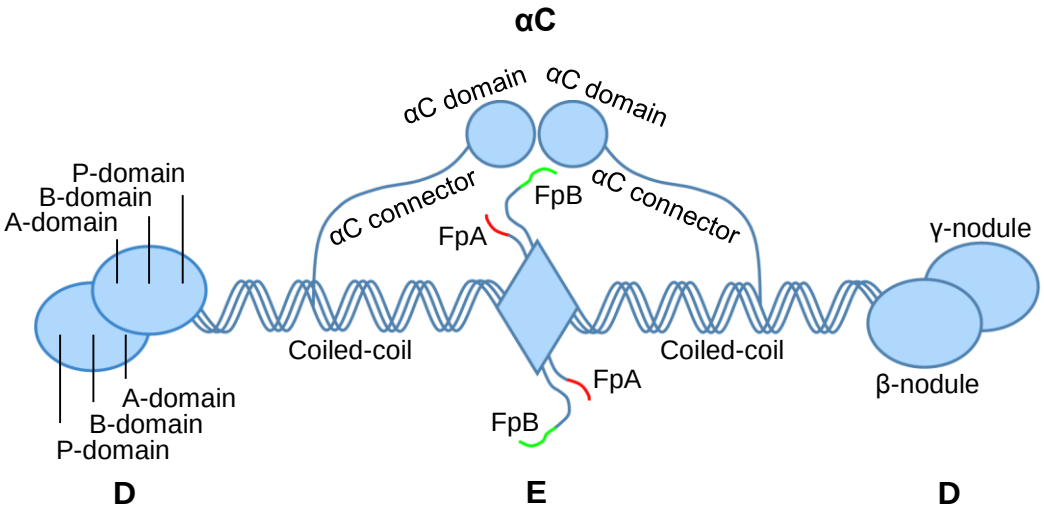

Figure 6. Structure of fibrinogen. Schematic diagram of fibrinogen illustrating two sets of three polypeptide chains (Aα, Bβ and γ) connecting a central E region to two outer D regions via coiled-coil connectors. The central E region comprises the N-termini of the polypeptide chains, including FpA and FpB shown in red and green respectively. The distal D regions include the β- and γ-nodules, each with A-, B- and P-domains. A fourth region consists of the αC domains, which are connected to the coiled-coils by the αC connectors. The αC domains interact with each other and are tethered to the E region via FpB.

1.2.3.1. Disulphide bonds

The two sets of polypeptide chains in fibrinogen are held together by 29 disulphide bonds between cysteine residues (Henschen, 1964), catalysed by protein disulphide isomerase ERp57 (Tamura et al., 2013). Cyanogen bromide cleavage of fibrinogen has revealed that the central portion of fibrinogen contains 11 disulphide bonds between the N-termini of the six polypeptide chains. Five of these hold the two sets of chains together: one between two Aα chains (Cys28), two between two γ chains (Cys8 and Cys9) and two linking Cys36 of one Aα chain to Cys65 of one Bβ chain, and vice versa (Blomback and Blomback, 1972, Blomback et al., 1976, Huang et al., 1993a). The

remaining six occur at the N-terminal side of the coiled-coil region of fibrinogen, three per half molecule (Bβ76-Aα49, Bβ80-γ19, γ23-Aα45). An additional six disulphide bonds occur at the C-terminal end of the coiled-coil region (Bβ193-Aα165, Bβ197-γ135, γ139-Aα161), three per half molecule, giving a total of 17 interchain disulphide bonds (Doolittle et al., 1978). Twelve intrachain disulphide bonds form loops between proximal cysteine residues: Aα442-472; Bβ201-286, 211-440 and 394-407; γ153-182 and 326-339 (Blomback et al., 1976, Henschen, 1978, Bouma et al., 1978). The N-terminal bonds are required for both assembly and secretion of fibrinogen. The most C-terminal disulphide bonds of the coiled-coil region are not necessary for assembly, but fibrinogen cannot be secreted in their absence, most likely due to mis-folding (Zhang and Redman, 1994, Zhang and Redman, 1996).

1.2.3.2. Crystal Structures

Several crystal structures of proteolysed fibrinogen fragments have been reported, including fragments D, double D and E, and the γ chain C-terminal (Spraggon et al., 1997, Madrazo et al., 2001, Yee et al., 1997). Native fibrinogen, however, has proved difficult to crystallise due to its high flexibility. This was initially achieved using chicken fibrinogen at a resolution of 5.5 angstroms (Å) (Yang et al., 2000b), a success attributed to the lack of flexible tandem repeats in the αC regions. This method revealed a sigmoidal-shaped structure of 460 Å in length, in agreement with previous findings using rotary-shadowed fibrinogen (Williams, 1981). Subsequently, Kollman et al. (2009) determined the crystal structure of human fibrinogen at 3.3 Å resolution; they observed structural differences in the bending and twisting of the coiled-coil regions, suggesting the canonical sigmoid structure becomes distorted in circulation. The αC regions could not be detected, providing further evidence of their motility. Until very recently, the complete three-dimensional structure of fibrinogen remained elusive. Protopopova et al. (2014) have now visualised the αC regions of fibrinogen using an alternative approach of high resolution atomic force microscopy. This revealed αC protrusions with an average length of 21 nm and average height of 0.4 nm, which is less than that of the coiled-coil connectors. This study also elucidated the involvement of the αC regions in fibrin polymerisation, as discussed below.

1.2.4. Functions of fibrinogen in clot formation

The initial response to vessel damage involves platelet activation and aggregation at the site of injury. Although largely mediated by vWF, fibrinogen secreted from activated platelets contributes to this process by binding integrin GPIIbIIIa on the platelet surface, as well as $\alpha_v\beta_3$ on endothelial cells (Parise and Phillips, 1985, Cheresh, 1987). The

resulting platelet plug is sufficient to temporarily prevent blood loss, but on its own is fragile. During the secondary stage of haemostasis, aggregated platelets become surrounded by a network of fibrin fibres, forming a stable clot to seal the vessel wall. Fibrinogen is the precursor to this vital process. Thrombin generation in response to sub-endothelial TF exposure and clotting factor activation leads to cleavage of N-terminal peptides from fibrinogen Aα and Bβ chains (Blomback et al., 1967), triggering polymerisation and fibre formation. The resulting clot is further stabilised by covalent cross-links between fibrin α and γ chains, promoting fibre thickness, elasticity and clot stiffness (Duval et al., 2014). Cross-linking by FXIII is also important for incorporation of fibrinolytic proteins, to facilitate clot degradation when wound healing is complete. The balance between clot formation and degradation is critical. Clot structure is an important determinant of resistance to fibrinolysis, and is therefore relevant to thrombotic diseases. The following sections outline the processes involved in fibrin clot formation, as well as the importance of clot structure, in greater detail.

1.2.4.1. Fibrin polymerisation

In 1978, Blomback et al. proposed the widely accepted two-step model of fibrin polymerisation (figure 7A). This model of fibrin polymerisation was enhanced by obtaining the crystal structure of fibrinogen, enabling characterisation of the various interactions at each stage (Yang et al., 2000a). In this model, thrombin cleaves FpA and FpB sequentially from fibrinogen Aα and Bβ chains at the AαArg16-glycine (Gly)17 and BβArg14-Gly15 bonds, yielding fibrin monomers. A third bond – AαArg19-Val20 – is cleaved more slowly (Blomback et al., 1967). The initial fibrinopeptide A cleavage exposes polymerisation site 'E_A' in the central E region, which binds a complementary pocket 'D_a' in the D region of a neighbouring molecule. The resulting end-to-middle E_A:D_a associations generate intermediate protofibrils, in which fibrinogen molecules are arranged end-to-end as part of a double-stranded, half-staggered oligomer, typically of 15 units in length (Bale et al., 1982). Initial lateral interactions primarily occur between γ-nodules, involving segments γ350-360 and γ370-380 (Yang et al., 2000a). Several studies have demonstrated that the initial rate of FpB cleavage is very low, but is accelerated subsequent to FpA cleavage and protofibril formation (Higgins et al., 1983, Martinelli and Scheraga, 1980, Hanna et al., 1984). Pechik et al. (2006) have provided structural evidence for this, with FpA located in the vicinity of fibrinogen-bound thrombin, and FpB some distance away due to its length and orientation. Furthermore, Pechik et al. suggested that the D:E:D interactions during protofibril formation lead to binding of BβN domains to the D regions and consequent repositioning of FpB in proximity to the active site of thrombin. The lag period preceding FpB cleavage dictates

its effects on lateral aggregation rather than earlier steps of assembly and is crucial for normal protofibril and fibre formation (Weisel et al., 1993). Yang et al. have proposed that, upon FpB removal, binding of 'E_B' to its complementary pocket 'D_b' in an adjacent molecule repositions the β-nodules away from the coiled-coils, enabling a second type of lateral, intermolecular contact between β-nodules. Consequently, two protofibrils can associate with a half-stagger (figure 7B). Removal of FpB also causes several conformational changes in the αC region leading to dissociation of the αC domains from the central E region, making them available for lateral, intermolecular interaction with adjacent αC domains (figure 7A) (Gorkun et al., 1994, Rudchenko et al., 1996). In this way, αC domains enhance lateral aggregation of protofibrils to produce thicker fibres (Collet et al., 2005a). A scanning electron micrograph of fibrin fibres is displayed in figure 7C.

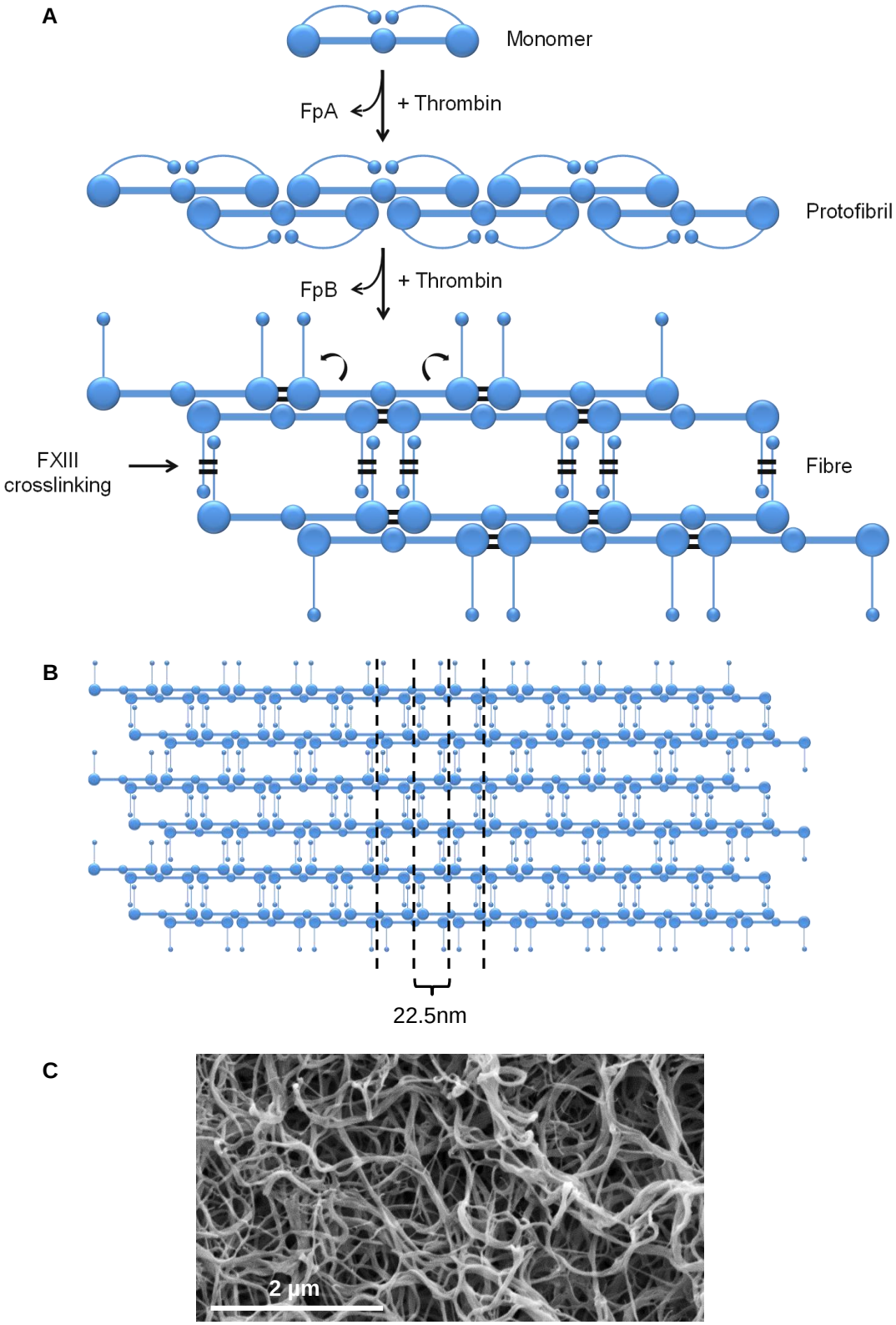

Figure 7. Protofibril and fibre formation. A) Two-step model of fibre formation. Fibrinopeptide A cleavage causes end-to-middle associations between the central E region and the D region of an adjacent molecule, leading to formation of double-stranded protofibrils. Protofibrils aggregate laterally after FpB cleavage into a fibrin fibre. Factor XIII cross-links α and γ chains to form a stable fibrin clot. B) Fibrin D:E region interactions form a half-stagger arrangement in the resulting fibre with 22.5nm periodicity. C) Scanning electron micrograph of fibrin fibres at 50,000X magnification.

In disrepute with the popular two-step model, Rocco et al. (2014) have recently proposed an alternative 'Y-ladder-to-double-stranded' (YL→DS) model. Using X-ray and light scattering techniques, they identified structures that were thinner than those predicted by the classic two-step method generating half-staggered, double stranded protofibrils. The YL→DS model involves a single E_A:D_a association between two fibrin monomers, creating a Y-shape which is repeated along the elongating single stranded protofibril. A second E_A:D_a interaction completes double stranded protofibril formation, ready for lateral aggregation. Since then, investigations by Protopopova et al. (2014), involving visualisation of αC regions in polymerising fibrin, have shed light on the contribution of this functional domain to fibre formation. In addition to the αC-mediated aggregation of protofibrils, Protopopova et al. presented a novel finding that αC regions contribute to the initial E:D region interactions, dampening previous speculations that they are only available for interaction after FpB cleavage, which normally anchors them to the E region (figure 7A) (Litvinov et al., 2007). Furthermore, Protopopova et al. observed an additional method of fibre thickening, whereby single fibrin molecules could join the growing fibre, facilitated by long-range αC-αC contacts. Again, this does not fit with the two-step model of polymerisation, but does partially support the YL→DS model. These recent findings bring a new level of complexity to the established model of fibrin assembly. Protopova et al. describe a new model which encompasses lateral aggregation of protofibrils, fibre thickening by addition of single fibrin molecules, and lengthening of fibres with single stranded protofibrils. Advances in high resolution imaging and crystallography techniques will continue to feed our comprehension of this process.

1.2.4.2. Fibre branching

Growing fibrin fibres frequently form branch points, producing a three-dimensional network. There are two opportunities for branching to occur: i) during protofbril extension by end-to-end association of fibrin monomers, and ii) during lateral aggregation of protofibrils, which may diverge into two separate fibres upon interference from a third fibrin molecule. These situations give rise to trimolecular or tetramolecular branch points, respectively (Mosesson et al., 1993). Trimolecular branching occurs when an extraneous fibrin molecule bridges unpaired polymerisation sites within two separate fibrils. This produces three branches of equal linear density and is more common in clots with thinner fibres. Tetramolecular branching, or divergence of protofibrils, produces a third branch that has twice the linear density of its constituents. This form of branching predominates in clots composed of thicker fibres. Typically there is a mixture of the two, with approximately 1 million fibrin molecules

between branch points (Collet et al., 2005b). The degree of fibrin branching can be influenced by a number of factors. Fogelson and Keener (2010) have shown that divergence of protofibrils is dependent on fibrin monomer supply rate, and therefore is influenced by thrombin concentration and the rate of fibrinopeptide cleavage. There is also a reported relationship between branching and fibre thickness, as well as clot stiffness (Ryan et al., 1999). The process of lateral aggregation is constrained by higher degrees of branching, but enhanced by greater distances between branch points (Baradet et al., 1995). Hence, clot structures with increased branching tend to have thinner fibres, and vice versa. Clots with elevated branching also tend to exhibit increased rigidity. Thus, it is apparent that the branching pattern of a clot impacts its structural and functional properties.

1.2.4.3. Cross-link formation by FXIII

Networks of fibrin fibres are stabilised by FXIII-mediated cross-linking. Factor XIII is a transglutaminase enzyme which catalyses the incorporation of reciprocal, antiparallel ε–amino(γ-glutamyl)lysine covalent crosslinks between lysine and glutamine residues in fibrin(ogen) α and γ chains. In plasma, the zymogen form of FXIII (FXIII-A2B2) is a 320 kDa heterotetramer with two identical A subunits (75 kDa) non-covalently bound to two identical B subunits (88 kDa) (Schwartz et al., 1973). The A subunits contain the active site for cross-linking activity, while the B subunits may serve to protect the zymogen from proteolytic degradation and facilitate its interaction with fibrin(ogen) (Souri et al., 2008, Smith et al., 2011). Thrombin activates FXIII-A2B2 by cleaving the Arg37-Gly38 bond within one FXIII-A subunit (Takagi and Doolittle, 1974). In this way, an N-terminal activation peptide is cleaved from the FXIII-A subunit but remains attached to the enzyme, occluding its active site. This proteolytic separation weakens the interaction between A and B subunits (Radek et al., 1993). The binding of calcium ions (Ca^{2+}) leads to dissociation of the A subunits from the B subunits and unmasking of the active site cysteine via conformational change in the separated FXIII-A2, yielding FXIII-B2 and catalytically active FXIII-A2 (FXIII-a) (Lorand et al., 1993, Hornyak and Shafer, 1991).

1.2.4.3.1. Fibrin α and γ chain cross-links

Factor XIII forms covalent cross-links between fibrin α and γ chains during clot formation. Fibrin γ chain cross-links are introduced prior to lateral aggregation of protofibrils, while they are still easily accessible by FXIII (Dyr et al., 1989). Active FXIII cross-links γ chain Lys406 with glutamine (Gln)398 or Gln399 of another γ chain, generating γ-γ dimers (Purves et al., 1987). These isopeptide bonds confer the

elasticity of cross-linked fibrin, which is able to stretch up to 1.8-fold and subsequently recover its original form (Roska and Ferry, 1982). They also play a role in determining fibre density (Duval et al., 2014). The process of γ-γ dimer formation is very rapid (0-5 minutes) and reinforces growing protofibrils prior to their lateral association (McKee et al., 1970). Following FpB cleavage, the rearrangement of αC domains enables additional cross-linking at multiple sites within the αC regions, generating α-α oligomers and high molecular weight α polymers. McKee et al. demonstrated that this reaction is much slower than γ-γ dimer formation (60-90 minutes), possibly due to FXIII diffusion constraints within the polymerising fibre, as well as the motility of αC domains. Four glutamine acceptor sites – Gln221, Gln237, Gln328, Gln366 - and multiple lysine donor sites – Lys539, Lsy556, Lys580, Lys601 – have been identified within the fibrinogen Aα chain (Cottrell et al., 1979, Matsuka et al., 1996, Sobel and Gawinowicz, 1996). Fibrin α chains can also be cross-linked to γ chains (α-γ). Clot stiffness is increased 2.5-fold by α-α cross-links, while α-γ cross-links have minimal effect (Standeven et al., 2007). Fibre thickening, straightening and resistance to fibrinolysis are also significantly promoted by α chain cross-linking (Gaffney, 1980, Duval et al., 2014). Binding of FXIII to the fibrinogen αC region enhances its cross-linking activity (Lewis et al., 1985); this interaction is reviewed in section 1.3.1. Cross-linked fibrin fibres are insoluble and form an extensive three-dimensional network.

1.2.4.4. Fibrin clot structure

Fibrin clot structure is influenced by a variety of factors, including genetic and environmental factors (section 1.2.1), post translational modifications (section 1.4), and cardiovascular disease (discussed below). These factors can influence the activity, function or plasma concentrations of the various clotting factors. Changes to clot structure can have a critical effect on haemostasis, due to altered mechanical and fibrinolytic stability. Clots with thicker fibres and increased branching tend to be more rigid, exhibiting higher degrees of inelasticity (Weisel, 2007, Ryan et al., 1999). On an individual basis, fibres with larger diameters take longer to lyse due to a greater number of fibrin molecules. However, clot lysis times are dependent on fibre number, branching and density. Typically, lysis is slower in clots with a more compact structure, with thinner fibres and increased branching, in comparison to clots with thicker fibres and a looser structure (Gabriel et al., 1992, Carr and Alving, 1995, Collet et al., 2000). This is at least in part due to the increased density, hindering penetration of fibrinolytic proteins through the fibre network.

1.2.4.4.1. Clinical implications

Structural changes to fibrin clots have been observed in a number of diseases. Premature coronary artery disease (CAD) results in clots with increased density and reduced permeability (Collet et al., 2006), while peripheral arterial disease (PAD), venous thromboembolism (VTE), acute myocardial infarction (AMI) and ischemic stroke all cause a reduction in permeability, along with increased fibre thickness and resistance to fibrinolysis (Bhasin et al., 2009, Undas et al., 2009b, Undas et al., 2008, Undas et al., 2009a). In addition, the increased incidence of myocardial infarction with elevated circulating fibrinogen levels can, to some extent, be attributed to an increase in clot stiffness. Diabetes and metabolic syndrome generate clots with reduced permeability and fibre thickness, increased clot density and branching, and longer lysis times (Dunn et al., 2005, Carter et al., 2007). Although complex and variable, the common denominator of these structural changes is a reduction in clot permeability, which results in slower fibrinolysis, thereby yielding a pro-thrombotic phenotype. Thus, an awareness of changes to fibrin clot morphology in relevant pathologies and the risks they pose to the patient is highly important.

1.3. Structure and function of the fibrinogen Aα chain

The fibrinogen Aα chain comprises three major zones of approximately 200 residues each: an N-terminal coiled-coil sequence, a central flexible domain with tandem repeats, and a C-terminal globular domain (αC domain) (Doolittle et al., 1979). The N-terminal zone (Aα1-194) is connected to the Bβ and γ chains via two disulphide rings, in between which lies the coiled-coil region (Doolittle et al., 1978). Although largely unstructured, the coiled-coils, which adopt an α-helical conformation, bring some order to the N-terminus. Following a short interzonal stretch, the central zone is composed of residues Aα240-424. Within this zone lie eight sets of tandem repeats (Aα270-372), each with 13 residues (Rixon et al., 1983). The tandem repeats have a high proportion of polar glycine, serine, proline or threonine residues, yet the majority of fibrinogen Aα chain non-polar tryptophan residues are also located in this region. It has been suggested that proteins with proline-rich tandem repeats adopt a helical poly-L-proline type II (PPII) conformation (Williamson, 1994). This conformation describes a left-handed helix with three residues per turn, which is stabilised by forming hydrogen bonds with water molecules. Such a conformation would explain the high hydration status of fibrinogen and also contribute some order to the C-terminal portion of the Aα chain (Doolittle, 1973).

The αC region of fibrinogen (Aα221-610) makes up two thirds of the Aα chain and contributes approximately 25 % of the mass of fibrinogen. It is composed of an N-terminal αC connector containing the tandem repeat sequences, and a C-terminal αC domain (Aα392-610). The low content of non-polar residues in the tandem repeats of the αC connectors confers flexibility rather than a compact structure. In contrast, an abundance of non-polar amino acid side chains in the αC domains are likely to form a compact core (Rixon et al., 1983). Tsurupa et al. (2002) have demonstrated that the αC domain is indeed folded into a compact, globular structure, as inferred by heat-induced unfolding transitions in αC domain fragments using spectroscopy and thermoanalytical techniques. This was not observed in αC connector fragments, but their behaviour was typical of the extended helical PPII conformation. These findings were supported by more recent nuclear magnetic resonance studies (Burton et al., 2006). Burton et al. identified a β-hairpin structure in an αC domain fragment (Aα374-538), with one face consisting mostly of uncharged residues and the other of charged residues that are highly conserved among species. They proposed that an adjacent hydrophobic region may interact with the charged surface of the β-hairpin to form a compact unit. In addition, the isolated αC domain was found to be unstable, which may explain its propensity for inter- and intramolecular interactions. Subsequent work revealed a second β-hairpin, formed by residues Aα459-476, with an unstable β-sheet structure

(Burton et al., 2007). Oligomerisation of αC domain fragments increased their stability, suggesting that αC-αC interactions are thermodynamically driven.

1.3.1. Interaction with plasma proteins

The N-terminal zone of the fibrinogen Aα chain is functionally important for fibrin polymerisation via cleavage of FpA (residues Aα1-19) by thrombin; residues 1-5 are important in this interaction, particularly in phosphorylated FpA (Maurer et al., 1998). However, the majority of interactions involve the αC region of fibrinogen. Figure 8 in section 1.5.1 illustrates the key sites of interaction in the Aα chain in relation to fibrinogen phosphorylation sites. Proteins that bind the αC region include FXIII, plasminogen, tPA, α2-AP, PAI-2 and fibronectin, as discussed below. Binding of FXIII to fibrinogen promotes its cross-linking activity (Lewis et al., 1985). Using surface plasmon resonance, Smith et al. (2011) localised the binding of inactive FXIII-A2B2 to fibrinogen αC residues 371-425 and deemed this a high affinity interaction, with a K_d of less than 35 nM. Calcium-dependent binding of active FXIII-A subunit with residues 389-403 was also reported (K_d of 2.35 μM), and Glu389 highlighted as a key residue. Further characterisation of this interaction revealed that fibrinogen Aα389-403 binds within a cleft in the β-sandwich domain of activated FXIII-A2 (FXIII-a2), exposed following cleavage of the activation peptide (Smith et al., 2013). This binding facilitates cross-linking to acceptor residue Gln366 by localising it to the active site of FXIII-a2. Inhibition of the FXIII-a2–fibrinogen interaction caused a reduction in fibrin α and γ chain cross-linking as well as cross-linking of α2-AP to the fibrinogen αC region. Hence, the binding of FXIII to fibrinogen is important for its function in stabilising clots and incorporating fibrinolytic proteins.

Fibrin(ogen) controls its own degradation by binding fibrinolytic proteins plasminogen and tPA, as well as their inhibitors, α2-AP and PAI-1, to achieve a localised action. Plasminogen binds to fibrin fragments D and E, as well as to the αC domain (residues 392-610) with high affinity (K_d of 32 nM) (Varadi and Patthy, 1983, Varadi and Patthy, 1984, Lucas et al., 1983, Tsurupa and Medved, 2001b). Residues Aα148-160 in the D region of fibrinogen enhance the rate of plasminogen activation by tPA by binding both proteins with equal affinity (K_d ~ 1 μM) (Voskuilen et al., 1987, Yakovlev et al., 2000). However, the large molar excess of plasminogen in the blood indicates that in physiological conditions this binding region may be saturated with plasminogen. Tsurupa and Medved (2001b) also discovered high affinity binding of tPA to the αC domain (K_d of 33 nM) at an independent site to that of plasminogen, and demonstrated that both plasminogen and tPA bind to sites that are cryptic in fibrinogen but exposed in

fibrin (Tsurupa and Medved, 2001a). Similarly, α2-AP binds with high affinity to fibrin fragments D1 and the D-D dimer, and to the αC region (Tsurupa et al., 2010). Again, these binding sites are only exposed in fibrin, not fibrinogen, with the exception of adsorbed fibrinogen. Tsurupa et al. proposed that the binding of α2-AP to fibrin induces a suitable orientation for subsequent cross-linking. Plasminogen activator inhibitor-1 also binds to the fibrin α chain N-terminus at residues 20-88 at sites that are cryptic in fibrinogen (Smolarczyk et al., 2005).

Additional proteins that interact with the fibrinogen Aα chain include thrombospondin and fibronectin. Both of these proteins are extracellular matrix glycoproteins that mediate intercellular and cell-matrix interactions. The thrombospondin binding region on the Aα chain has been localised to N-terminal residues 92-147; this interaction is thought to play a role in platelet aggregation (Bacon-Baguley et al., 1990). Conversion of fibrinogen to fibrin also enables a high affinity interaction between fibronectin and the fibrin αC region, localised to residues 221-391 (Makogonenko et al., 2002). This binding is thought to promote matrix formation, thereby encouraging cell adhesion and migration during vessel repair.

1.3.1.1. Cross-linking to fibrinolytic proteins

Several proteins are covalently cross-linked to the Aα chain by FXIII, in particular those of the (anti-)fibrinolytic system. In this way, the developing clot incorporates a timely mechanism to regulate its own destruction, enabling vessel repair while preventing problematic clot growth. Alpha-2-antiplasmin is cross-linked to the αC connectors at Lys303 (Kimura and Aoki, 1986b). Interestingly, Fraser et al. (2011) have demonstrated that covalent incorporation of α2-AP is the principal determinant of the antifibrinolytic function of FXIII, rather than fibrin α and γ chain cross-linking. The FXIII-mediated cross-linking of α2-AP has a half-life of approximately 20 minutes, which demonstrates the incorporation of antifibrinolytic agents into new thrombi (Robinson et al., 2000). Inhibitors PAI-2 and TAFI are also cross-linked to the fibrin α chain. Plasminogen activator inhibitor-2 is cross-linked to N-terminal Lys148, Lys176, and Lys183, as well as Lys230 in the αC connectors, and Lys413 and Lys457 in the αC domain, leading to increased resistance to fibrinolysis (Ritchie et al., 2000, Ritchie et al., 2001). Cross-links are formed between unidentified fibrinogen lysine residues and the activation peptide of TAFI (Gln2, Gln5), as well as the mature enzyme (Gln292), and may facilitate activation of this inhibitor, enhance its antifibrinolytic activity or prevent it from further proteolytic degradation (Valnickova and Enghild, 1998). Thus, it is apparent that the fibrinogen Aα chain, in particular the αC region, has a major role in the regulation of fibrinolysis.

1.3.2. Cell surface interactions

In addition to its role in binding plasma proteins, fibrinogen is also able to bind to integrins on cell surfaces, including platelets and endothelial cells. The fibrinogen Aα chain contains two Arg-Gly-Asp (RGD) recognition motifs for integrin binding – one in the N-terminus (residues 95-97) and one in the C-terminus (residues 572-574) – in addition to a γ chain C-terminal Ala-Gly-Asp-Val (AGDV) attachment site (Hawiger et al., 1989, Kloczewiak et al., 1984). Contrary to previous speculation, it has been shown that only the fibrinogen γ chain AGDV domain is needed for interaction with activated GPIIbIIIa on the platelet surface (Cheresh et al., 1989, Liu et al., 1997). The Aα chain RGD sequences, on the other hand, are important for endothelial cell binding. Initial interactions with endothelial cells are dependent of the C-terminal RGD motif as the N-terminal site is buried within the coiled-coil domain, and is therefore not readily available for interaction (Doolittle et al., 1978, Ugarova et al., 1993). Binding of the fibrinogen αC region to integrin $\alpha_V\beta_3$ on the surface of endothelial cells induces a conformational change in fibrinogen, leading to exposure of the second Aα95-97 RGD motif (Cheresh et al., 1989, Ugarova et al., 1993). This serves to anchor aggregating platelets and localise clot formation to the damaged sub-endothelium.

1.4. Post-translational modification of fibrinogen

The complexity of the human proteome far outweighs that of the human genome. The International Human Genome Sequencing Consortium (2004) reported that there are only 20,000 to 25,000 human genes, yet there are over 1 million proteins (Jensen, 2004). Initiation of transcription by alternative promoters, differential termination of transcription, alternative mRNA splicing, and genetic recombination are the four basic mechanisms that contribute to the diversity of the human transcriptome, producing multiple mRNA transcripts (approximately 100,000 in total) from single genes (Ayoubi and Van De Ven, 1996). This complexity is exponentially amplified by post-translational modification (PTM) of proteins. Post-translational modifications are chemical modifications that regulate functional aspects of the protein in question, such as activity, localisation, or interaction with other proteins, molecules or cells. This is a highly abundant and important phenomenon, and approximately 5 % of the human genome encodes enzymes that effectuate post translational modification (Rogers and Overall, 2013). Protein properties can be changed in a timely manner in response to specific circumstances or stimuli, and PTMs provide a significant expansion in combinatorial molecular states. In order of the number of reported cases in PubMed (Seo and Lee, 2004), common PTMs include phosphorylation, methylation, cysteine oxidation, glycosylation, acetylation, acylation, ubiquitination, deamidation, nitrosylation, SUMOylation and nitration. Proteolysis is also a form of post-translational modification involving cleavage of peptide bonds by proteases. Proteolysis has a variety of biological functions, including regulation of protein activity, cleavage of signal peptides and pro-proteins during biosynthesis, and protein degradation to remove abnormal or misfolded proteins, or to maintain physiological protein concentrations.

There are numerous reports of fibrinogen PTMs *in vivo* that occur naturally, or in response to certain drugs or pathophysiological conditions. Naturally-occurring modifications may also be elevated by disease. Phosphorylation of fibrinogen is the focus of this thesis and is discussed in more detail in section 1.5. Importantly, post-translational modification of fibrinogen leads to altered function and fibrin clot properties. Individual fibrinogen PTMs and their specific effects are described below and summarised in table 1.

Modification	Site	Functional effects	References
Naturally-occurring fibrinogen PTMs			
Phosphorylation	Aα: S3, S345	↑ Resistance to fibrinolysis, enhanced thrombin-binding	Blomback et al., 1966, Seydewitz et al., 1984, Martin et al., 1992, Maurer et al., 1998
N-glycosylation	Bβ: N364; γ: N52	↓ Clot formation, ↑ fibre thickness, ↓ branching, ↑ porosity	Blomback et al., 1972, Topfer-Peterson et al., 1976, Langer et al., 1988, Zauner et al., 2012
O-glycosylation	αC region (unknown sites)		
Sulphation	γ': Y418, Y422	Enhanced thrombin-binding	Hortin, 1989, Meh et al., 2001, Lovely et al., 2003
Deamidation	Aα, Bβ, γ (unknown sites)	Unknown	Henschen-Edman, 2001
Hydroxylation	Bβ: P31	Unknown	Henschen et al., 1991
Glutamine cyclisation	Bβ: Q1	Protection from aminopeptidases	Blomback et al., 1966
Proteolysis	Aα: A1-D2	Unknown	Blomback et al., 1966
	Aα: K583-M584	Unknown	Rudchenko et al., 1996
	Aα: V610-R611	Unknown	Rixon et al., 1983
	Aα: N269-P270, G297-G298, P309-G310	↓ clot formation, ↑ fibre density, ↓ fibre thickness, ↓ porosity, ↑ clot stiffness	Nakashima et al., 1992, Holm et al., 1985, Kaijzel., 2006
Abnormal fibrinogen PTMs			
Glycation	Lysine residues	↑ fibre density, ↑ clot stiffness, ↑ resistance to fibrinolysis	Alzahrani and Ajjan, 2010, Undas and Ariens, 2011

Nitration	Bβ:Y292, Y424	↑ Clot formation, ↓ fibrinolysis, altered clot structure, ↑ clot stiffness.	Vadseth et al., 2004, Parastatidis et al., 2008
Methionine-oxidation	Aα: M476; Bβ M367; γ: M78	↓ Clot formation, ↑ fibre density, ↓ fibre thickness, ↓ porosity, ↓ clot stiffness	Weigandt et al., 2012
Metal-ion catalysed oxidation	Aα, Bβ (unknown sites)	↓ Clot formation, ↓ fibre thickness	Belisario et al., 1997, Shacter et al., 1995
Acetylation	Aα: K191, K208, K224, K429, K457, K539, K562; Bβ: K233; γ: K170, K273.	↑ Clot formation and fibrinolysis, ↑ fibre thickness, ↑ porosity, ↓ fibre thickness	Svensson et al., 2012, Ajjan et al., 2009, Williams et al., 1998, He et al., 2001
Homocysteinylation	Cysteine and lysine residues	↑ Fibre diameter, ↑ branching, ↓ permeability, ↑ clot stiffness, ↑ resistance to fibrinolysis	Lauricella et al., 2006, Undas et al., 2006, Rojas et al., 2009, Sauls et al., 2011

Table 1. Post-translational modification of fibrinogen. Modifications are divided into naturally-occuring PTMs and abnormal PTMs that occur with drugs or disease. Modified sites on the Aα, Bβ and γ chains of fibrinogen are displayed (S: serine, N: asparagine, Y: tyrosine, P: proline, Q: glutamine, A: alanine, D: aspartic acid, V: valine, R: arginine, G: glycine, M: methionine, K: lysine) with their functional effects on fibrin clot formation. The table is adapted and updated from Henschen-Edman (2001).

1.4.1. Glycosylation

Glycosylation involves covalent attachment of carbohydrate to a protein during biosynthesis via an N-glycosidic or O-glycosidic bond. The terminal monosaccharide of an N-glycosylating carbohydrate is usually sialic acid, which carries a negative charge and influences the glycoprotein's structural and functional properties. Fibrinogen is N-glycosylated at asparagine (Asn)52 in the Bβ chain and Asn364 in the γ chain, both comprising biantennary digalactosylated mono- or di-sialylated structures (Blomback et al., 1972, Adamczyk et al., 2013, Topfer-Peterson et al., 1976). Increased glycosylation of fibrinogen has been reported in foetal fibrinogen and liver disease (Galanakis et al., 1983, Martinez and Barsigian, 1987). The use of deglycosylated fibrinogen has indicated that glycosylation hinders lateral aggregation and clot formation, and produces clots with reduced fibre thickness, increased branching and reduced porosity (Langer et al., 1988). Although the Aα chain is not N-glycosylated, mass spectrometric-based approaches have recently revealed O-glycosylation of the αC region (Zauner et al., 2012, Nagel and Meyer, 2014). Nagel and Meyer identified O-glycosylation of six distinct Aα chain peptides, corresponding to residues 262-271, 301-305, 328-337, 505-512, 529-554 and 557-580. The exact residues and their functional implications remain to be characterised.

1.4.2. Sulphation

Tyrosine-O-sulphation is catalysed by type 1 and type 2 tyrosylprotein sulphotransferases in the *trans*-Golgi compartment during protein biosynthesis (Baeuerle and Huttner, 1987, Blomback et al., 1972). This modification was originally discovered in FpB of bovine fibrinogen (Bettelheim, 1954), and has since also been detected in fibrinogen γ' at Tyr418 and Tyr 422 (Hortin, 1989, Meh et al., 2001). The fibrinogen γ chain contains a low affinity thrombin-binding site in the E domain, while γ' also has a high affinity thrombin-binding site within its C-terminal extension (γ'408-427) (Meh et al., 1996). Tyrosine-sulphated residues in fibrinogen γ' reside within this binding site and are important for optimal thrombin binding, with doubly sulphated γ' chains exhibiting 4 to 8-fold greater affinity (Lovely et al., 2003, Meh et al., 2001).

1.4.3. Deamidation, hydroxylation and cyclisation

Deamidation, proline hydroxylation and glutamine cyclisation have been reported in fibrinogen but are not well understood. Partial deamidation is present on all three fibrinogen chains at asparagine and glutamine residues, but the exact position and

function of this hydrolysis reaction are yet to be characterised (Henschen-Edman, 2001). Similarly, an N-terminal residue of the fibrinogen Bβ chain – Pro31 – is hydroxylated with unknown function (Henschen et al., 1991). Blomback et al. (1966) have also identified cyclisation of Bβ Gln1 to pyroglutamic acid, which may protect fibrinogen from degradation by aminopeptidases.

1.4.4. Proteolysis

The fibrinogen Aα chain cDNA sequence predicts an additional 15 amino acids at the C-terminal end of the polypeptide chain (Aα611-625), which does not appear in plasma fibrinogen, suggesting that fibrinogen may be first exposed to proteolysis during biosynthesis (Rixon et al., 1983). This peptide is likely to be removed by cellular proprotein convertases, given that a prediction score for proprotein cleavage at position Arg611 (0.451) falls just short of the threshold (>0.5) using ProP 1.0 Server (Duckert et al., 2004), which only has a 62 % sensitivity for general (non-furin) proprotein convertase-specific networks. By introducing an Arg611Gly mutation into the fibrinogen Aα chain, Farrell et al. (1993) found that fibrinogen could be assembled and secreted in the presence or absence of this peptide, and could be clotted upon activation by thrombin in either case. Thus, cleavage of this peptide is not required for biological activity, and its function remains unclear.

Post-synthesis, the fibrinogen Aα chain is highly susceptible to proteolytic degradation in plasma. This predominantly affects the αC region, however the first residue of the N-terminus is also cleaved by an amino-peptidase in 10 % of Aα chains (Blomback et al., 1966). Blomback et al. demonstrated that this cleavage is protected by phosphorylation of FpA at Ser3. Cleavage of C-terminal Lys583 by plasmin reportedly occurs in 25 % of fibrinogen molecules, but with unknown function (Rudchenko et al., 1996, Henschen-Edman, 2001). Proteolysis of the αC region in plasma also generates a 305 kDa low molecular weight (LMW) fibrinogen, with one intact and one degraded Aα chain, and a 270 kDa LMW’ fibrinogen with two degraded Aα chains (Holm et al., 1985). Approximately 70 % of circulating fibrinogen molecules are the normal high molecular weight (HMW) fibrinogen (340kDa), while LMW and LMW’ fibrinogens represent just 25 % and 5 % of the plasma pool respectively. Generation of LMW and LMW’ fibrinogen occurs via cleavage of the Aα chain at Asn269, Gly297 and proline (Pro)309 (Nakashima et al., 1992). Sites of fibrinogen cleavage have been determined by N-terminal sequence analyses using a variety of proteases (Blomback et al., 1966, Nakashima et al., 1992, Henschen-Edman, 2001). However, most enzymes (thrombin, snake venom enzymes, leukocytes elastase, trypsin) attack from the N-terminal end of

fibrinogen, while those that target the C-terminal end (plasmin, leukocyte elastase, matrix metalloproteinases) cleave the Aα chain before Asn269 – the earliest cleavage site present in plasma. The molecular weights of the Aα chain fragments also differ from those of LMW and LMW' fibrinogen. The relevant protease therefore remains a mystery.

Clottability is impaired in proteolysed fibrinogen; Holm et al. (1985) reported clottability values of 98 % for HMW fibrinogen, 92 % for LMW fibrinogen and 80 % for LMW' fibrinogen. The clotting time of LMW (20 minutes) and LMW' fibrinogens (25 minutes) were also delayed when compared to HMW fibrinogen (14 minutes). Scanning electron microscopy of fibrin clots formed from HMW and LMW fibrinogen revealed significant differences in clot structure (Kaijzel et al., 2006). Clots composed of LMW fibrin exhibited increased fibre density, reduced fibre thickness, reduced porosity and increased clot stiffness. These findings demonstrate the importance of the αC region in fibrin polymerisation and clot morphology, and highlight the need for tight regulation of Aα chain proteolysis in plasma.

The relative proportions of the three fibrinogens are altered in acute phase conditions. Reganon et al. (1993) reported an increase in the circulating fraction of HMW fibrinogen from 70 % to 95 % in the plasma of AMI patients, and proposed that this is caused by the increased synthesis of fibrinogen in acute phase conditions, rather than reduced proteolytic activity. The rise in HMW fibrinogen coincided with elevated phosphorylation of Ser3 in FpA, and resulted in faster coagulation. Reganon et al. have therefore postulated that HMW fibrinogen and phosphorylation of FpA are risk factors for thrombosis. In contrast, the proportion of circulating LMW fibrinogen is significantly increased in individuals with diabetes (Lipinski and Lipinska, 2000). Hence, changes in abundance of HMW, LMW and LMW' fibrinogens may contribute to pathophysiological processes.

1.4.5. Glycation

Glycation of proteins involves a non-enzymatic reaction between the ε-amino group of a lysine residue and the aldehyde group of a sugar molecule, such as glucose or fructose. Complex rearrangements, as well as dehydration, β-elimination and condensation reactions lead to formation of covalently cross-linked advanced glycation end products (AGEs). Formation of AGEs has been implicated in several pathologies, including Alzheimer's disease, renal disease, and vascular damage in atherosclerosis and diabetes (Bierhaus et al., 1998). Protein glycation is particularly prevalent in diabetes due to hyperglycaemia; glycation of fibrinogen is significantly elevated in the

absence of glycaemic control (Pieters et al., 2007, Hammer et al., 1989). Glycated fibrinogen produces clots that are denser, stiffer and more resistant to fibrinolysis, possibly due to modification of lysines that would normally be targeted by plasmin (Undas and Ariens, 2011, Alzahrani and Ajjan, 2010). Fibrinogen can also be modified by glycoaldehyde – a by-product of glycation – leading to delayed polymerisation, thinner fibrin fibres and increased resistance to fibrinolysis (Andrades et al., 2009).

1.4.6. Nitration

Vadseth et al. (2004) have reported increased nitration of fibrinogen in patients with coronary artery disease. They demonstrated that nitrated fibrinogen exhibits faster clot formation and FXIII cross-link incorporation, suggesting a pro-thrombotic effect of this PTM. Clots formed from fibrinogen exposed to nitrating oxidants were comprised of thinner fibres with higher porosity, and could be more easily deformed by mechanical stress. Nitration of fibrinogen did not influence the rate of fibrinolysis, or platelet aggregation and binding. Parastatidis et al. (2008) have also highlighted fibrinogen Bβ chain tyrosine nitration as a pro-thrombotic risk factor. Using high resolution liquid chromatography-tandem mass spectrometry (LC-MS/MS) they identified nitration of Tyr292 and Tyr424 in the C-terminus of the Bβ chain *in vivo*. This modification resulted in four functional consequences: i) faster clot formation, ii) altered clot structure, with apparent 'fibrin clusters' but no effect on fibre diameter, iii) increased clot stiffness, and iv) slower fibrinolysis. Parastatidis et al. have suggested that tyrosine nitration may facilitate E_B:D_B interactions, accelerating lateral aggregation. Overall these studies demonstrate a link between nitrative stress and thrombosis, mediated to some extent by fibrinogen.

1.4.7. Oxidation

Reactive oxygen species can lead to formation of dityrosine, methionine sulphoxides and carbonyl groups (aldehydes and ketones) on amino acid side chains. Fibrinogen is highly susceptible to oxidative modification (Shacter et al., 1994), and may be exposed to reactive oxygen species *in vivo* during the oxidative stress associated with ischemia-reperfusion injury and inflammation (Cohen, 1989, Cao et al., 1988, Fantone and Ward, 1982, Weitzman and Gordon, 1990). The functional effects of fibrinogen oxidation have been studied *in vitro* using metal-ion catalysed oxidation and hypochlorite (Weigandt et al., 2012, Belisario et al., 1997, Shacter et al., 1995). Metal-ion catalysed oxidation induced dityrosine and carbonyl formation in fibrinogen, leading to delayed fibrin polymerisation and thinner fibres. Incubation of fibrinogen with hypochlorite resulted in

oxidation of the following methionine (Met) residues: AαMet476, BβMet367 and γMet78, which impaired clot formation, increased fibre density, reduced fibre thickness, reduced porosity and reduced clot stiffness.

1.4.8. Acetylation

Acetylation of fibrinogen is relevant to the treatment of diabetic patients with aspirin (acetylsalicylic acid). Fibrinogen incubated with aspirin is acetylated at multiple lysine residues on its Aα chain, plus two residues on its Bβ chain, and one on its γ chain (Svensson et al., 2012). Interestingly, some of the identified acetylated residues in the Aα chain – Lys208, Lys224, Lys429 and Lys539 – are involved in FXIII-mediated cross-linking of fibrin chains, providing a potential mechanistic explanation for enhanced fibrinolysis in the presence of aspirin. In addition, clot formation and lysis rates are increased in the presence of aspirin, while the developed clots have a looser structure with increased fibre thickness, increased porosity and reduced rigidity (Ajjan et al., 2009, Williams et al., 1998, He et al., 2001). Hence, acetylation of fibrinogen has significant effects on clotting dynamics as well as structural properties.

1.4.9. Homocysteinylation

Homocysteinylation of proteins involves acylation of the ε-amino group of lysine residues by a metabolite of homocysteine – homocysteine thiolactone, or oxidation of thiol groups in cysteine residues by free homocysteine. Homocysteine is present in plasma due to a cellular export mechanism (Christensen et al., 1991). Disruption of this mechanism leads to hyperhomocysteinemia, which is associated with vascular and thrombotic diseases (D'Angelo and Selhub, 1997). Homocysteinylation of fibrinogen occurs with elevated plasma homocysteine levels and significantly affects clot properties, leading to a more compact structure with increased fibre diameter and branching, reduced permeability, increased stiffness and increased resistance to fibrinolysis (Lauricella et al., 2006, Undas et al., 2006, Rojas et al., 2009, Sauls et al., 2011). Hence, homocysteinylated fibrinogen is a risk factor for thrombosis.

1.5. Fibrinogen phosphorylation

Phosphorylation is a fundamental form of post-translational modification which can activate or deactivate a protein, label it for destruction, facilitate its subcellular trafficking or affect its interactions with other proteins. The mechanism of phosphorylation involves transfer of the terminal γ-phosphate of an adenosine triphosphate (ATP) molecule to a serine, threonine or tyrosine residue in a protein. This reaction is catalysed by serine/threonine or tyrosine protein kinases. Kinases represent the largest enzyme family in the human genome, comprising approximately 2% with over 2,000 genes (Manning et al., 2002). Roughly 30% of all human proteins are phosphorylated by one or more of over 500 known protein kinases, which may represent only a quarter of the actual number (Hunter, 1994). Different kinases exhibit substrate specificity via the sequences around their active site that target the enzyme to a particular consensus motif in the protein, usually several amino acids around the site of phosphorylation (Ubersax and Ferrell, 2007). However, meeting the sequence requirements does not guarantee phosphorylation of a protein, nor do the phosphorylation sites always conform to the consensus motif. An additional specificity determinant is the location of the kinase. For example, they may reside along the secretory pathway for phosphorylation of secretory proteins during biosynthesis. The localisation of kinases is dictated by targeting subunits within the kinase, which direct the catalytic subunit to the target locus – an organelle, membrane, or cytoplasm – in proximity to its substrate or away from inhibitors (Hubbard and Cohen, 1993).

Phosphorylation is a reversible process and phosphorylated proteins are also subjected to dephosphorylation by phosphatases, which catalyse the removal of phosphate by hydrolysis. This is important to regulate the degree of phosphorylation, in order to limit its function to the appropriate time and conditions. Phosphatases also have an important role in proofreading the activity of kinases, whereby a requirement for more than one phosphorylation site allows time for error correction by phosphatases, before the second (or *n*th) phosphorylation site induces function (Swain and Siggia, 2002). The process of phosphorylation is very complex and, in the past, has largely been studied using *in vitro* assays. This has been less than ideal as kinases exhibit reduced substrate specificity *in vitro*. More recent developments have enabled analysis of *in vivo* phosphorylation sites by mass spectrometry (Mann et al., 2002). This will lead to further characterisation of this highly abundant modification and its functional significance in individual proteins.

1.5.1. Ser3 and Ser345 phosphorylation

In 1962, Blomback et al. reported the presence of phosphate in a peptide cleaved from fibrinogen by thrombin and tentatively identified this as a phosphoserine at residue 3. Further investigations revealed that human and bovine fibrinogen have similar phosphate contents of 9.4 µg/100 mg and 14.5 µg/100 mg respectively (Blomback et al., 1963). However, fibrinogen from haemophiliacs with FVIII- or FIX-deficiency had slightly lower phosphate contents (7.8 µg/100 mg and 8.0 µg/100 mg respectively). During clotting assays, only 25-40 % of fibrinogen-bound phosphate was lost after thrombin digestion, and it was suggested that only 30-40 % of FpA was released. Incubation of fibrinogen with calf intestinal alkaline phosphatase achieved a 70-80 % removal of phosphate, without any major change in size or shape. Dephosphorylation prolonged the clotting time of human fibrinogen, but had no effect on bovine fibrinogen. Blomback et al. (1966) later reported that approximately 25 % of cleaved FpA from human plasma fibrinogen contained phosphate. Furthermore, only trace amounts of N-terminal alanine were detected in the clot, excluding the possibility of incomplete cleavage of FpA, as previously speculated. These findings pointed towards the presence of additional phosphorylated residues in fibrinogen.

The phosphorylation of FpA was further characterised using recombinant fibrinogen expressed in CHO cells (Binnie et al., 1993). Gorkun et al. (1997) have demonstrated that recombinant fibrinogen expressed in this way typifies plasma fibrinogen in terms of fibrinopeptide release, polymerisation and FXIII cross-linking. Upon separation of thrombin digestion products by high performance liquid chromatography (HPLC), Binnie et al. identified two separate peaks corresponding to phosphorylated and non-phosphorylated FpA, and deduced from this a 22 % degree of phosphorylation. As recombinant fibrinogen was used, this finding indicated that partial phosphorylation of FpA is regulated at the synthesis stage rather than in circulation. With regards to its function, Hanna et al. (1984) reported accelerated cleavage of phosphorylated FpA due to enhanced binding of thrombin. Subsequent work by Maurer et al. (1998) supported this result, with phosphorylation of Ser3 causing a 65 % enhancement of substrate specificity for thrombin, thereby aiding enzyme-substrate complex formation and facilitating FpA cleavage. They proposed that the phosphate serves as an anionic linker, binding basic residues in thrombin to promote binding of FpA residues 1-5.

In 1984, Seydewitz et al. determined the phosphate content of adult and foetal human fibrinogen by alkaline hydrolysis, analysing each polypeptide individually. They found a ratio of 0.9 mol phosphate/mol fibrinogen for adult fibrinogen, and an elevated proportion of 1.4 mol phosphate/mol fibrinogen for foetal fibrinogen. In addition, the

phosphate content of fibrinogen was exclusively on the Aα chain, which supports previous findings of a high degree of Aα chain phosphorylation in dog, pig and sheep fibrinogen (Kudryk et al., 1982, Cierniewski and Krajewski, 1974). For both adult and foetal fibrinogen, approximately 50 % of the phosphate was lost after thrombin digestion, suggesting that a second phosphorylation site in the Aα chain is modified to the same extent. This site was identified by Seydewitz et al. as Ser345, located in the αC connectors. More recently, a novel approach using liquid chromatography-electrospray ionisation-tandem mass spectrometry has clearly confirmed exclusive phosphorylation of human fibrinogen Aα chain at Ser3 and Ser345 *in vivo* (Wind et al., 2003). This was again demonstrated, using the same approach, by Nagel and Meyer (2014).

Given that there are two phosphorylation sites per Aα chain, and thus four per fibrinogen molecule, the degree of phosphorylation reported by Seydewitz et al. (1984) (0.9 mol phosphate/mol fibrinogen) is equivalent to 22.5 %, the same as that of recombinant fibrinogen (Binnie et al., 1993). Whether all 22.5 % of molecules were fully phosphorylated, or represented a mixture of one, two or three phosphorylation sites, was not determined. Recently, Nagel and Meyer (2014) have reported a 1:1:1 ratio of non-, mono- and di-phosphorylated fibrinogen Aα chains, indicating that approximately two thirds of fibrinogen molecules (55-75 %) contain either one or two phosphate groups.

The function of the Ser345 phosphorylation site has not yet been investigated. Figure 8 shows Aα chain residues 1-220 (N-terminus) and 221-610 (C-terminus), with the Ser3 and Ser345 phosphorylation sites in relation to various functional regions, as reviewed in section 1.3. The illustration highlights potential functions of the two phosphorylation sites, particularly Ser345, in the FXIII-mediated cross-linking of fibrin chains and fibrinolytic proteins to the αC region, interaction with FXIII-A2B2 and other proteins or cells, and exposure or protection of plasmin cleavage sites. Several *in vitro* studies have investigated the effect of fibrinogen phosphorylation on fibrin clot formation and resistance to fibrinolysis, as discussed below.

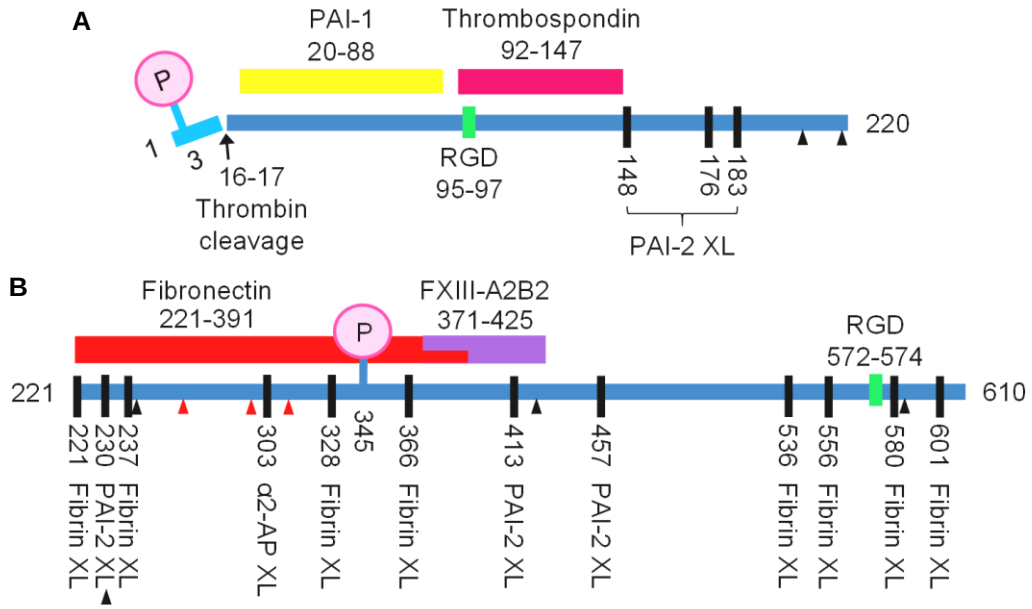

Figure 8. The location of fibrinogen Aα chain phosphorylation sites. Fibrinogen Aα chain residues are shown in blue with the Ser3 and Ser345 phosphorylation sites (P). A) N-terminal residues 1-220; B) C-terminal residues 221-610 (αC region). Protein binding regions (coloured bars), cross-linking (XL) donor and acceptor sites (black bars), and RGD sequences (green) are indicated at the appropriate locations. Thrombin cleavage of FpA (light blue) at the Arg16-Gly17 bond is also indicated with an arrow. Upward arrows represent plasmin cleavage sites (▲), or sites of proteolytic degradation in circulation (▲) generating LMW and LMW' fibrinogen. Additional proteins that bind the αC region at undefined sites are not displayed. The figure highlights the functional significance of the fibrinogen Aα chain, including potential functions of the phosphorylation sites.

1.5.2. *In vitro* phosphorylation of fibrinogen

A variety of protein kinases have been demonstrated to phosphorylate the fibrinogen Aα chain in vitro, including protein kinases (PK) A and C, and casein kinases (CK) 1 and 2 (Engstrom et al., 1980, Papanikolaou et al., 1982, Guasch et al., 1986, Itarte et al., 1983), causing alteration of clot properties. Phosphorylation with CK2 augments clot turbidity and significantly enhances the rate of whole blood coagulation *in vitro*, an effect which is synergistic with polycationic compounds thought to increase CK2 activity (Heldin, 1987, Suk et al., 1997). Conversely, phosphorylation with PKC causes reversible reductions in fibre thickness and clot turbidity; this is coupled with an irreversible inhibition of plasmin-mediated fibrinolysis, as demonstrated with alkaline phosphatase, which removed approximately 80% of fibrinogen phosphate content (Forsberg, 1989, Forsberg and Martin, 1990, Heldin et al., 1987b). In 1991, Martin et al. compared the effects of fibrinogen phosphorylation by three kinases: PKA, CK1 and CK2. Phosphorylation with PKA resulted in thinner fibres, while phosphorylation with

the casein kinases increased fibre thickness, in support of previous findings. In each case, a rise in fibre thickness was observed after dephosphorylation with alkaline phosphatase and the rate of plasmin degradation was slower than for control fibrinogens, which persisted after phosphate removal. It was proposed that phosphorylation may serve to protect fibrinogen from plasmin digestion in circulation, with the non-reversible nature of this regulatory mechanism perhaps explicable by a phosphorylation-induced conformational change, impeding interaction between fibrinogen and plasmin(ogen). Indeed, it was later confirmed that both PKC- and CK2-phosphorylated fibrinogens undergo a conformational change to their secondary structure, while phosphorylation with PKA or PKC caused changes in the tertiary structure of fibrinogen around tryptophan residues. These conformational changes resulted in a decreased rate of proteolysis by plasmin, which was again shown to be irreversible (Martin and Bjork, 1990).

Subsequent characterisation of *in vitro* phospho-acceptor residues in the fibrinogen Aα chain following incubation with PKC or CK2 has identified multiple sites, predominantly in the αC domain, strengthening the notion that the C-terminal peptide cleavage by plasmin is hindered after phosphorylation by these kinases. Protein kinase C was found to phosphorylate Ser557, Ser558, Ser559 and Ser599, as well as additional sites in the central portion of the polypeptide chain near to, and not excluding, Ser345 (Heldin and Humble, 1987). On the other hand, CK2 phosphorylated Ser523 and Ser590, plus other undefined serine and threonine residues between amino acids 259 and 268 (Heldin, 1987). Heldin and colleagues did not demonstrate phosphorylation of Ser3 or Ser345 with these particular enzymes; however, this does not rule out a potential role for PKC or CK2 in the cellular phosphorylation of fibrinogen, since kinases are known to exhibit altered substrate specificity *in vitro* (Olsen et al., 2006). It is not yet clear which particular kinase phosphorylates fibrinogen *in vivo*. A summary of identified fibrinogen phosphorylation sites and their effects on clot formation are summarised in table 2.

1.5.3. *In vivo* phosphorylation of fibrinogen

Despite the lower specificity, it is plausible that the additional sites phosphorylated *in vitro* by CK2 or PKC do exist under physiological circumstances, being modified extracellularly in circulation when several protein kinases and pools of ATP are released from platelet granules during platelet activation. The earliest evidence for phosphorylation of fibrinogen by platelet kinases came from Krust et al. (1983), who found that treatment of patients with interferon, which increases platelet kinase activity,

leads to phosphorylation of a 70-72 kDa protein, identified as the fibrinogen Aα chain. Similarly, a low platelet count in patients with Argentine haemorrhagic fever coincided with a reduction in the level of fibrinogen phosphorylation (Lerer et al., 1991). In contrast, an elevated degree of fibrinogen phosphorylation has been reported in systemic lupus erythematous (SLE), and was associated with platelet activation (Ekdahl et al., 1997). Most recently, Zahedi et al. (2008) have determined the phosphoproteome of resting human platelets by enriching phosphopeptides and analysing phosphorylation sites by nano-liquid chromatography-tandem mass spectrometry or precursor ion scanning. They identified multiple phosphorylated residues on platelet fibrinogen: Ser345, Thr393, Ser505, Ser527, Ser530 and Ser590. Despite these findings, phosphorylation of recombinant fibrinogen, and the presence of phosphorylated fibrinogen in circulation under basal, non-stimulated conditions, implies that phosphorylation of Ser3 and Ser345 occurs via a different mechanism, most likely during biosynthesis (Binnie et al., 1993, Blomback et al., 1962). The reason for additional phosphorylation of fibrinogen by activated platelets is unknown; however, it is plausible that different protein kinases with distinct spatial and temporal dispositions may regulate multiple functions of fibrinogen as appropriate for the given milieu. Martin et al. (1992) have demonstrated that *in vivo* fibrinogen phosphorylation, elevated in acute phase conditions, produces clots with increased fibre thickness and an irreversible 50 % reduction in susceptibility to plasmin digestion. This was not associated with platelet activation and likely represents an increase in Ser3 and Ser345 phosphorylation, as other studies have reported elevated phosphorylation of FpA in acute phase conditions (refer to section 1.5.5).

Kinase	Phosphorylation sites	Functional effects	References
In vitro phosphorylation			
PKA	Unknown	↓ Fibre thickness, ↑ resistance to fibrinolysis	Martin et al. 1991
PKC	S557, S558, S559, S599, additional sites in the central zone	↓ Fibre thickness, ↑ resistance to fibrinolysis, conformational change	Forsberg, 1989, Forsberg and Martin, 1990, Heldin et al. 1987, Martin et al., 1991, Martin and Bjork, 1990, Heldin and Humble, 1987
CK1	Unknown	↑ Fibre thickness, ↑ resistance to fibrinolysis	Martin et al., 1991, Itarte et al., 1983
CK2	S523, S590, additional residues between 259 and 268	↑ Fibre thickness, ↑ resistance to fibrinolysis, conformational change	Guasch et al., 1986, Heldin, 1987, Suk et al., 1997, Martin et al., 1991, Martin and Bjork, 1990
In vivo phosphorylation			
Unknown (normal conditions)	S3, S345	S3: enhanced thrombin-binding; S345: unknown	Blomback et al., 1966, Seydewitz et al., 1984, Maurer et al., 1998
Unknown (acute phase conditions)	S3 (other sites not investigated)	↑ Fibre thickness, ↑ resistance to fibrinolysis	Seydewitz and Witt 1985, Reganon et al. 1993, Martin et al.1992

Table 2. *In vitro* and *in vivo* fibrinogen phosphorylation. Kinases that have been demonstrated to phosphorylate fibrinogen *in vitro* are shown with identified phosphorylation sites (S: serine) and their functional effects on fibrinogen structure and fibrin clot formation. The sites and effects of *in vivo* fibrinogen phosphorylation in normal and acute phase conditions are also shown for comparison, but the kinases are unknown.

1.5.4. Potential fibrinogen kinases

As mentioned, the specificity of kinases for their substrates is largely dependent on a consensus sequence recognition motif. Consensus motifs for the kinases that have been demonstrated to phosphorylate fibrinogen *in vitro* are as follows: PKA, R-R-X-S/T-Y, where Y tends to be a hydrophobic amino acid; PKC, R-X-X-S/T-X-R-X; CK1, pS-X-X-S/T; CK2, S/T-D/E-X-E/D/pS (Ubersax and Ferrell, 2007, Pearson and Kemp, 1991). The Ser3 and Ser345 fibrinogen phosphorylation sites contain sequence homology conforming to S-X-E. Based on this homology, Seydewitz et al. (1984) postulated that CK2 may phosphorylate fibrinogen *in vivo*, as the sequence is similar to the requirements of CK2. Martin et al. (1992) also hypothesised that CK2 may be the *in vivo* fibrinogen kinase, as fibrinogen with elevated phosphorylation, from patients undergoing hip replacement surgery, had similar effects on clot formation to those observed by *in vitro* phosphorylation of fibrinogen by CK2 (Heldin, 1987, Martin et al., 1991). Another possibility that has not yet been explored is the Golgi casein kinase (G-CK). Despite their names, it is now known that CK1 and CK2 do not phosphorylate casein *in vivo*, and that G-CK is the true casein kinase. The G-CK phosphorylates secretory proteins at S-X-E consensus motifs, distinct from that of CK2 and exactly matching the fibrinogen phosphorylation sites (Lasa-Benito et al., 1996). Recently, Tagliabracci et al. (2012) identified the G-CK as a family of secreted protein kinases: Fam20A, Fam20B, Fam20C, Fam198A and Fam198B. They discovered that Fam20C phosphorylates a variety of secretory proteins involved in biomineralisation processes. Interestingly, it has also been suggested that the G-CK has a prominent role in generating the human plasma phosphoproteome (Salvi et al., 2010). Plasma phosphoproteins represent a distinct set of substrates from that of CK2, and the majority of phosphorylation sites satisfy the S-X-E consensus motif. In further support of this possibility, FpA has been phosphorylated *in vitro* by a casein kinase isolated from the Golgi apparatus of bovine mammary glands (Szymanski and Farrell, 1982). It is therefore likely that the G-CK may phosphorylate fibrinogen *in vivo*.

1.5.5. Elevated fibrinogen phosphorylation

Elevated levels of fibrinogen phosphorylation have been observed in various pathological states, suggesting a possible link to the development of thrombosis. Firstly, Ogata et al. (2006) reported up-regulated phosphorylation of the fibrinogen Aα chain in ovarian cancer patients. This is interesting as there is a well-known association between cancer and VTE, and a high VTE incidence has been reported in ovarian cancer patients (Tateo et al., 2005). Secondly, SLE leads to a substantial increase in

fibrinogen (Ekdahl et al., 1997). This disease is also associated with arterial or venous thrombosis, occurring in more than 10 % of SLE patients, possibly exceeding 50 % in high risk patients, and causing approximately one quarter of deaths (Love and Santoro, 1990, Cervera et al., 2003). Thirdly, patients with VTE itself have exhibited an increase in fibrinogen phosphorylation (Leeksma et al., 1986, Seydewitz et al., 1987). Seydewitz et al. reported a rise from control levels (20-25 %) to 35 %, followed by a further increase to 50-70 % after two days of receiving thrombolytic therapy. Finally, several studies have reported an association between acute phase conditions and an elevated degree of fibrinogen phosphorylation. Seydewitz and Witt (1985) observed increased phosphorylation of FpA in patients following hip replacement surgery. The degree of phosphorylation increased significantly 24 hours post-operation, and declined to normal levels after 1 week. This was supported by a subsequent investigation, whereby the phosphate content of fibrinogen doubled 24 hours after hip replacement surgery (Martin et al., 1992). As mentioned previously (section 1.5.3), Martin et al. characterised the effects of this increase in phosphorylation on clot formation, and found a direct relationship between phosphate content and fibre thickness. Susceptibility to plasmin digestion was also compromised, however this remained the case after 8 days, by which time the phosphate content had returned to normal. This suggests that increased phosphorylation of fibrinogen in acute phase conditions has an irreversible effect on fibrinolysis, supporting findings from *in vitro* phosphorylation of fibrinogen (section 1.5.2).

Increased fibrinogen phosphorylation in AMI patients undergoing thrombolytic therapy has also been reported. Patients exhibited a three-fold increase in the degree of fibrinogen phosphorylation, approaching the theoretical maximum of 4 mol phosphate/mol fibrinogen (Haglund et al. 2000). In addition, Reganon et al. (1993) found an initial 30% increase in FpA phosphorylation prior to treatment, rising to 65% after 5 hours of streptokinase therapy; this was accompanied by faster FpA release and clotting of the newly synthesised fibrinogen. Elevated phosphorylation of fibrinogen may therefore be a risk factor for thrombosis. They also found that the fraction of HMW fibrinogen in AMI patients receiving thrombolytic treatment was elevated beyond physiological levels, representing approximately 95% of total fibrinogen. Thrombolytic therapy depletes circulating fibrinogen and triggers synthesis of new HMW molecules, which have higher coagulability than other fibrinogen species (Vila et al. 1990). As fibrinogen is secreted in its phosphorylated form, it has been hypothesised that the increase in fibrinogen turnover rate and HMW fibrinogen may account for the concomitant rise in phosphorylation with thrombolytic therapy (Leeksma et al., 1986). However, given that fibrinogen is only partially phosphorylated when secreted (22 %)

(Binnie et al., 1993), and only one phosphorylation site (Ser345) is lost in LMW and LMW' fibrinogen, it is unlikely that this would cause a such a significant elevation. It remains to be determined whether the balance of kinase and phosphatase activity is altered in acute phase conditions. Importantly, these studies collectively highlight a role of fibrinogen phosphorylation in haemostasis, with pro-thrombotic effects. Elevated fibrinogen phosphorylation may promote coagulation and present a risk factor for reocclusion in AMI patients.

1.5.5.1. Ser3 phosphorylation and VTE

In a recent study testing for gene associations with blood metabolites, loci from three functionally-linked genes were found to be associated with phosphorylation of fibrinogen Aα chain Ser3: i) the *ABO* gene encoding ABO blood group, ii) the *FUT2* gene encoding fucosyltransferase 2, also involved in determining blood group and iii) the *ALPL* gene encoding a tissue non-specific alkaline phosphatase (Suhre et al., 2011). Both the *ALPL* and *ABO* loci are associated with circulating levels of alkaline phosphatase (Yuan et al., 2008), suggesting their influence on the degree of fibrinogen phosphorylation may be mediated by this enzyme. Notably, the *ABO* locus is also associated with VTE risk, whereby non-O blood group individuals have a higher risk than O blood group carriers (Tregouet et al., 2009). This highlights a potential role of fibrinogen phosphorylation in the underlying pathology of VTE. Hence, Suhre et al. have provided the first evidence of a genetic link between fibrinogen phosphorylation and thrombosis.

To summarise, phosphorylation of fibrinogen occurs at Aα chain Ser3 and Ser345 and is elevated in acute phase conditions and thrombosis, suggesting an important contribution to haemostatic processes. However, the mechanism and functional effects of this modification are yet to be determined. Fibrinogen can be phosphorylated by several kinases *in vitro* with conflicting effects on clot structure, but the *in vivo* fibrinogen kinase has not been identified. With regards to function, existing research has focused on Ser3 phosphorylation in relation to enhanced thrombin binding and FpA cleavage but little is known about the role of Ser345 phosphorylation. As Ser345 is positioned between FXIII cross-linking acceptor sites and close to the FXIII-A2B2 binding region, this site might be implicated in the regulation of α chain crosslinking. It may also coordinate fibrinolysis as several fibrinolytic proteins interact with the αC region of fibrinogen. Advancing understanding of the regulation of fibrinogen phosphorylation and its effects on clot formation and fibrinolysis may prove valuable for the management of thrombosis.

1.6. Aims and hypothesis

1.6.1. Hypothesis

Elevated phosphorylation of fibrinogen, as occurs in acute phase conditions, is directly responsible for inducing pro-thrombotic changes in the fibrin network, and is mediated by increased activity of a hepatocellular kinase.

1.6.2. Aims

This project aims to provide an in-depth investigation into the cellular mechanism and functional role of *in vivo* fibrinogen phosphorylation at Aα chain Ser3 and Ser345. The function of the individual phosphorylation sites will be investigated by expression of recombinant wild-type (WT) fibrinogen and variant fibrinogens with mutations at Ser3 and/or Ser345 to prevent phosphorylation. This will be achieved using an established expression system in Chinese hamster ovary (CHO) cells (Binnie et al., 1993). Preliminary analysis by matrix assisted laser desorption ionisation (MALDI)-time of flight (TOF)/TOF mass spectrometry has confirmed that CHO cells are capable of phosphorylating WT fibrinogen at Ser3 and Ser345 (Appendix 3). Purified recombinant fibrinogens will be compared in a variety of functional studies designed to investigate the impact of each phosphorylation site on fibrin clot properties, including structure, polymerisation and lysis rates, and interactions with other haemostatic plasma components, such as FXIII, plasmin(ogen) and α2-AP. To characterise the mechanism of fibrinogen phosphorylation, methods will be developed to visualise and quantify phosphorylated fibrinogen inside, or secreted from, human hepatoma (HepG2) cells. These methods will be used to determine the subcellular location of fibrinogen phosphorylation, as well as the relevant fibrinogen kinase. The effect of acute phase cytokine interleukin-6 (IL-6) on fibrinogen expression, phosphorylation and kinase activity will also be examined.

The key aims of this thesis are summarised below:

1. To express and purify recombinant WT fibrinogen and fibrinogen variants lacking the Ser3 and/or Ser345 phosphorylation sites using a CHO cell expression system.

2. To investigate the functional effect of fibrinogen phosphorylation on fibrin clot structure and function, including clot formation, FXIII-mediated clot stabilisation, interaction with fibrinolytic proteins, and plasmin digestion of fibrin(ogen).

3. To characterise the mechanism of fibrinogen phosphorylation by identifying the subcellular location and *in vivo* fibrinogen kinase, as well as changes to this regulatory process in acute phase conditions.

Chapter 2

Materials and Methods

2.1. Recombinant Fibrinogen Expression

Full-length recombinant WT fibrinogen was expressed in CHO cells and purified by affinity chromatography. The integrity and functionality of this fibrinogen was then analysed using a variety of methods. To investigate the function of the Ser3 and Ser345 phosphorylation sites, a plasmid coding for the Aα chain of fibrinogen was mutated to change the serine residues of interest to alternative amino acids. The resulting vectors were transfected into CHO and Expi293F cells for expression of variant fibrinogen lacking the phosphorylation sites of interest.

2.1.1. Expression of recombinant WT fibrinogen in CHO cells

Chinese hamster ovary cells previously transfected with plasmids containing human fibrinogen Aα, Bβ and γ chain cDNA for expression of recombinant WT fibrinogen (CHO-WT) (kindly donated by Prof Susan Lord, University of North Carolina at Chapel Hill) were cultured in 10 x 100 mm dishes with 10 ml growth medium per dish (Appendix 1) and incubated at 37°C, 5 % carbon dioxide (CO_2). When confluent, cells were split using trypsin-ethylenediamine tetraacetic acid (EDTA) solution (Sigma-Aldrich, USA) and transferred to 10 x 2 L roller bottles, each with 200 ml growth medium containing 4 g Cytodex 1 dextran microcarrier beads (60-87 µm) (Sigma-Aldrich) previously swollen in phosphate buffered saline (PBS) pH 7.4 (Appendix 1), autoclaved at 120°C and resuspended in growth medium after sedimentation. The microcarrier beads were added to roller bottles to increase surface area for cell adhesion and growth. Roller bottle cultures were incubated in a rolling incubator at 37°C, 5 % CO_2. After 3 days, or when confluent, cells were incubated overnight in 100ml serum-free growth medium per bottle for adjustment to serum-free conditions. The cells were then cultured in insulin transferrin selenium (ITS)-supplemented medium (Appendix 1), using ITS as a growth factor supplement in place of serum for easier downstream protein purification. Fibrinogen-containing medium (100 ml) was harvested from each roller bottle and replaced with 100ml fresh ITS medium every 2-3

days for approximately 3 months. Harvested medium was filtered and stored at -20°C with serine protease inhibitor phenylmethylsulfonyl fluoride (PMSF) (Sigma-Aldrich) [150 nM] until purification. An aliquot of medium was taken from each harvest for an enzyme-linked immunosorbent assay (ELISA) to quantify fibrinogen (method 2.1.2); this was performed every 2 weeks to monitor the degree of fibrinogen secretion and the culture was terminated once productivity was seen to significantly decline.

2.1.2. ELISA for quantification of fibrinogen in harvested medium

A 96-well microtiter plate was coated with 100 µl per well of polyclonal anti-human fibrinogen antibody (DAKO, Denmark) diluted 1/4000 [1.5 µg/ml] in Buffer A (Appendix 1) and incubated at 4°C overnight. Following incubation, the plate was washed with 3 x 300 µl Buffer B (Appendix 1). To generate a standard curve, Calbiochem® human fibrinogen from plasminogen-depleted plasma (Millipore, USA) was diluted to eight known concentrations ranging from 0.016 to 1 µg/ml in Buffer B. The fibrinogen standards were added to the plate in duplicate, along with samples of medium containing recombinant WT fibrinogen – undiluted, or diluted 1/10, 1/20 and 1/40 in Buffer B – and incubated for 2 hours at room temperature on a shaker. The plate was washed with 3 x 300 µl Buffer B and 100 µl per well of a horseradish peroxidase (HRP)-conjugated anti-fibrinogen antibody (abcam, UK) diluted 1/16,000 [0.625 µg/ml] in Buffer B was applied for 1 hour at room temperature. After a final wash step with Buffer B, bound fibrinogen was detected using 100 µl per well of o-phenylenediamine dihydrochloride (OPD) substrate (DAKO) dissolved in distilled water (dH_2O) to 0.5 mg/ml. Hydrogen peroxide was added at 0.01 % (v/v) to catalyse the oxidation of OPD by horseradish peroxidase; this produces a yellow colour with intensity proportionate to the amount of fibrinogen in the well. The reaction was stopped with 100 µl per well of 1 M sulphuric acid and absorbance was measured at 490 nm using an MRX-TC plate reader (Dynex, USA).

2.1.3. Purification of recombinant WT fibrinogen

2.1.3.1. Ammonium sulphate precipitation of fibrinogen

Harvested cell culture medium was mixed with a protease inhibitor cocktail (Appendix 1) to prevent proteolytic degradation. The cocktail was buffered with 2-(*N*-morpholino)ethanesulfonic acid (MES) at pH 5.6, the isoelectric point (pI) of fibrinogen, to encourage precipitation. Saturated ammonium sulphate solution was prepared by dissolving 1520 g ammonium sulphate (Fisher Scientific, USA) in 2 L dH_2O heated to

90°C. The solution was cooled at 4°C overnight, or until crystals had formed, and added dropwise to the culture medium by passing through filter paper. The volume of 100 % (v/v) saturated ammonium sulphate required for a final concentration of 40 % (v/v) when mixed with the media was calculated using the following formula: $V_{AS} = 0.667V_M$, where V_{AS} is the volume of ammonium sulphate to add, and V_M is the starting volume of media. The solution was incubated overnight at 4°C with gentle stirring to precipitate the fibrinogen. The following day, the precipitate mix was centrifuged at 9000 rpm, 4°C for 45 minutes without braking (Sorvall instrument RC5C) and the pellets resuspended in 1.2 ml pellet cocktail (Appendix 1) containing protease inhibitors and Tris buffer at physiological pH (7.4). Resuspended pellets were pooled and centrifuged at 19,000 rpm, 4°C for 30 minutes with braking (Sorvall, SS-34) and the supernatants containing the fibrinogen were decanted and stored at -20°C until purification.

2.1.3.2. Affinity chromatography with IF-1 anti-fibrinogen antibody

A BioCad Sprint Perfusion Chromatography System was used for purification of recombinant WT fibrinogen by affinity chromatography. The column consisted of an anti-fibrinogen IF-1 monoclonal antibody (Kamiya Biomedical, USA) coupled to a cyanogen bromide-activated sepharose 4B resin (GE Healthcare, UK) in IF-1 equilibration buffer (Appendix 1). Fibrinogen-containing supernatants were mixed with calcium chloride ($CaCl_2$) [10 mM] prior to loading on the column, as the IF-1 antibody recognises an epitope within the D-domain of fibrinogen in a calcium dependent manner. The column was equilibrated with 1 column volume (CV) (7.599ml) of IF-1 equilibration buffer before injecting 5ml supernatant; this volume of supernatant was reduced from 15 ml to 5 ml to prevent overloading and loss of fibrinogen in the flow through. IF-1 wash buffers I and II (Appendix 1) were applied sequentially to the column to remove any unbound sample before eluting fibrinogen with 6 CV of IF-1 elution buffer (Appendix 1). Elution was achieved with EDTA (Sigma-Aldrich) to chelate calcium ions from binding pockets in the fibrinogen D domain, impeding its interaction with the IF-1 column. The concentration of eluted fibrinogen in selected fractions was verified by reading absorbance at 280 nm (A_{280} nm) using a NanoDrop ND-1000 spectrophotometer (Thermo Scientific) and extinction coefficient 1.51. All fractions containing a reasonable amount of fibrinogen were pooled and stored at -80°C.

2.1.3.3. Concentration and dialysis of purified fibrinogen

Dialysis tubing (25 mm) with a 12 kDa molecular weight cut off (MWCO) (Sigma-Aldrich) was prepared by heating in dH_2O with 10 mM EDTA (Sigma-Aldrich) to remove

divalent cations and prevent binding of protein to the membrane. Purified samples were transferred to dialysis tubing and placed in Tris-buffered saline (TBS)-1 pH 7.4 (Appendix 1), three samples per litre, with gentle stirring at 4˚C overnight. The buffer was changed the following morning and stirred for a further hour. Samples were concentrated to approximately 1 mg/ml by centrifugation at 3,000 g (Hettich Rotanta 460R) using Vivaspin 20 concentrator tubes with a 100 kDa MWCO (Life Technologies, USA). Finally, samples were pooled, divided into aliquots and stored at -80˚C. Fibrinogen from later harvests was pooled separately in case of degradation, as determined by sodium dodecyl sulphate polyacrylamide gel electrophoresis (SDS-PAGE) (method 2.1.4).

2.1.4. SDS-PAGE

All materials and reagents were purchased from Life Technologies unless otherwise stated. Samples containing 15 µg protein were mixed with 10X reducing agent, 4X lithium dodecyl sulphate (LDS) sample buffer and dH_2O to a final volume of 40 µl. The samples were then heated to 95°C for 15 minutes to denature proteins and reduce disulphide bonds, cooled on ice for 2 minutes and centrifuged briefly (Eppendorf MiniSpin Plus). Reduced samples (40 µl) were loaded onto pre-cast 4-12 % Bis-Tris polyacrylamide gels (1.0 mm, 10 well) with a Precision Plus Protein WesternC standard (molecular weight marker) (7.5 µl) (BIO-RAD, USA), consisting of 10 pre-stained recombinant proteins of known size ranging from 10-250 kDa. Electrophoresis was carried out at 200 V for 40 minutes in 500 ml MES running buffer, prepared by diluting a 20X concentrated stock solution with filtered dH_2O. Gels were rinsed for 30 minutes in dH_2O to remove residual buffer, stained with GelCode Blue Stain Reagent (Thermo Scientific, USA) for 1 hour at room temperature with shaking, destained in dH_2O overnight and imaged the next day by transillumination with Chemi-imager software (Alpha Innotech, USA).

2.1.5. Expression and purification of recombinant FXIII-A

For use in functional studies with recombinant WT fibrinogen, recombinant FXIII-A (rFXIII-A) was expressed in *Escherichia Coli* (*E. Coli*) and purified by glutathione S-transferase (GST)-affinity chromatography, according to methods described by Smith et al. (2011).

2.1.5.1. Expression of recombinant GST-FXIII-A in *E. Coli*

The expression construct for recombinant GST-FXIII-A, kindly provided by Dr Penelope Adamson, had previously been transformed into BL21-Gold (DE3) competent *E. Coli* cells (Stratagene, USA), as described in method 2.1.8.3. Two starter cultures, each with 180 ml terrific broth, 20 ml phosphate buffer (Appendix 1) and 200 µl 100 mg/ml ampicillin, were inoculated with 10 µl of a glycerol stock of the transformed *E. Coli* and incubated for 16 hours at 37°C, 225 rpm. All buffers are detailed in Appendix 1 and were autoclaved before use. The next day, each starter culture was used to inoculate a new expression culture containing 1.8 L terrific broth, 200ml phosphate buffer and 2ml 100mg/ml ampicillin and incubated at 37°C, 180rpm for 2 hours. Expression of GST-FXIII-A was induced using isopropyl β-D-1-thiogalactopyranoside [1 mM] and the cultures were incubated for 16 hours at 30°C, 180 rpm. Cells were harvested by centrifugation at 5450 rpm, 4°C for 10 minutes (Sorvall instrument RC5C) and the bacterial pellets were resuspended in ice cold *E. Coli* wash buffer (180 ml per 2 L culture) (Appendix 1). An additional centrifugation step at 4600 rpm, 4°C for 1 hour was performed to remove the wash buffer; this was discarded and the pelleted cells were stored at -20°C until lysis and rFXIII-A purification.

2.1.5.2. Cell lysis of BL21-Gold *E. Coli*

All reagents were purchased from Sigma-Aldrich. Frozen cell pellets from method 2.1.5.1 were thawed and resuspended in 176 ml ice cold PBS pH 7.4 (Appendix 1) by stirring for 1 hour at room temperature. Bacterial cells were lysed with lysozyme [1 mg/ml] in the presence of dithiothreitol (DTT) [1 mM] to increase binding of the GST fusion protein to glutathione during subsequent affinity chromatography purification; the mixture was stirred gently for an additional 30 minutes at room temperature. A protease inhibitor cocktail containing aprotinin [2 µg/ml], pepstatin A [1 µM], leupeptin [10 µM] and benzamidine dihydrochloride [4 mM] was added to the culture and stirred at 4°C for 30 minutes, before addition of PMSF [0.5 mM] and 0.05 % (v/v) sodium deoxycholate – an ionic detergent used to solubilise cell membranes. After 30 minutes of stirring at room temperature, the culture was transferred back to 4°C and mixed vigorously for a further 10 minutes with 1 % (v/v) triton X-100 to aid solubilisation of proteins, plus DNase I [5 µg/ml] with magnesium chloride [5 mM] for DNA degradation. The DNase activity was halted by chelation of magnesium ions with EDTA [6 mM]. To separate soluble recombinant GST-FXIII-A from insoluble cellular components, lysates were centrifuged at 13,570 rpm for 20 minutes, 4°C (Sorvall instrument RC5C). The supernatant was carefully decanted, mixed briefly with 2 g streptomycin sulphate to precipitate nucleic acids, and centrifuged again at 13,570 rpm for 20 minutes, 4°C.

Finally, the supernatant was filtered through a 0.22 µm vacuum filter (Thermo Scientific) and made up to a 300 ml volume with PBS pH 7.4, ready for purification by GST-affinity chromatography.

2.1.5.3. Purification of rFXIII-A by GST affinity chromatography

An ÄKTA prime chromatography system (GE Healthcare, UK) was used for purification of GST-FXIII-A from cell lysate by exploiting the high affinity interaction between GST and glutathione. The system was fitted with 3 x 5 ml GSTrap Fast Flow affinity columns (GE Healthcare) pre-packed with Glutathione Sepharose media to bind the GST fusion protein. All buffers used during purification contained 15 % (v/v) glycerol for protein stability and are detailed in Appendix 1. The columns were equilibrated with 50 ml GST equilibration buffer pH 7.4 at 5 ml/min before loading 300 ml lysate at a reduced flow rate of 0.5 ml/min. To remove any unbound sample and wash the bound GST-FXIII-A, 250 ml GST wash buffer was applied at a flow rate of 0.5 ml/min. The flow rate was gradually increased and a further 60 ml GST wash buffer was applied at 1.5 ml/min, followed by a final equilibration step with 420 ml equilibration buffer at 2.5 ml/min.

Upon completion of the loading and washing steps, the GSTrap Fast Flow columns containing the bound GST-FXIII-A were removed from the ÄKTA prime and manually loaded with PreScission Protease (GE Healthcare) for cleavage of the GST tag from FXIII-A. PreScission Protease is a fusion protein consisting of the human rhinovirus 3C protease and GST. Its action involves simultaneous interaction of GST with glutathione and site-specific cleavage of GST between the glutamine (Q) and glycine (G) residues of the following amino acid sequence: LQVLFQ/GP. The PreScission Protease (2 U per 100 µg protein) was added to 15 ml equilibration buffer and injected manually into the GSTrap Fast Flow columns, which were then incubated horizontally at 4°C for a minimum of 8 hours. Following cleavage, the columns were re-fitted to the ÄKTA prime, with an additional fourth 5 ml GSTrap Fast Flow column at the bottom to prevent loss of FXIII-A. The cleaved FXIII-A was eluted with 35 ml PBS equilibration buffer pH 7.4 at a flow rate of 1 ml/min, whilst collecting 1 ml fractions. The bound GST was subsequently eluted in 2 ml fractions using 35 ml GST elution buffer pH 8.0 containing 20 mM glutathione at a flow rate of 1 ml/min. The columns were regenerated at 5 ml/min with 45 ml 5 M urea, 45 ml equilibration buffer, 45 ml 70 % (v/v) ethanol and a further 100 ml equilibration buffer. Fractions from the FXIII-A (peak 2) and GST elution peaks were pooled separately and the FXIII-A was concentrated using Vivaspin concentrator tubes with a 30 kDa MWCO (Life Technologies). A NanoDrop ND-1000 spectrophotometer was used to determine the concentration of FXIII-A at A_{280}nm with extinction coefficient 1.58. Purified FXIII-A (7 µg) and GST (4 µl at unknown

concentration) samples were analysed by SDS-PAGE (method 2.1.4) and western blotting using an HRP-conjugated FXIII-A antibody (method 2.1.6; table 3). The blot was developed by addition of 1-2 ml 3,3',5,5'-Tetramethylbenzidine (Sigma-Aldrich); the reaction was quenched with dH_2O before imaging by transillumination using a Kodak Image Station 2000R and Kodak 1D Image Analysis Software (Labtech International, UK). Finally, the activity of the purified FXIII-A was analysed by means of a biotin-pentylamine incorporation FXIII-A activity assay (method 2.1.7.2).

2.1.6. Western blotting

Samples were subjected to SDS-PAGE as described in method 2.1.4, loading nanogram quantities of protein with 5µl Precision Plus Protein WesternC standard to compensate for the more sensitive detection. Each protein within the molecular weight standard has a synthetic *Strep*-tag of 8 amino acids in length, which binds StrepTactin – an engineered form of streptavidin – with high affinity, enabling detection. After electrophoresis, gels were rinsed for 10 minutes in transfer buffer pH 8.1-8.4 (Appendix 1) on an orbital shaker. Immobilon-P polyvinylidene-difluoride (PVDF) transfer membrane (Millipore) (0.45 µm pore size) was cut to 3 x 2.5 inches and pre-wetted in methanol for 15 seconds, rinsed in dH_2O for 2 minutes and equilibrated in chilled transfer buffer for 2 minutes. Filter paper and sponges of the same size were also pre-soaked in transfer buffer before assembling into blotting cassettes in the following order: sponge – filter paper – SDS-PAGE gel – PVDF membrane – filter paper – sponge. Cassettes were inserted into a tank containing an ice pack and filled with chilled transfer buffer. The transfer was run at 100 V for 1 hour and the buffer was stirred gently throughout to maintain even temperature and ion distribution. After 1 hour, membranes were carefully removed from the tank and washed 3 x 10 minutes in TBS-2-Tween 20 pH 7.4 (Appendix 1). A blocking solution of TBS-2-Tween 20 with 5 % (w/v) skimmed milk powder was added for 1 hour at room temperature, or 4°C overnight, to prevent non-specific binding of antibodies during subsequent incubation steps. The membrane was washed 3 x 10 minutes with TBS-2-Tween 20. The primary antibody was diluted in 10 ml blocking solution and incubated with the membrane for 1 hour at room temperature on a roller. Another three wash steps were performed with TBS-2-Tween 20. A secondary HRP-conjugated antibody directed against the primary antibody species, plus a Precision Protein StrepTactin-HRP Conjugate (BIO-RAD) (1/5000) for detection of the molecular weight marker, were diluted in 10 ml blocking solution and incubated with the membrane for 1 hour at room temperature. Primary and secondary antibodies used for western blotting are listed in table 3. The membrane was washed 3 x 10 minutes with TBS-2-Tween 20 prior to development with

SuperSignal West Pico Chemiluminescent Substrate (Thermo Scientific) or Clarity ECL Substrate (BIO-RAD). Enhancer and peroxide solutions were mixed in a 1:1 ratio, added to the blot and left for 5 minutes. Blots were imaged by chemiluminescence using a Kodak Image Station 2000R with Kodak 1D Image Analysis Software, or a G:BOX F3 with GeneSys software (Syngene, UK), for varying lengths of exposure depending on the amount of protein.

Antibody	Host species	Clonality	Dilution
Anti-FXIII-A HRP (Enzyme Research Laboratories)	Sheep	Polyclonal	1/2000
Anti-fibrinogen (DAKO)	Rabbit	Polyclonal	1/1000
Anti-fibrinogen Aα 290-348/349-406 (Accurate Chemical, USA)	Mouse	Monoclonal	1/1000
Anti-fibrinogen γ 15-35 (Accurate Chemical)	Mouse	Monoclonal	1/5000
Anti-phosphoserine (abcam)	Rabbit	Polyclonal	1/100
Anti-phosphoserine (Millipore)	Mouse	Monoclonal	1/1000
Anti-rabbit HRP (DAKO)	Goat	Polyclonal	1/1000
Anti-mouse HRP (DAKO)	Rabbit	Polyclonal	1/1000

Table 3. Western blotting antibodies. Primary and secondary antibodies used for detection of fibrinogen, fibrinogen Aα chain or phosphoserine by western blotting are listed with details of host species, clonality and working dilution.

2.1.7. Functional studies with recombinant WT fibrinogen

2.1.7.1. Turbidity and lysis assay

Formation and lysis of a clot can be monitored *in vitro* by recording changes in optical density, or turbidity, during these dynamic processes. Turbidity increases with lateral aggregation of protofibrils and fibre formation in the presence of thrombin and calcium, and declines with proteolytic clot degradation by plasmin. Additional haemostatic proteins may be added to examine their influence on clot turbidity and lysis. All reagents were diluted to the desired concentrations in sufficient TBS-1 pH 7.4 for a

final volume of 150 µl per well. Recombinant WT fibrinogen (0.5 mg/ml) was added to a 96 well microtiter plate in duplicate ± rFXIII-A [1.1 µg/ml] in an 80 µl volume per well. This was overlaid with 35 µl plasminogen (Enzyme Research Laboratories) (35 µg/ml) and the plate was inserted into the preheated chamber of an EL_x808 Absorbance Microplate Reader (BIO-TEK, USA) at 37°C. For activation, 35 µl of a mix containing recombinant tPA [0.3 µg/ml] (Technoclone, Austria), thrombin (Calbiochem) [0.5 U/ml] and $CaCl_2$ [2.5 mM] were added to each well in one step and the plate was immediately shaken. Absorbance at 340 nm was recorded for 59 minutes in 12 second intervals and a customised software application was used for calculation of turbidimetric variables (Carter et al., 2007): lag time (Lag), representing the onset of lateral aggregation of protofibrils preceding exponential increase in turbidity; maximum absorbance (MaxAbs), representing fibre thickness and clot compactness; clotting rate; time to 50 % lysis ($Lys50_{MA}$); lysis rate; and lysis area, which encompasses clot formation, MaxAbs and fibrinolysis (figure 9).

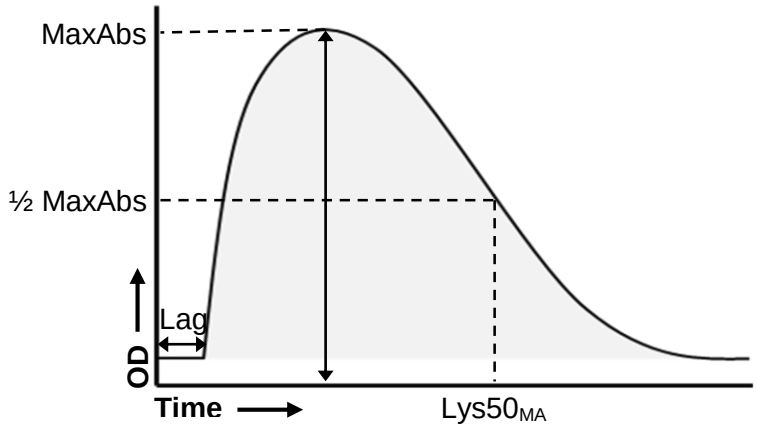

Figure 9. Turbidity and lysis curve analysis. The graph displays a typical curve with change in OD over time during a turbidity and lysis assay. The Lag phase is shown as the period prior to the onset of increase in turbidity; maximum absorbance (MaxAbs) can be read from the peak of the curve, while half this value (½ MaxAbs) is used to determine time to 50 % lysis ($Lys50_{MA}$); lysis area is depicted by the grey shading.

2.1.7.2. Biotin-pentylamine incorporation FXIII-A activity assay

The FXIII-A activity assay relies on cross-linking of biotin-pentylamine to fibrinogen via its primary amine group, catalysed by the transglutaminase activity of FXIII-A. The degree of cross-linked biotin-pentylamine is hence used as a measure of FXIII activity. All reagents were from Sigma-Aldrich unless otherwise stated. Recombinant WT

fibrinogen and a Calbiochem® fibrinogen control were added to a 96-well microtiter plate in duplicate for six different time points ± rFXIII-A. The plate was coated with 100 µl per well of fibrinogen [40 µg/ml] in TBS-3 pH 8.3 (Appendix 1) for 40 minutes at room temperature and the surface blocked with 300 µl per well 1 % (w/v) bovine serum albumin (BSA)-TBS-1 at 37°C pH 8.3 for 90 minutes. The plate was washed with 4 x 300 µl TBS-1, and 10 µl of rFXIII-A diluted to 11 µg/ml in TBS-1 were added to each well, giving a final concentration of 1.1 µg/ml after addition of the master mix. Using a multi-channel pipette, 90 µl of master mix containing DTT [0.1 mM], 5-(biotinamido) pentylamine (Thermo Scientific) [2.7 µM], $CaCl_2$ [1 mM] and thrombin [1 U/ml] in TBS-1 were added to each well for 0-25 minutes in 5 minute intervals and reactions were stopped using 200 µl per well of 200 mM EDTA to chelate calcium ions. For the zero time point, EDTA was added prior to addition of the master mix. The plate was washed with 4 x 300 µl TBS-3-Tween 20 pH 8.3 (Appendix 1) and 100 µl per well of streptavidin alkaline phosphatase [2 µg/ml], diluted in 1 % (w/v) BSA-TBS-3-Tween 20, was added for 1 hour at 37˚C to bind incorporated biotin-pentylamine via a high affinity interaction between streptavidin and biotin. After a final four washes with TBS-3-Tween 20, biotin-pentylamine was detected by addition of 100 µl per well of p-nitrophenol phosphate (PNPP) – a substrate for streptavidin alkaline phosphatase – dissolved in dH_2O to a final concentration of 1 mg/ml. Once the colour had developed, reactions were stopped using 100 µl per well of 4 M sodium hydroxide and absorbance was measured at 405 nm using a Dynex MRX-TC plate reader.

2.1.7.3. Fibrin polymerisation time course experiment by SDS-PAGE

Recombinant WT fibrinogen [0.5 mg/ml] and rFXIII-A [1.1 µg/ml] were diluted in TBS-1 pH 7.4 to 15 µl and mixed with 5 µl activation mix containing thrombin [0.05 U/ml] and $CaCl_2$ [1.5 mM], also diluted in TBS-1. Eight separate reactions were prepared and activation mix was added at controlled time points. After addition of the activation mix, each reaction was immediately transferred to a hot block at 37˚C for 0, 5, 10, 20, 30, 60, 120 or 180 minutes. Reactions were stopped at the aforementioned time points by addition of 4X LDS sample buffer and 10X reducing agent. Each sample, plus a fibrinogen-only control, was reduced by heating at 95°C for 15 minutes and loaded onto a 4-12 % Bis-Tris polyacrylamide gel with 7.5 µl Precision Protein WesternC standard. Samples were electrophoresed at 150 V for 85 minutes in 700 ml 3-(N-morpholino)propanesulfonic acid (MOPS) SDS running buffer (Life Technologies), prepared from a 20X concentrated stock by diluting in filtered dH_2O. Electrophoresis conditions differed to method 2.1.4, with a lower voltage, extended running time and use of MOPS buffer to aid separation of high molecular weight fibrin α-α, α-γ and γ-γ

polymers. The gel was washed twice in dH_2O, stained for 1 hour with GelCode Blue Stain Reagent and rinsed in dH_2O overnight before imaging by transillumination the next day.

2.1.8. Generation of variant fibrinogen Aα chain constructs

In order to substitute fibrinogen Aα chain Ser3 and Ser345 for residues which cannot be phosphorylated, relevant nucleotides within the Aα chain DNA sequence were mutated by site directed mutagenesis. Site directed mutagenesis can be used to create single or multiple base substitutions within a known DNA sequence. Base changes are designed in such a way to encode a different amino acid of choice at a particular location within the transcribed protein.

Three expression vectors, created from the pMLP vector (figure 10) by insertion of fibrinogen Aα (pMLP-Aα), Bβ (pMLP-Bβ) or γ (pMLP-γ) chain cDNA into the multiple cloning site (figure 11), were kindly provided by Prof Susan Lord, University of North Carolina at Chapel Hill. For expression of fibrinogen variants, Aα chain Ser3 and Ser345 residues within the pMLP-Aα vector were mutated to asparagine, glutamic acid or alanine residues; the effects of each amino acid on the expression and secretion of fibrinogen variants were compared in a series of transfection experiments. Serine codons were initially changed to asparagine as these two residues have similar charge and polarity. Alanine has similar charge but different polarity to serine and is commonly used for transfection due to its structural simplicity, which is unlikely to disrupt secondary protein structure. Glutamic acid was employed as a phosphomimetic by exploiting its negative charge, resembling that of a phosphate group. The properties of these four amino acids are compared in table 4.

	Serine	Asparagine	Glutamic Acid	Alanine
Abbreviations	Ser (S)	Asn (N)	Glu (E)	Ala (A)
Structure	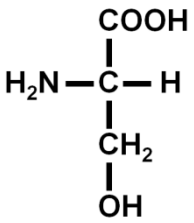	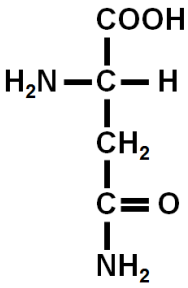	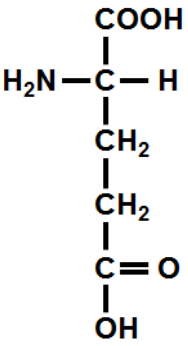	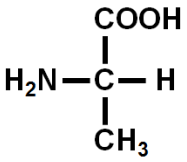
Charge	Uncharged	Uncharged	**Negative*	Uncharged
Polarity	Polar	Polar	Polar	***Nonpolar*
Functional group	Hydroxyl	Amide	Carboxyl	Methyl

Table 4. Comparison of amino acid properties. The table details the structure, charge, polarity and side chain functional groups of the four amino acids involved in site directed mutagenesis of Ser3 and Ser345 phosphorylation sites: serine, asparagine, glutamic acid and alanine. Serine and asparagine share similar chemical properties, while glutamic acid differs by its negative charge (*) and alanine by its polarity (**).

Mutagenesis of pMLP-Aα was carried out using polymerase chain reaction (PCR) with primers designed to introduce the desired mutations. The variant constructs were then transformed into *E. Coli* for amplification, harvested by cell lysis and purified. Analyses of DNA quality and sequence integrity were performed prior to transfection into CHO cells. Seven new pMLP-Aα vectors were created in this way for expression of fibrinogen variants with the following Aα chain mutations:

1. Ser3Asn (S3N)
2. Ser345Asn (S345N)
3. Ser3/345Asn (S3/345N) (double variant)
4. Ser3Glu (S3E)
5. Ser345Glu (S345E)
6. Ser3/345Glu (S3/345E) (double variant)
7. Ser345Ala (S345A)

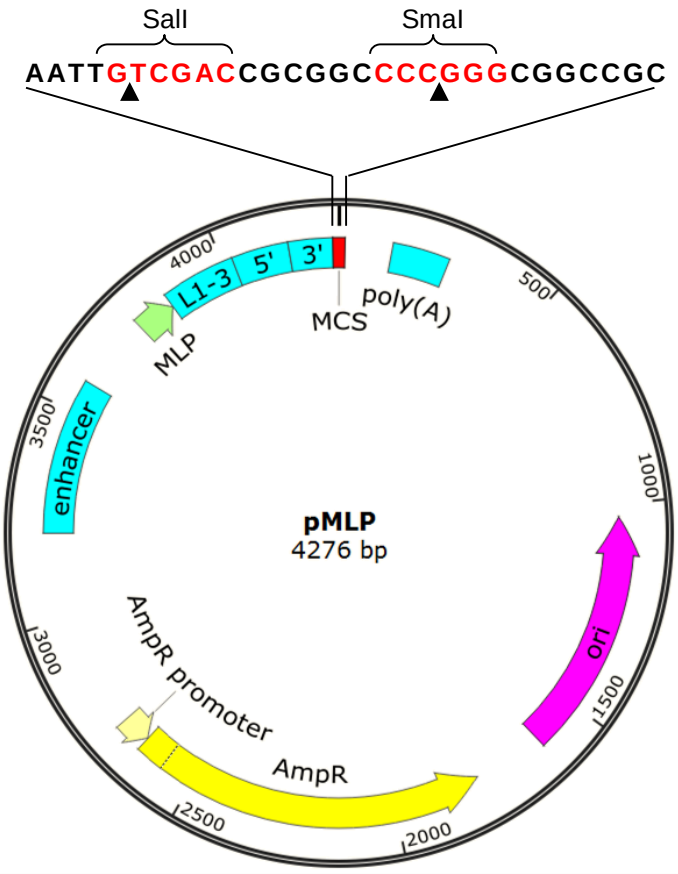

Figure 10. pMLP vector map. Downstream of the SV40 enhancer, the pMLP vector contains the major late promoter (MLP) and tripartite leader sequence (L1-3) from adenovirus 2, 5' and 3' splice sites, a multiple cloning site (MCS) and the SV40 mRNA polyadenylation (poly(A)) signal. The MCS is detailed above the map; restriction sites used for insertion of Aα (SmaI), Bβ (SalI and SmaI) or γ (SmaI) chain cDNA are highlighted in red, with cleavage sites indicated by arrows (▲). The vector also contains an origin of replication (ori), ampicillin resistance gene (AmpR) and AmpR promoter in the opposite orientation.

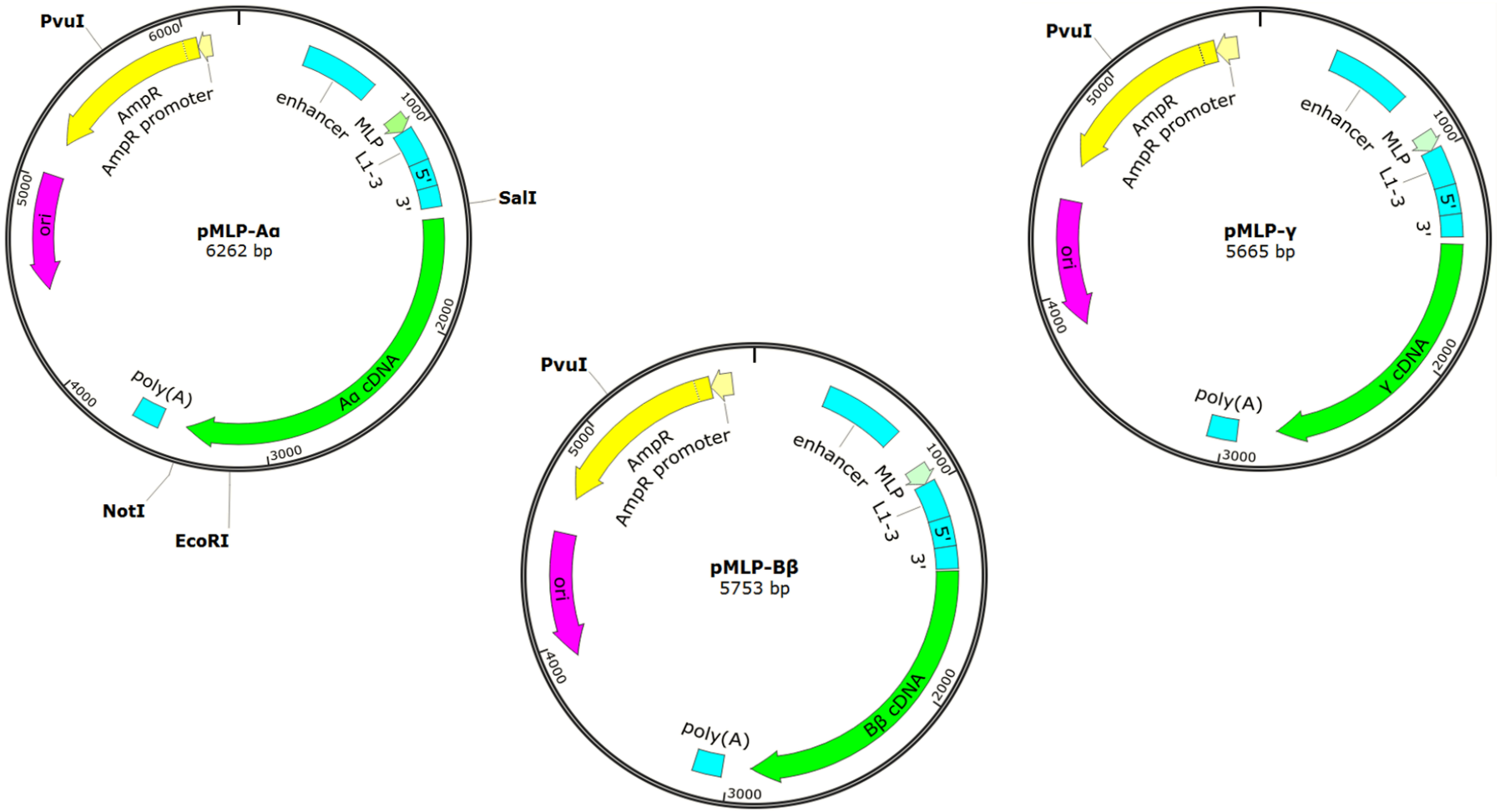

Figure 11. pMLP-Aα, -Bβ and -γ vector maps. The vector maps show pMLP with fibrinogen Aα, Bβ or γ chain cDNA inserts in the multiple cloning site. Expression of these polypeptide chains is driven by the adenovirus 2 major late promoter (MLP). The locations of restriction sties used to linearise the vectors (PvuI and EcoRI), as well as those used to remove the Aα chain insert from pMLP-Aα (NotI and SalI), are also indicated.

2.1.8.1. Primer design for site directed mutagenesis

A Quikchange Primer Design tool by Agilent Technologies (USA) was used to design primers in accordance with the Quikchange II site directed mutagenesis kit manual. Serine 3 and Ser345 codons (AGT and AGC respectively) were located within the Aα chain sequence. Forward and reverse primers of 25-45bp in length were designed to target these regions with complementary sequence either side of the codon of interest, while primer bases within the Ser3 and Ser345 codons were changed to introduce codons transcribing the desired amino acids (table 5). Primers were designed to have 40-60% guanine/cytosine (GC) content, including a G or C at the beginning and end of each primer, and a melting temperature (T_m) of approximately 80°C to ensure good annealing to the template. All custom oligonucleotides were purchased from Life Technologies.

Primer	Sequence (5' to 3')	Length (nt)	T_m (°C)
S3N F	GCACAGCATGGACTGCAGATAATGGTGAAGGTG	33	79.14
S3N R	CACCTTCACCATTATCTGCAGTCCATGCTGTGC	33	79.14
S345N F	CCTGGAATCCTGGCAACTCTGAACGCGGAAG	31	80.31
S345N R	CTTCCGCGTTCAGAGTTGCCAGGATTCCAGG	31	80.31
S3E F	GGCACAGCATGGACTGCAGATGAGGGTGAAGGTGACTTTCTAG	43	78.85
S3E R	CTAGAAAGTCACCTTCACCCTCATCTGCAGTCCATGCTGTGCC	43	78.85
S345E F	GAACCTGGAATCCTGGCGAGTCTGAACGCGGAAGTGC	37	78.42
S345E R	GCACTTCCGCGTTCAGACTCGCCAGGATTCCAGGTTC	37	78.42
S345A F	CCTGGAATCCTGGCGCCTCTGAACGCGGAAG	31	81.69
S345A R	CTTCCGCGTTCAGAGGCGCCAGGATTCCAGG	31	81.69

Table 5. Ser3 and Ser345 primers used for site directed mutagenesis. 5' to 3' sequences of forward (F) and reverse (R) primers are displayed, with the altered codons of interest highlighted in red, as well as nucleotide (nt) length and T_m of each primer.

2.1.8.2. Site directed mutagenesis

Polymerase chain reaction was performed using a Quikchange II site directed mutagenesis kit (Stratagene) in accordance with the manufacturer's instructions. All

templates and primers were diluted in molecular grade BDH® H_2O (VWR International, USA). Each cDNA template (1 ng) was mixed with the relevant forward and reverse primers listed in table 5 (125 ng each), 10X reaction buffer, 1 µl of deoxynucleotide triphosphate (dNTP) mix, 2.5 U *PfuUltra* high fidelity DNA polymerase and molecular grade H_2O up to a final volume of 50 µl in a PCR reaction tube. The cDNA was amplified during a process of thermal cycling in a PTC-200 thermal cycler (MJ Reseasrch, Canada) using the following conditions:

1.	Initiation	95°C	30 seconds	
2.	Denaturation	95°C	30 seconds	x 18
3.	Annealing	55°C	1 minute	
4.	Elongation	68°C	7 minutes	

The extension time represented 1 minute per kilobase of pMLP-Aα plasmid length (6.2 kb). A two-step site directed mutagenesis was performed to generate the Ser3/345Asn double variant, whereby pMLP-Aα Ser3Asn cDNA was used as the template in a reaction with Ser345Asn primers. Upon completion of PCR, all reactions were stored overnight at 4°C and the parental (non-mutated) template was digested the following day with 10 U DpnI for 1 hour at 37°C in a PTC-200 thermal cycler. This restriction enzyme has specificity for methylated-DNA and is therefore unable to cleave plasmid cDNA which has been propagated *in vitro*. Reactions were returned to 4°C until transformation.

2.1.8.3. Transformation into *E. Coli*

XL-1 Blue supercompetent *E. Coli* cells (Stratagene) were transformed with the PCR-amplified pMLP-Aα expression vectors in accordance with the manufacturer's instructions. Plasmid DNA (1 µl) was added to 50µl cells and incubated on ice for 30 minutes. Cells were heat-shocked at 42°C for 45 seconds to facilitate uptake of DNA and incubated on ice for a further 2 minutes. Pre-warmed lysogeny broth (LB) (Appendix 1) (500 µl) was added to the cells and incubated for 1 hour at 37°C, 225 rpm before spreading the transformed cells (50-100 µl) onto pre-warmed LB agar (Appendix 1) containing ampicillin [100 µg/ml]. Plates were incubated inverted overnight at 37°C, checked for the appearance of single colonies the following day and stored at 4°C until plasmid purification.

2.1.8.4. Plasmid purification (Mini-prep)

A QIAprep Mini-prep Kit (QIAGEN, Netherlands) was used for purification of up to 20 µg high-copy plasmid DNA. Single bacterial colonies were picked from agar plates

using a 10 µl inoculation loop and used to inoculate starter cultures of 4.5 ml LB/ampicillin (100 µg/ml). These cultures were incubated overnight in an orbital shaker at 37°C, 300 rpm. Bacterial cells were harvested by centrifugation in a bench-top centrifuge at 13,000 rpm (Eppendorf MiniSpin Plus) for 2 minutes, resuspended in 250 µl Buffer P1 and lysed with SDS under alkaline conditions by mixing with 250 µl Buffer P2. Chromosomal DNA and proteins are denatured under the alkaline conditions used for bacterial cell lysis, while plasmid DNA remains stable for subsequent purification. After a maximum of 5 minutes, 350 µl neutralising Buffer N3 was mixed with the lysate, causing precipitation of the denatured protein and genomic DNA, cellular debris and SDS. Precipitate was removed by centrifugation for 10 minutes at 13,000 rpm and the resulting supernatant was applied to a QIAprep spin column. The sample was then centrifuged at 13,000 rpm for 1 minute to enable binding of plasmid DNA to the membrane. The column was washed with 750 µl Buffer PE and centrifuged again to remove residual buffer (13,000 rpm, 1 minute). Plasmid DNA was eluted from the column into a clean 1.5 ml microcentrifuge tube with 50 µl molecular grade H_2O and centrifuged at 13,000 rpm for 1 minute. The concentration of DNA within the eluate was analysed at A_{260}nm using a NanoDrop ND-1000 spectrophotometer, while qualitative assessment of the Mini-preps was carried out by agarose gel electrophoresis (method 2.1.8.7).

2.1.8.5. Plasmid purification (Maxi-prep)

A QIAprep Maxi-prep Kit (QIAGEN) was used for purification of up to 100 µg high-copy plasmid DNA. Starter cultures were prepared in the same way as for a Mini-prep (method 2.1.8.4) and incubated for 8 hours at 37°C, 300 rpm. A second culture with 100 ml LB/ampicillin [100 µg/ml] was inoculated with 200 µl starter culture and incubated at 37°C overnight, 300 rpm. The culture was centrifuged (Hettich Rotanta 460R) the next day for 30 minutes at 4,600 x g, 4°C to pellet the cells. Pelleted cells were resuspended in 10 ml Buffer P1 and lysed with 10 ml Buffer P2. Buffer P3 (10 ml) was added to precipitate debris and the lysate was filtered through a QIAfilter Maxi Cartridge. For removal of endotoxins, the filtered lysate was mixed with 2.5 ml Buffer ER and incubated on ice for 30 minutes. A QIAGEN-tip 500 was equilibrated with 10 ml Buffer QBT and the filtered lysate passed through the tip by gravity flow for binding of plasmid DNA to the resin. After washing with 2 x 30 ml Buffer QC, DNA was eluted with 15 ml Buffer QN and precipitated by addition of 10.5 ml room temperature isopropanol. The solution was centrifuged for 1 hour at 4,600 x g, 4°C to pellet the DNA. The supernatant was discarded and pelleted DNA was washed with 5 ml endotoxin-free, room temperature 70 % ethanol before a final centrifugation step for 1 hour at

4,600 x g, 4°C. The supernatant was again carefully decanted and the DNA pellet air-dried for 5 minutes before re-dissolving in 30 µl molecular grade H_2O. The DNA concentration at A_{260}nm was determined with a NanoDrop ND-1000 spectrophotometer and the Maxi-prep quality was analysed by agarose gel electrophoresis (method 2.1.8.7).

2.1.8.6. Restriction digestion of plasmid DNA

Restriction digestion was used to linearise plasmid DNA for analysis by agarose gel electrophoresis. Restriction enzymes recognise and cleave specific sequences of DNA; an online restriction mapping tool – Webcutter 2.0 – was used to identify enzymes which cleave at only one site within the pMLP vector sequences to enable linearisation without producing multiple fragments. Plasmid DNA (pMLP) (350 ng) was digested with 30 U EcoRI restriction enzyme in a 30 µl reaction mix containing 10X EcoRI buffer, BSA [100 µg/ml] and molecular grade H_2O for 16 hours at 37°C. Reagents were supplied by New England Biolabs.

2.1.8.7. Agarose gel electrophoresis

Linearised plasmids were electrophoresed to assess their quality. Agarose gels were prepared by mixing 1 % or 2 % (w/v) electrophoresis-grade agarose (Life Technologies), for large (>1000 bp) or small (<1000 bp) strands of DNA respectively, with 120 ml Tris-acetate EDTA (TAE) buffer (Appendix 1) by heating until molten and clear. After cooling to 50°C, 8 µl ethidium bromide (0.5 mg/ml) (Sigma-Aldrich) was added for fluorescent staining of nucleic acids and the agarose was immediately poured into a cast with a well comb and left for 30 minutes to set. Linearised plasmid DNA samples were mixed with 6X DNA loading buffer (Appendix 1) and loaded onto the gel. Hyperladder I (200-10,000 bp) or Hyperladder IV (100-1000 bp) (Bioline, UK) was used as a molecular weight marker. Samples were electrophoresed at 100 V for 90 minutes in TAE buffer and the DNA imaged under ultraviolet (UV)-transillumination using Chemi-imager software.

2.1.8.8. Sequencing of variant Aα chain cDNA open reading frames

The mutations introduced into the pMLP vectors did not introduce unique restriction sites; hence the success of mutagenesis could only be verified by DNA sequencing. Samples were sent to a DNA sequencing service (DNA Sequencing & Services, University of Dundee), which uses automated high-throughput sequencing with dye-labelled dideoxynucleotide triphosphates as chain terminators. Isolated plasmid DNA

from selected clones was reacted individually with four forward primers designed to bind regions spanning the entire fibrinogen Aα chain open reading frame. Primers were designed using GenScript DNA Sequencing Primers Design Tool and adapted to satisfy the criteria detailed by DNA Sequencing & Services. Primer sequences are listed in table 6. For analysis, sequencing data was compared to the original DNA sequences to highlight any errors. Nucleotide sequences for the original and mutated plasmids were then translated into protein sequence using ExPASy Translate Tool and aligned using a Basic Local Alignment Search Tool (BLAST) (National Center for Biotechnology Information, USA) to highlight and verify the desired mutations (Appendix 2).

Primer	Position (nt)	Sequence (5' to 3')	Length (nt)
Aα forward 1	1398	CTCTCGAGTGAATTGTCG	18
Aα forward 2	1936	AAATGTTAGGGCCCAGTTGGTTGA	24
Aα forward 3	2572	TGCTGGGCACTGGACCTCTG	20
Aα forward 4	3175	CCCTTCCCGTGGTAAATCTT	20

Table 6. Aα chain sequencing primers. Forward primers used for sequencing of the pMLP-Aα open reading frame are listed with their starting position in the pMLP vector (6262 bp; open reading frame: nucleotides 1466-3400), 5' to 3' sequences and nucleotide (nt) length.

2.1.9. Transfection of pMLP-Aα variants into CHO-Bβγ cells

Calcium phosphate ($CaPO_4$) precipitation was used for transfection of pMLP-Aα vectors into CHO cells; this technique relies upon complex formation between DNA and precipitated $CaPO_4$ to enable entry of DNA into the cells. Chinese hamster ovary cells previously transfected with pMLP-Bβ and pMLP-γ constructs by the same method were cultured in 100 mm dishes with 10 ml growth medium containing 400 µg/ml neomycin analogue G418 and incubated at 37°C, 5 % CO_2. Cells were split (1:10) 1 day ahead of transfection and medium was replaced with a fresh 10 ml G418 medium 2 hours ahead of transfection. For transfection, 10 µg pMLP-Aα DNA was combined with 10X less (1 µg) pMSVHis selection vector (provided by Prof Susan Lord, University of North Carolina at Chapel Hill), filter-sterilised cell culture-grade $CaCl_2$ [250 mM] and filter-sterilised dH_2O up to a final volume of 500 µl. The DNA/$CaCl_2$ mixture was combined with 500 µl 2X HEPES-buffered saline (HeBS) (Appendix 1); the HeBS solution was bubbled using a mechanical pipettor and the DNA/$CaCl_2$ mixture was simultaneously

added dropwise using a Pasteur pipette to encourage $CaPO_4$ precipitation. The transfection mix was vortexed for 15 seconds and incubated at room temperature for 30 minutes before adding 500 µl to each dish of cells. Dishes were incubated for 4 hours at 37°C, 5 % CO_2 and the cells were subjected to an osmotic shock for by addition of 2 ml per dish of 10 % (v/v) glycerol solution in G418 medium for 3 minutes to facilitate intracellular transport of DNA to the nucleus. The dishes were washed with 3 x 5 ml growth medium and incubated for 2 days in 10 ml G418 medium at 37°C, 5 % CO_2. At the end of this incubation period, transfected cells were trypsinised, re-plated at varying dilutions in growth medium (1:10, 1:20 and 1:40) and returned to 37°C, 5 % CO_2. The following day, 10 ml growth medium containing 400 µg/ml G418 and 250 µM L-histidinol dihydrochloride (Sigma-Aldrich) were added to each dish to achieve stable transfection. The medium was replaced every 2-3 days until the appearance of large, healthy and well-separated colonies. Approximately 24 colonies were selected by aspirating medium, sealing glass cloning cylinders over the colonies using sterile Vaseline, and adding a few drops of trypsin/EDTA solution to each cylinder for 5 minutes at room temperature. Cells were transferred to a 24-well plate with 0.5 ml L-histidinol/G418 selection medium per well and incubated overnight at 37°C, 5 % CO_2 to adhere. Fresh selection medium was added the next day and clones were cultured without medium change until 60-70% of the wells had reached confluence. At this point, medium from each clone was removed and screened for fibrinogen content by ELISA, according to section 2.1.2. Selected clones were then trypsinised and transferred to 60 mm dishes with 4 ml selection medium. Cells were cultured at 37°C, 5 % CO_2 until confluent and ready for further screening by ELISA or storage in liquid nitrogen (method 2.1.10). Due to problems with expression, clones were further analysed for the presence of intracellular fibrinogen using a variety of methods outlined in section 2.1.11.

2.1.10. Freezing cells for storage in liquid nitrogen

Confluent cells were trypsinised from plates using trypsin/EDTA solution and mixed with a 4X excess of growth medium before centrifuging at 1000 rpm for 15 minutes (Eppendorf Centrifuge 5702 R). Cell pellets were resuspended in 2 ml per dish of sterile freeze solution, containing 90 % (v/v) newborn calf serum (Fisher Scientific) with 10 % (v/v) cryoprotective dimethyl sulfoxide (DMSO) (Sigma-Aldrich), and divided into 1 ml aliquots in cryovials (Fisher Scientific). The cryovials were placed in an isopropanol chamber and stored at -80°C overnight for slow cooling (approximately -1°C/minute), before transferring to liquid nitrogen the next morning.

2.1.11. Analysis of intracellular CHO fibrinogen

Expression of variant fibrinogen Aα chain in transfected CHO cells was investigated by cell lysis, western blotting with cell lysate and conditioned medium, immunofluorescence, and end-point reverse transcription PCR (RT-PCR), as detailed below.

2.1.11.1. Lysis of CHO cells and harvest of conditioned medium for western blotting and ELISA

In order to investigate fibrinogen expression and secretion from CHO cells transfected with the variant Aα chain constructs, selected clones were cultured in 60 mm dishes and lysed using a non-denaturing Mammalian-Protein Extraction Reagent (M-PER) (Thermo Scientific). A 1 ml aliquot of medium was removed, mixed with protease inhibitor cocktail (1:100) (Sigma), and stored at -20°C until further analysis. The remaining medium was aspirated and cells were washed once with 1X PBS pH 7.4, containing $CaCl_2$ and magnesium chloride ($MgCl_2$) to minimise cell detachment (Appendix 1), before adding 250 µl M-PER pre-mixed with protease inhibitor cocktail (1:100). The plates were incubated on a shaker at room temperature for 5 minutes and cell lysate was collected into a centrifuge tube using a pipette. Lysates were centrifuged at 14,000 x g for 10 minutes in a bench top centrifuge (Eppendorf MiniSpin Plus) to pellet cell debris, while the supernatant was transferred to a clean tube and stored at -20°C. Lysates were concentrated 5X using centrifugal filters with a 30 kDa MWCO (Millipore). Both lysate and medium (30 µl) from each clone were loaded onto a 4-12 % Bis-Tris polyacrylamide gel for SDS-PAGE, followed by western blotting with a rabbit polyclonal anti-fibrinogen antibody and goat anti-rabbit HRP secondary antibody (methods 2.1.4 and 2.1.6; table 3). The western blot results revealed an additional band between the fibrinogen Aα and Bβ chain bands, which was investigated further by repeating the western blot without the primary antibody incubation step, probing only with goat anti-rabbit HRP and StrepTactin HRP before developing with SuperSignal West Pico Chemiluminescent Substrate. This confirmed it to be a non-specific band, rather than fibrinogen-related (refer to 3.1.3). In a repeat cell lysis experiment, harvested medium was also concentrated 5X so that sufficient fibrinogen was loaded onto the gel. The western blot was probed with a mouse monoclonal anti-fibrinogen Aα chain antibody followed by a rabbit anti-mouse HRP secondary antibody (table 3).

2.1.11.2. Immunofluorescent detection of fibrinogen Aα chain in CHO cells

For details of immunofluorescence methodology and assay development, refer to section 2.3.2. Briefly, CHO cells transfected with variant fibrinogen Aα chain constructs, as well as CHO-WT and CHO-Bβγ cells, were fixed onto a microscope slide, permeabilised and probed with a mouse monoclonal anti-fibrinogen Aα chain primary antibody (table 3), followed by a Cy3-AffiniPure donkey anti-mouse secondary antibody (1/500) (Stratech, UK). Slides were imaged by laser-scanning confocal microscopy (LSCM) (method 2.3.2.3), using the same settings for control and experiment wells to enable comparison of fluorescence intensity.

2.1.11.3. RNA extraction from CHO cells

Extraction of RNA from CHO cells cultured in 6-well plates or 60 mm dishes was carried out using an RNeasy plus mini kit (QIAGEN), complete with genomic DNA-eliminator spin columns, according to the accompanying instructions. Work was carried out in a DNA/RNA laboratory to minimise risk of contamination with RNases and filter pipette tips (Gilson, USA) were used throughout the procedure to avoid cross-contamination of samples. Cells were lysed directly by addition of 350 µl Buffer RLT; the lysate was collected using a cell lifter (Sigma-Aldrich) and homogenised by passing at least five times through a 20-gauge needle. Homogenised lysate was transferred to a genomic DNA-eliminator spin column in a 2 ml collection tube and centrifuged for 30 seconds at 10,000 rpm in a bench top centrifuge (Eppendorf MiniSpin Plus). The column was discarded and the flow through mixed with 1 ml 70 % ethanol for precipitation of RNA. The sample was transferred to an RNeasy spin column in a 2 ml collection tube and centrifuged for 15 seconds at 10,000 rpm to allow RNA to bind the column. Flow-through was discarded and the column was washed with 700µl Buffer RW1 by inverting the tube several times and centrifuging for 15 seconds, 10,000rpm. Two more wash steps were performed with 500 µl Buffer RPE for 15 seconds and 2 minutes at 10,000 rpm. The column was then placed in a clean collection tube and centrifuged for an additional minute to remove residual wash buffer. Finally, the spin column was again placed in a clean 1.5 ml microcentrifuge tube and 30 µl RNase-free H_2O was added directly to the membrane before centrifuging for 1 minute to elute the RNA. The RNA yield was determined by measuring A_{260} nm using a NanoDrop ND-1000 spectrophotometer and samples were stored at -20°C.

2.1.11.4. Reverse transcription-PCR with RNA from transfected CHO cells

Clones of CHO cells transfected with S3N and S345N Aα chain constructs were screened for expression of fibrinogen Aα by RT-PCR; CHO-WT and untransfected CHO cells were included as positive and negative controls respectively. The extracted RNA was reverse transcribed and amplified in a single reaction using a QIAGEN OneStep RT-PCR Kit, with primers specific to the Chinese hamster fibrinogen Aα chain nucleotide sequence (table 7). Forward and reverse primers were designed using Primer-BLAST (National Center for Biotechnology Information, USA) – an online tool for finding specific primers to a given sequence. Primers were designed to be 18-30 nucleotides in length with 40-60 % GC content and an annealing temperature 5°C below the T_m.

Optimal reaction conditions were achieved with 100 ng RNA template and 40 cycles of amplification. Reactions were set up to contain 10 µl 5X OneStep RT-PCR buffer, 2 µl dNTP mix (with each dNTP at a final concentration of 400 µM), 3 µl each of forward primer and reverse primers [0.6 µM], 2 µl OneStep RT-PCR enzyme mix and 28 µl RNase-free H_2O up to a final volume of 50 µl. Reactions were placed in a PTC-200 thermal cycler and subjected to the following cycling conditions:

1.	Reverse transcription		50°C	30 minutes
2.	PCR activation		95°C	15 minutes
3.	Amplification:			
		a. Denaturation	94°C	30 seconds
		b. Annealing	55°C	1 minute
		c. Extension	72°C	1 minute
4.	Final extension		72°C	10 minutes

x 40

Reactions were stored at 4°C overnight upon completion. Five microlitres of each reaction were mixed with 3 µl 6X loading dye and 10 µl molecular grade H_2O before loading on a 1 % agarose gel with 5 µl Hyperladder IV. Electrophoresis and imaging were carried out according to method 2.1.8.7.

Primer	Sequence (5' to 3')	Length (nt)	T_m (°C)	% GC
FGA Forward	TCTGGCTGCAGGATGAAAGG	20	60.03	55
FGA Reverse	CAATGTCCACCTCCAGTCGT	20	59.68	55

Table 7. Reverse transcription PCR primers for analysis of fibrinogen Aα chain expression in CHO cells. Forward and reverse primer sequences for amplification of fibrinogen Aα chain (FGA) cDNA are displayed with nucleotide (nt) length, T_m and GC content.

2.1.12. Optimisation of CHO cell transfection for fibrinogen expression

Due to difficulties across research groups with expression of fibrinogen Aα chain variants using the established method of CHO cell transfection, and taking into account the successful expression of Bβ and γ chain variants, the constructs for individual chains were transfected in a different order to investigate whether this would permit expression and secretion of fibrinogen. Whole vectors were sequenced to check for errors and each vector was linearised prior to transfection to improve integration efficiency. New CHO cells were purchased from ATCC (USA) and transfected first of all with pMLP-Bβ via the standard method as described in section 2.1.9. Clones were analysed for Bβ chain expression by real-time PCR and the best clone was co-transfected with pMLP-Aα and pMLP-γ for fibrinogen expression. An overview of this process is illustrated in figure 12.

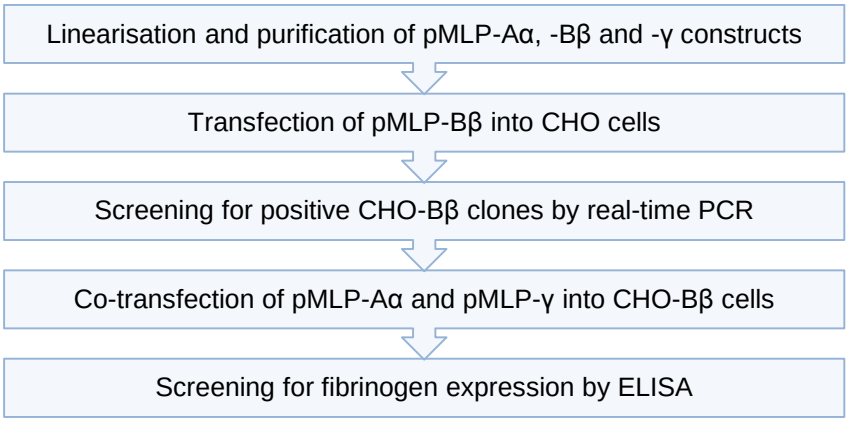

Figure 12. The process of pMLP-Aα and pMLP-γ co-transfection into CHO-Bβ cells for recombinant fibrinogen expression. Each of the pMLP constructs was linearised by restriction digestion prior to transfection. A CHO-Bβ cell line was formed by transfection of pMLP-Bβ into CHO cells and selection of the most productive clone using real-time PCR. The pMLP-Aα and pMLP-Bβ expression constructs were co-transfected for expression of fibrinogen, which was analysed by ELISA with medium harvested from each clone.

2.1.12.1. Testing CHO cells for resistance to selection reagents

All selection reagents were purchased from Source BioScience, UK. New CHO cells were incubated with potential selection reagents to check for resistance and to find the most effective and suitable reagents for selection of positive clones. Cells were passaged and seeded in 100 mm dishes to approximately 50 % confluence in normal growth medium. The medium was replaced the next day with selection medium containing G418 [400 µg/ml or 700 µ/ml], L-histidinol dihydrochloride [250 µM], hygromycin [125 µg/ml], puromycin [50 µg/ml] or zeocin [175 µg/ml] diluted in growth medium. After 2 days, cells were split 1:10 into the same selection medium and monitored for cell death over 1 week.

2.1.12.2. Sequencing of pMLP-Aα, -Bβ and -γ constructs

Whole pMLP-Aα WT, -Bβ and -γ constructs were sequenced by DNA Sequencing & Services, University of Dundee (see method 2.1.8.8). Forward and reverse sequencing primers designed using GenScript DNA Sequencing Primers Design Tool are listed in table 8. Sequencing data was compared to original DNA sequences to screen for errors.

Primer	Sequence (5' to 3')	Length (nt)
Forward -1	CGGGACTATGGTTGCTGAC	19
Forward 0	CAGTACTCTTGGATCGGAAACC	22
Forward 1	CTCTCGAGTGAATTGTCG	18
Forward 8	CATGTCTGGATCCTCTACGC	20
Forward 9	CAAACGTTTCGGCGAGAAG	19
Forward 10	GCCTTATCCGGTAACTATCGTC	22
Forward 11	CTCAGCGATCTGTCTATTTCG	21
Forward 12	GACTGGTGAGTACTCAACCAAGTC	24
Forward 13	GATGTTGCAAGTGTGGCG	18
Reverse 1	CCTCTACAAATGTGGTATGGCTG	23
Reverse 2	GACTCCTGCATTAGGAAGCAG	21

Table 8. pMLP sequencing primers. Forward and reverse primers used for sequencing of entire pMLP vectors are listed with their 5' to 3' sequences and nucleotide (nt) length.

2.1.12.3. Linearisation of pMLP vectors

To increase efficiency of viable plasmid DNA integration into the host genome, the pMLP-Aα WT, pMLP-Bβ and pMLP-γ vectors were linearised at a restriction site located within the Ampicillin resistance gene to ensure that recombination occurred outside of the Aα, Bβ and γ chain open reading frames. Restriction digestion reagents were supplied by New England Biolabs. Plasmid DNA (30 µg) was digested with 50 U PvuI restriction enzyme in a 35 µl reaction mix containing 10X Buffer 3, 100X BSA and ultrapure H_2O for 3 hours at 37°C.

2.1.12.4. Agarose gel electrophoresis and gel extraction

Linearised pMLP vectors were separated on a 1 % agarose gel using the method outlined in section 2.1.8.7. Relevant bands were excised from the gel and DNA was extracted using a QIAquick Gel Extraction Kit (QIAGEN), as per the manufacturer's instructions. In brief, agarose bands were dissolved in a supplied buffer (Buffer QG) with an equal volume of isopropanol, and each applied to a spin column that binds the DNA. The bound DNA was washed with Buffer PE. Additional wash steps were included to remove contaminants and promote purity of DNA samples. The DNA was eluted from the columns in 30 µl ultrapure H_2O and the concentration determined using a NanoDrop ND-1000 spectrophotometer at A_{260} nm.

2.1.12.5. Transfection of pMLP-Bβ into CHO cells

Linearised pMLP-Bβ (10 µg) was transfected into new, untransfected CHO cells using protocol 2.1.9. A pSELECT-neo selection vector (Source BioScience) (1µg) was co-transfected to confer resistance to G418. On day 3, transfected cells were split into varying dilutions and re-plated straight into 10 ml selection medium containing G418 [700 µg/ml]. Selection pressure was applied until the appearance of large healthy colonies, which were selected and transferred to 2 x 60 mm dishes per clone in selection medium. As individual fibrinogen chains are not secreted, expression of the Bβ chain in 12 selected clones was compared by reverse transcription of cellular RNA and real-time PCR.

2.1.12.6. Reverse transcription of CHO-Bβ RNA

Ribonucleic acid was extracted from CHO-Bβ clones according to method 2.1.11.3 and was reverse transcribed using an Applied Biosystems High Capacity cDNA Reverse Transcription Kit (Life Technologies). Template RNA was diluted to 200 ng/µl in RNase-free H_2O and reactions were set up with 2 µl 10X buffer, 0.8 µl 25X dNTP mix,

2 µl 10X RT primers (random), 10 µl template RNA [100 ng/µl], 1 µl MultiScribe reverse transcriptase and 4.2 µl RNase-free H_2O up to a 20 µl total volume. Reactions were held at 25°C for 10 minutes, 37°C for 120 minutes and 85°C for 5 minutes in a PTC-200 thermal cycler before proceeding to real-time PCR.

2.1.12.7. Real-time PCR with CHO-Bβ cDNA

Reverse transcribed cDNA was amplified by quantitative real-time PCR using SYBR Green I. This dye binds to any double stranded DNA, resulting in emission of a fluorescence signal which follows a sigmoidal trend during the reaction. The point at which the fluorescence of a given reaction exceeds a cycle threshold value (Ct) reflects the relative amount of cDNA template. This Ct value can be used to calculate fold-differences in expression after normalisation to the Ct value of an internal control – an endogenous housekeeping gene – and a reference sample.

Primers were designed to amplify the following templates reverse transcribed from Chinese hamster RNA i) fibrinogen Bβ chain cDNA and ii) glyceraldehyde 3-phosphate dehydrogenase (GAPDH) cDNA, to be used as an internal control (method 2.1.11.4; table 9). Reverse transcription reactions were diluted 1:10 in RNase-free H_2O before preparing PCR reactions, each with 10 µl Light Cycler 480 SYBR Green I Master Mix (Roche, Switzerland), 1 µl each of forward and reverse primers [0.2 µM], 2 µl pre-diluted cDNA template and 6 µl RNase-free H_2O to a 20 µl total volume. Each template was analysed with triplicate reactions. A Light Cycler 480 Instrument (Roche) was used for thermal cycling and quantification of SYBR green fluorescence over 40 cycles with the conditions detailed below:

1.	Activation	95°C	5 minutes	
2.	Amplification			
	a. Denaturation	95°C	10 seconds	x 40
	b. Annealing	55°C	20 seconds	
	c. Extension	72°C	30 seconds	

A melting curve was included at the end of each PCR experiment to distinguish between specific amplification products and any non-specific products such as primer dimers. Reactions were held at 95°C for 30 seconds and 45°C for 1 minute before increasing the temperature up to 97°C at a rate of 0.11°C per second, with 5 fluorescence data acquisitions for every +1°C. Finally, samples were cooled to 40°C for 10 seconds.

Light Cycler 480 Software (Version 1.5) (Roche) was used for calculation of Ct values and melting curve analysis. Real-time PCR data for fibrinogen β chain expression was analysed using the ΔCt method, whereby ΔCt is the experiment Ct value normalised to that of the endogenous housekeeping gene, GAPDH ($Ct_{experiment}$ - $Ct_{control}$ = ΔCt). The relative expression level in each clone was compared using a $2^{-\Delta Ct}$ calculation.

Primer	Sequence (5' to 3')	Length (nt)	T_m (°C)	% GC
FGB Forward	AGGAGGGTTTCTTCAGTGCC	20	59.60	55
FGB Reverse	GCTTCTGCCTCTTTTGCCAC	20	60.04	55
GAPDH Forward	GCTTCTGCCTCTTTTGCCAC	20	59.96	55
GAPDH Reverse	GCTTCTGCCTCTTTTGCCAC	20	60.03	60

Table 9. Real-time PCR primers for analysis of fibrinogen Bβ chain expression in CHO cells. Forward and reverse primer sequences for amplification of fibrinogen Bβ chain (FGB) and GAPDH cDNA are displayed with nucleotide (nt) length, T_m and GC content.

2.1.12.8. Co-transfection of pMLP-Aα and pMLP-γ into CHO-Bβ cells

Linearised pMLP-Aα WT and pMLP-γ vectors (10 µg each) were co-transfected into the selected CHO-Bβ cell line, along with pSELECT-zeo-mcs selection vector (Source BioScience) (2 µg) for resistance of transfected cells to antibiotic zeocin. Refer to section 2.1.9 for details of the transfection method. After splitting and diluting cells (day 3), they were re-plated into selection medium containing G418 [700 µg/ml] and zeocin [200 µg/ml]. As no colonies survived selection, the concentration of zeocin was optimised as described below. The transfection was then repeated using the optimal zeocin concentration.

2.1.12.9. Transfection of pSELECT-zeo-mcs into CHO cells and optimisation of zeocin concentration for selection

Selection vector pSELECT-zeo-mcs was transfected (1 µg) into CHO cells using the $CaPO_4$ precipitation method (method 2.1.9), with the aim of optimising zeocin concentration in selection medium for effective selection pressure. Two days post-transfection, cells were trypsinised, diluted 1:20 and 1:40 and re-plated in selection medium containing three different concentrations of zeocin: 50 µg/ml, 100 µg/ml and

150 µg/ml. Medium was replaced with fresh selection medium every 2-3 days until colony formation.

2.1.13. Recombinant fibrinogen expression in Expi293F cells

Due to difficulties with expression of fibrinogen variants in CHO cells, an alternative Expi293^{TM} expression system (Life Technologies) was employed for expression of recombinant fibrinogen. This system involves transient transfection of non-adherent Expi293F cells, which have been isolated from a human embryonic kidney (HEK) 293 cell line by selecting for cells with a higher protein productivity. These cells can also be seeded at high density for maximal transfection efficiency and protein expression. The expression system includes optimised lipid-based transfection reagent ExpiFectamine and transfection enhancers, as well as Expi293 expression medium to support high density suspension cultures with serum-free conditions. All reagents were purchased from Life Technologies unless otherwise stated.

2.1.13.1. Counting cells with a haemocytometer

Cultured cells were counted using a haemocytometer chamber and trypan blue dye. First, the apparatus was cleaned with 70 % ethanol and the coverslip was moistened with water to affix to the haemocytometer. Trypan blue is a “vital stain”, which is excluded from healthy cells and selectively taken up by dead cells. After thorough mixing, an aliquot of cells was removed from a cell suspension and diluted with trypan blue. Ten microliters of this mixture were pipetted into either side of the haemocytometer, in between the coverslip and chamber. The haemocytometer was viewed under a CKX41 inverted optical microscope (OLYMPUS, Japan) with a 10X objective lens. Cells inside both central grids, including boundaries, were counted using a hand tally counter and averaged. The haemocytometer is designed such that, when the coverslip is in place, each grid has a volume of 1 mm^3 (0.1 µl). Hence, the number of cells in the starting culture was calculated using the equation below, where d = dilution factor, c = average number of cells within the grid, and v = the original volume of suspension or culture containing the cells (ml):

$$\text{Total number of cells} = dcv \times 10^4$$

2.1.13.2. Transient transfection of pMLP-Aα, -Bβ and –γ vectors into Expi293F cells

For transfection of pMLP-Aα, -Bβ and –γ constructs, viable cells were counted using a haemocytometer chamber and the trypan blue (Sigma-Aldrich) dye exclusion method

as detailed above. Cells were seeded at a density of 2.0 x 10^6 viable cells/ml culture in Expi293 expression medium and cultured in suspension in a 125 ml spinner flask at 37°C, 8 % CO_2 with gentle stirring. Cell density and viability were monitored again the following day to ensure the cells were in excess of 3.0 x 10^6 cells/ml with greater than 95 % overall viability in order to proceed with transfection. For a 30 ml transfection culture, a volume of culture containing 7.5 x 10^7 cells was added to a new flask and made up to 25.5 ml with Expi293 expression medium. Each plasmid DNA (10 µg) was diluted in OptiMEM I reduced serum medium (Life Technologies) to a final volume of 1.5 ml. Eighty microliters of ExpiFectamine293 transfection reagent were also diluted in OptiMEM I medium to a final volume of 1.5 ml and both mixes were incubated at room temperature for 5 minutes. The diluted DNA and ExpiFectamine293 were combined, mixed gently and incubated at room temperature for 30 minutes to allow DNA-ExpiFectamine293 complex formation; the mixture (3ml) was then added to the flask containing Expi293F cells for transfection. Cells were incubated on a stirrer at 37°C, 8 % CO_2 for approximately 16-18 hours. Following incubation, 150 µl ExpiFectamine293 Transfection Enhancer 1 and 1.5 ml ExpiFectamine293 Transfection Enhancer 2 were added to the flask, giving a final volume of 30 ml. The transfected culture was then incubated on a stirrer at 37°C, 8 % CO_2 for 7 days and an aliquot of cell suspension was removed on days 3, 5 and 7 for analysis of protein expression. Harvested aliquots were centrifuged at 14,000 x g for 10 minutes in a bench top centrifuge (Eppendorf MiniSpin Plus) to pellet cells; medium supernatant was transferred to a clean 1.5 ml tube, mixed with protease inhibitor cocktail (Sigma-Aldrich) (1:500) and stored at -20°C.

On day 7, the remaining 27 ml cell suspension was harvested by centrifugation at 400 x g for 10 minutes, 4°C (Eppendorf Centrifuge 5702 R). Medium supernatant was transferred to a separate tube and pelleted cells were resuspended in 10 ml Dulbecco's PBS (Life Technologies), re-pelleted at 400 x g for 10 minutes at 4°C, snap-frozen on liquid nitrogen and stored at -80°C. Protease inhibitor cocktail (1:500), phosphatase inhibitor cocktail 2 (Sigma-Aldrich) (1:1000) and phosphatase inhibitor cocktail 3 (Sigma-Aldrich) (1:1000) were added to the medium to prevent proteolytic degradation and loss of phosphate from fibrinogen. The medium was then centrifuged at 4,600 x g for 15 minutes, 4°C (Hettich Rotanta 460R) and the supernatant filtered through a 0.22 µm bottle top filter. Filtered medium was snap-frozen on liquid nitrogen and stored at -80°C.

2.1.13.3. Analysis of harvested Expi293 medium

Aliquots of medium removed on days 3, 5 and 7 were first of all analysed for fibrinogen content by ELISA according to method 2.1.2. Medium was diluted 1/10, 1/50, 1/100, 1/200 and 1/400, and added to a 96-well microtiter plate in duplicate. A Calbiochem® fibrinogen standard curve ranging from 0-1 µg/ml was used to determine the concentration of fibrinogen in each sample. The integrity of secreted fibrinogen in medium samples was verified by reducing SDS-PAGE and western blotting with a polyclonal anti-fibrinogen antibody (methods 2.1.4 and 2.1.6). Prior to SDS-PAGE, the medium was concentrated 4X using an Amicon Ultra-0.5 Centrifugal Filter Unit (Millipore) with a 100 kDa MWCO; the membrane was washed twice with 500 µl 20 mM Hepes by centrifugation at 14,000 x g in a bench top centrifuge (Eppendorf MiniSpin Plus) before concentrating 400 µl of media to 100 µl in the same way.

2.1.13.4. Cloning of fibrinogen Aα, Bβ and γ chain cDNA into pmaxCloning

Expression of recombinant fibrinogen in Expi293F cells was successful, but the yield of fibrinogen was still low. In attempt to enhance expression levels, the Aα, Bβ and γ chain open reading frames from the pMLP vectors were cloned into a new vector – pmaxCloning (pmC) (figure 13) – kindly provided by Dr Paul Cordell, University of Leeds. The pmC vector contains a cytomegalovirus (CMV) promoter which enables high protein expression and is optimal for the Expi293 expression system. The cloning process involved i) introducing restriction sites into PCR-amplified fragments containing the Aα, Bβ and γ chain open reading frames, ii) restriction digestion of purified PCR fragments and pmC, iii) ligation of PCR fragments with the pmC vector and iv) amplification of ligated pmC-Aα, -Bβ and –γ vectors in *E. Coli* and isolation using a QIAprep Maxi-prep Kit for transfection.

A

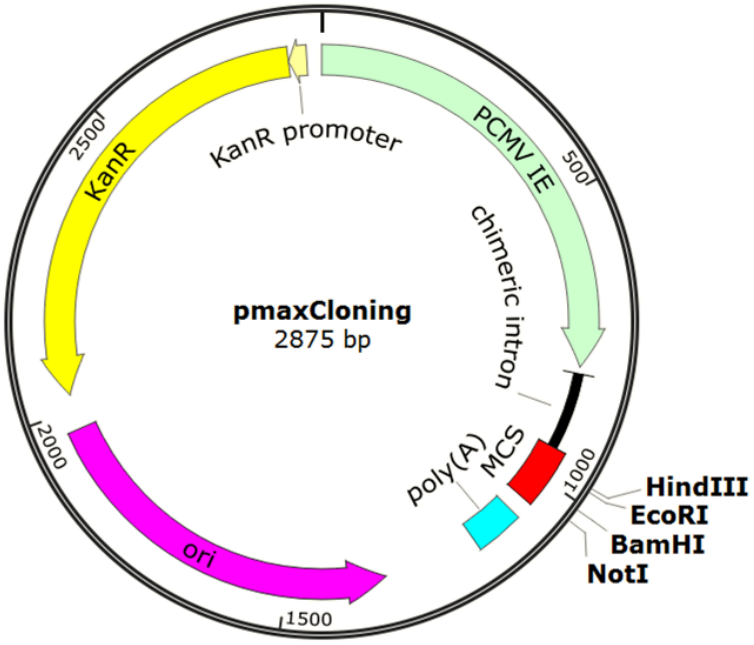

B

Hind III Eco RI

GGTACCGCCATCATGAAGTTTAAACAAGCTTGAATTCTCTAGAGATATCCTG

Bam HI Not I

CAGAGATCTGGATCCCTCGAGGCTAGCGCGGCCGCGTTTAAACAGAGCTC

Figure 13. pmaxCloning. A) Vector map. The pmaxCloning vector contains the immediate early promoter of cytomegalovirus (PCMV IE) for high protein expression, a chimeric intron which enhances gene expression, a multiple cloning site (MCS) and an SV40 late mRNA polyadenylation (poly(A)) signal. In the opposite orientation, the vector contains an origin of replication, as well as a kanamycin resistance (KanR) gene and its promoter for bacterial cloning. Restriction sites within the MCS used for insertion of fibrinogen Aα, Bβ and γ cDNA (HindIII, EcoRI, BamHI, NotI) are indicated on the map. B) Multiple cloning site. The 102 bp MCS sequence is shown with sequence recognition motifs for restriction enzymes used to insert fibrinogen Aα, Bβ and γ cDNA highlighted in red and specific cleavage sites indicated by arrows (▲).

2.1.13.4.1. Polymerase chain reaction: introducing restriction sites

Due to incompatibility between restriction sites in the pMLP vectors and the multiple cloning site of pmaxCloning, new restriction sites were introduced either side of Aα, Bβ and γ chain cDNA fragments; fragments containing the desired restriction sites were amplified from pMLP by PCR using the primers listed in table 10. Forward and reverse

primers were designed to be complementary to regions either side of the start and stop codons respectively, with a short sequence outside of the open reading frame substituted with the chosen restriction site. Criteria for selection of appropriate restriction sites included confirmation by restriction mapping that sites were unique within the whole vector, as well as maximal compatibility with the original sequence to promote primer annealing. Primers were between 30 and 40 bp long with a GC content of 40-60 % and a T_m close to 70°C; the annealing temperature during PCR was set to 5°C below the T_m of the primers. Custom primers were purchased from Life Technologies.

Polymerase chain reaction was carried out using an Expand High Fidelity PCR System (Roche, UK). Primers were diluted to 10 µM and pMLP-Aα (WT, S3N and S345N), pMLP-Bβ and pMLP-γ vectors were diluted to 100 ng/µl, all in molecular grade H_2O. Each reaction consisted of 1 µl template DNA (100 ng), 5 µl 10X buffer with $MgCl_2$, 1 µl dNTP mix [200 µM], 1.5 µl each of forward and reverse primers [0.3 µM], 1 µl enzyme mix and 39.2 µl molecular grade H_2O up to a final volume of 50 µl. Reactions were prepared and mixed in PCR tubes and subjected to the following thermal cycling conditions in a PTC-200 thermal cycler:

1.	Initial denaturation	94°C	2 minutes	
2.	Denaturation	94°	15 seconds	x 10
3.	Annealing	64°C (Aα and γ) or 67°C (Bβ)	30 seconds	
4.	Elongation	72°C	2 minutes	
5.	Denaturation	94°C	15 seconds	x 20
6.	Annealing	64°C (Aα and γ) or 67°C (Bβ)	30 seconds	
7.	Elongation	72°C	2 minutes + 5 seconds/cycle	
8.	Final elongation	72°C	7 minutes	

Primer	Sequence (5' to 3')	Length (nt)	T_m (°C)
Aα forward + HindIII	CCAGCCCC**A/AGCTT**AGAAAAG**ATG**TTTTCCATGAGG	36	70.1
Aα reverse + NotI	GAATT**GCGGCC/GC**CCATTTAACTTAGT**CTA**GGG	33	70.2
Bβ forward + EcoRI	TGCGCCGCTCTCGAGT**G/AATTC**TCGAC**ATG**AAAAGA	36	73.1
Bβ reverse + NotI	AATT**GCGGCC/GC**CCGTATTGGGGA**CTA**TTG	30	72.2
γ forward + EcoRI	CCCGG**G/AATTC**AGACATC**ATG**AGTTGGTCCTTG	33	69.8
γ reverse + BamHI	CTCTTT**GGATC/C**GGTCTT**TTA**AACGTCTCCAGC	33	68.6

Table 10. PCR primers used to introduce restriction sites either side of fibrinogen Aa, Bβ and γ cDNA fragments. 5' to 3' primer sequences are displayed with restriction sites highlighted in red and start/stop codons underlined, as well as nucleotide (nt) length and T_m of each primer.

2.1.13.4.2. Polymerase chain reaction product purification

On completion of PCR reactions, PCR products were purified using a QIAquick PCR Purification Kit (QIAGEN), following the manufacturer's instructions. In brief, five volumes of Buffer PB (250 µl) were mixed with one volume of PCR sample (50 µl), added to a QIAquick spin column and centrifuged at 14,000 x g for 1 minute in a bench top centrifuge (Eppendorf MiniSpin Plus) for binding of the DNA to the membrane. The flow-through was discarded and the QIAquick column was washed with 3 x 750 µl Buffer PE by centrifugation at 14,000 x g for 1 minute each time. After discarding flow-through, the column was centrifuged for an additional 1 minute to remove residual buffer and placed in a clean 1.5 ml tube. To elute DNA, 30 µl molecular grade H_2O was added directly to the membrane and left to stand for 1 minute before a final centrifugation step at 14,000 x g for 1 minute. The concentration of purified DNA was determined at A_{260} nm using a NanoDrop ND-1000 spectrophotometer and samples were stored at -20°C until restriction digestion.

2.1.13.4.3. Double digestion of PCR products and pmaxCloning

The PCR-amplified Aα, Bβ and γ chain cDNA fragments were double digested with the relevant restriction enzymes: Aα chain fragments with HindIII and NotI (high fidelity), the Bβ chain fragment with EcoRI and NotI (high fidelity), and the γ chain fragment with EcoRI and BamHI. The pmaxCloning vector was also digested with each pair of restriction enzymes to enable sticky-end ligation of fragments into vector. Restriction digestion reagents were supplied by New England Biolabs. For both fragment and pmaxCloning digestion, 4 µg DNA was mixed with 30 U of each required enzyme, 10X buffer 2 or buffer 4 (determined using the online Double Digest Finder tool by New England Biolabs), BSA [100 µg/ml] and molecular grade dH_2O up to a final volume of 30 µl. Reactions were incubated at 37°C for 3 hours. Digested DNA products were purified from the reaction mix by agarose gel electrophoresis and gel extraction (method 2.1.12.4). The DNA yield was determined at A_{260} nm using a NanoDrop ND-1000 spectrophotometer.

2.1.13.4.4. Ligation of Aα, Bβ and γ cDNA fragments with pmaxCloning

Ligation was performed using a 1:3 ratio of vector to insert, with 100 ng total DNA per reaction. Fragments and vectors were diluted to a concentration 25 ng/µl and, for each reaction, 1 µl vector was mixed with 3 µl fragment DNA, 10X DNA ligase buffer (Promega, USA), 1 U T4 DNA ligase (Promega) and molecular grade dH_2O up to a final volume of 20 µl. Reactions were incubated at 4°C for 16 hours before transformation into XL-1 blue cells (1 µl in 50 µl cells) the following day (method 2.1.8.3). Plasmids were purified from selected colonies using a QIAprep Maxi-Prep kit (method 2.1.8.5) and quantified by measuring absorbance at A_{260} nm with a NanoDrop ND-1000 spectrophotometer. Plasmid size and integrity were verified by restriction digestion with EcoRI (method 2.1.8.6) and agarose gel electrophoresis with Hyperladder I (200-10,000bp; Bioline) (method 2.1.8.7). Annotated vector maps of the new fibrinogen Aα, Bβ and γ chain expression constructs – named pmC-Aα WT or S345N, pmC-Bβ and pmC-γ – are displayed in figure 14.

2.1.13.4.5. Transient transfection of pmC-Aα, -Bβ and –γ vectors into CHO cells

To test the viability of the new pmC constructs prior to transfection into Expi293F cells, each vector was transiently transfected into CHO cells by $CaPO_4$ precipitation (method 2.1.9) and the cells were assayed for fibrinogen Aα, Bβ or γ chain expression by lysis and western blotting (methods 2.1.11.1 and 2.1.6 respectively). For each vector, 10 µg

plasmid DNA was transfected individually, in the absence of selection vector, into untransfected CHO cells, subjected to osmotic shock and assayed 48 hours post-transfection. Cells lysate (20 µl) was mixed with 10X reducing agent, 4X LDS sample buffer and dH_2O in a 40 µl total volume and subjected to SDS-PAGE and western blotting. Blots were probed for fibrinogen using a polyclonal anti-rabbit primary antibody and goat anti-rabbit HRP secondary antibody (table 3).

2.1.13.4.6. Transient transfection of pmC-Aα, -Bβ and –γ vectors into Expi293F cells

Following confirmation of successful expression of individual fibrinogen chains in CHO cells using the pmC-Aα, Bβ and γ vectors, transfection of Expi293F cells with the WT vectors was carried out, as well as with pmC-Aα S345N, -Bβ and -γ for expression of the Ser345 variant (method 2.1.13.2). Secreted fibrinogen was analysed according to method 2.1.13.3; briefly, the fibrinogen was visualised by SDS-PAGE and western blotting, while the concentration in medium harvested on day 7 was determined by ELISA to establish whether there is increased fibrinogen expression using the pmC vectors compared to the pMLP vectors.

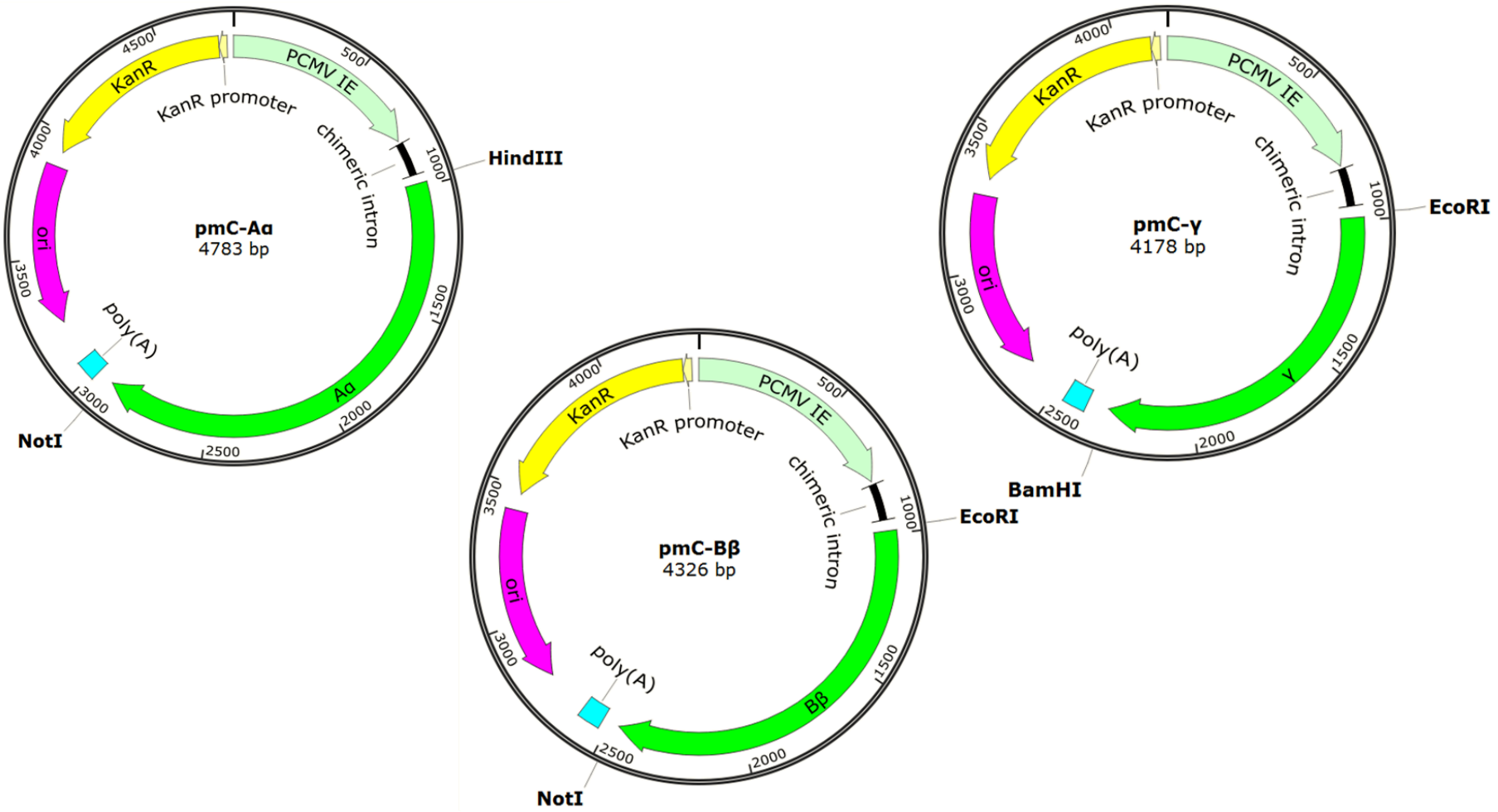

Figure 14. pmC-Aα, -Bβ and -γ vector maps. The vector maps show the pmaxCloning (pmC) vector with fibrinogen Aα, Bβ or γ chain cDNA inserts in the multiple cloning site. Strong, constitutive expression of these polypeptide chains is driven by the upstream cytomegalovirus promoter (PCMV IE). The restriction sites used to insert the cDNA fragments (HindIII, NotI, EcoRI and BamHI) are indicated on each map.

2.2. Functional studies with fibrinogen phosphorylation isoforms

As an alternative approach to expression of variant fibrinogen, the naturally occurring 20-25 % degree of fibrinogen phosphorylation in plasma was exploited, using chromatography to enrich the phosphorylated fraction. Fibrinogen phosphorylation isoforms were then compared in several functional assays to determine the effect of phosphorylation on FXIII cross-linking activity, plasmin digestion, α2-antiplasmin incorporation and fibrin clot structure.

2.2.1. Preparation of fibrinogen phosphorylation isoforms

2.2.1.1. Purification of commercial fibrinogen

Calbiochem® human fibrinogen from plasminogen-depleted plasma was purified by ammonium sulphate precipitation (AP-fibrinogen) (Smith et al., 2011); this was kindly provided by Dr Kerrie Smith, University of Leeds for use in chromatography and functional experiments. Calbiochem® fibrinogen was also purified by IF-1 affinity chromatography using an ÄKTA avant 25 system (GE Healthcare), and dialysed against TBS-1 pH 7.4, following the same process as that used for purification of recombinant fibrinogen (section 2.1.3). Coming from the same source, both of these fibrinogen samples were confirmed to have a 25 % degree of phosphorylation, using the malachite green assay as described below.

2.2.1.2. Malachite green assay

A malachite green assay was used to determine the degree of fibrinogen phosphorylation in purified samples of fibrinogen. Phosphate standards were prepared by diluting appropriate volumes of a stock solution of potassium dihydrogen phosphate (KH_2PO_4) in TBS-1 pH 7.4 to a 300 µl volume, giving a final concentration range of 0-5 µM KH_2PO_4 (0-1000 pmol phosphate). An equivalent volume of fibrinogen sample at 3 µM was also prepared. For alkaline hydrolysis of protein-bound phosphate, 40 µl of 8 M sodium hydroxide were added to each standard and fibrinogen sample before heating to 95˚C for 15 minutes. Samples were cooled and centrifuged (Eppendorf MiniSpin Plus), mixed with 120 µl 5 M hydrochloric acid and incubated on ice to encourage precipitation of proteins. Precipitate was removed by centrifugation at 20,000 x g, 4˚C for 15 minutes in a bench-top centrifuge (Jouan MR1822). Each standard and fibrinogen sample was added to a 96-well microtiter plate in duplicate, with 200 µl per well. Finally, 100 µl Malachite Green Solution A (Millipore) was added to

each well and the absorbance measured at 630 nm after 10, 20 and 30 minutes using an EL_x808 Absorbance Microplate Reader. Ammonium molybdate in Malachite Green Solution A reacts with free inorganic phosphate (P_i) under acidic conditions (H^+), yielding an intermediate which reacts with malachite green and causes a colour change from yellow to green:

1. $P_i + (NH_4)_2MoO_4 \xrightarrow{H^+} H_3PMo_{12}O_{40}$
   Ammonium molybdate

2. $H_3PMo_{12}O_{40} + HMG^{2+} \xrightarrow{H^+} (MG^+)(H_2PMo_{12}O_{40}) + 2H^+$
   Malachite Green (Yellow, λmax 446nm) (Green, λmax 640nm)

2.2.1.3. Anion exchange chromatography

Anion exchange chromatography was employed for the separation of phosphorylated and non-phosphorylated fibrinogen molecules using AP-fibrinogen. Anion exchange was the method of choice because, with a pI of approximately 5.6, fibrinogen has a net negative charge at physiological pH. Figure 15 illustrates the relationship between pH and the net charge of a protein at pH values exceeding the pI. Protein phosphorylation causes a shift to a more acidic pI due to alteration of the net charge by the negatively charged phosphate groups. By this principle, phosphorylated proteins bind a positively charged matrix with higher affinity than their non-phosphorylated counterparts and will therefore elute later upon application of a buffer gradient with increasing ionic strength.

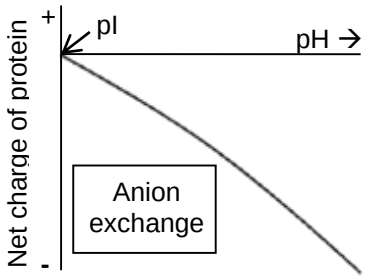

Figure 15. The relationship between pH and net charge of a protein. At pH values above the isoelectric point (pI), proteins have a net negative charge and can therefore be manipulated by anion exchange chromatography.

Separation of phosphorylated and non-phosphorylated fibrinogen was performed using an ÄKTA prime chromatography system with three connected 1 ml HiTrap Diethylaminoethanol (DEAE) Sepharose Fast Flow columns (GE Healthcare). For the first run, the columns were equilibrated with 10 ml 20 mM Tris-hydrochloride (HCl) pH 8.0 before injection of 1 ml AP-fibrinogen diluted to 2 mg/ml in equilibration buffer. A flow rate of 1 ml/min was used throughout. After sample addition, 0.5 ml fractions were collected for the remainder of the method. A further 10 ml equilibration buffer was passed through the column before applying a concentration gradient of 1 M sodium chloride (NaCl), increasing from 0-100 % over a 20 ml volume, diluted with equilibration buffer. Finally, the column was washed with 30 ml equilibration buffer. Fractions corresponding to elution peaks were pooled, concentrated using Vivaspin 20 concentrators (100 kDa MWCO) and analysed for the presence of fibrinogen by SDS-PAGE (method 2.1.4).

Various parameters were optimised from the initial method to promote separation and resolution. Initially, the pH of the equilibration buffer was lowered to pH 6.8, closer to the pI of fibrinogen. Gradient time was increased from 20 ml (6.7 CV) to 90 ml (30 CV), and then further to 180 ml (60 CV), while binding flow rate was decreased to 0.2 ml/min, collecting 2 ml fractions. Fibrinogen from each peak was pooled separately and dialysed overnight against TBS-1 pH 7.4 using dialysis tubing (10 mm) with a 12 kDa MWCO (Sigma-Aldrich) (method 2.1.3.3). The malachite green assay (method 2.2.1.2) was used to measure the degree of phosphorylation of fibrinogen from each peak. Despite optimisation, there was still insufficient separation of phosphorylated and non-phosphorylated fibrinogen using this method; therefore, alternative approaches were sourced and tested.

2.2.1.4. Phos-tag™ affinity chromatography

As an alternative method for the chromatographic separation of phosphorylated fibrinogen from non-phosphorylated fibrinogen, Phos-tag™ Agarose (400 µl) (figure 18; section 2.3.4) was purchased from Alpha Laboratories, UK and packed into an empty Tricorn 5/50 High Performance Column (GE Healthcare) with two adaptors, giving a final bed volume of 0.353 µl. Refer to section 2.3.4 for information on Phos-tag™. Chromatography was performed using an ÄKTA avant 25 system (GE Healthcare), following a protocol described by Kinoshita et al. (2005), which was adapted to encourage binding of phosphorylated fibrinogen to the Phos-tag™ Agarose. Alterations to the method included reduction of binding flow rate from 0.25 ml/min to 0.1 ml/min and alteration of the elution buffer composition; phosphorylated fibrinogen was eluted with 50 mM EDTA rather than NaH_2PO_4, as trace amounts remaining after dialysis

interfered with the highly sensitive malachite green assay. See Appendix 1 for buffer compositions. The amount of fibrinogen loaded per run was also optimised to give sufficient yield of phosphorylated fibrinogen after elution.

The final optimised method was as follows. Firstly, the storage buffer was removed with 15 CV of wash buffer at a flow rate of 0.5 ml/min. The column was then equilibrated with 30 CV of equilibration buffer, followed by 2 CV of binding buffer, both at 0.5 ml/min. Fibrinogen (4 mg) was diluted in binding buffer to a 2.5 ml volume and was loaded at a flow rate of 0.1 ml/min, collecting 0.5 ml fractions. Phosphorylated fibrinogen was eluted by applying a gradient from 0-100 % elution buffer diluted with filtered dH_2O over 20 CV at 0.25 ml/min, again collecting 0.5ml fractions. Finally, a second wash step was performed with 5 CV wash buffer at 0.5 ml/min, followed by 5 CV storage buffer at 0.5 ml/min. The fibrinogen concentration in each fraction was measured at A_{280} nm using the ÄKTA avant with Unicorn 6 control software and a NanoDrop ND-1000 spectrophotometer with extinction coefficient 1.51. Flow through and elution peaks were pooled, concentrated to 200 µl using Vivaspin concentrator tubes (100 kDa MWCO) and dialysed against TBS-1 pH 7.4 using a Slide-A-Lyzer Mini Dialysis Unit with a 7 kDa MWCO (Thermo Scientific). A maximum of 100 µl fibrinogen was added to each unit and dialysed for 2 hours at 4°C with gentle stirring, followed by an additional hour with fresh TBS-1. Fibrinogen was stored at -80°C until use and the degree of fibrinogen phosphorylation in each peak, as well as control fibrinogen, was analysed using the malachite green assay (method 2.2.1.2). This method yielded two fibrinogen samples for use in functional investigations: 13 % phosphorylated and 33 % phosphorylated.

2.2.1.5. Dephosphorylation of fibrinogen

Dephosphorylation of fibrinogen was performed according to the method detailed by Kinoshita et al. (2005). Calbiochem® fibrinogen was dissolved in 50 mM Tris pH 9.0 to a concentration of approximately 8 mg/ml. The dephosphorylation reaction mix was prepared with 6 mg fibrinogen, 405 U bovine intestinal alkaline phosphatase (Sigma-Aldrich), $MgCl_2$ [400 µM] and 50 mM Tris pH 9.0 to a final volume of 3 ml. The reaction was incubated overnight at 37°C. Fibrinogen was purified from the reaction mix by IF-1 affinity chromatography (method 2.1.3.2) using an ÄKTA avant 25 system, concentrated by centrifugation using Vivaspin concentrator tubes (100 kDa MWCO) and dialysed against TBS-1 pH 7.4 using a Slide-A-Lyzer Mini Dialysis Unit (7 kDa MWCO), as explained in method 2.2.1.4. Dephosphorylated fibrinogen was stored at -80°C. Removal of phosphate was confirmed by malachite green assay (method 2.2.1.2).

2.2.1.6. Fibrinogen samples for functional studies

As previously mentioned, Calbiochem® fibrinogen was purified by IF-1 affinity chromatography using an ÄKTA avant 25 system, and the degree of phosphorylation determined by malachite green assay (method 2.2.1.2). This fibrinogen was used as the control sample in functional assays, representing physiological phosphorylation levels (25 %). The two fibrinogen samples from Phos-tag™ affinity chromatography (13 % and 33 % phosphorylation) and dephosphorylated fibrinogen were also used in subsequent functional assays.

2.2.2. Biotin-pentylamine (lysine donor) incorporation FXIII-A activity assay

The effect of phosphate on FXIII cross-linking of lysine analogue pentylamine to glutamine acceptor residues within fibrinogen was examined by comparison of phosphorylated (13 %, 25 % and 33 %) and dephosphorylated fibrinogen samples. The FXIII-A activity assay was performed in accordance with the method outlined in section 2.1.7.2 with triplicates of each sample. In both assays, the FXIII-A-mediated incorporation of lysine donor 5-(biotinamido) pentylamine to the phosphorylation isoforms was compared at 0, 5, 10, 15, 20 and 25 minutes. The experiment was repeated to give three independent data sets.

2.2.3. Plasminogen binding assay

A 96-well microtiter plate was coated with 100 µl per well of phosphorylated (13 %, 25 % and 33 %) and dephosphorylated fibrinogen in triplicate at 40 µg/ml in 50 mM sodium carbonate (Na_2CO_3) pH 9.6 and incubated at 4°C overnight. The wells were washed with 3 x 300 µl TBS-4-Tween 20 pH 7.4 (Appendix 1) and blocked with 300 µl per well of 3 % (w/v) BSA-TBS-4-Tween 20 for 90 minutes at 37°C. The plate was washed with 3 x 300 µl TBS-4-Tween 20 and 100 µl per well of plasminogen was added at increasing concentrations from 3.75 to 240 nM, diluted in TBS-4 pH 7.4 (Appendix 1). Plasminogen was incubated in the plate for 1 hour at 37°C before washing 3 x 300 µl TBS-4-Tween 20. To detect bound plasminogen, 100 µl per well of goat anti-human plasminogen HRP antibody (Enzyme Research Laboratories) diluted 1/2000 in 1 % (w/v) BSA-TBS-4-Tween 20 was added for 1 hour at 37°C. Finally, the plate was washed 3 x 300 µl TBS-4-Tween 20 and developed using OPD substrate as previously described (section 2.1.2). Absorbance at 490 nm was measured with a Dynex MRX-TC plate reader. Three independent experiments were performed.

2.2.4. Plasmin digestion time course experiment by SDS-PAGE

An initial plasmin digestion experiment was carried out to optimise the concentration of plasmin needed to digest 10 µg fibrinogen in 40 minutes. A concentration range of plasmin from 27.5 to 440 nM was tested to find the lowest concentration that could give sufficient digestion of fibrinogen into X, Y and D fragments. Fibrinogen [1.1 µM; 374 µg/ml] and plasmin (Enzyme Research Laboratories) were diluted in TBS-1 pH 7.4 to a final volume of 27 µl and incubated at 37°C for 40 minutes. Reactions were stopped by addition of 9 µl 4X LDS sample buffer to denature proteins, and analysed by non-reducing SDS-PAGE (method 2.1.4 without reducing agent). The optimal concentration of plasmin was found to be 220 nM (18.3 µg/ml) (section 3.2.2.4). The experiment was repeated using 220 nM plasmin at different time points, from 0-40 minutes in 5 minute intervals. As fibrinogen was almost completely digested within 5 minutes, the time course was shortened from 40 to 4 minutes, with 30 second intervals. To determine the influence of phosphorylation on plasmin-mediated fibrinogen digestion, the above method was used for digestion of phosphorylated (13 %, 25 % or 33 %) and dephosphorylated fibrinogen samples. After non-reducing SDS-PAGE, bands corresponding to fibrinogen fragments Y (145 kDa) and D1 (92 kDa) were analysed by densitometry using ImageJ 1,23y image analysis software (National Institutes of Health, USA), normalising the intensity of each band to total protein in the lane.

2.2.5. α2-antiplasmin incorporation assay

A 96 well microtiter plate was coated with 100 µl per well of phosphorylated (25 %, 13 %, 33 %) and dephosphorylated fibrinogen, each in triplicate, at 80 µg/ml in TBS-2 pH 7.4 (Appendix 1) for 40 minutes at room temperature. The plate was washed with 3 x 300 µl TBS-2 and incubated overnight at 4°C with 300 µl per well of 3% (w/v) BSA-TBS-2 to block for non-specific binding. Blocking was continued for 1 hour at 37°C the next morning before washing with 3 x 300 µl TBS-2-Tween 20 pH 7.4. For conversion of fibrinogen to fibrin, 100 µl per well of activation mix containing thrombin [1 U/ml] and $CaCl_2$ [5 mM] in TBS-2 was added for 45 minutes at room temperature and cleaved fibrinopeptides were removed with 4 x 300 µl high salt washing buffer (TBS-5-Tween 20 pH 7.4; Appendix 1), followed by 4 x 300 µl regular TBS-2-Tween 20. Ten microliters of rFXIII-A master mix [1.1 µg/ml] were added to each well before addition of 90 µl FXIII reaction mix containing DTT [100 µM], α2-AP [10 µg/ml], thrombin [1 U/ml] and $CaCl_2$ [5 mM] in TBS-2. Reactions were stopped at 0, 10, 20, 30, 40 and 50 minutes by addition of 200 µl 200 mM EDTA stop solution. The plate was washed with

4 x 300 µl 6 M urea, followed by 4 x 300 µl TBS-2-Tween 20, and incubated with 100 µl per well of goat polyclonal anti-α2-AP HRP antibody (Enzyme Research Laboratories) diluted 1/1000 in 3 % (w/v) BSA-TBS-2-Tween 20 for 1 hour at room temperature. A final wash step with 4 x 300 µl TBS-2-Tween 20 was carried out before developing the plate with ODP substrate (method 2.1.2) and measuring absorbance at 490 nm using an EL_x808 Absorbance Microplate Reader. The assay was repeated in three independent experiments.

2.2.6. Clot-based plasmin generation assay

The plasmin generation assay relies on plasmin-mediated cleavage of pNitroaniline (pNA) from chromogenic S-2251 substrate (Chromogenix, USA) in the following reaction:

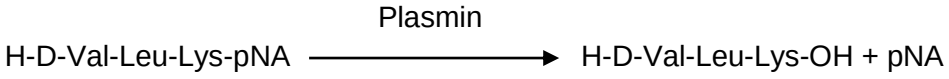

The pNA produced absorbs light at 405 nm and the increase in absorbance at 405 nm is directly proportional to plasmin activity; hence, this assay was used as a measure of plasmin activity in clots formed *in vitro* with phosphorylated (13 %, 25 %, 33 %) and dephosphorylated fibrin. Clots were formed in the presence of FXIII-A ± α2-AP to examine how phosphorylation affects covalent incorporation of α2-AP.

Fibrinogen samples were diluted to 0.25 mg/ml in TBS-6-Tween 20 pH 7.4 (Appendix 1) and 94 µl were added to each well, followed by plasminogen [312.5 µg/ml] and rFXIII-A [1.4 µg/ml] ± α2-AP [1.65 µg/ml] to a final volume of 100 µl. The plate was inserted into an EL_x808 Absorbance Microplate Reader pre-heated to 37°C and overlaid with 50 µl per well of activation mix containing thrombin [0.75 U/ml] and $CaCl_2$ [3.75 mM] diluted in TBS-6-Tween 20. Absorbance at 340 nm was measured every 12 seconds for 15 minutes, ensuring full clot formation. The plate was then overlaid with 50 µl per well of lysis mix containing tPA [0.05 µg/ml] and S-2251 substrate [0.6 mM], diluted in TBS-6-Tween 20 with 0.1% (w/v) BSA. Plasmin generation was monitored over 4 hours at 37°C by measuring absorbance at 405 nm every 48 seconds. Data were collected from three independent experiments.

2.2.7. Turbidity analysis

The effect of fibrinogen phosphorylation on fibre thickness and polymerisation was examined using the clot formation stage of the plasmin generation assay, as detailed above (section 2.2.6). Briefly, clots were formed using phosphorylated (13 %, 25 %, 33 %) and dephosphorylated fibrinogen, in the presence of plasminogen and rFXIII-A. Clotting was activated by thrombin and $CaCl_2$ before measuring absorbance at 340 nm for 15 minutes. Five independent experiments were performed and data were analysed using a customised software application for calculation of MaxAbs and clotting rate (Carter et al., 2007).

2.2.8. Scanning electron microscopy of fibrin clots

Fibrin clots formed from phosphorylated (25 %, 13 %, 33 %) and dephosphorylated fibrinogen were imaged by scanning electron microscopy (SEM) for visualisation and measurement of the effect of phosphorylation on fibre diameter. Fibrinogen [1 mg/ml], thrombin [1 U/ml] and $CaCl_2$ [10 mM] were combined in TBS-1 pH 7.4 to a final volume of 110 µl. Seventy five microliters of this mix were pipetted into the lid of a 0.5 ml Eppendorf tube, already pierced several times with a needle to facilitate subsequent wash steps, and wrapped in parafilm to prevent leakage during clot formation. The developing clots were incubated for 2 hours at room temperature in a humidity chamber. Washing, fixation and dehydration steps were all performed at room temperature with gentle stirring in a 50 ml volume. The clots were washed by removing the parafilm and placing in a beaker containing 50 mM sodium cacodylate pH 7.4 for 3 x 20 minutes. Sodium cacodylate is commonly used during specimen preparation for electron microscopy because the cacodylate does not form a precipitate with residual ions, as phosphate buffers may do if there is insufficient washing before fixation. Clots were transferred to a 2 % (v/v) gluteraldehyde (Sigma-Aldrich) solution in sodium cacodylate buffer for fixation, and washed again with sodium cacodylate buffer for 3 x 20 minutes.

A stepwise dehydration of the clots was carried out by sequentially transferring them to acetone solutions of increasing concentrations for 10 minutes each: 30 %, 50 %, 70 %, 80 %, 90 %, 95 % and 100 %. Two further 10 minute incubations in 100 % acetone were performed before transferring to fresh 100 % acetone for the final time. Fibrin clot structures were then subjected to a process known as critical point drying, which enables complete dehydration of biological samples whilst preserving surface morphology. During this process, water within samples is replaced with liquid CO_2; when temperature and pressure are raised beyond the critical point for CO_2 (31°C and

1200 pounds/square inch), the liquid CO_2 vaporises without change in density, thereby avoiding changes to surface tension which would distort surface ultrastructure. Critical point drying was conducted by Martin Fuller, University of Leeds using an E3000 critical point dryer (Quorum Technologies Ltd, UK).

On completion of drying, the clots were mounted onto 0.5 inch aluminium specimen stubs covered with 12 mm carbon tabs (Agar Scientific, UK) and coated with a 7 nm layer of platinum-palladium using a 208HR High Resolution Sputter Coater (Cressington, UK). The samples were individually imaged over 5 different areas using a Quanta 200F FEGESEM field-emission scanning electron microscope (FEI, USA) and fibre diameters (n=100) measured using ImageJ software.

2.2.9. Statistical analysis

Statistical analysis was performed where appropriate ($n \geq 3$). Data were analysed using Microsoft Excel to calculate mean values from independent experiments and standard error of the mean. Differences between mean values of different groups were analysed for statistical significance using a paired, two-tailed student's t-test, with significance accepted at $p<0.05$. Data are presented as mean ± standard error of the mean, with the level of significance denoted by * ($p<0.05$), ** ($p<0.01$), *** ($p<0.005$), or **** ($p<0.001$).

2.3. Characterisation of intracellular fibrinogen phosphorylation

Methods were developed to investigate the mechanism of *in vivo* fibrinogen phosphorylation, in particular the cellular location of fibrinogen phosphorylation and the kinase responsible. Intracellular phosphorylated fibrinogen Aα chains were visualised by proximity ligation assay (PLA). Other methods, such as SDS-PAGE, western blotting, ELISA and isoelectric focusing, were optimised for comparison of phosphorylation levels of secreted fibrinogen from cells incubated with various stimulators and inhibitors.

2.3.1. HepG2 cell culture

A human hepatoma cell line – HepG2 (ATCC) – was enlisted for investigations into cellular fibrinogen phosphorylation as these cells express fibrinogen naturally. Human hepatoma cells were cultured at 37°C, 5 % CO_2 in full growth medium supplemented with L-glutamine, as detailed in Appendix 1. Cells were cultured in 100 mm dishes and passaged once a week by incubating with 3 ml trypsin/EDTA solution for up to 30 minutes before diluting to 10 ml with growth medium. The cells were then passed three times through a 19 gauge needle to minimise clumping and re-plated at a 1:10 dilution in growth medium. Medium was replaced every 2-3 days.

2.3.2. Immunofluorescent detection of cellular fibrinogen Aα chains

Immunofluorescence was used to optimise an anti-fibrinogen Aα antibody, as well as markers for the ER and Golgi apparatus, prior to detection of phosphorylated fibrinogen Aα chains by PLA.

2.3.2.1. Slide preparation

Human hepatoma cells were trypsinised and counted using a haemocytometer chamber and the trypan blue dye exclusion method (method 2.1.13.1). For immunofluorescence, cells were seeded on LabTek-II 8-well chamber slides (Sigma-Aldrich) at a density of 100,000 cells per well in 500 µl growth medium (Appendix 1) and incubated overnight at 37˚C, 5 % CO_2. For fixation, cells were washed quickly with 800 µl PBS pH 7.4 (Appendix 1) and incubated with 500 µl 3 % (w/v) paraformaldehyde (Sigma-Aldrich) solution in PBS, containing $CaCl_2$ [100 µM] and $MgCl_2$ [100 µM], for 20 minutes at room temperature. After an additional three washes with PBS, cells were incubated with 500 µl 50 mM ammonium chloride solution in PBS for 10 minutes at

room temperature. Three final wash steps with PBS were performed before storing slides in PBS at 4˚C for up to 2 weeks.

2.3.2.2. Assay procedure

Slides were incubated in ice-cold methanol at -20˚C for 10 minutes to permeabilise cells. After three washes with PBS, slides were incubated in 0.2 % (w/v) fish skin gelatin (Sigma-Aldrich) solution in PBS (1X FSG) at room temperature for a minimum of 30 minutes to block for non-specific binding. Primary antibody solution in 1X FSG was added for 2 hours at room temperature in a humidified chamber, with 50 µl per well. After 3 x 5 minute washes with 1X FSG, 50 µl per well of secondary antibody solution in 1X FSG was added for 1 hour at room temperature in a humidified chamber covered with foil. Slides were washed four times with 1X FSG, once with PBS and once with 0.01X PBS, for 5 minutes each time, covered with foil. Once dry, slides were mounted using 15 µl per well of Duolink In Situ mounting medium containing 4',6-diamidino-2-phenylindole (DAPI) nuclei stain (Sigma-Aldrich); glass coverslips were positioned and sealed with colourless nail varnish. Slides were stored at -20˚C in the dark and brought to room temperature before imaging. Images were captured by LSCM as outlined below.

2.3.2.3. Laser scanning confocal microscopy

Slides prepared for immunofluorescence were imaged by LSCM using an LSM 700 inverted confocal microscope with Zen imaging software (Carl Zeiss Microscopy, Germany). Images were captured using a 63x oil objective lens with four solid-state lasers (405 nm, 488 nm, 555 nm and 635 nm); those to be compared were taken using the same pinhole (1 µm), detector gain and offset settings.

2.3.2.4. Antibody optimisation

Various primary and secondary antibodies used for immunofluorescence are listed in table 11. Three antibodies were tested for successful detection of fibrinogen Aα chain in CHO cells and HepG2 cells, using CHO-Bβγ as a negative control; only the anti-fibrinogen Aα 290-348/349-406 was validated for this purpose and therefore used in future experiments. Antibodies directed against ER and Golgi markers – anti-protein disulphide isomerise (anti-PDI) (ER) and anti-TGN46 (*trans*-Golgi) – were also optimised by immunofluorescence using the concentrations detailed below (table 11).

Antibody	Host Species	Clonality	Concentration/dilution	
			Tested	Optimal
Anti-fibrinogen Aα (Abnova, UK)	Rabbit	Polyclonal	1.5-5 µg/ml	N/A
Anti-fibrinogen Aα (Stratech)	Rabbit	Polyclonal	1/10-1/50	N/A
Anti-fibrinogen Aα 290-348/349-406 (Accurate Chemical)	Mouse	Monoclonal	1.5-5 µg/ml	1.5 µg/ml
Anti-phosphoserine (abcam)	Rabbit	Polyclonal	2.5-20 µg/ml	2.5 µg/ml
Alexa Fluor 488 anti-PDI (New England Biolabs)	Rabbit	Monoclonal	1/25-1/100	1/50
Anti-TGN 46 (abcam)	Sheep	Polyclonal	1/200-1/400	1/200
Anti-cleaved caspase 3 (New England Biolabs)	Rabbit	Monoclonal	N/A	1/400
Alexa Fluor 488-AffiniPure donkey anti-rabbit (Stratech)	Donkey	Polyclonal	N/A	1/1000
Cy3-AffiniPure donkey anti-mouse (Stratech)	Donkey	Polyclonal	N/A	1/1000
Alexa Fluor 647-AffiniPure donkey anti-sheep (Stratech)	Donkey	Polyclonal	N/A	1/1000

Table 11. Antibodies used for immunofluorescent techniques. The table lists primary and secondary antibodies used for immunofluorescence or the proximity ligation assay, as well as their respective species, clonality and chosen dilutions.

2.3.3. Detection of phosphorylated fibrinogen Aα chains in HepG2 cells by proximity ligation assay

The proximity ligation assay was developed to detect and quantify intracellular phosphorylated fibrinogen. This technique was used to i) investigate the location of fibrinogen phosphorylation using secretion inhibitor Brefeldin A (BFA) (section 2.3.3.3), ii) determine whether intracellular phosphorylation of fibrinogen increases in acute phase conditions (section 2.3.6), and iii) identify the *in vivo* fibrinogen kinase using broad spectrum kinase inhibitor staurosporine (STSP) (section 2.3.7).

2.3.3.1. Assay principle

Proximity ligation assay is a recently developed technique (Fredriksson et al., 2002) which enables highly specific detection *in situ* of two distinct entities in close proximity, residing less than 45 nm apart. The general method for PLA can be broken down into six stages, as illustrated in figure 16. After fixation of cells or tissues on a microscope slide, they are firstly incubated with two primary antibodies from different species. Oligonucleotide-conjugated PLA probes with plus or minus strands are added to detect each primary antibody; the plus and minus strands of the probes hybridise when in proximity. Hybridised oligonucleotides ligate to form a complete circle, which provides a template for rolling circle amplification in the presence of a polymerase. Finally, each amplification product is detected with fluorescently-labelled probes and appears as an individual spot when imaged by fluorescent microscopy. This novel technique can be used to detect and quantify protein-protein interactions, post-translational modifications and protein expression. Here, this method has been applied for the detection and quantification of phosphorylated human fibrinogen Aα chains in CHO cells and HepG2 cells (figure 17). All reagents are available commercially as part of the Duolink In Situ kit from Olink Bioscience, distributed in the UK by Sigma-Aldrich.

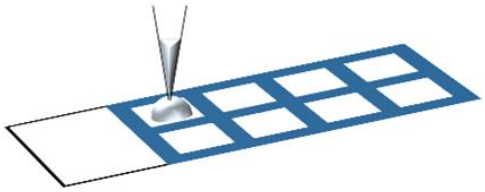

STEP 1: Fix cells onto microscope slide.

STEP 2: Add two primary antibodies.

STEP 3: Add PLUS and MINUS PLA probes.

STEP 4: Ligate hybridised DNA.

STEP 5: Amplify ligated DNA template and detect with fluorescent probes.

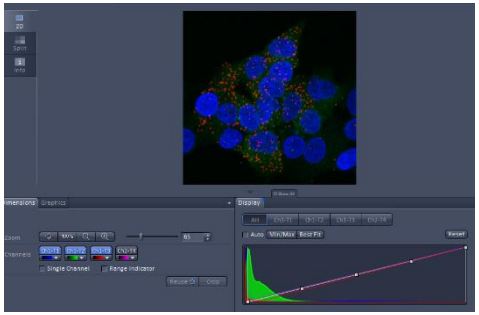

STEP 6: Image by confocal microscopy.

Figure 16. The six stages of a proximity ligation assay. 1) Cultured cells are fixed onto a microscope slide using formaldehyde. 2) Cells are blocked for non-specific binding and incubated with two different primary antibodies. 3) Cells are incubated with PLA probes directed against each primary antibody; the PLA probes are conjugated to plus and minus strands of DNA which hybridise when in close proximity. 4) Hybridised probes are ligated upon incubation with a DNA ligase, forming a circular DNA template. 5) A polymerase is added and the DNA is amplified by rolling circle amplification. Fluorescently labelled oligonucleotides that can hybridise with the amplification product are used for detection. 6) Cells are imaged by LSCM. Image modified from Gullberg et al. (2011).

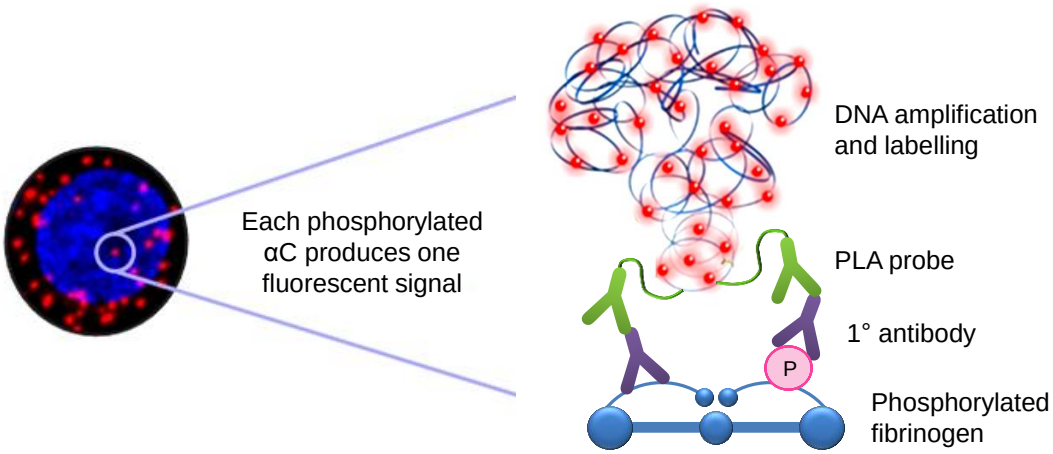

Figure 17. Detection of phosphorylated fibrinogen Aα chain by proximity ligation. Primary antibodies directed to the fibrinogen Aα chain (αC) (left) and phosphoserine (P) (right) are detected with oligonucleotide-conjugated PLA probes. Ligation and amplification of PLA probes enables fluorescent detection, whereby each individual signal corresponds to one phosphorylated α chain. Image modified from Gullberg et al. (2011).

2.3.3.2. PLA method

In all experiments, HepG2 cells were incubated with 20 µg/ml BFA for 8 hours prior to fixing to increase the signal (refer to method 2.3.3.3 for more details). To investigate the mechanism of fibrinogen phosphorylation, cells were also incubated with 10 ng/ml IL-6 for 24 hours or 250-500 nM kinase inhibitor STSP for 8 hours (sections 2.3.6 and 2.3.7). Subsequent fixation, permeabilisation, blocking and primary antibody incubation steps were followed according to sections 2.3.2.1 and 2.3.2.2. The following primary antibodies were used: i) mouse polyclonal anti-fibrinogen Aα chain, ii) rabbit polyclonal anti-phosphoserine and iii) sheep polyclonal anti-trans-*Golgi* network 46 (TGN46) (table 3). Primary antibody concentrations were optimised by immunofluorescence as described previously (method 2.3.2.4). The anti-phosphoserine antibody was optimised by PLA (table 11) by selecting the concentration which gave the highest signal-to-noise ratio; this was determined by subtracting the number of spots in images of control CHO-Bβγ cells from the signal in phosphorylated Aα chain-positive CHO-WT cells. After incubating cells with the primary antibody solution, Duolink In Situ PLA probes – anti-mouse PLUS and anti-rabbit MINUS (Sigma-Aldrich) – were diluted 1:5 in 1X FSG and incubated at room temperature for 20 minutes before adding to cells. During this time, slides were washed 4 x 5 minutes with 1X FSG on an orbital shaker. Slides were incubated in a humidified chamber for 1 hour at 37°C with 40 µl per well of PLA probe solution and washed 2 x 5 minutes with Wash Buffer A (Appendix 1). Detection was

performed using a Duolink In Situ Detection Reagent (orange; 554 nm) (Sigma-Aldrich). The supplied 5X ligation stock and ligase were diluted 1:5 and 1:40 respectively in filtered dH_2O, added to cells with 40 µl per well and incubated in a humidified chamber at 37°C for 30 minutes. Similarly, 40 µl per well of the 5X amplification stock and a DNA polymerase diluted 1:80 in Milli-Q H_2O were added for 100 minutes at 37°C in the dark, followed by 2 x 5 minute washes with Wash Buffer A. Alexa Fluor 488 anti-PDI and Alexa Fluor 647-AffiniPure donkey anti-sheep antibodies (table 11) were diluted in 1X FSG and added to cells for 1 hour at room temperature in the dark. The final washing and mounting procedures are detailed in section 2.3.2.2.

2.3.3.3. Inhibition of the secretory pathway with BFA

Brefeldin A inhibits the secretory pathway in cells, specifically blocking movement of proteins from the ER to the Golgi apparatus. This fungal metabolite leads to disassembly of the Golgi apparatus, with redistribution of *cis*- and *medial*-Golgi (but not *trans*-Golgi) components to the ER, disrupting a dynamic membrane recycling process between these two organelles (Lippincott-Schwartz et al., 1989). Brefeldin A was used to investigate the subcellular location of fibrinogen phosphorylation and to increase signal in PLA experiments. The concentration and incubation time were optimised by immunofluorescence with 5-20 µg/ml BFA for 4-8 hours. For PLA, cells were incubated with 20 µg/ml BFA diluted in 500 µl growth medium per well, for 8 hours prior to fixation.

2.3.3.4. LSCM and image analysis

Slides from PLA experiments were imaged using an LSM 700 inverted confocal microscope with Zen imaging software, as outlined in section 2.3.2.3. Z-stacks were captured with 1 µm intervals from the top to the bottom of cells within the field of view. Individual z-stack images were combined to form a maximum intensity projection, which was used for image analysis to quantify spots from whole cells. The maximum intensity projection images were analysed using a macro for ImageJ, designed by Gareth Howell, University of Leeds; the macro locates the nucleus and cytoplasmic area of each cell within the image and quantifies the number of spots per cell.

2.3.4. Detection of phosphorylated fibrinogen using Phos-tag™

In 2002, the Department of Functional Molecular Science at Hiroshima University developed a novel phosphate-capturing molecule – Phos-tag™. The Phos-tag™ molecule binds divalent metal cations, enabling high affinity interactions with phosphate

monoester di-anions (figure 18A). This presents a wide range of valuable applications for the field of phosphoproteomics, which is still largely dependent on the use of radioactive isotopes and limited by poor phosphoserine and phosphothreonine antibody specificity and sensitivity. Phos-tag™ Biotin, Phos-tag™ Agarose and Phos-tag™ SuperSep SDS-PAGE gels were purchased from Alpha Laboratories. Phos-tag™ Biotin (10 mg) was dissolved in 1.3 ml TBS-4 pH 7.4 containing 10 % (v/v) methanol to give a 10 mM stock solution. The applications of Phos-tag™ enlisted for this thesis are illustrated in figure 18B-D and detailed below.

2.3.4.1. Phos-tag™ affinity SDS-PAGE

Pre-cast Phos-tag™ SuperSep 12.5 % polyacrylamide gels containing 50 µM Phos-tag™ with 100 µM zinc chloride were used for the capture and slowed migration of phosphorylated proteins during electrophoresis. Ammonium sulphate precipitated fibrinogen (25 % phosphorylation) and dephosphorylated fibrinogen (200 ng) were combined with 4X reducing agent and 10X LDS sample buffer, zinc nitrate [500 µM] to quench the equivalent molar concentration of EDTA in the LDS sample buffer, and dH_2O to a final volume of 20 µl. Samples were heated to 95°C for 15 minutes, cooled on ice for 2 minutes and centrifuged briefly (Eppendorf MiniSpin Plus) to collect condensation before loading 15 µl per well. Electrophoresis was performed at 20 milliamperes (mA)/gel in 500 ml Tricine SDS-PAGE running buffer prepared from a 20X stock solution (Life Technologies) diluted in filtered dH_2O. For details of the standard western blotting procedure, refer to section 2.1.6. This was adapted to include a preliminary 10 minute wash step in transfer buffer containing 1 mM EDTA to chelate Zn^{2+} ions, followed by the usual 10 minute wash in transfer buffer without EDTA. Blots were probed with a mouse anti-fibrinogen Aα chain antibody and rabbit anti-mouse HRP secondary antibody (table 3) before developing by chemiluminescence with Clarity ECL Substrate.

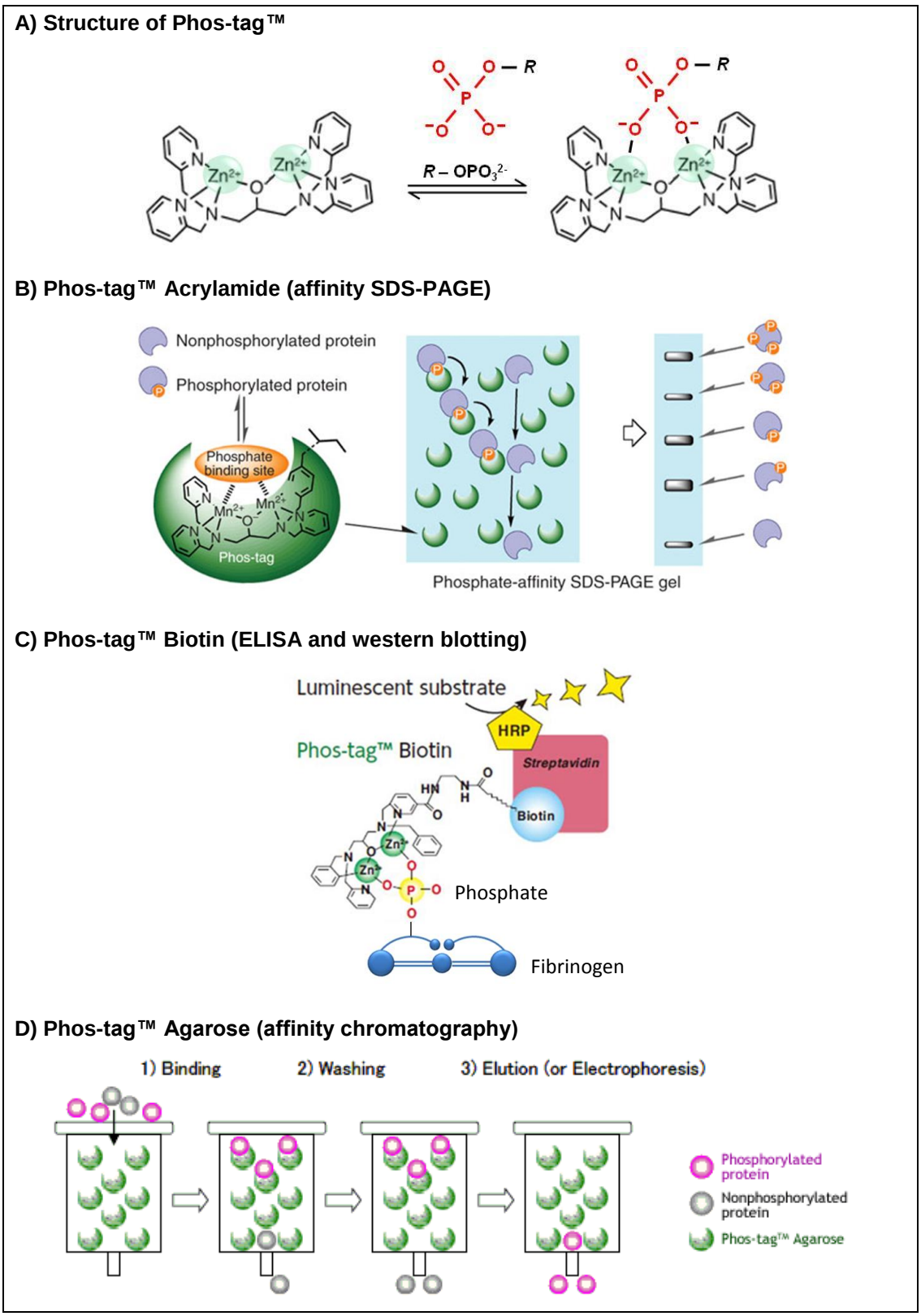

Figure 18. Applications of Phos-tag™. A) Phos-tag™ structure and Zn^{2+}-mediated interaction with protein-bound phosphate. B) Separation of proteins according to phosphorylation state by SDS-PAGE with Phos-tag™ Acrylamide. C) Detection of fibrinogen-bound phosphate by ELISA or western blotting using Phos-tag™ Biotin and streptavidin HRP. D) Chromatographic enrichment of phosphoproteins with Phos-tag™ Agarose. Images adapted from Kinoshita et al. (2009); Wako n.d. *Phos-tag™ Series*. Available from: http://www.wako-chem.co.jp/english/labchem/product/life/Phos-tag/pdf/Phos-tag.pdf [Accessed: 10 July 2014].

2.3.4.2. ELISA with Phos-tag™ Biotin

The high affinity interaction between biotin and streptavidin was exploited for the development of an assay to quantify the degree of fibrinogen phosphorylation in conditioned medium from HepG2 cells, using Phos-tag™ Biotin. A 96-well microtiter plate was coated with 100 µl per well of rabbit polyclonal anti-fibrinogen antibody (1/4000) in 50 mM sodium carbonate pH 9.6, at 4°C overnight. The plate was washed with 3 x 300 µl TBS-4-Tween 20 pH 7.4 and incubated with 300 µl per well of 3 % (w/v) BSA-TBS-4-Tween 20 blocking solution at 37°C for 90 minutes. Another wash step was performed before adding 100 µl per well of AP-fibrinogen at 170-680 ng/ml (approximately 50-200 fmol phosphate) in duplicate, diluted in TBS-4-Tween 20 for 2 hours at room temperature on a shaker. Blank wells containing TBS-Tween 20-only were included as a negative control. For preparation of a Phos-tag™ Biotin-bound Streptavidin HRP conjugate, a 500 µl mix containing Phos-tag™ Biotin [20 µM], zinc nitrate [400 µM], 1 µl streptavidin HRP (GE Healthcare) and TBS-4-Tween 20 was incubated at room temperature for 30 minutes. This was scaled up depending on the desired final volume. The mixture was then concentrated to less than 10 µl using a centrifugal filter device (30 kDa MWCO) to remove excess, unbound Phos-tag™. The remaining solution was diluted in 500 µl TBS-4-Tween 20 per microliter of Phos-tag™ Biotin added to the initial mix (1/500). A serial dilution of Zn^2-Phos-tag™ Biotin-Streptavidin HRP in TBS-4-Tween 20 was carried out to give a concentration range of 1/500 to 1/8000. After 3 x 300 µl washes with TBS-4-Tween 20, the prepared dilutions of Zn^2-Phos-tag™ Biotin-Streptavidin HRP were added to the plate with 100 µl per well for 1 hour at room temperature on a shaker. The plate was washed with 3 x 300 µl TBS-4-Tween 20 and developed with OPD substrate, reading absorbance at 490 nm with a Dynex MRX-TC plate reader.

To check for non-specific binding, a subsequent assay included a streptavidin-only negative control, whereby the same amount of streptavidin was diluted in TBS-4-Tween 20 to 500 µl without Phos-tag™ Biotin or zinc nitrate. The results demonstrated that streptavidin HRP was binding non-specifically to fibrinogen; therefore, streptavidin alkaline phosphatase was used in its place in future experiments. Due to inconsistencies within and between data sets, the Phos-tag™ Biotin and streptavidin alkaline phosphatase were added separately, rather than as a pre-prepared complex. After normal coating procedure (described above) and incubation with 100 µl per well of AP-fibrinogen and dephosphorylated fibrinogen at 1 µg/ml, or TBS-4-Tween 20 only, the plate was washed 3 x 300 µl TBS-4-Tween 20 and 100 µl per well of Phos-tag™ Biotin, diluted to 1 mM in TBS-4-Tween 20 containing zinc nitrate [100 mM], were added to each well for 1 hour at room

temperature on a shaker. Duplicate wells were incubated with TBS-4-Tween 20-only at this stage to give a control for non-specific binding of streptavidin alkaline phosphatase. Unbound Phos-tag™ Biotin was washed off with 3 x 300 µl TBS-4-Tween 20 before detecting bound Phos-tag™ Biotin with 100 µl per well of streptavidin alkaline phosphatase diluted to 10 nM in TBS-4-Tween 20; this was added for 1 hour at room temperature. A final 3 x 300 µl TBS-4-Tween 20 wash step was performed and the plate developed with PNPP in the same way as detailed in method 2.1.7.2.

2.3.4.3. Western blotting with Phos-tag™ Biotin

A serial dilution of AP-fibrinogen from 500 ng to 62.5 ng was prepared for gel loading by mixing with 4X reducing agent, 10X LDS sample buffer and dH_2O; samples were then heated to 95°C for 15 minutes before electrophoresis. The protein was blotted onto a PVDF membrane following method 2.1.6. After blotting, the membrane was soaked in 100 ml TBS-4-Tween 20 pH 7.4 with gentle shaking for 1 hour at room temperature. During this time, a Phos-tag™ Biotin-bound Streptavidin HRP conjugate was prepared as described in method 2.3.4.1, except the remaining solution after centrifugation was diluted with 20 ml TBS-4-Tween 20. The membrane was incubated with 10 ml of the Zn^2-Phos-tag™ Biotin-Streptavidin HRP complex for 30 minutes at room temperature with gentle rotation. Finally, the membrane was washed in 100 ml TBS-4-Tween 20 for 2 x 5 minutes and developed using SuperSignal West Pico Chemiluminescent Substrate and a G:BOX F3 with GeneSys software. An additional experiment was performed in the same way, but with an additional blot probed with streptavidin HRP-only (no Phos-tag™ Biotin) as a negative control for non-specific binding.

2.3.5. Developing methods for the detection of phosphorylated fibrinogen using anti-phosphoserine antibodies

2.3.5.1. Fibrinogen-phosphoserine ELISA

Antibodies to fibrinogen and phosphoserine were used to develop an ELISA for the quantification of phosphorylated fibrinogen in conditioned medium. A 96 well microtiter plate was coated with rabbit polyclonal anti-fibrinogen antibody (1/250) overnight at 4°C in sodium carbonate pH 9.6, washed with 3 x 300 µl TBS-2-Tween 20 pH 7.4 and blocked with 3 % (w/v) BSA-TBS-2-Tween 20. After additional washing, AP-fibrinogen (25 % phosphorylation) and dephosphorylated fibrinogen were diluted to 1 µg/ml in TBS-2-Tween 20 and added to the plate (100 µl per well) for 2 hours at room temperature. The plate was washed with 3 x 300 µl TBS-2-Tween 20 and incubated

with a concentration range of phosphoserine antibody Q5 (1/10-1/80) or mouse monoclonal anti-phosphoserine at 1/100. Details of antibodies can be found in table 3 below the western blotting protocol. Both antibodies were diluted in 1 % (w/v) BSA-TBS-2-Tween 20 and incubated overnight at 4°C with rolling. Wells were washed with 3 x 300 µl TBS-2-Tween 20 before addition of 100 µl per well of rabbit anti-mouse HRP secondary antibody diluted in TBS-2-Tween-20 (1/1000) for 1 hour at room temperature, followed by a final washing step. The plate was developed with OPD substrate and absorbance measured at 490 nm using a Dynex MRX-TC plate reader.

To reduce non-specific binding, the method was repeated with a 10 % BSA-TBS-2-Tween 20 blocking solution and the mouse monoclonal anti-phosphoserine antibody was diluted in 5 % (w/v) BSA-TBS-2-Tween 20 at 4°C overnight. These improved blocking conditions were incorporated in subsequent experiments. For the final experiment, a plate was coated with mouse anti-fibrinogen γ chain antibody (1/4000) and later incubated with a rabbit polyclonal anti-phosphoserine antibody (1/100), followed by goat anti-rabbit HRP (1/1000).

2.3.5.2. Phosphoserine western blots

The western blotting protocol for phosphoserine detection was adapted from the general protocol in section 2.1.6. Ammonium sulphate precipitated fibrinogen (25 % phosphorylation) (0.1-5 µg) was electrophoresed and blotted onto PVDF before blocking in 10 % (w/v) BSA-TBS-2-Tween 20 pH 7.4 for 2 hours at room temperature. A mouse monoclonal anti-phosphoserine primary antibody was diluted in 5 % (w/v) BSA-TBS-2-Tween 20 and incubated with the blot overnight at 4°C. The blot was washed 4 x 15 minutes in TBS-2-Tween 20 and the rabbit anti-mouse HRP secondary antibody (1/5000), plus StrepTactin HRP, were added in 5 % (w/v) milk-TBS-2-Tween 20 for 1 hour at room temperature. After 3 x 10 minute washes in TBS-2-Tween 20, the blot was develop by chemiluminescence with Clarity ECL Substrate. The same procedure was repeated using 2 µg AP-fibrinogen and dephosphorylated fibrinogen with a rabbit polyclonal anti-phosphoserine primary antibody and goat anti-rabbit HRP secondary antibody. In experiment blots, a mouse monoclonal anti-fibrinogen γ chain antibody was included during the primary antibody incubation step, plus an additional secondary antibody incubation with goat anti-rabbit HRP prior to addition of rabbit anti-mouse HRP at 1/10,000 for γ chain detection. Probing for the fibrinogen γ chain enabled normalisation of phosphorylated Aα chain bands to γ chain bands during densitometry analysis with GeneTools software (Syngene). Refer to table 3 for details of antibodies and dilutions.

2.3.6. Investigations into the effect of IL-6 on fibrinogen expression and phosphorylation in HepG2 cells

HepG2 cells were incubated with recombinant human IL-6 (expressed in HEK cells) (Sigma-Aldrich) to mimic acute phase conditions, addressing the question of whether elevated fibrinogen phosphorylation in the acute phase is due to modification inside the cell or in circulation. In an initial experiment, a concentration range from 5 to 80 ng/ml was added to the cells for 24 hours and the change in fibrinogen expression monitored by real-time PCR (method 2.3.6.1) to identify the optimal concentration.

Quantification of intracellular phosphorylated fibrinogen Aα chains in the presence and absence of 10 ng/ml IL-6 for 24 hours was performed by PLA, as described in method 2.3.3.2. For analysis of secreted fibrinogen, six dishes (60 mm) of HepG2 cells were cultured to confluence, washed once with serum-free medium and incubated with serum-free medium ± 10 ng/ml IL-6 in triplicate for 24 hours. Conditioned medium was harvested, mixed with protease and phosphatase inhibitor cocktails (Sigma-Aldrich) (1/500) and incubated on ice during the RNA extraction procedure (method 2.1.11.3). Harvested medium was subsequently concentrated to 50 µl using Amicon Ultra-0.5 Centrifugal Filter Units with a 100 kDa MWCO and stored at -80°C until further analysis. The concentration of fibrinogen in each sample was measured by ELISA (method 2.1.2) and the degree of phosphorylation compared by SDS-PAGE and western blotting with an anti-phosphoserine antibody (method 2.3.5.2). Relative fibrinogen expression levels in the presence and absence of IL-6 were quantified by reverse transcription and real-time PCR, described below.

2.3.6.1. Real-time PCR: quantifying the change in fibrinogen and casein kinase expression with IL-6

Ribonucleic acid extracted from HepG2 cells incubated in the presence and absence of 10 ng/ml IL-6 was reverse transcribed into cDNA (methods 2.1.11.3 and 2.1.12.6). The protocol for real-time PCR is outlined in section 2.1.12.7, with adaptations described here. Forward and reverse primers were designed to amplify the following human cDNA: fibrinogen Aα chain, CK2, Fam20A, Fam20B, Fam20C, Fam198A, Fam20B and 18S rRNA as an internal control (table 12). Refer to section 2.1.11.4 for primer design and details of fibrinogen Aα chain primers. For experiments comparing fibrinogen expression, templates were diluted 1:10 or 1:200 for experiment and control reactions respectively. For experiments comparing kinase expression, RNA was diluted to 100 ng/µl instead of 200 ng/µl (due to lower yield) prior to reverse transcription and cDNA templates were added to reactions undiluted (experiment) or diluted 1:100 (18S

rRNA control). All reactions were performed in triplicate. Real-time PCR data were analysed using the ΔΔCt method by i) normalising experiment Ct values to endogenous control 18S rRNA Ct values ($Ct_{experiment}$ - $Ct_{control}$ = ΔCt), ii) subtracting ΔCt values from the reference ΔCt value of the control sample (i.e. without IL-6), and iii) determining the relative expression in experiment samples using a $2^{-\Delta\Delta Ct}$ calculation.

Primer	Sequence (5' to 3')	Length (nt)	T_m (°C)	% GC
CK2 Forward	GCTTCCACCACAGCTCTATCA	21	59.79	52.38
CK2 Reverse	GTGTAAACTCTGGCCCTGCT	20	59.96	55
Fam20A Forward	CTGGAACAGGCGACACAAGA	20	60.25	55
Fam20A Reverse	TGCTCGCTGGAGAGACAAAG	20	60.04	55
Fam20B Forward	CAAATTGGCCAGGTGGGAGTA	21	60.27	52.38
Fam20B Reverse	CCAAAGACATCCAAGGCCACT	21	60.55	52.38
Fam20C Forward	CCATGAAACAAACGAGGGAGC	21	59.80	52.38
Fam20C Reverse	GAGCTTCTTGTCCCGTGTGA	20	59.97	55
Fam198A Forward	TGGAGGGCATAGATGGGTTTC	21	59.51	52.38
Fam198A Reverse	TCCTCGTCCCTGAAGAGTGT	20	59.89	55
Fam198B Forward	CAGAGTTCATCCAAGCAGCAG	21	59.26	52.38
Fam198B Reverse	CCAAATGCCTTGGGTCATGC	20	60.11	55
18S rRNA Forward	GTAACCCGTTGAACCCCATTC	21	59.19	52.38
18S rRNA Reverse	ACCATCCAATCGGTAGTAGCG	21	59.66	52.38

Table 12. Real-time PCR primers for analysis of kinase expression in HepG2 cells. Forward and reverse primer sequences for amplification of casein kinase and 18S rRNA cDNA are displayed with nucleotide (nt) length, T_m and GC content.

2.3.7. Incubation of HepG2 cells with STSP

Staurosporine is a potent and promiscuous ATP-competitive kinase inhibitor, which characteristically has no effect on G-CK activity due to a long β1-β2 loop structure around the ATP binding site of Fam20 proteins, impeding interaction with the inhibitor (Xiao et al., 2013, Meggio et al., 1995). Therefore, cells were incubated with STSP to determine whether fibrinogen is phosphorylated by the G-CK. As STSP induces

apoptosis, the best concentration would provide effective kinase inhibition with minimal cell death; a concentration range of 0.5-10 µM STSP (Millipore) was added to HepG2 cells, which were then screened for the appearance of cleaved caspase 3 – a marker for apoptosis – by immunofluorescence using an anti-cleaved caspase 3 antibody (table 11; method 2.3.2).

A proximity ligation assay was carried out with the addition of 250-500 nM STSP for 8 hours prior to fixing cells (method 2.3.3.2) and the number of phosphorylated fibrinogen Aα chains in control or STSP-treated cells was compared using ImageJ (method 2.3.3.4). The phosphorylation status of secreted fibrinogen was also compared by western blotting. HepG2 cells were cultured to confluence in 60 mm dishes in full growth medium, washed once with serum-free medium and incubated with 0-200 nM STSP diluted in serum-free medium for 24 hours. Conditioned medium was harvested and mixed with protease and phosphatase inhibitor cocktails (1/500) before concentrating to 50 µl using Amicon Ultra-0.5 Centrifugal Filter Units (100 kDa MWCO). In a subsequent experiment, cells were cultured ± 200 nM STSP for 24 hours and harvested medium was concentrated to 1 ml for immunoprecipitation of fibrinogen (method 2.3.8). All samples were analysed by SDS-PAGE and western blotting with an anti-phosphoserine antibody (method 2.3.5.2).

2.3.8. Immunoprecipitation of fibrinogen from conditioned medium

Fibrinogen was purified from conditioned HepG2 medium by immunoprecipitation using Dynabeads® Magnetic Separation Technology (Life Technologies) according to the manufacturer's instructions. A polyclonal anti-fibrinogen antibody (10 µg) was diluted in 200 µl PBS-Tween 20 pH 7.4 (Appendix 1) and incubated with Dynabeads® Protein G for 10 minutes at room temperature with rotation. The tube was placed on a magnetic rack and the supernatant removed with a pipette. In this way, the Dynabeads-antibody complexes were washed with 200 µl PBS-Tween 20 before addition of target antigen; after removal of wash buffer, 1 ml fibrinogen-containing medium was added to the tube and incubated at room temperature for 1 hour with rotation. Supernatant was removed and the Dynabeads-antibody-fibrinogen complexes were washed with 3 x 200 µl PBS-Tween 20. For elution of fibrinogen, the supernatant was removed and 20 µl 50 mM glycine pH 2.8 were added to the tube with 7.5 µl 4X LDS sample buffer and 3 µl 10X reducing agent. The mixture was heated to 95°C for 15 minutes before loading the supernatant on a 4-12 % Bis-Tris polyacrylamide gel. Immunoprecipitated fibrinogen was subjected to SDS-PAGE and western blotting with anti-phosphoserine and anti-fibrinogen gamma chain antibodies (method 2.3.5.2), followed by Clean-Blot IP

Detection Kit (HRP) (Thermo Scientific) diluted 1/200 in 5 % (w/v) milk-TBS-2-Tween 20 pH 7.4 for detection of primary antibodies without interference from denatured IgG bands.

2.3.9. Reverse transfection of Fam20A siRNA into HepG2 cells

To investigate whether Fam20A phosphorylates fibrinogen, Fam20A siRNA and a scrambled control siRNA (Santa Cruz Biotechnology, USA) were reverse transfected into HepG2 cells using Lipofectamine RNAiMAX, adhering to the protocol from Life Technologies. Each siRNA was resuspended in an appropriate volume of supplied RNase-free H_2O to give a stock concentration of 10 µM. The concentration of siRNA for transfection was optimised using a range from 5 to 50 nM in 5 nM intervals and the relative knockdown in Fam20A expression determined by RNA extraction and real-time PCR (method 2.3.6.1). The optimised transfection protocol is described below.

HepG2 cells were cultured to confluence in 100 mm dishes and medium was replaced one day ahead of transfection. In each well of a 6 well plate, 5 µl lipofectamine RNAiMAX and 1.5 µl Fam20A or scrambled control siRNA [5 nM] were diluted in 500 µl OptiMEM I reduced serum medium and incubated for 10-20 minutes at room temperature. Cells were trypsinised, counted using a haemocytometer (method 2.1.13.1) and diluted to 100,000 cells/ml in antiobiotic-free growth medium before adding 2.5 ml (250,000) cells per well. The plate was shaken gently to evenly distribute cells and incubated at 37°C, 5 % CO_2. Medium was replaced after 24 hours and incubated for a further 48 hours without change. Cells were assayed by RNA extraction and real-time PCR, while conditioned medium was harvested for analysis by SDS-PAGE and western blotting with an anti-phosphoserine antibody (method 2.3.5.2). Harvested medium was immediately placed on ice and mixed with protease and phosphatase inhibitor cocktails (1/500) before concentrating to 50 µl using Amicon Ultra-0.5 Centrifugal Filter Units with a 100 kDa MWCO. The fibrinogen concentration was determined by fibrinogen ELISA with serial dilution of each sample (method 2.1.2).

As harvested medium contained insufficient fibrinogen for downstream analysis of phosphoserine content, several steps were taken to improve the yield. To maximise cell viability, culture medium was replaced with fresh medium 12 hours post-transfection and cells were incubated for a further 60 hours before analysis. The number of cells seeded per well was also increased to the upper recommended limit of 375,000. A final experiment was performed in the presence of 10 ng/ml IL-6 to increase fibrinogen expression and determine whether Fam20A is responsible for the elevated cellular fibrinogen Aα chain phosphorylation observed previously with IL-6; the

cytokine was added to cells 12 hours post-transfection for 60 hours. Harvested medium was concentrated to 1 ml and fibrinogen was immunoprecipitated before analysis of phosphoserine content by western blotting (method 2.3.8).

2.3.10. Statistical analysis

Data from experiments conducted three times or more ($n \geq 3$) were analysed for statistically significant differences using a paired, two-tailed student's t-test, according to section 2.2.9.

Chapter 3

Results

3.1. Recombinant fibrinogen expression

Recombinant WT fibrinogen was expressed using an established in-house CHO cell expression system. Site directed mutagenesis and transfection of mutated fibrinogen Aα chain constructs into CHO and Expi293F cells was carried out for expression of variant fibrinogen without the Ser3 and Ser345 phosphorylation sites, ultimately to investigate their function by comparison to WT fibrinogen.

3.1.1. Expression and purification of recombinant WT fibrinogen

During expression of recombinant WT fibrinogen in CHO cells, an aliquot of conditioned medium was removed from each harvest for further screening by ELISA to monitor fibrinogen secretion over time (figure 19). The average fibrinogen concentration from harvests 1-36 was 1.6 µg/ml, giving an estimated total of 48 mg fibrinogen in 30 L. The CHO cell expression system was terminated after 13 weeks (39 harvests) due to a steady decline in productivity.

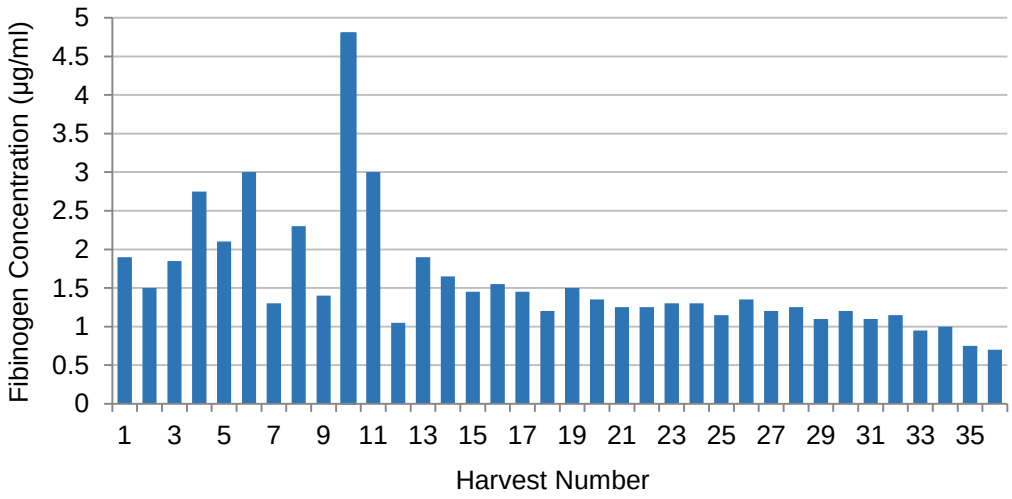

Figure 19. Concentration of recombinant WT fibrinogen in each harvest of cell culture medium (1-36). Medium from CHO cells expressing recombinant WT fibrinogen was harvested every 2-3 days for 3 months. Productivity of the cells was monitored by measuring the fibrinogen concentration in each harvest of medium by ELISA.

Recombinant WT fibrinogen was precipitated out of the large volume of medium using ammonium sulphate and resuspended in pellet buffer. Fibrinogen was purified by IF-1 affinity chromatography; figure 20 shows a large flow through peak, followed by a smaller fibrinogen-containing elution peak which was collected in fractions. On average, 950 µg fibrinogen were eluted per run from 5 ml supernatant. Fractions containing fibrinogen from later harvests were pooled separately in case of degradation. The final quantity of purified fibrinogen after concentration and dialysis was 21.96 mg.

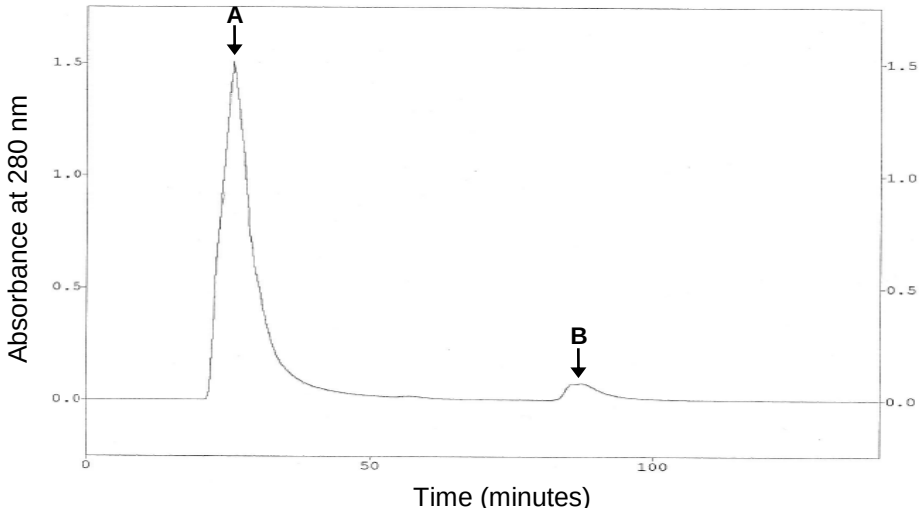

Figure 20. Chromatogram of recombinant WT fibrinogen purification by affinity chromatography. Ammonium sulphate-precipitated fibrinogen was loaded onto an IF-1 column in the presence of 10mM $CaCl_2$ and eluted with 50 mM EGTA. A) Flow through peak; B) fibrinogen elution peak. Chromatography was performed using an ÄKTA prime system.

3.1.1.1. Functional analysis of recombinant WT fibrinogen

The quality of purified recombinant WT fibrinogen was assessed by reducing SDS-PAGE. An equal quantity of fibrinogen (15 µg) from each of the three samples of pooled harvests was loaded separately to compare quality, in case of degradation in later harvests. Figure 21 shows fibrinogen from harvests 1-29 (lane 1), 30-34 (lane 2) and 35-39 (lane 3). Three bands corresponding to the Aα (66kDa), Bβ (54kDa) and γ (48kDa) chains of fibrinogen were present in equal proportions and there appeared to be no degradation or reduction in quality of fibrinogen purified from later harvests.

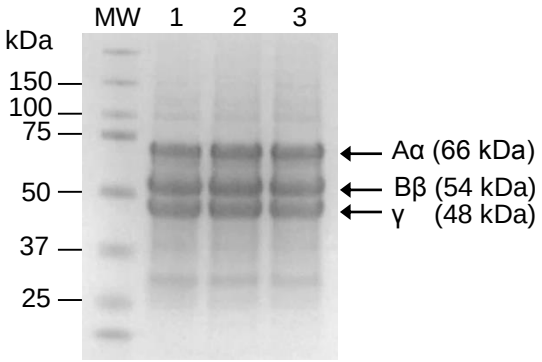

Figure 21. Reducing SDS-PAGE of purified recombinant WT fibrinogen. Samples of purified fibrinogen (15µg) pooled from different harvests of CHO cell medium were separated by reducing SDS-PAGE. The Aα, Bβ and γ chains of fibrinogen are indicated with arrows and their respective molecular weights. MW: molecular weight marker; lane 1: harvests 1-29; lane 2: 30-34; lane 3: 35-39.

The functionality of purified recombinant WT fibrinogen was verified by means of turbidity and lysis assay, biotin-pentylamine incorporation rFXIII-A activity assay and a fibrin polymerisation time course experiment. Clot formation and fibrinolysis followed a typical trend (figure 22), with almost identical Lag and MaxAbs values in the presence or absence of rFXIII-A, plus negligible differences in clotting rate, lysis rate and $Lys50_{MA}$ (table 13).

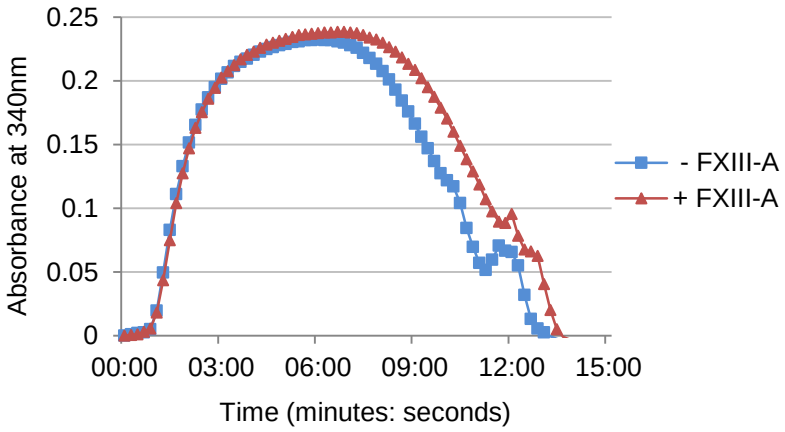

Figure 22. Turbidity and lysis curves with recombinant WT fibrinogen. Recombinant WT fibrinogen at 0.5 mg/ml was incubated with plasminogen [35 µg/ml] in the presence (▲) and absence (■) of rFXIII-A [1.1 µg/ml], before addition of an activation mix containing 0.5 U/ml thrombin, 2.5 mM $CaCl_2$ and 0.3 µg/ml tPA. The graph displays the change in absorbance at 340 nm over time during clotting and lysis. Absorbance values are an average of duplicate wells (n=1).

	Lag (s)	MaxAbs	Clotting rate	Lys50$_{MA}$ (s)	Lysis rate
- rFXIII-A	40	0.230	7.18 x 10^{-4}	240	-5.18 x 10^{-4}
+ rFXIII-A	40	0.237	6.37 x 10^{-4-}	258	-5.85 x 10^{-4-}

Table 13. Turbidity and lysis curve analysis. Turbidity and lysis curves generated using recombinant WT fibrinogen ± rFXIII-A were analysed using customised software for calculation of turbidimetric variables. Values are calculated from duplicate wells (n=1).

For assays involving cross-linking, rFXIII-A was expressed in *E. Coli* and purified by GST affinity chromatography, with a yield of 952 µg. Reducing SDS-PAGE and western blotting showed a strong rFXIII-A band at 83kDa with some minor degradation products and co-elution with GST (figure 23A and B). Incorporation of biotin-pentylamine was used as a measure of rFXIII-A activity to confirm that recombinant WT fibrinogen is a functional substrate for this enzyme. The results showed normal rFXIII-A-mediated cross-linking of pentylamine to WT fibrinogen increasing over time (figure 23C).

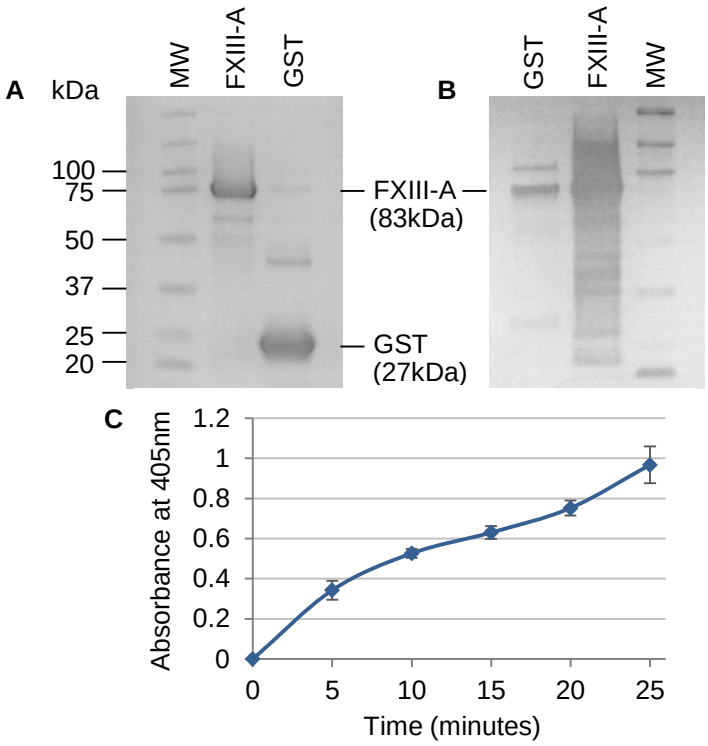

Figure 23. SDS-PAGE, western blotting and activity assay of purified rFXIII-A. A) SDS-PAGE of purified rFXIII-A (7 µg) and GST elution fractions (4 µl). B) Western blotting of rFXIII-A and GST elution fractions with a sheep polyclonal anti-FXIII-A antibody (1/2000). MW: molecular weight marker; lane 1: Purified rFXIII-A; lane 2: GST elution fractions. C) FXIII-A activity assay. Incorporation of biotin-pentylamine [2.7 µM] to recombinant WT fibrinogen [40 µg/ml] by rFXIII-A [1.1µg/ml] in the presence of 1 U/ml thrombin and 1mM $CaCl_2$ was determined by absorbance at 405 nm. Average absorbance values from duplicate wells are displayed with error bars representing standard deviation (n=1).

Fibrin clots formed in the presence of rFXIII-A were reduced and run on an SDS-PAGE gel to visualise α-α, α-γ and γ-γ chain polymer formation (figure 24) and to demonstrate cross-linking of fibrinogen chains. The γ-γ polymers appeared first at 10 minutes, increasing in intensity over time. Bands corresponding to α-α and α-γ polymers appeared from 30 minutes onwards. Coinciding with cross-linked polymer formation, there was a visible reduction in fibrin α and γ chain monomers.

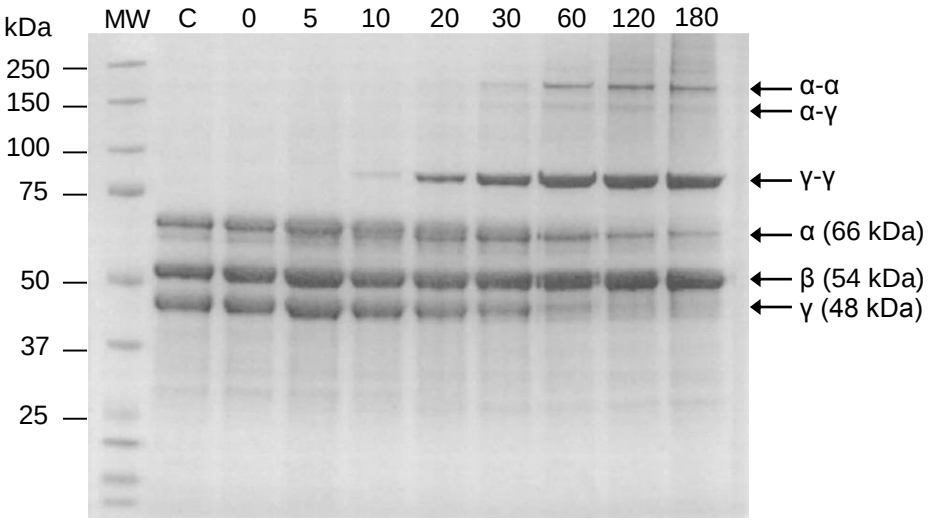

Figure 24. Reducing SDS-PAGE fibrin polymerisation time course. Recombinant WT fibrinogen [0.5 mg/ml] was incubated with rFXIII-A [1.1 µg/ml] in the presence of 0.05 U/ml thrombin and 1.5 mM $CaCl_2$ for 0-180 minutes. Reduced samples were separated on a 4-12 % Bis-Tris polyacrylamide gel in MOPS running buffer. Fibrin α, β and γ chains and HMW cross-linked dimers are indicated with arrows. MW: molecular weight marker (kDa); C: control fibrinogen (no rFXIII-A).

3.1.2. Generation of pMLP-Aα variants by site directed mutagenesis

Site directed mutagenesis was carried out to produce variant fibrinogen Aα chain constructs for expression of recombinant fibrinogen without the Ser3 and Ser345 phosphorylation sites. Agarose gel electrophoresis confirmed the integrity of purified DNA after the mutagenesis procedure, with clean bands at the correct molecular weight (6,265bp) indicating good quality templates with no degradation. Plasmids were also sequenced to ensure the desired mutations were present before transfection. For each variant, the sequencing data revealed base changes exclusive to the codons of interest, producing the correct protein sequences with the exception of Ser3 and Ser345 when translated using ExPASy Translate Tool. Excerpts of sequencing data demonstrating successful mutations can be found in Appendix 2. Variant constructs for

expression of fibrinogen Aα S3N, S345N, S3/345N, S3E, S345E, S3/345E and S345A were generated in this way.

3.1.3. Transfection of pMLP-Aα variants into CHO-Bβγ cells

Initially, CHO-Bβγ cells were transfected with pMLP-Aα S345N and the pMSVHis selection vector. Uptake of DNA by the cells was successfully achieved, as inferred from the growth of healthy colonies under selective pressure. However, when screening an aliquot of medium from each of the 24 selected clones by fibrinogen ELISA, none of the clones were found to be positive for fibrinogen secretion. To investigate this further, several clones were selected at random and cultured in 60 mm dishes for 1 week without medium change. Conditioned medium was harvested and the ELISA was repeated. Again, no secreted fibrinogen was detected for any of the clones. At this point, it was unclear whether the absence of positive clones was due to an inability of the cells to express non-phosphorylated fibrinogen, or due to a problem with the transfection method.

The process of pMLP-Aα S345N transfection was repeated in the same way, coupled with transfection of pMLP-Aα WT as a control. One out of six selected WT clones was positive for fibrinogen expression, albeit at a low concentration of 15 ng/ml. In contrast, the S345N clones remained blank during the ELISA. Subsequent transfections of pMLP-Aα S3N and pMLP-Aα S3/345N had the same outcome. To investigate whether this may be an effect of losing the phosphoserine residues, phosphomimetics pMLP-Aα S3E and S345E, which would replace Ser3 and Ser345 with negatively charged glutamic acid, were also transfected into CHO-Bβγ cells. Again, the 24 well plate fibrinogen ELISA revealed a complete absence of secreted fibrinogen, suggesting that i) the phosphate groups itself, rather than its negative charge, is required for secretion, or ii) the problem lies within the transfection process – a conclusion which is somewhat weakened by the viability of pMLP-Aα WT transfection and expression. A final attempt to express variant fibrinogen in CHO cells was made by transfection of pMLP-Aα S345A to change Ser345 to alanine, which is more typically used for transfection due to its small, inoffensive structure. Unfortunately this still did not permit expression and no positive clones were detected.

Intracellular analysis of fibrinogen was performed to establish whether the variants were either: i) not expressed by the cells, or ii) expressed but not secreted without the phosphorylation sites. Chinese hamster ovary cells transfected with WT fibrinogen constructs prior to this thesis (CHO-WT), and used for expression and purification of recombinant WT fibrinogen, were used as a positive control in these experiments.

Transfected CHO cells were lysed and both lysate and conditioned medium were analysed for fibrinogen content by western blotting. Blots were probed with a polyclonal anti-fibrinogen antibody (figure 25) or monoclonal anti-fibrinogen Aα chain antibody (figure 26). In figure 26, medium was concentrated 5X for stronger detection of fibrinogen; lysate was concentrated in both cases. In figure 25, the Aα, Bβ and γ chains of fibrinogen were all detected in lysate and conditioned medium from CHO-WT cells. An additional non-specific band between the Aα and Bβ chains (approximately 60 kDa) also appeared in the cell lysates. To determine if this band was fibrinogen-related, the blot was repeated without the anti-fibrinogen antibody incubation step. The results demonstrated that the band is a result of cross-reactivity of the secondary goat anti-rabbit HRP antibody to another protein in CHO cells, or endogenous peroxidase activity. In CHO cells transfected with the S345N variant, fibrinogen bands were present in the lysate but were very faint. This most likely indicates unequal loading of fibrinogen on the gel, and could be improved by performing a cell count prior to seeding cells. The Bβ and γ chains of S345N fibrinogen were clearly present, while the Aα chain band was only just visible. In a repeat experiment, in which the blot was probed with a monoclonal anti-fibrinogen Aα chain antibody (figure 26), an Aα chain band was clearly detected for S345N fibrinogen in cell lysate, with no band in the medium. In contrast, the WT fibrinogen presented as a very faint band in the lysate and a strong band in the medium. Again, this experiment would benefit from cell counting and seeding cells at equal densities. The results suggest that the CHO cells were able to express the variant Aα chain but could not secrete it, or at least not at a sufficient level for detection. The question remains whether the absence of fibrinogen in the medium is due to very low expression levels and problems with the transfection, or whether this is a direct effect of mutating the phosphorylation sites.

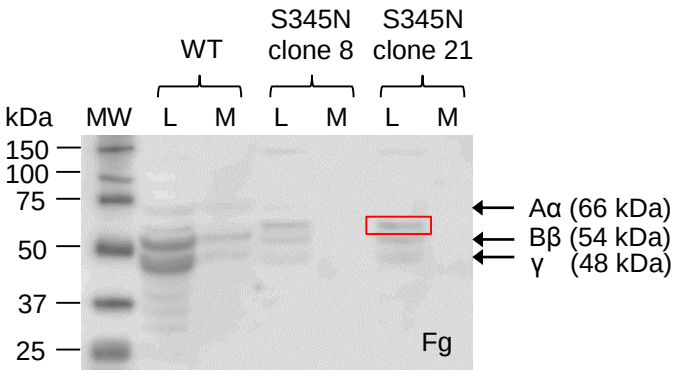

Figure 25. Western blotting of WT and S345N fibrinogen from CHO cell lysate and medium. Chinese hamster ovary cells transfected with constructs for expression of WT or S345N fibrinogen (clones 8 and 21) were incubated in serum-free medium for 5 days prior to lysis and harvest of medium. Lysate was concentrated 5X using centrifugal filters. Lysate (L) and conditioned medium (M) (30 µl) were separated by reducing SDS-PAGE and probed with a rabbit polyclonal anti-fibrinogen antibody (Fg) (1/1000). The red box highlights a non-specific band in CHO cell lysates. MW: molecular weight marker.

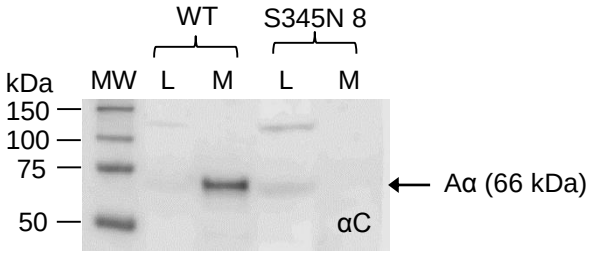

Figure 26. Western blotting of WT and S345N fibrinogen Aα chain from CHO cell lysate and medium. Lysate (L) and conditioned medium (M) from CHO cells transfected with WT or S345N fibrinogen constructs (clone 8) were harvested after 5 days in serum-free medium. Loading conditions differ to figure 25, with a 5X concentration of harvested medium for clear detection of the fibrinogen Aα chain. Samples (30 µl) were separated by reducing SDS-PAGE and probed with a mouse monoclonal anti-fibrinogen Aα chain antibody (αC) (1/1000). MW: molecular weight marker.

Contrary to the aforementioned lysis and blotting, further investigations into fibrinogen expression by immunofluorescence failed to detect any variant fibrinogen Aα chain in CHO cells, despite positive signal in CHO-WT cells (figure 27). Ideally, more than one clone per variant would be screened. However, the S345N clone was the same as used for cell lysis and blotting, which detected low levels of Aα chain. The same anti-fibrinogen Aα chain antibody was also used for both techniques. The absence of Aα chain by immunofluorescence suggests a lack, or very low level, of expression. Immunofluorescence may not be sensitive enough to detect these low levels of Aα chain.

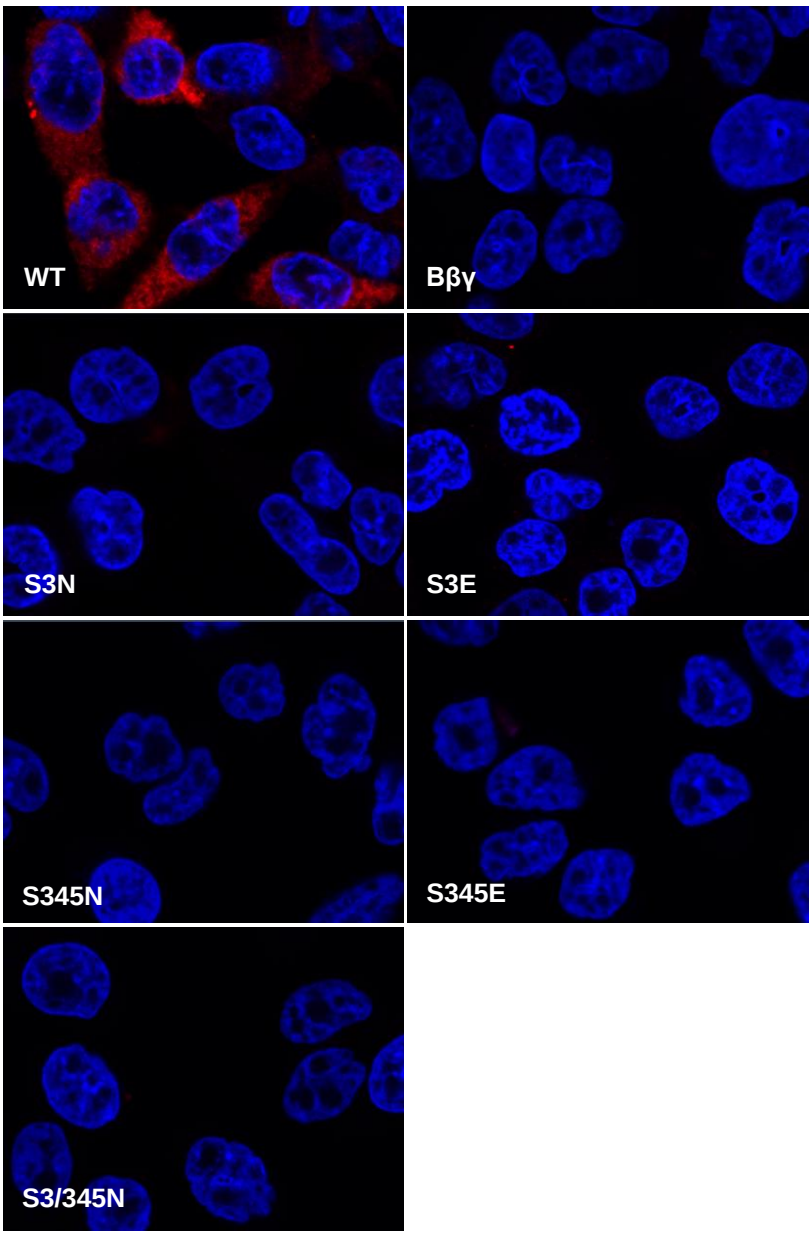

Figure 27. Immunofluorescent staining of fibrinogen Aα chain in CHO cells. CHO-WT, CHO-Bβγ and CHO cells transfected with variant fibrinogen Aα chain constructs (S3N, S3E, S345N, S345E, S3/345N) were fixed onto an 8-well chamber slide and incubated with mouse monoclonal anti-fibrinogen Aα chain (red) (1.5 µg/ml) and Cy3-AffiniPure donkey anti-mouse (1/1000) antibodies. Mounting medium contained DAPI nucleic acid stain (blue). Images were captured by LSCM with a 60x oil objective lens.

Finally, fibrinogen Aα chain expression levels in CHO cells transfected with the S3N and S345N variant constructs were compared by RNA extraction and end-point RT-PCR in a single experiment. Reactions were analysed by agarose gel electrophoresis and the results are displayed in figure 28. A strong band at 325bp, representing the fibrinogen Aα chain amplification product, was present in the CHO-WT reaction but was absent in all of the four selected S3N clones. Faint duplicate bands

appeared for the S345N clones, but the lower of the two bands was also present in the CHO-Bβ negative control, indicating contamination. The upper band is also likely to be contamination given its faint appearance, as well as the limitations of end-point RT-PCR in detecting changes in expression levels, beyond confirming presence or absence. Real-time PCR with melting curve analysis would confirm whether or not these amplification products correspond to the fibrinogen Aα chain, and enable comparison of expression levels. The lack of fibrinogen Aα chain mRNA in transfected CHO cells points to a problem with transfection. However, a higher number of clones should be screened to ascertain if this is the case.

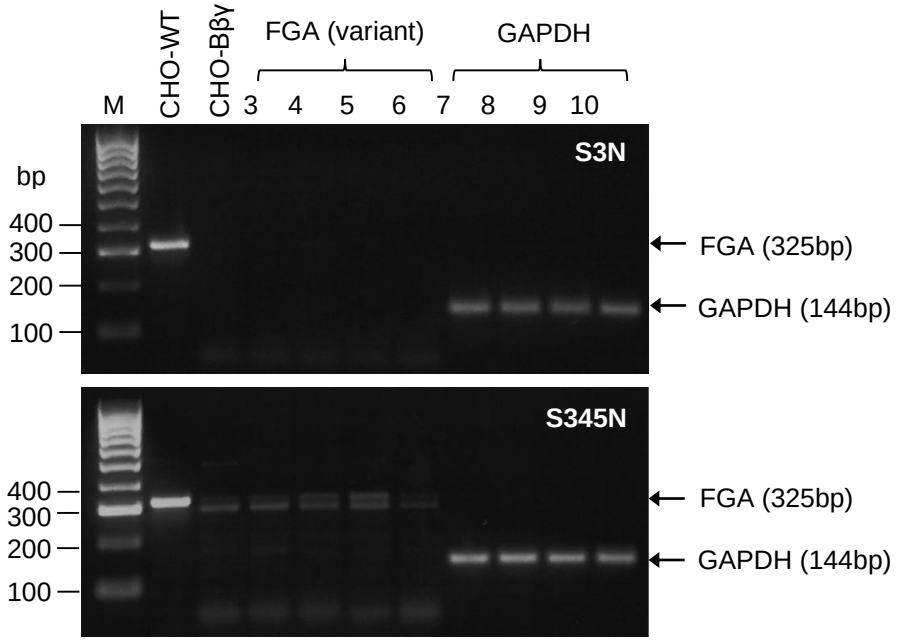

Figure 28. RT-PCR analysis of S3N and S345N variant fibrinogen Aα chain mRNA expression in CHO cells. RNA was extracted from CHO-Bβγ cells (negative control) and transfected CHO cells expressing WT (positive control), S3N, or S345N fibrinogen. Extracted RNA (100 ng) was reverse transcribed and amplified using primers specific to the fibrinogen Aα chain [0.6 µM] (FGA; lanes 1-6) or GAPDH control (lanes 7-10) for 40 cycles. The data are from a single experiment (n=1). The PCR products were visualised by 2% agarose gel electrophoresis. M: Hyperladder I molecular weight marker; lane 1: CHO-WT; lane 2: CHO-Bβγ; lanes 3-6: S3N or S345N clones amplified with FGA primers; lanes 7-10: S3N or S345N clones amplified with GAPDH primers. S3N clones (left to right): 1, 7 12, 24. S345N clones (left to right): 8, 11, 21, 32.

3.1.4. Co-transfection of pMLP-Aα and –γ into CHO-Bβ cells

To test the hypothesis that expression of recombinant fibrinogen in CHO cells may be affected by the order of transfection of Aα, Bβ and γ chain cDNA constructs, transfections were repeated with co-transfection of pMLP-Aα and –γ into a CHO-Bβ cell line. Prior to transfection, each pMLP construct was sequenced to verify sequence integrity. This highlighted some minor errors in the previously recorded sequences, however the open reading frames were of correct nucleotide sequence for translation of the corresponding polypeptide chains. Sequences of pMLP-Aα, -Bβ and –γ are displayed in Appendix 2.

New CHO cells were purchased and transfected with linearised pMLP-Bβ and pSELECT-neo selection vector to establish a CHO-Bβ cell line. As individual fibrinogen chains are not secreted, expression of the Bβ chain in 12 selected clones was compared by RNA extraction and real-time PCR. Clone 12 exhibited significantly higher expression than other clones (figure 29) and was therefore the cell line of choice for subsequent co-transfection of Aα and γ chain constructs.

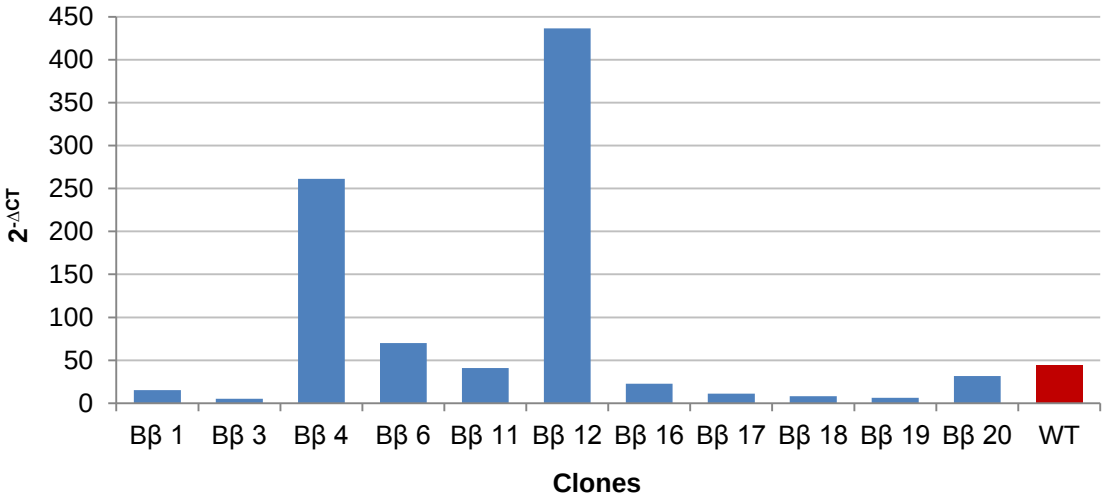

Figure 29. Comparison of fibrinogen Bβ chain expression in clones of transfected CHO cells by real-time PCR. CHO cells transfected with pMLP-Bβ were cultured in selection medium to form stable clones. Individual clones were screened for fibrinogen Bβ chain expression by RNA extraction and real-time PCR. Extracted RNA (20 ng) was amplified using primers specific to the Bβ chain [0.2 µM] for 40 cycles and the relative expression in each clone was compared using a $2^{-\Delta CT}$ calculation. The clone with the highest expression (clone 12) was used for subsequent co-transfection of Aα and γ chain constructs.

The established CHO-Bβ cell line was co-transfected with pMLP-Aα WT or S345N, pMLP–γ and pSELECT-zeo-ncs selection vector. Cells were split into varying dilutions after transfection and cultured in selection medium containing zeocin at a final concentration of 200 µg/ml to obtain stable clones expressing fibrinogen. With application of selection pressure, only one set of S345N dishes (split 1/80) survived and formed colonies. These were transferred to a 24 well plate and screened by fibrinogen ELISA. The results showed that none of the medium samples contained fibrinogen. No colonies had formed in the other S345N dishes or any of the WT dishes and the cells died within a few days, suggesting one of three things: i) the transfection was unsuccessful, ii) the cells were diluted too much before adding selection medium, or iii) the concentration of zeocin in the selection medium was too high. As there had not previously been any problems with uptake of selection vector and stable colony formation, the latter two options seemed more likely. Therefore, a subsequent experiment was conducted to optimise zeocin concentration by transfection of pSELECT-zeo-mcs into CHO cells via the normal method, and incubation of transfected cells with medium containing a concentration range of zeocin. Cells were plated at different dilutions and the highest concentration of zeocin that permitted colony formation (150 µg/ml) was selected as the optimal concentration. The optimal dilution factor for cells before selection was in this case 1/40. However, a repeat attempt at co-transfection of pMLP-Aα and –γ was again unsuccessful, failing to produce healthy colonies despite plating cells at a lower dilution with less zeocin. This process was not repeated further due to the lengthy nature of CHO cell transfections; instead, a new transient transfection method using Expi293F cells was tested for expression of variant fibrinogen.

3.1.5. Recombinant fibrinogen expression in Expi293F cells

The pMLP constructs used for transfection of CHO cells were transiently transfected into Expi293F cells for expression of recombinant fibrinogen. Initially, pMLP-Aα WT, pMLP-Bβ and pMLP-γ were transfected for expression of WT fibrinogen. An aliquot of medium was removed on days 3, 5 and 7 post-transfection for analysis of fibrinogen expression by ELISA. Fibrinogen was present in the medium, with very similar concentrations for each day, suggesting an optimal time course of 7 days. The concentration of fibrinogen in medium from day 7 was 4 µg/ml, giving an overall yield of 200 µg fibrinogen from a 50 ml culture, some of which would also be lost during purification. Secreted fibrinogen was visualised by western blotting with an anti-fibrinogen antibody, which showed three clean bands at the correct molecular weights for the fibrinogen Aα, Bβ and γ chains (figure 30).

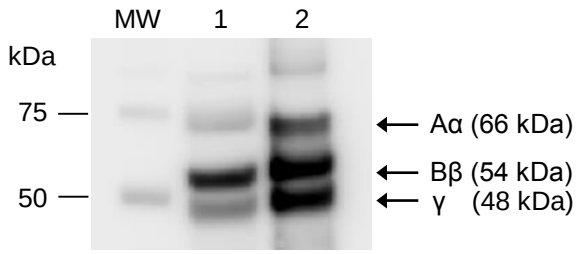

Figure 30. Western blot of recombinant fibrinogen secreted by Expi293F cells transfected with the pMLP constructs. Conditioned medium from Expi293F cells transiently transfected with pMLP-Aα, -Bβ and -γ was harvested, concentrated and analysed by reducing SDS-PAGE and western blotting with a rabbit polyclonal anti-fibrinogen antibody (1/1000). MW: molecular weight marker; lane 1: Expi293F fibrinogen (20 µl); AP-fibrinogen control (300 ng).

In attempt to achieve a more proficient yield, Aα WT, Aα S345N, Bβ and γ chain cDNAs were removed from pMLP by restriction digestion and inserted into the pmC vector. This vector contains a CMV promoter, which is recommended for high protein expression in Expi293F cells. The new constructs were analysed by agarose gel electrophoresis which revealed clean bands at the correct molecular weights of 4783 bp, 4326 bp and 4178 bp for pmC-Aα, -Bβ or –γ respectively, indicating successful ligation of vector and insert (figure 31). Prior to Expi293F transfection, each pmC construct was individually transfected into CHO cells to test their viability for protein expression, as this is a more cost effective method. Cells were lysed and analysed by western blotting (figure 32). After the first attempt, only the γ chain was detected in the medium. A repeat attempt confirmed expression of the Bβ chain as well, but the WT Aα chain was not detected; this may be due to variability in transfection efficiency between experiments. An additional band above the Bβ chain, of approximately 60 kDa, is a result of non-specific interaction of the secondary antibody or intrinsic peroxidase acitivty, as discussed previously in section 3.1.3.

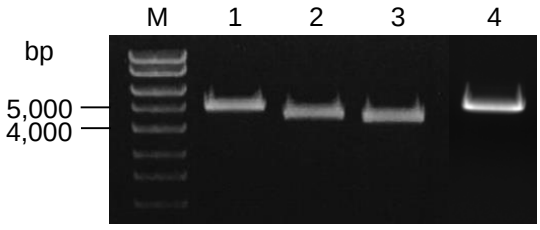

Figure 31. Agarose gel electrophoresis of the pmC fibrinogen expression constructs. Restriction digestion reactions were prepared with 4 µg pmC-Aα WT (lane 1), pmC-Bβ (lane 2), pmC–γ (lane 3) or pmC-Aα S345N (lane 4) maxi-preps and 30 U EcoRI. Reactions were incubated for 16 hours at 37°C and analysed by agarose gel electrophoresis on a 1 % gel in TE buffer. M: Hyperladder I molecular weight marker.

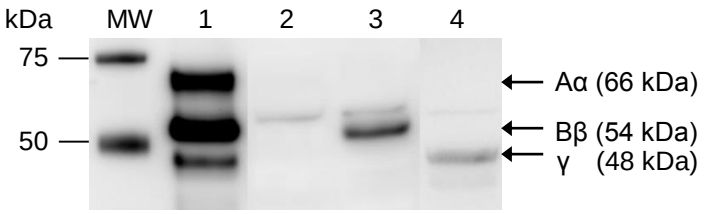

Figure 32. Western blot of lysate from CHO cells transfected with the pmC expression constructs. Fibrinogen expression constructs pmC-Aα WT, -Bβ and –γ were transiently transfected into CHO cells and the cells were lysed 2 days later. Cell lysate (20 µl) was analysed by SDS-PAGE and western blotting with a rabbit polyclonal anti-fibrinogen antibody (1/1000) to screen for expression of the individual chains. MW: molecular weight marker; lane 1: AP-fibrinogen control (100 ng); lanes 2-4: lysate of CHO cells transfected with pmC-Aα (2), -Bβ (3) and –γ (4). A non-specific band of approximately 60 kDa is present in lysate lanes (2-4).

With confirmation that Bβ and γ chains could be expressed in CHO cells, pmC-Aα WT or S345N, pmC-Bβ and pmC-γ were transfected together into Expi293F cells for fibrinogen expression. Medium was harvested on day 7 and analysed by ELISA and western blotting. Both WT and S345N fibrinogen were successfully expressed using this system (figure 33). Wild-type fibrinogen was at a concentration of 10 µg/ml and S345N fibrinogen was at 16 µg/ml, giving a yield of 300 µg or 480 µg respectively from a 30 ml culture. This outcome demonstrates for the first time that fibrinogen can be expressed without the Ser345 phosphorylation site; however, the γ chain in S345N fibrinogen exhibited a slightly higher molecular weight (approximately 50 kDa) compared to the normal 48 kDa, which warrants further investigation. In addition, there was only a marginal improvement in yield after cloning into pmC. Given the high cost and low yield, this approach did not seem suitable for large-scale expression of recombinant fibrinogen variants.

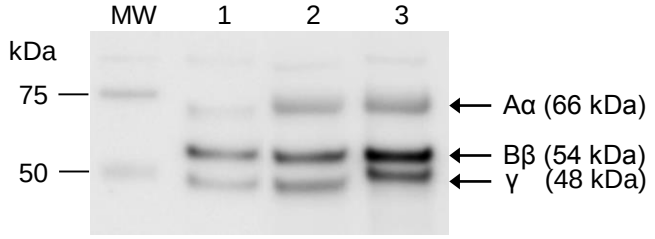

Figure 33. Western blot of recombinant fibrinogen secreted by Expi293F cells transfected with the pmC constructs. Conditioned medium from Expi293F cells transiently transfected with pmC-Aα WT or S345N, pmC-Bβ and pmC-γ was harvested and concentrated before measuring the fibrinogen concentration by ELISA. Fibrinogen (50 ng) was analysed by SDS-PAGE and western blotting with a rabbit polyclonal anti-fibrinogen antibody (1/1000). MW: molecular weight marker; lane 1: Calbiochem® fibrinogen control; lane 2: Expi293F WT fibrinogen; lane 3: Expi293F S345N fibrinogen.

3.2. Functional studies with fibrinogen phosphorylation isoforms

Normally, plasma fibrinogen is approximately 20-25% phosphorylated. Due to problems with expression of recombinant fibrinogen lacking the Ser3 and Ser345 phosphorylation sites, another approach was sought to investigate the function of this modification; this involved separation of phosphorylated from non-phosphorylated fibrinogen by chromatography. Functional studies were then conducted using these samples.

3.2.1. Preparation of fibrinogen phosphorylation isoforms

3.2.1.1. Separation of phosphorylated and non-phosphorylated fibrinogen by DEAE anion-exchange chromatography

With a pI of 5.6, fibrinogen has a net negative charge at physiological pH. The addition of phosphate to fibrinogen makes the protein more negatively charged. Therefore, a positively charged DEAE Fast Flow column was used to bind fibrinogen, with a greater affinity for the phosphorylated form. Initially fibrinogen eluted as a single peak, therefore several parameters were optimised. The pH of the equilibration buffer was lowered from 8 to 6.8 and gradient time was doubled from 4 CV to 8 CV, but unfortunately there was still no separation of the phosphorylation isoforms. Extension of the gradient time to 30 CV and reduction of the binding flow rate to 0.2 ml/min resulted in two elution peaks, but the second peak was very small and not distinct from the first peak. Further doubling of the gradient time to 60 CV did not improve resolution or the size of the second peak. Figure 34 displays a chromatogram of the elution phase. The degree of phosphorylation of fibrinogen in each peak was assessed using the malachite green assay. The amount of phosphate in each well was determined from a standard curve and used to calculate the mol phosphate/mol fibrinogen. This was converted to a percentage of phosphorylation based on the assumption that fibrinogen has a theoretical maximum of 4 mol phosphate/mol fibrinogen (two sites per Aα chain). The results of this assay confirmed a slight enrichment of phosphorylated fibrinogen in the second anion exchange elution peak, from 25 % (1 mol phosphate/mol fibrinogen) for control AP-fibrinogen to 36 % phosphorylation (1.45 mol phosphate/mol fibrinogen). The first elution peak was only slightly reduced from 25.0 % to 24 % phosphorylation (0.94 mol phosphate/mol fibrinogen).

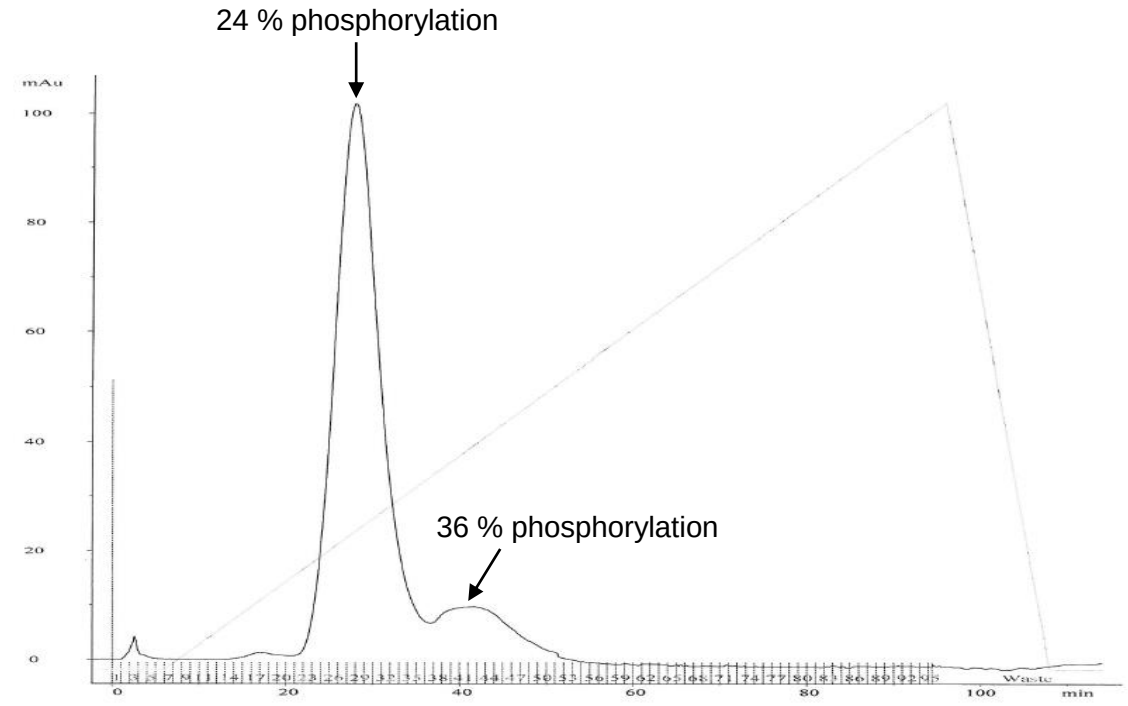

Figure 34. Anion exchange chromatography with fibrinogen. Calbiochem® fibrinogen (2 mg) was applied to a DEAE Sepharose Fast Flow column and eluted with an increasing concentration of NaCl up to 1M. The chromatogram shows the elution phase with two peaks of 24 % and 36 % phosphorylated fibrinogen, as determined by malachite green assay. Chromatography was performed using an ÄKTA prime system.

3.2.1.2. Separation of phosphorylated and non-phosphorylated fibrinogen by Phos-tag™ affinity chromatography

Phos-tag™ chromatography was employed as an alternative to anion exchange chromatography in attempt to achieve greater separation of phosphorylated and non-phosphorylated fibrinogen. During the first trials of this method, all of the loaded fibrinogen (1 mg) came through the column in the flow through and there was no detectable elution of bound fibrinogen. Loading more fibrinogen (4 mg) at a reduced flow rate of 0.1 ml/min resulted in an elution peak which was collected, dialysed against TBS-1 pH 7.4 and analysed by malachite green assay. An aliquot of phosphate buffer-only was also dialysed against TBS-1 pH 7.4 and included in the malachite green assay as a control for residual NaH_2PO_4; unfortunately the control sample and the eluted fibrinogen sample both appeared overly green in the assay, indicating contamination with phosphate from the elution buffer due to insufficient dialysis. Therefore, the elution buffer was changed to 50 mM EDTA, which had an equally effective outcome in terms of the resulting elution peak and enabled subsequent analysis of phosphate content by malachite green assay. Fibrinogen in the flow through

and elution fractions was 18 % and 50 % phosphorylated respectively. As this produced a greater range in degree of phosphorylation than the anion exchange method, Phos-tag™ chromatography was repeated several times to obtain enough fibrinogen from each peak for functional studies. Figure 35 shows a typical chromatogram of this method with flow through and elution peaks. The phosphate content of fibrinogen from each peak was determined by malachite green assay: 13 % (0.5 mol phosphate/mol fibrinogen) and 33 % (1.3 mol phosphate/mol fibrinogen) phosphorylation for fibrinogen from flow through and elution peaks respectively. Details of these samples are summarised in table 14, section 3.2.1.4. Unfortunately there was far less enrichment of phosphorylated fibrinogen than the first attempt. However, there was a 2.5-fold difference between the 13 % and 33 % samples, which mimics the rise in phosphorylation during the acute phase (from 20-25 % to approximately 50-70 %).

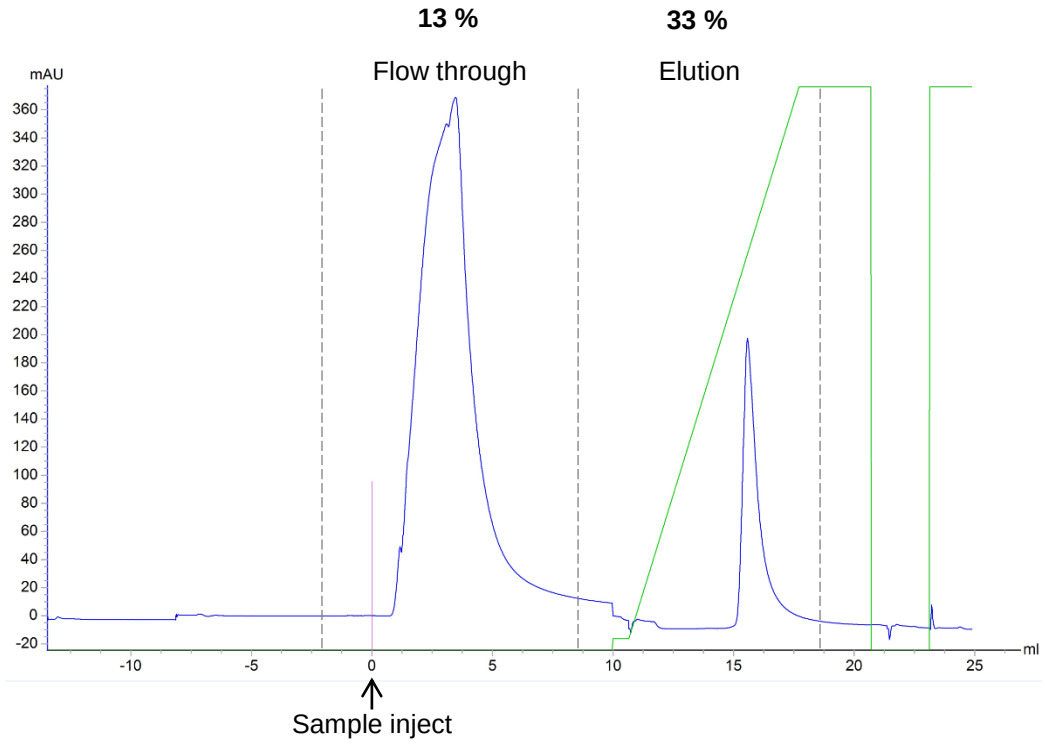

Figure 35. Phos-tag™ Agarose affinity chromatography with fibrinogen. Calbiochem® fibrinogen (4 mg) was loaded onto a Phos-tag™ Agarose column and the bound phosphorylated fibrinogen was eluted with a gradient of EDTA up to 50 mM. The chromatogram shows the point of sample inject as well as flow through and elution peaks, containing 13 % and 33 % phosphorylated fibrinogen respectively. The green lines represent EDTA concentration. Chromatography was performed using an ÄKTA avant 25 system.

3.2.1.3. Dephosphorylation of fibrinogen

Ammonium sulphate-precipitated fibrinogen was dephosphorylated using bovine intestinal alkaline phosphatase and purified from the reaction mix by IF-1 affinity chromatography. Dephosphorylation was confirmed by malachite green assay which revealed a 4 % degree of phosphorylation (0.16 mol phosphate/mol fibrinogen) in the purified fibrinogen sample – an 84 % reduction from control levels (0.98 mol phosphate/mol fibrinogen) (table 14).

3.2.1.4. Fibrinogen samples for functional studies

As previously described in section 3.2.1.2, phosphorylated and non-phosphorylated fibrinogen were separated by Phos-tag™ affinity chromatography. Control Calbiochem® fibrinogen and dephosphorylated Calbiochem® fibrinogen were also purified by IF-1 affinity chromatography. Collectively, this produced four fibrinogen samples with varying degrees of phosphorylation:

1. **Control** IF-1 purified Calbiochem® fibrinogen (25 % phosphorylation)
2. **Dephosphorylated** fibrinogen (4 % phosphorylation)
3. Phos-tag™ chromatography flow through fibrinogen (**13 %** phosphorylated)
4. Phos-tag™ chromatography eluted fibrinogen (**33 %** phosphorylated)

The degree of phosphorylation of each sample was determined using the malachite green assay. Table 14 shows a summary of malachite green assay data, including the percentage phosphorylation of each sample. The four samples were then compared in a variety of assays to investigate the functional effects of fibrinogen phosphorylation.

	Control	Dephosphorylated	Flow through	Elution
pmol phosphate	245	40	125	325
mol phos/mol fg	0.98	0.16	0.50	1.30
% phosphorylation	25	4	13	33

Table 14. Malachite green assay with Phos-tag™ chromatography peaks and dephosphorylated fibrinogen. The degree of phosphorylation of fibrinogen from Phos-tag™ chromatography flow through and elution peaks, as well as IF-1 purified control and dephosphorylated Calbiochem® fibrinogen, was determined by malachite green assay. The data are based on duplicate wells from a single experiment. For each sample, pmol phosphate was divided by 250 pmol fibrinogen to convert to mol phosphate/mol fibrinogen. This value was divided by four to calculate the percentage phosphorylation, assuming a theoretical maximum of 4 mol phosphate/mol fibrinogen.

3.2.2. The effect of fibrinogen phosphorylation on the interaction between fibrinogen and other plasma components

Fibrin(ogen) interacts with several other plasma proteins during coagulation, including FXIII, α2-AP and plasmin(ogen). Given that these proteins bind or become covalently cross-linked to the αC region of the fibrinogen Aα chain, in proximity to Ser345, it is possible that phosphorylation of fibrinogen may regulate these interactions in some way. Studies were therefore conducted to investigate the effect of fibrinogen phosphorylation on FXIII cross-linking activity, including fibrin chain cross-linking and incorporation of α2-AP, as well as plasminogen binding and the rate of plasmin digestion of fibrinogen.

3.2.2.1. FXIII-mediated cross-linking of fibrin α and γ chains

A biotin pentylamine incorporation assay was used to investigate the effect of fibrinogen phosphorylation on the cross-linking of fibrin α and γ chains by rFXIII-A, using phosphorylated (13 %, 25 %, 33 %) and dephosphorylated fibrinogen substrates. The results showed a similar trend of biotin-pentylamine incorporation over time for the varying degrees of phosphorylation (figure 36). The same trend was observed in three independent experiments and suggests that phosphorylation does not influence clot stabilisation via inter-chain fibrin cross-linking.

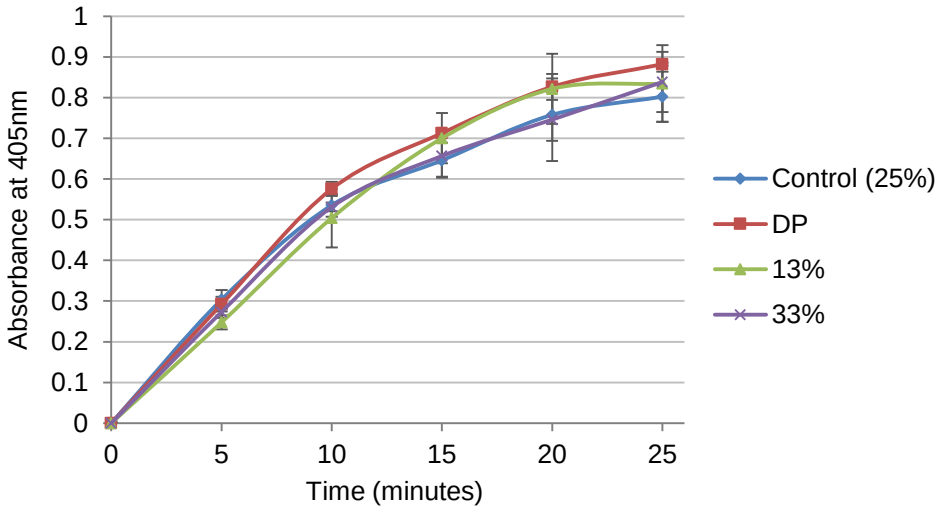

Figure 36. Biotin-pentylamine incorporation by rFXIII-A. Cross-linking of biotin-pentylamine [2.7 µM] to phosphorylated (13 %, 25 % and 33 %) and dephosphorylated (DP) fibrinogen [40 µg/ml] by rFXIII-A [1.1 µg/ml] in the presence of 1 U/ml thrombin and 1mM $CaCl_2$ was measured over 25 minutes and detected with streptavidin alkaline phosphatase and PNPP substrate. The data shown are an average of three wells from a single experiment, with error bars representing standard deviation. The data are representative of three independent experiments (n=3).

3.2.2.2. Incorporation of α2-AP

Two separate assays were used to monitor cross-linking of α2-AP to the fibrin α chain: an α2-AP incorporation assay and a clot-based plasmin generation assay. For the incorporation assay, phosphorylated (13 %, 25 %, 33 %) and dephosphorylated fibrinogen samples were converted to fibrin in the presence of thrombin and $CaCl_2$ before adding a master mix containing rFXIII-A and α2-AP. Incorporation of α2-AP was measured over 50 minutes. Figure 37 shows the graph from one of three independent experiments, all of which demonstrated no difference in α2-AP incorporation with the varying degrees of phosphorylation.

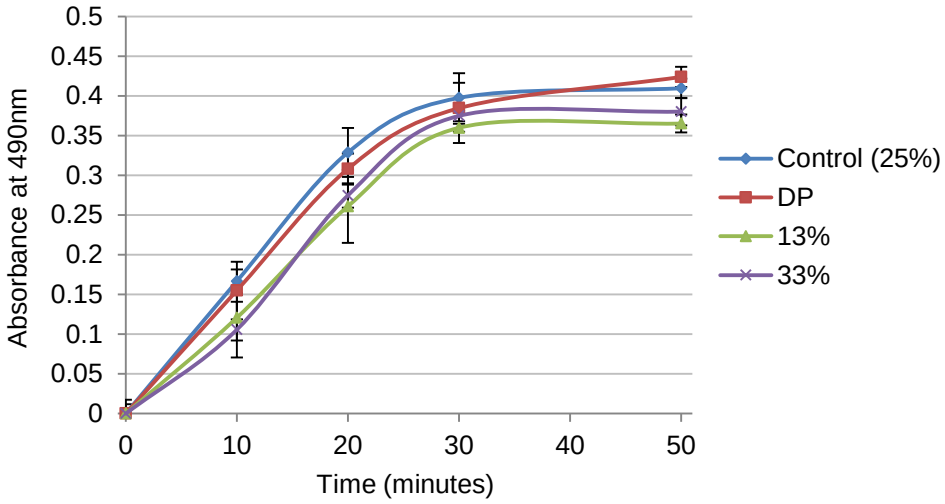

Figure 37. α2-AP incorporation by rFXIII-A. Fibrin was formed by incubation of fibrinogen [80 µg/ml] with 1 U/ml thrombin and 5 mM $CaCl_2$. Cross-linking of α2-AP [10 µg/ml] to phosphorylated (13 %, 25 % and 33 %) and dephosphorylated (DP) fibrin by rFXIII-A [1.1 µg/ml] was measured over 50 minutes and detected with a HRP-conjugated anti-α2-AP antibody (1/1000) and OPD substrate. The data shown are an average of three wells from a single experiment, with error bars representing standard deviation. The data are representative of three independent experiments (n=3).

For the plasmin generation assay, formation of a chromogenic substrate was used as a measure of plasmin activity, in the presence or absence of α2-AP. Results are displayed in figure 38. As expected, the increase in plasmin activity over time was delayed by the addition of plasmin inhibitor α2-AP, reaching the same plateau at approximately 1 hour 30 minutes without α2-AP and 2 hours 30 minutes with α2-AP. However, plasmin activity in clots formed from the different fibrinogen samples was identical whether α2-AP was included or not. This outcome was observed in three independent experiments. Taken together, the data from these two assays indicate that phosphorylation of fibrinogen neither promotes nor inhibits cross-linking of α2-AP to

Lys303 in the α chain, and therefore does not impact the rate of plasmin-mediated fibrinogen degradation by this means.

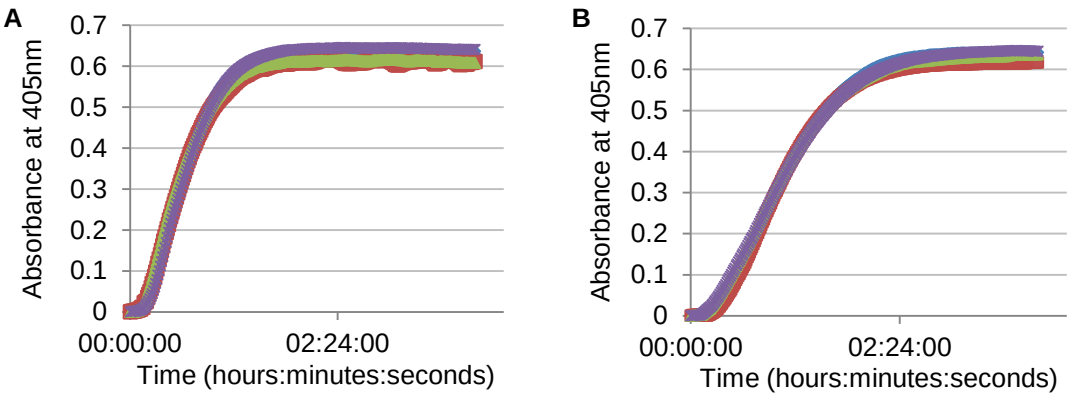

Figure 38. Plasmin generation assay. Clots composed of phosphorylated (13 %, 25 % and 33 %) and dephosphorylated (DP) fibrin were formed by incubation of fibrinogen samples at 0.25 mg/ml with plasminogen [312.5 µg/ml] and rFXIII-A [1.4 µg/ml] in the absence (A) or presence (B) of α2-AP [1.65 µg/ml]. Clotting was activated with 0.75 U/ml thrombin and 3.75 mM $CaCl_2$. Absorbance was monitored over 3 hours after addition of a lysis mix containing tPA [0.05 µg/ml] and S225-1 chromogenic substrate [0.6 mM] as an indicator of plasmin activity. Blue: control (25 %); red: dephosphorylated; green: 13 %; purple: 33 %. The data are an average of three wells from a single experiment, and are representative of three independent experiments (n=3).

3.2.2.3. Plasminogen binding

Binding of plasminogen to phosphorylated (13 %, 25 %, 33 %) and dephosphorylated fibrinogen was measured by ELISA at seven concentrations of plasminogen (3.75-240 nM), reflecting the published binding affinity of plasminogen to fibrin Aα221-610 of 32 nM (Tsurupa and Medved 2001). Three separate experiments revealed no difference in trend between the fibrinogen samples (figure 39), implying that plasminogen binding to the fibrinogen αC region is not altered by phosphorylation.

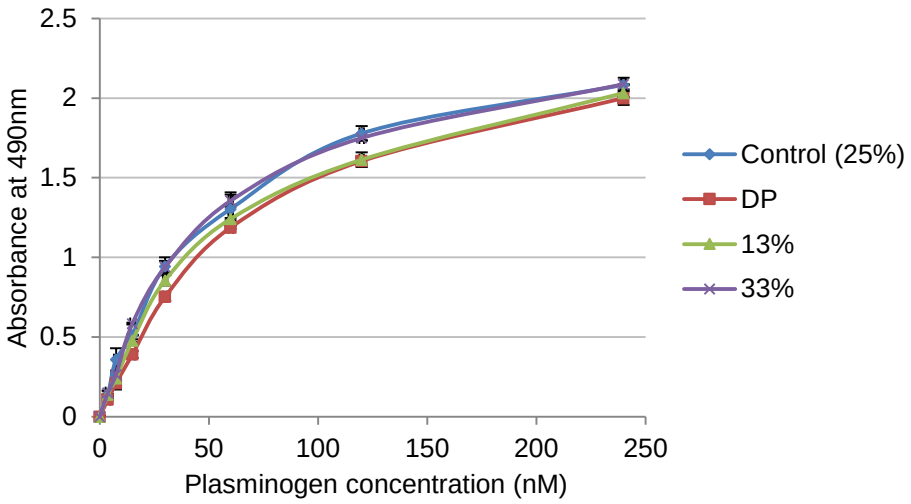

Figure 39. Plasminogen binding assay. Phosphorylated (13 %, 25 % and 33 %) and dephosphorylated (DP) fibrinogen [40 µg/ml] were incubated with increasing concentrations of plasminogen (0-240 nM) for 1 hour. Bound plasminogen was detected with an anti-plasminogen HRP antibody (1/2000) and OPD substrate. The data shown are an average from three wells of a single experiment, with error bars of standard deviation. The data are representative of three independent experiments (n=3).

3.2.2.4. Plasmin digestion of fibrinogen

The effect of fibrinogen phosphorylation on the rate of plasmin digestion was analysed using a time course experiment and non-reducing SDS-PAGE. A concentration range of plasmin from 27.5 nM to 440 nM at 0 and 40 minutes was tested in the first experiment and the optimal concentration of plasmin found to be 220 nM. At this concentration, fibrinogen was almost completely degraded and the bands representing fibrinogen fragments were clearly defined (figure 40A). A second experiment was conducted to optimise the time-scale, using a range of time points from 5 to 40 minutes. The results demonstrated almost complete digestion in just 5 minutes (figure 40B). Hence, a total duration exceeding 5 minutes would not be useful for monitoring a steady progression. One option to improve this method would have been to lower the plasmin concentration, however in the previous experiment there was still a lot of intact fibrinogen at the top of the lane using 110 nM plasmin. The time-course was therefore shortened from 40 minutes to 4 minutes with 30 second intervals for subsequent experiments.

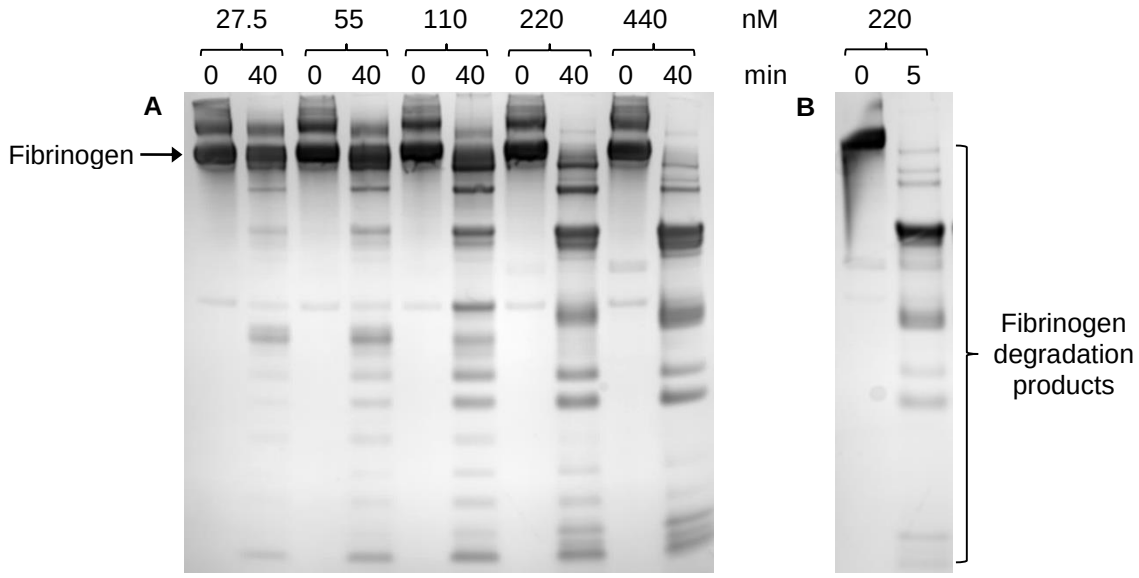

Figure 40. Optimisation of a plasmin digestion time course experiment. Fibrinogen (25 % phosphorylated) (10 µg) was digested with plasmin for controlled time periods before inhibiting with LDS sample buffer. Each reaction was separated by non-reducing SDS-PAGE. A) Incubation of fibrinogen with 27.5-440 nM plasmin for 0 and 40 minutes. B) Incubation of fibrinogen with 220 nM plasmin for 0 and 5 minutes, showing rapid degradation of fibrinogen.

Phosphorylated (13 %, 25 %, 33 %) and dephosphorylated fibrinogen were compared using this method. Figure 41 shows an example gel with 0 to 4 minutes plasmin digestion of control fibrinogen (25 % phosphorylated) and the appearance of fibrinogen degradation products over time. The intensity of fragment Y and fragment D1 in stained SDS-PAGE gels were analysed by densitometry, normalising to total protein. The results, expressed as a percentage of total protein, are plotted against time in figure 42. The graphs represent data averaged from two independent experiments and show an increase in fragment Y and fragment D1 over time. There was no difference in fragment Y formation over time between the fibrinogen samples, but a slight decrease in fragment D1 formation with more phosphorylation. However, this was not significant and the DP sample did not fit with this trend, so it is unclear whether this effect is genuine or due to experimental error. A more sensitive assay may be needed to clarify this result.

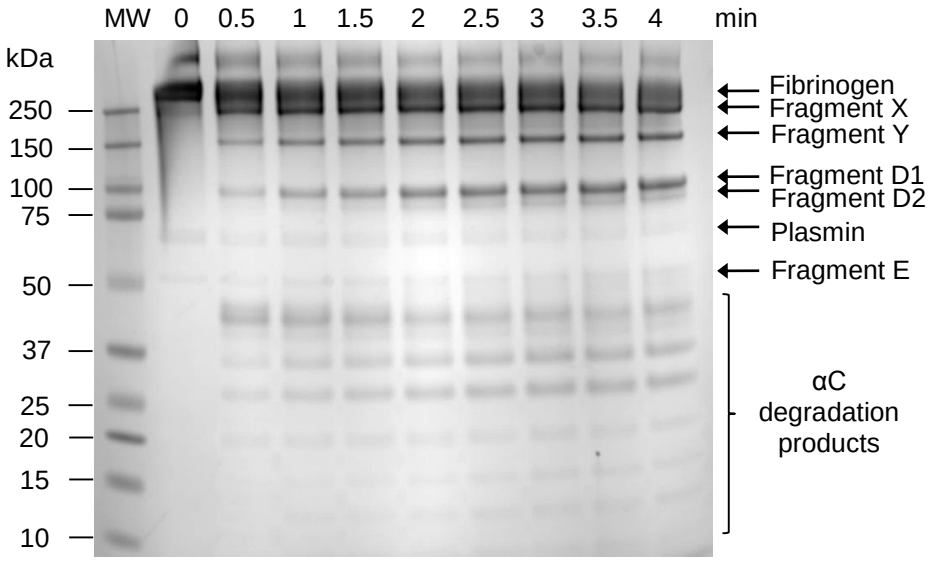

Figure 41. Plasmin digestion of fibrinogen. Fibrinogen (25 % phosphorylated) (10 µg) was incubated with 220 nM plasmin for 0-4 minutes in 30 second intervals and reactions were inhibited with LDS sample buffer. Each reaction was separated by non-reducing SDS-PAGE to visualise the fibrinogen degradation products (indicated by arrows) and Aα chain (αC) degradation products. MW: molecular weight marker. The above gel is an example from one of two experiments with phosphorylated (13 %, 25 % and 33 %) and dephosphorylated fibrinogen.

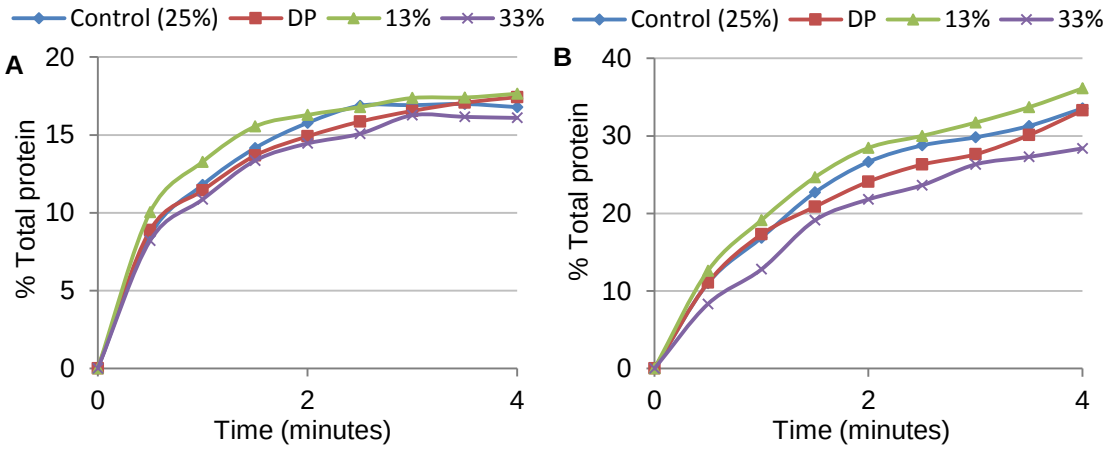

Figure 42. Densitometry of fibrinogen degradation products over time with plasmin digestion. Phosphorylated (13 %, 25 %, 33 %) and dephosphorylated fibrinogen samples (10 µg) were incubated with 220 nM plasmin for 0-4 minutes in 30 second intervals and separated by non-reducing SDS-PAGE. The intensity of bands corresponding to fragment Y (A) and fragment D1 (B) over time were analysed by densitometry and normalised to total protein in each lane. Results are expressed as a percentage of total protein and represent average values from two independent experiments (n=2).

3.2.3. The effect of fibrinogen phosphorylation on clot structure

3.2.3.1. Turbidity analysis

Comparison of fibrin fibre diameter and overall clot structure was conducted by spectrophotometric turbidity analyses and electron microscopy of clots composed of phosphorylated (13 %, 25 %, 33 %) and dephosphorylated fibrin. Turbidity data averaged from five independent experiments were analysed using a customised programme for calculation of MaxAbs and clotting rate variables. The results demonstrated a relationship between the degree of phosphorylation and fibre thickness. Higher phosphate content produced lower MaxAbs values, with a significant reduction from 0.068 for dephosphorylated fibrin to 0.036 for 33 % phosphorylated fibrin (p=0.0011) (figure 43A and B). Despite this trend, there was a negligible difference between MaxAbs values for the 25 % (0.044) and 13 % phosphorylated samples (0.046) (p=0.7727), and only a small difference between the 25 % and 33 % phosphorylated samples (p=0.0728). However, the decline in MaxAbs from 13 % to 33 % phosphorylation was statistically significant (p=0.0247). The observed reduction in MaxAbs indicates thinner fibres with increasing phosphorylation. Clotting rate showed a similar trend to MaxAbs, with increasing phosphorylation levels leading to slower clot formation, but with less of a difference between each sample (figure 43C). Again, incremental differences from 13 % to 25 %, and from 25 % to 33 % phosphorylation were non-significant (p=0.8484 and p=0.1292 respectively), but the difference in clotting rate between 13 % and 33 % phosphorylation was found to be significant (p=0.0256). Clotting rate for dephosphorylated fibrin was higher than for each of the other three fibrinogens (13 %, 25 % and 33 % phosphorylation), with an overall reduction from 2.069×10^{-4} to 1.549×10^{-4} absorbance units/second (p=0.0033). Lag time was too short for comparable measurement using this method, so the effect of phosphorylation on the rate of lateral aggregation of protofibrils could not be inferred. The experiment could be repeated using a lower thrombin concentration to slow down this initial stage and enable comparison.

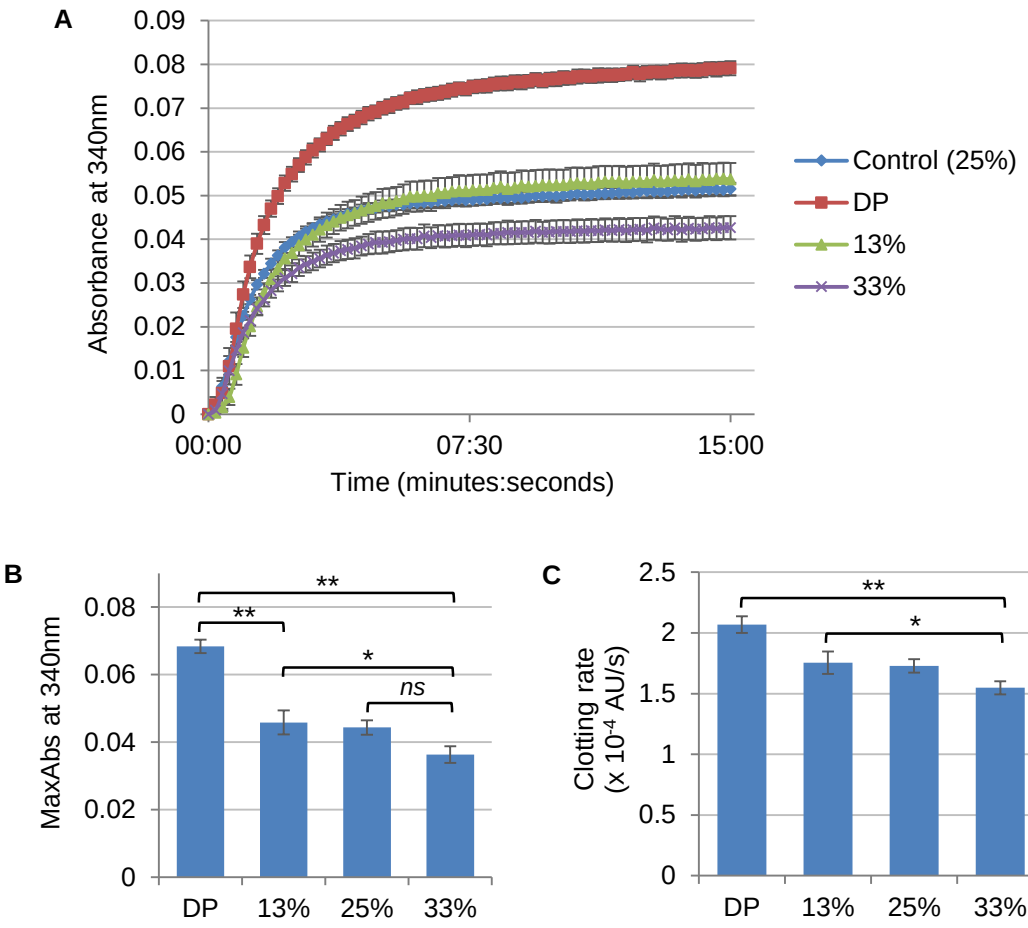

Figure 43. Analysis of fibrin clot turbidity. A) Clots composed of phosphorylated (13 %, 25 % and 33 %) and dephosphorylated (DP) fibrin were formed by incubation of fibrinogen samples at 0.25 mg/ml with plasminogen [312.5 µg/ml] and rFXIII-A [1.4 µg/ml], plus an activation mix containing 0.75 U/ml thrombin and 3.75 mM $CaCl_2$. The absorbance at 340 nm was recorded over 15 minutes. A customised software application was used for calculation of MaxAbs (B) as an indication of fibre thickness, and clotting rate (C) in absorbance units per second (AU/s). The data in A, B and C are an average of five independent experiments (n=5), with error bars representing standard error of the mean. Statistical significance between mean MaxAbs and clotting rate values is indicated by * ($p<0.05$), ** ($p<0.01$) or *ns* (non-significant).

3.2.3.2. SEM of fibrin clots

Electron micrographs of clots showed a visible reduction in fibre diameter with higher degrees of phosphorylation (figure 44), supporting the turbidity data. This was analysed further using image analysis software, measuring the diameters of 20 fibres from five different images (a total of 100 fibres) per sample. Average fibre diameters were

58.6 nm, 40.6 nm, 35.6 nm and 31.7 nm for dephosphorylated fibrin, and 13 %, 25 % and 33 % phosphorylated fibrin respectively (figure 45A). Statistical analysis revealed significant differences between mean fibre diameter for each increment in phosphorylation level, from dephosphorylated fibrin to 13 % phosphorylation ($p=0.0002$), from 13 % to 25 % phosphorylation ($p=0.0006$), and from 25 % to 33 % phosphorylation ($p=0.0055$). Highly significant differences were found between dephosphorylated and 33 % phosphorylated fibrin, and between 13 % and 33 % phosphorylated fibrin ($p<0.0001$). The trend of lower turbidity with increasing phosphorylation was similar to that observed by turbidity analysis, but with more pronounced differences when comparing the 13 % and 33 % phosphorylated samples to control fibrinogen (25 % phosphorylation). A comparison of turbidity and electron microscopy results is displayed in figure 45B. By qualitative speculation, the electron micrographs also point to increased branching of fibres with more phosphate (figure 44), but this was not confirmed by quantitative means and warrants further investigation.

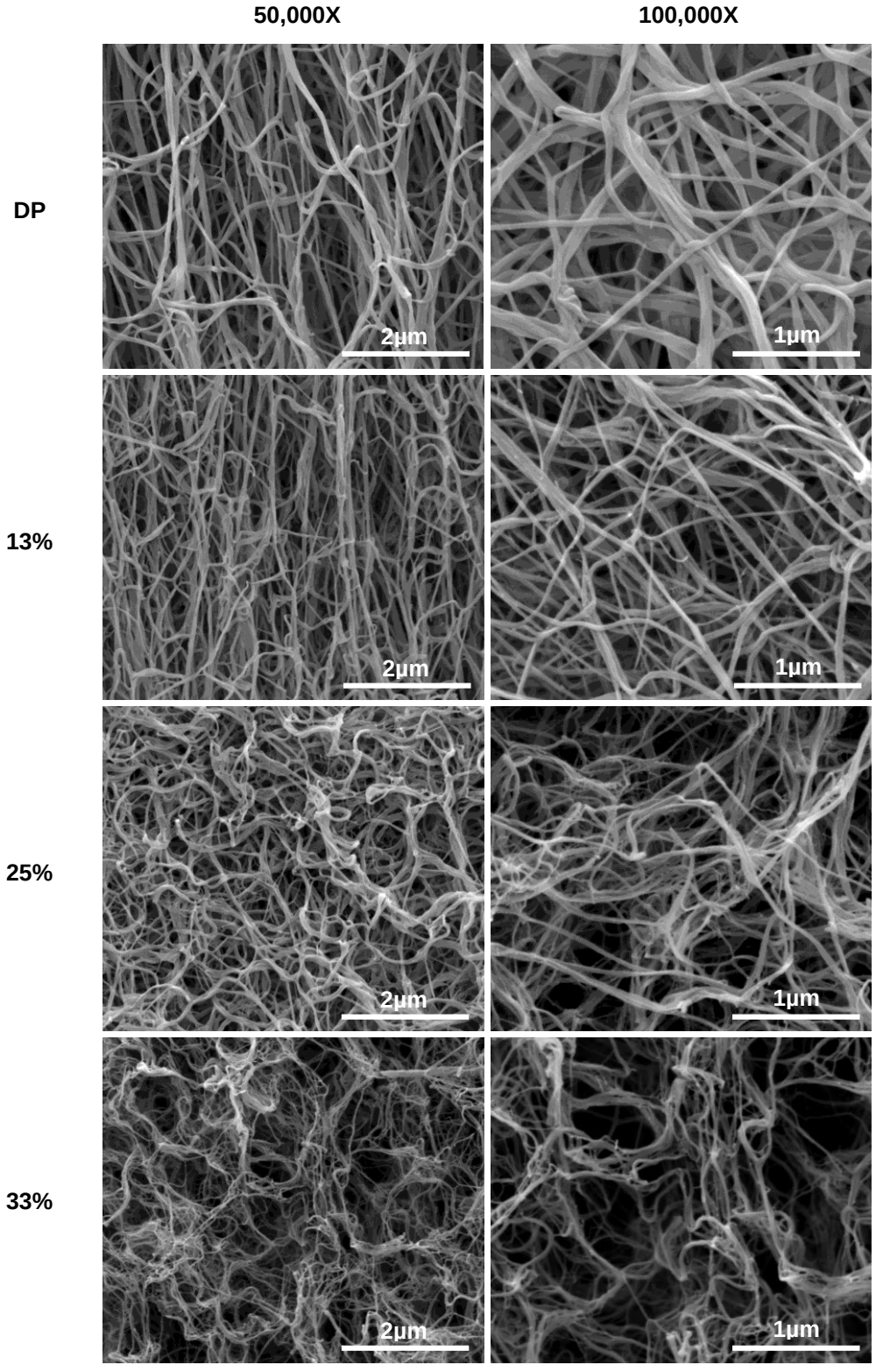

Figure 44. Scanning electron micrographs of fibrin clots. Phosphorylated (13 %, 25 % and 33 %) and dephosphorylated (DP) fibrinogen samples at 1 mg/ml were incubated with 1 U/ml thrombin and 10 mM $CaCl_2$ for clot formation. Clots were fixed in 2 % (v/v) gluteraldehyde, dried and coated with 7nm platinum-palladium before imaging by SEM at 50,000X and 100,000X magnification. Five different areas from a single clot were imaged per fibrinogen sample for analysis of fibre diameter. True dimensions are indicated by scale bars.

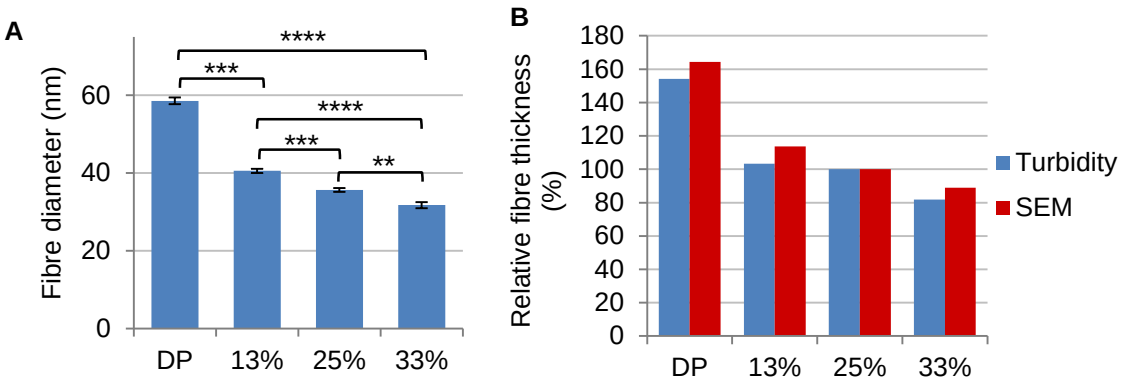

Figure 45. Comparison of fibrin fibre diameter. A) Diameters of phosphorylated (13 %, 25 % and 33 %) and dephosphorylated (DP) fibrin fibres in SEM images at 50,000X magnification were measured using ImageJ software. A total of 100 fibres were measured over five different areas per clot (20 fibres per image) (n=5). Average values are displayed with error bars representing standard error of the mean. Statistical significance between mean fibre diameters is indicated by ** ($p<0.01$), *** ($p<0.001$), or **** ($p<0.0001$). B) Comparison of the effect of fibrinogen phosphorylation on fibre thickness as determined by turbidity assay (MaxAbs) and SEM. Data are expressed as a percentage of the control sample (25 % phosphorylation).

Taken together, the results of the turbidity and SEM experiments demonstrate that phosphorylation of fibrinogen has a notable impact on clot structure. In addition to the slower clotting rate, an elevated degree of phosphorylation is likely to produce clots with thinner fibres and increased density due to more extensive branching – a typical pro-thrombotic clot structure. This highlights a detrimental role of fibrinogen phosphorylation in thrombosis.

3.3. Characterisation of intracellular fibrinogen phosphorylation

Studies were carried out using HepG2 cells to investigate the intracellular mechanism of fibrinogen phosphorylation in control and acute phase conditions. The main aims were to i) identify the subcellular site of fibrinogen phosphorylation, ii) identify the relevant kinase, and iii) determine whether the rise in fibrinogen phosphorylation in acute phase conditions occurs intracellularly or in circulation. Several methods were employed, including western blotting, ELISA and PLA.

3.3.1. Immunofluorescent detection of cellular fibrinogen Aα chains

Immunofluorescence was used to optimise various antibodies for subsequent PLA experiments. First, three different fibrinogen Aα chain antibodies were tested at varying concentrations to see which one gave the strongest signal in CHO-WT cells, with minimal background in CHO-Bβ cells (negative control). Neither of the rabbit polyclonal antibodies detected the fibrinogen Aα chain (figure 46A and B), but the mouse monoclonal antibody worked well at an optimal concentration of 1.5 µg/ml (figure 46C).

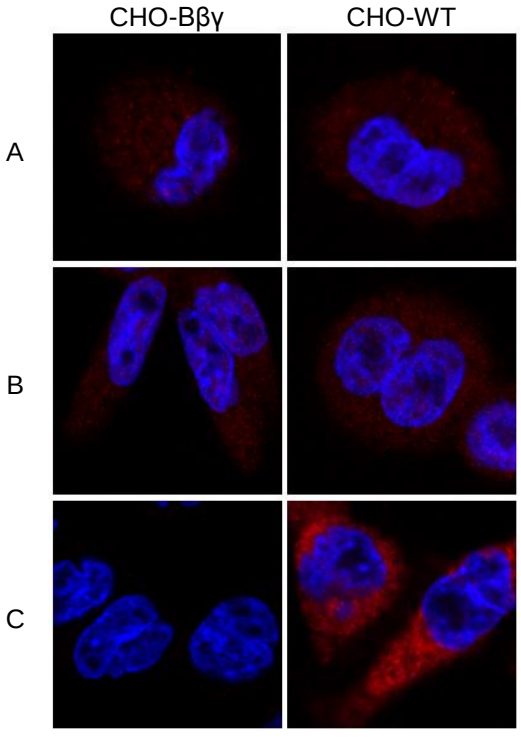

Figure 46. Validating antibodies for immunofluorescent detection of the fibrinogen Aα chain in CHO cells. CHO-WT and CHO-Bβ cells were fixed onto an 8-well chamber slide and incubated with antibodies to the fibrinogen Aα chain (red) at a range of concentrations. A and B: rabbit polyclonal anti-fibrinogen Aα chain; C: mouse monoclonal anti-fibrinogen Aα chain. Primary antibodies were detected with Alexa Fluor 488-Affini-Pure donkey anti-rabbit (1/1000) or Cy3-AffiniPure donkey anti-mouse (1/1000) secondary antibodies. Mounting medium contained DAPI nucleic acid stain (blue) and images were taken by LSCM with a 60x oil objective lens.

Antibodies against PDI and TGN46 were optimised for the detection of ER and *trans*-Golgi respectively. The concentrations that gave the highest signal:background ratio were selected for experiments; anti-PDI was used at a 1/50 dilution and anti-TGN46 was used at a 1/200 dilution. Figure 47 shows the immunofluorescent detection of fibrinogen Aα chains, PDI, TGN46 and nuclei in HepG2 cells. There was significant overlap between fibrinogen Aα chain and ER staining, which may represent pools of Aα-γ complexes in the ER (Yu et al., 1984, Xia and Redman, 2001). As expected, there was no significant co-localisation between the fibrinogen Aα chain and Golgi marker TGN46, implying that assembled fibrinogen travels quickly through the cell for secretion.

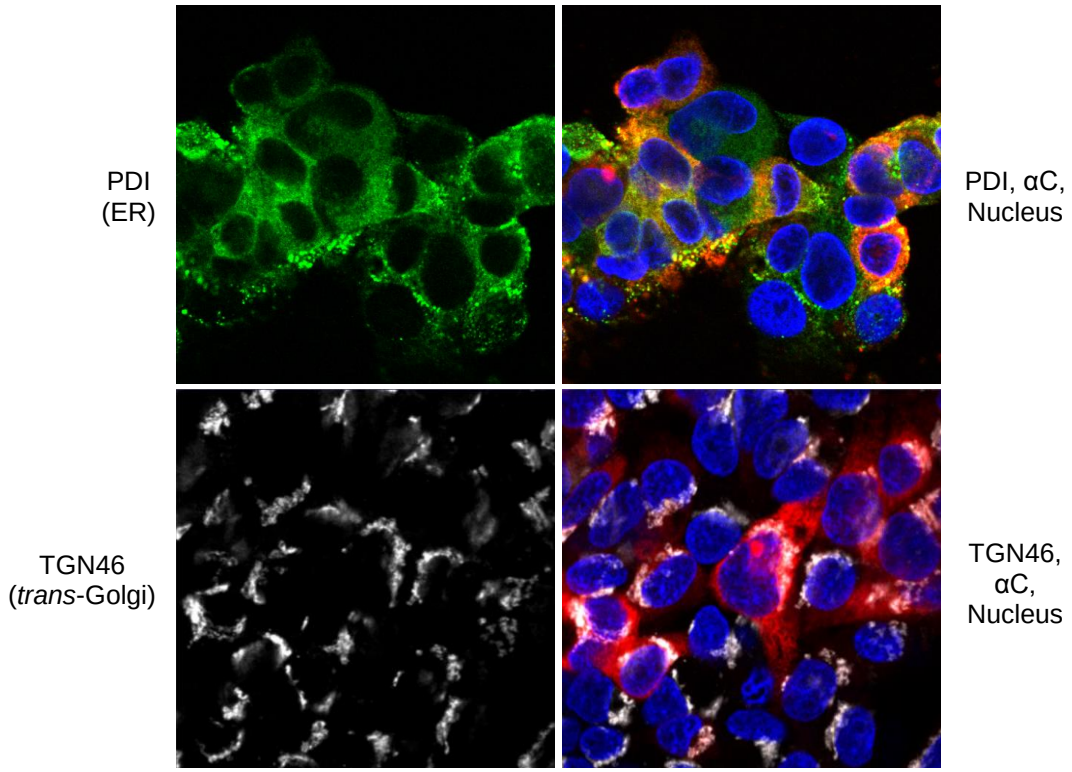

Figure 47. Immunofluorescent detection of ER and Golgi markers in HepG2 cells. HepG2 cells were fixed onto an 8-well chamber slide and incubated with a mouse monoclonal anti-fibrinogen Aα chain antibody (red) (1.5 µg/ml) plus an anti-PDI (ER marker; green) (1/50) or anti-TGN46 (*trans*-Golgi marker; white) (1/200) antibody. Primary antibodies were detected with Cy3-AffiniPure donkey anti-mouse (1/1000) or Alexa Fluor 647-AffiniPure donkey anti-sheep secondary antibodies (1/1000). Mounting medium contained DAPI nucleic acid stain (blue) and images were taken by LSCM with a 60x oil objective lens.

3.3.2. Detection of phosphorylated fibrinogen Aα chains in HepG2 cells by proximity ligation assay

Detection of a target by PLA requires two different primary antibodies to localise in close proximity. Having optimised the fibrinogen Aα chain primary antibody by immunofluorescence, a proximity ligation assay was performed with a concentration range of the second primary antibody – rabbit polyclonal anti-phosphoserine. For optimisation purposes, phosphorylated fibrinogen was detected in CHO-WT so that CHO-Bβγ cells could be used as a negative control. The optimal concentration of anti-phosphoserine that produced a reasonable signal, but with low background, was 2.5 µg/ml. In subsequent experiments, phosphorylated fibrinogen was detected in HepG2 cells, as these cells express fibrinogen naturally. Markers for the ER and *trans*-Golgi were included to investigate the subcellular location of fibrinogen phosphorylation. However, phosphorylated fibrinogen did not co-localise with either marker and the signals were fairly sparse (figure 48). This may suggest that, once phosphorylated, fibrinogen is secreted rapidly from the cell and therefore not detected as a build-up of signal in one specific location. To investigate this further, BFA was added to the cells prior to fixation to inhibit protein secretion, as discussed below.

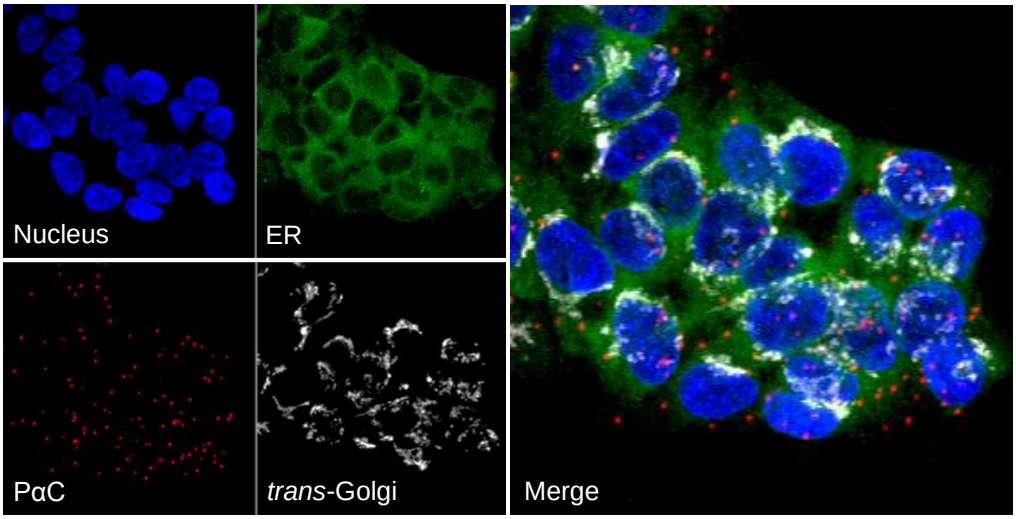

Figure 48. Proximity ligation assay to detect phosphorylated fibrinogen Aα chain in HepG2 cells. HepG2 cells were fixed onto an 8 well chamber slide and probed with mouse monoclonal anti-fibrinogen Aα chain (1.5 µg/ml) and rabbit polyclonal anti-phosphoserine (2.5 µg/ml) primary antibodies in a proximity ligation assay to detect phosphorylated Aα chain (PαC; red). Cells were also incubated with ER marker Alexa-Fluor 488 anti-PDI (green) (1/50), *trans*-Golgi marker sheep polyclonal anti-TGN46 (white) (1/200), and DAPI nucleic acid stain (blue). The anti-TGN46 primary antibody was detected with Alexa Fluor 647-AffiniPure donkey anti-sheep (1/1000). Images were taken by LSCM with a 60x oil-objective lens.

3.3.3. The effect of secretory pathway inhibitor Brefeldin A on fibrinogen phosphorylation in HepG2 cells

Secretory pathway inhibitor, BFA, was enlisted to facilitate identification of the subcellular site of fibrinogen phosphorylation, and to increase signal in later experiments. A BFA concentration of 20 µg/ml added for 8 hours gave the best result, with the largest increase in signal compared to control cells. This effect is shown in figure 49. The average number of phosphorylated fibrinogen Aα chains per cell, in the presence and absence of BFA, was calculated using ImageJ software. This figure increased significantly with BFA, from an average of 5.0 spots per cell to 16.8 spots per cell. Given that BFA blocks the exit of secretory proteins from the ER, but also causes redistribution of enzymes from the *cis*- and *medial*-Golgi back to the ER, this build-up of signal after addition of BFA suggests that fibrinogen is phosphorylated before it reaches the *trans*-Golgi compartment. This rules out the possibility of phosphorylation occurring in the *trans*-Golgi, secretory vesicles or at the cell surface. On the other hand, it suggests fibrinogen phosphorylation is likely to occur in the ER or an early Golgi compartment, making CK2 and the G-CK valid candidates for the *in vivo* fibrinogen kinase.

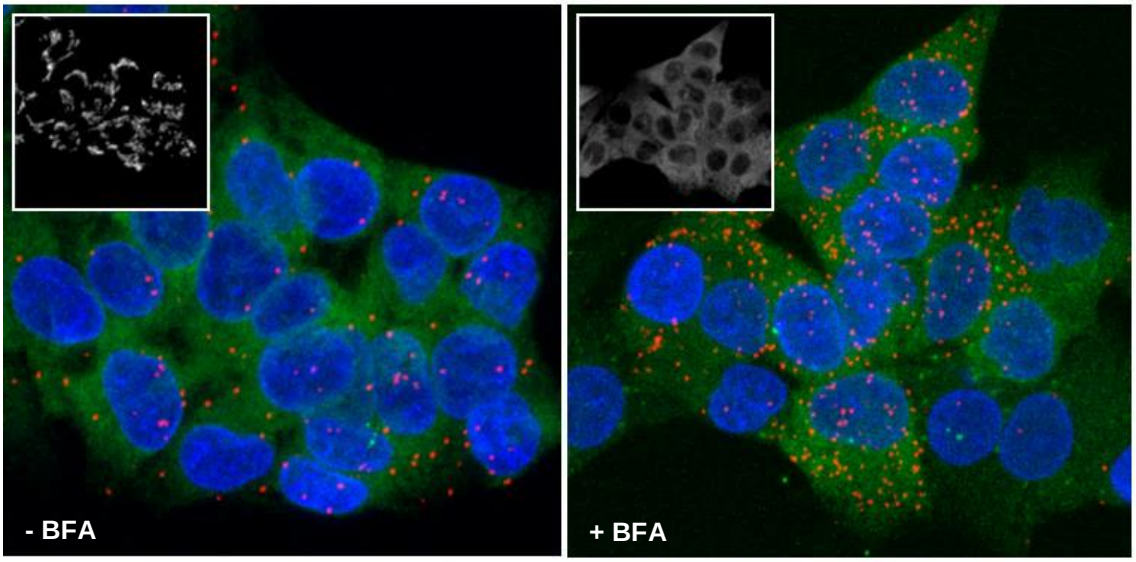

Figure 49. The effect of BFA on fibrinogen phosphorylation in HepG2 cells. HepG2 cells were incubated in the presence and absence of 20 µg/ml BFA for 8 hours before fixing. Cells were probed with mouse monoclonal anti-fibrinogen Aα chain (1.5 µg/ml) and rabbit polyclonal anti-phosphoserine (2.5 µg/ml) primary antibodies in a proximity ligation assay to detect phosphorylated Aα chain (PαC; red). Cells were also incubated with ER marker Alexa-Fluor 488 anti-PDI (green) (1/50) and DAPI nucleic acid stain (blue). Images were taken by LSCM with a 60x oil-objective lens. Three wells per group were imaged within a single experiment for subsequent quantitation of fibrinogen phosphorylation using ImageJ software (n=1).

3.3.4. Developing methods for the detection of phosphorylated fibrinogen using Phos-tag™

Alongside the intracellular detection of phosphorylated fibrinogen by PLA, several approaches were tested for the detection of phosphorylated fibrinogen in conditioned medium using Phos-tag™, including SDS-PAGE, ELISA and western blotting.

3.3.4.1. Phos-tag™ affinity SDS-PAGE

Control (25 % phosphorylated) and dephosphorylated fibrinogen were separated by Phos-tag™ affinity SDS-PAGE on a precast Phos-tag™ SuperSep gel, adhering to the manufacturer's instructions. Protein was blotted onto PVDF membrane and probed with an anti-fibrinogen Aα chain antibody, as shown in figure 50. As the interaction between Phos-tag™ and phosphate is zinc-dependent, EDTA in the sample buffer was quenched with an equivalent concentration of zinc nitrate. However, there was some band distortion which may be due to chelation of Zn^{2+} ions by EDTA – a common problem with this technique. There was no difference in density or position of the Aα chain bands between control and dephosphorylated fibrinogen samples, each producing one major band and one minor band of slightly lower molecular weight. This may indicate that fibrinogen is not phosphorylated heavily enough for sufficient interaction with Phos-tag™ molecules during migration through the gel. This could be confirmed by loading a protein with a higher degree of phosphorylation, such as β-casein (5 mol phosphate/mol protein), as a control. The concentration of fibrinogen or Phos-tag™ in the gel could be optimised to encourage interaction. The current could also be reduced for slower electrophoresis and increased contact time between Phos-tag™ and fibrinogen molecules.

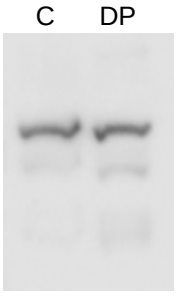

Figure 50. Phos-tag™ affinity SDS-PAGE and western blot. Control AP-fibrinogen (C; 25 % phosphorylated) and dephosphorylated (DP) fibrinogen (200 ng) were reduced and separated on a Phos-tag™ affinity SDS-PAGE gel containing 50 µM Phos-tag™ and 100 µM zinc chloride. Electrophoresis was performed at 20 mA/gel in Tricine SDS-PAGE running buffer. The gel was incubated in transfer buffer containing 1mM EDTA prior to western blotting. The blot was probed with a rabbit polyclonal anti-fibrinogen Aα chain antibody (1/1000).

3.3.4.2. ELISA with Phos-tag™ Biotin

The interaction between Phos-tag™ Biotin and streptavidin HRP was utilised for quantification of phosphorylated fibrinogen by ELISA. In the first experiment, a serial dilution of fibrinogen was overlaid with a concentration range of Zn^{2+}-Phos-tag™ Biotin-Streptavidin HRP complex. Absorbance values increased with higher concentrations of Phos-tag™, but showed little variation with increasing concentrations of fibrinogen, suggesting the Phos-tag™ may have been binding non-specifically. A second experiment included a Streptavidin HRP-only control, without Phos-tag™ Biotin. Unfortunately, signal was present in the streptavidin HRP-only wells, indicating non-specific binding of streptavidin HRP to fibrinogen or to the plate. This was also confirmed by western blotting with Phos-tag™ Biotin (described in section 3.3.4.3), which revealed non-specific interaction between streptavidin HRP and the fibrinogen Aα and Bβ chains. Therefore, streptavidin alkaline phosphatase was used in place of streptavidin HRP in subsequent assays, including a streptavidin alkaline phosphatase-only control each time. Phos-tag Biotin™ and streptavidin alkaline phosphatase were also added separately rather than as a pre-prepared complex. The streptavidin-only control remained blank during this experiment, making it a more suitable option that the HRP-conjugate. The absorbance value for AP-fibrinogen (25 % phosphorylated) (0.875) was slightly higher than for dephosphorylated fibrinogen (0.651), but the absorbance in the blank well with no fibrinogen was also high (0.498), suggesting non-specific binding of Phos-tag™ Biotin to the well or coating antibody. Furthermore, the absorbance values for experiment wells were very low after blank-subtraction, despite a long development time and high concentration of Phos-tag, indicating poor affinity of Phos-tag™ for phosphorylated fibrinogen.

3.3.4.3. Western blotting with Phos-tag™ Biotin

In tandem with the Phos-tag™ ELISA optimisation, Phos-tag™ Biotin was also applied for the detection of phosphorylated fibrinogen by western blotting. A concentration range of AP-fibrinogen was separated by SDS-PAGE, blotted and probed with Phos-tag™ Biotin, followed by streptavidin HRP. The resulting blot is shown in figure 51. Two bands corresponding to the Aα chain and the Bβ chain of fibrinogen were detected. Current literature provides no evidence of Bβ chain phosphorylation, hence it is likely that the presence of this chain is due to non-specific binding of Phos-tag™ or streptavidin HRP to fibrinogen. As the Aα and Bβ chains appear in similar intensity on this blot, it is likely that the Aα chain is also a result of non-specific binding, rather than detection of phosphate. A repeat experiment was performed in duplicate with i) Zn^{2+}-Phos-tag™ Biotin-streptavidin HRP or ii) streptavidin HRP-only. The Aα and Bβ

fibrinogen chains appeared in both blots, demonstrating non-specific binding of streptavidin HRP to fibrinogen. Hence, this approach could not be continued.

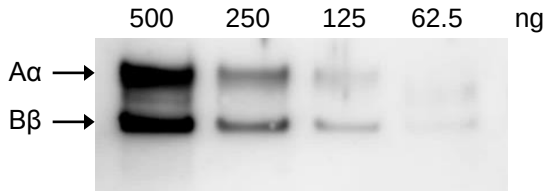

Figure 51. Western blot of fibrinogen with Phos-tag™ Biotin. AP-fibrinogen (62.5-500 ng) was separated by reducing SDS-PAGE and blotted onto PVDF membrane. The membrane was probed with 10 ml Phos-tag™ Biotin-bound Streptavidin HRP conjugate for 30 minutes to detect phosphorylation.

3.3.5. Developing methods for the detection of phosphorylated fibrinogen using anti-phosphoserine antibodies

As with the Phos-tag™ methods discussed above, anti-phosphoserine antibodies were also used to detect phosphorylation of secreted fibrinogen from HepG2 cells, by ELISA and western blotting.

3.3.5.1. Fibrinogen-phosphoserine ELISA

A sandwich assay was optimised for quantification of the degree of fibrinogen phosphorylation relative to a standard curve with an increasing amount of fibrinogen and phosphoserine. Initially, a blocking solution containing 3 % (w/v) BSA was used to prevent non-specific binding. The phosphoserine Q5 antibody produced high background with no specific detection of phosphorylated fibrinogen. The mouse monoclonal anti-phosphoserine demonstrated only a marginal difference in absorbance between AP-fibrinogen (1.295) and dephosphorylated fibrinogen (1.102) at the highest primary antibody concentration (1/100). The blank well at this concentration had an absorbance of 0.655, indicating non-specific binding to the plate. This also suggests non-specific interactions with fibrinogen, as the absorbance value for dephosphorylated fibrinogen was much higher than the blank. Appropriate controls confirmed that the primary antibody (mouse monoclonal anti-phosphoserine) was responsible for this. Therefore, the percentage of BSA was increased to 10 % (w/v) and the anti-phosphoserine antibody was added to the plate in a solution containing 5 % (w/v) BSA. The primary antibody incubation was also carried out at 4°C overnight for reduced binding kinetics in favour of specific antibody-antigen interactions. These changes abolished the non-specific binding of mouse monoclonal anti-phosphoserine to

fibrinogen, with absorbance values of 0.458 and 0.520 for the blank wells and dephosphorylated fibrinogen respectively. However, the background caused by non-specific binding of phosphoserine antibody to the plate was still fairly high, and the difference in absorbance between AP- and dephosphorylated fibrinogen remained slight (0.250). In a final experiment, the plate was coated with a mouse anti-fibrinogen γ chain antibody and fibrinogen-bound phosphate detected with a rabbit polyclonal anti-phosphoserine antibody. The HRP-catalysed reaction developed very slowly and the resulting absorbance values were very similar for AP-fibrinogen, dephosphorylated fibrinogen and the blank (no fibrinogen). This again demonstrated insufficient sensitivity and specificity of phosphoserine antibodies for this type of assay.

3.3.5.2. Phosphoserine western blots

As an alternative approach, fibrinogen was separated by SDS-PAGE and probed for phosphoserine by immunoblotting. The mouse anti-phosphoserine produced a clear Aα chain band with 1 to 5 µg AP-fibrinogen (figure 52A). However, there was also some non-specific detection of the Bβ chain. The rabbit polyclonal anti-phosphoserine produced one band corresponding to phosphorylated fibrinogen Aα chain with 2 µg AP-fibrinogen (figure 52B). The lane with dephosphorylated fibrinogen remained blank, demonstrating an acceptable specificity of this antibody with the conditions used. Hence, this antibody was used in subsequent investigations into the effect of IL-6, STSP and Fam20A siRNA on the degree of fibrinogen phosphorylation in HepG2 cells.

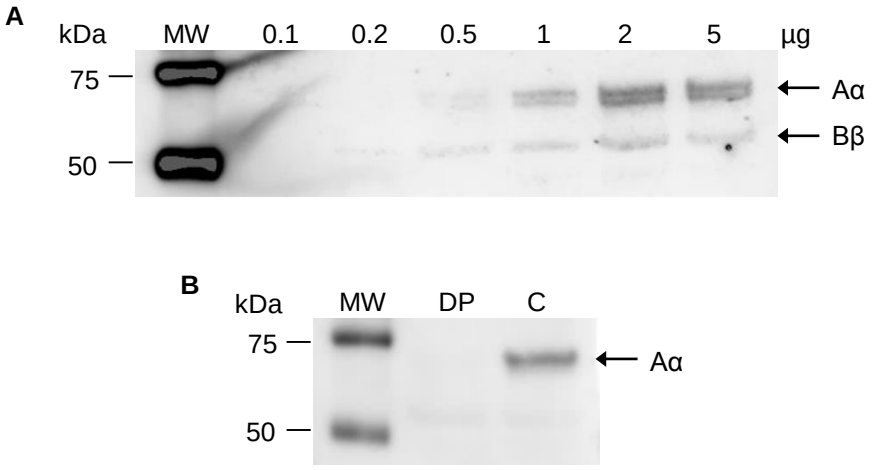

Figure 52. Western blotting of fibrinogen with anti-phosphoserine antibodies. AP-fibrinogen was separated by reducing SDS-PAGE and immunoblotted using anti-phosphoserine antibodies. A) Phosphorylated fibrinogen (0.1-5 µg) was probed with mouse monoclonal anti-phosphoserine antibody (1/1000) followed by rabbit anti-mouse HRP (1/5000). B) Phosphorylated control fibrinogen (C; 25 % phosphorylated) and dephosphorylated fibrinogen (DP) (2 µg each) were probed with rabbit polyclonal anti-phosphoserine (1/100) and goat anti-rabbit HRP (1/5000). MW: molecular weight marker.

The four fibrinogen samples of varying degrees of phosphorylation – control, dephosphorylated, 13 % and 33 % – were analysed using this method to qualitatively support the malachite green assay data and to validate the phosphoserine blot as a useful tool for comparison of fibrinogen phosphorylation. An anti-fibrinogen γ chain antibody was also included to monitor loading of fibrinogen, for normalisation purposes. The blot image matched the previously described trend with a near absence of phosphoserine in the dephosphorylated lane, and a rise in band intensity from 13 % to control (25 %), to 33 % phosphorylation (figure 53).

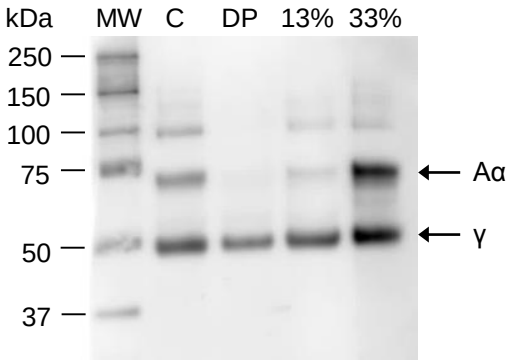

Figure 53. Phosphoserine western blot of fibrinogen phosphorylation isoforms. Phosphorylated (13 %, 25 % (C), 33 %) fibrinogens separated by Phos-tag™ affinity chromatography and dephosphorylated (DP) fibrinogen (2 µg each) were separated by reducing SDS-PAGE and blotted onto PVDF membrane. Blots were probed with rabbit polyclonal anti-phosphoserine (1/100) and mouse monoclonal anti-fibrinogen γ chain (1/5000) antibodies.

3.3.6. The effect of IL-6 on fibrinogen expression and phosphorylation in HepG2 cells

Human hepatoma cells were incubated with IL-6 to mimic the acute phase, providing a platform for investigating the mechanism of fibrinogen phosphorylation in these conditions. Real-time PCR was used to measure changes in expression of the fibrinogen Aα chain and relevant casein kinase enzymes with IL-6. Proximity ligation assay and phosphoserine immunoblotting were then used to determine the influence of IL-6 on the degree of fibrinogen phosphorylation after secretion from HepG2 cells.

3.3.6.1. Optimisation of IL-6 concentration and its effect on fibrinogen expression

The concentration of IL-6 was optimised using a range of 0-80 ng/ml. Interleukin-6 was added to the cells at increasing concentrations for 24 hours before extracting RNA for

analysis of fibrinogen Aα mRNA levels. Extracted RNA was reverse transcribed into cDNA and analysed by real-time PCR with primers specific to the fibrinogen Aα chain, normalising to housekeeping gene 18S rRNA. Figure 54A shows a graph of fold-change in fibrinogen Aα chain expression with increasing concentrations of IL-6. The expression increases rapidly up to 10 ng/ml IL-6 and then begins to plateau. This trend supports data published by Faber et al. (2012). Therefore, 10 ng/ml was selected as the optimal concentration of IL-6 for subsequent experiments. The effect of 10 ng/ml IL-6 on fibrinogen Aα chain expression was further characterised by incubation of HepG2 cells with the optimal concentration of IL-6 in three independent experiments. Ribonucleic acid was extracted from the cells each time after a 24 hour incubation period and reverse transcribed for real-time PCR. The data from each PCR experiment revealed a significant 3.5-fold increase in fibrinogen Aα chain expression in HepG2 cells incubated with IL-6 ($p=0.0442$) (figure 54B), in agreement with previous reports (Faber et al., 2012, Igaz et al., 1998).

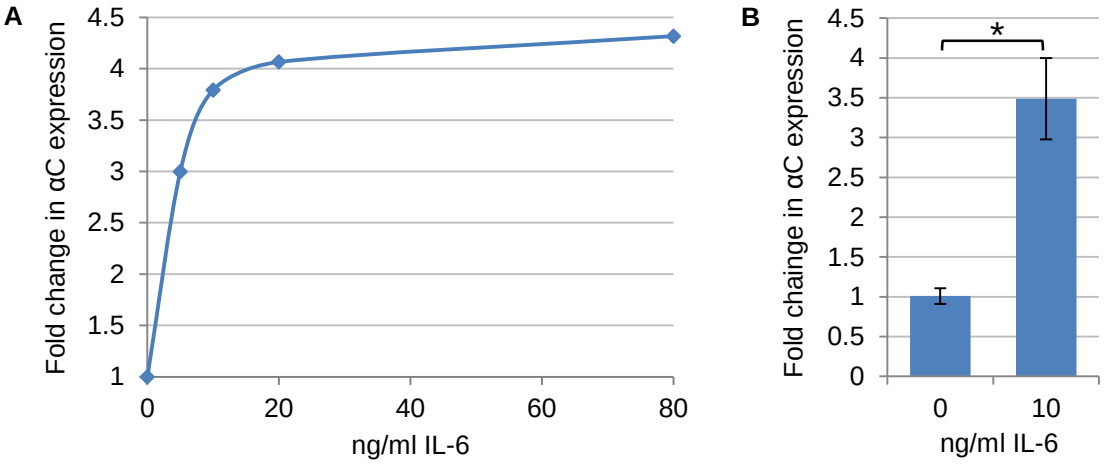

Figure 54. The effect of IL-6 on fibrinogen Aα chain expression. RNA extracted from HepG2 cells incubated with IL-6 was reverse transcribed into cDNA and amplified (20 ng) during real-time PCR with fibrinogen Aα chain primers [0.2 µM] for 40 cycles. Relative expression was compared using a $2^{-\Delta\Delta Ct}$ calculation, normalising to 18S rRNA. A) Optimisation of IL-6 concentration. The graph shows the fold increase in fibrinogen Aα chain (αC) expression with increasing concentrations of IL-6 from 0-80 ng/ml added for 24 hours. The data are an average of triplicate wells within a single experiment (n=1). B) The fold increase in fibrinogen Aα chain expression after incubation with 10 ng/ml IL-6 for 24 hours. The data are an average of three independent experiments (n=3), with error bars representing standard error of the mean. The fold change in Aα chain expression is statistically significant ($p<0.05$) (*).

3.3.6.2. The effect of IL-6 on kinase expression profiles in HepG2 cells

In searching for the kinase responsible for fibrinogen phosphorylation *in vivo*, HepG2 cells were first of all screened for expression of six likely candidates: CK2, Fam20A, Fam20B, Fam20C, Fam198A and Fam198B. These kinases are capable of phosphorylating the S-X-E motif present at both Ser3 and Ser345. They also reside along the secretory pathway in the ER or Golgi compartments. Briefly, HepG2 cells were cultured under normal conditions before RNA extraction and real-time PCR with primers specific to each of the kinases. Figure 55 shows the relative expression of each of the six kinases. Cycle threshold values for Fam198A and Fam198B were late (> 35 cycles), indicating very low expression of these two kinases. Expression of the other four kinases was easily detected, with CK2 exhibiting the highest mRNA levels. However, this experiment was not replicated and the relative expression levels should therefore be interpreted with caution, given that minor variations in starting RNA concentrations can result in major fluctuations in $2^{-\Delta\Delta Ct}$ values.

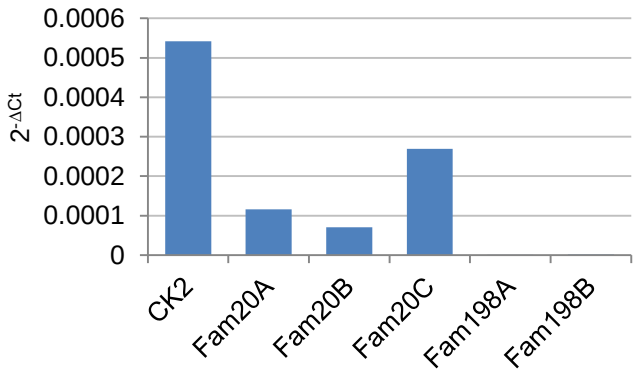

Figure 55. Relative expression of casein kinases in HepG2 cells. RNA extracted from HepG2 cells was reverse transcribed into cDNA and amplified (100 ng) during real-time PCR with primers specific to CK2 and Golgi casein kinases (Fam20A, Fam20B, Fam20C, Fam198A and Fam198B) [0.2 µM] for 40 cycles. Relative expression was compared using a $2^{-\Delta Ct}$ calculation, normalising to GAPDH. The data shown are from triplicate wells within a single experiment (n=1).

Having confirmed expression of CK2 and the Fam20 Golgi casein kinases in HepG2 cells, their expression profiles were compared in the presence and absence of IL-6, to give an indication of which enzyme might effectuate the elevation in fibrinogen phosphorylation during the acute phase response. HepG2 cells were incubated ± 10 ng/ml IL-6 for 24 hours and RNA was extracted for real-time PCR analysis with the kinase-specific primers. Interestingly, there was no change in expression of CK2,

Fam20B or Fam20C, but there was a large increase in Fam20A expression with IL-6 (figure 56A). The experiment was repeated three times, measuring only the fold-change in Fam20A expression each time. There was an average 6.0-fold increase in Fam20A expression, deemed significant by statistical analysis (p=0.0341) (figure 56B). As the p value reflects standard error, the dramatic rise in expression is likely to be more significant with a greater number of experimental repeats. This finding has exposed for the first time an important role of Fam20A in the hepatocellular response to acute phase conditions. Furthermore, it suggests that Fam20A may be responsible for phosphorylation of fibrinogen and/or other acute phase proteins that are secreted by hepatocytes and have the Golgi casein kinase S-X-E sequence recognition motif.

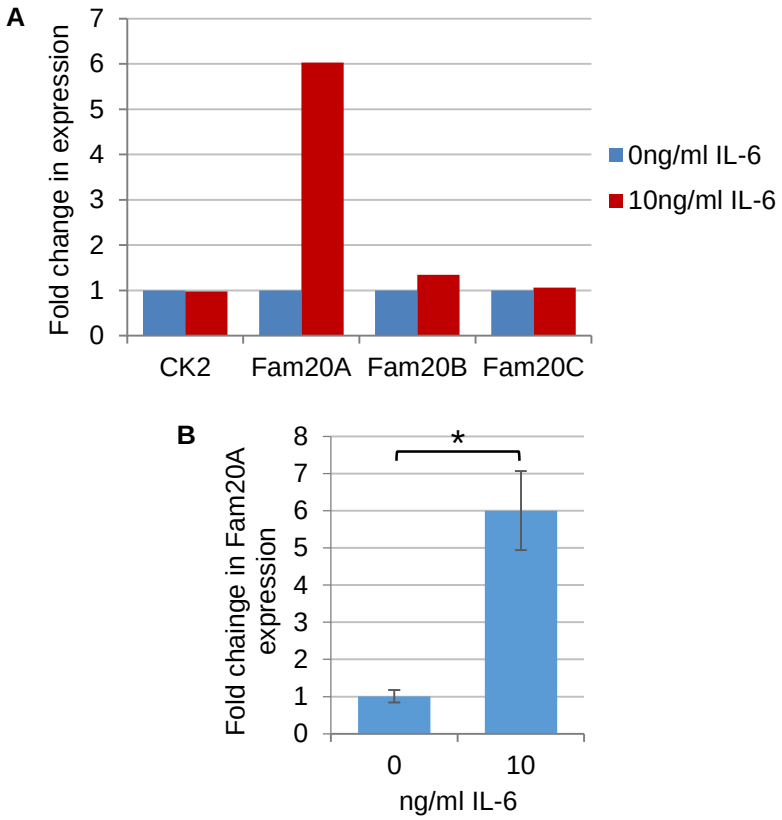

Figure 56. The effect of IL-6 on casein kinase expression. HepG2 cells were incubated ± 10 ng/ml IL-6 for 24 hours. Extracted RNA was reverse transcribed into cDNA and amplified (100 ng) during real-time PCR with kinase-specific primers [0.2 µM] for 40 cycles. Relative kinase expression was compared using a $2^{-\Delta\Delta Ct}$ calculation, normalising to 18S rRNA. A) Fold change in expression of CK2, Fam20A, Fam20B and Fam20C with IL-6. The data are an average of triplicate wells within a single experiment (n=1). B) Fold increase in Fam20A expression with IL-6. The data are an average of three independent experiments (n=3), with error bars representing standard error of the mean. The fold change in Fam20A expression is statistically significant ($p<0.05$) (*).

3.3.6.3. The effect of IL-6 on the degree of fibrinogen phosphorylation

Interleukin-6 was added to HepG2 cells to monitor its effect on the degree of phosphorylation of intracellular fibrinogen by PLA, and of secreted fibrinogen by western blotting. For proximity ligation, cells were cultured on an 8-well chamber slide and incubated ± 10 ng/ml IL-6 (three wells each) for 24 hours before fixing. The assay was performed with anti-fibrinogen Aα chain and anti-phosphoserine antibodies for detection of phosphorylated fibrinogen inside the cell by confocal microscopy (figure 57A). Images were then analysed using an ImageJ macro to determine the average number of spots per cell in each sample group. Interleukin-6 caused a 4.0-fold rise in the number of spots per cell from 2.1 to 8.3 (figure 57B), representing a greater number of phosphorylated fibrinogen molecules. However, this increase was only slightly higher than the 3.5-fold increase in fibrinogen expression, previously quantified by real-time PCR (section 3.3.7.1). In other words, the increase in phosphorylated fibrinogen was similar to that of the total number of fibrinogen molecules, suggesting the proportion, or percentage, of fibrinogen phosphorylation is unaltered by IL-6.

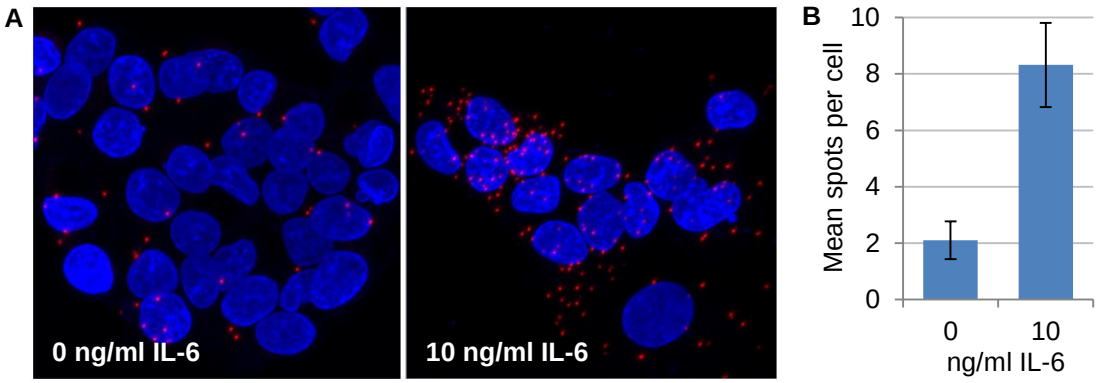

Figure 57. The effect of IL-6 on the quantity of phosphorylated fibrinogen Aα chains in HepG2 cells. HepG2 cells were incubated in the presence and absence of 10 ng/ml IL-6 for 24 hours before fixing. A) Cells were probed with mouse monoclonal anti-fibrinogen Aα chain (1.5 µg/ml) and rabbit polyclonal anti-phosphoserine (2.5 µg/ml) primary antibodies in a PLA to detect phosphorylated Aα chain (PαC; red). Nuclei (blue) were stained with DAPI during mounting. Images were taken by LSCM with a 60x oil-objective lens. B) Individual spots were counted using ImageJ software. The mean number of spots per cell ± IL-6 are presented as an average of three wells from a single experiment (n=1), with error bars representing standard deviation.

The phosphate content of secreted fibrinogen in the presence and absence of IL-6 was compared by SDS-PAGE and western blotting. Three dishes of HepG2 cells (n=1) were cultured ± 10 ng/ml IL-6 for 24 hours before harvesting conditioned medium for analysis by western blotting with anti-phosphoserine and anti-fibrinogen γ chain antibodies. Phosphorylated Aα chain bands where much darker in IL-6 lanes compared to control lanes, despite consistent loading of the fibrinogen γ chain (figure 58A). Densitometry analysis with ImageJ revealed a 3.1-fold increase in phosphorylated Aα chain:γ chain ratio from 0.8 to 2.5 (figure 58B). This is equivalent to an elevated degree of fibrinogen phosphorylation from the 25 % control value to 78 % – a similar rise to that reported previously during the acute phase, although slightly higher. This result demonstrates for the first time that the rise in fibrinogen phosphorylation in acute phase conditions is mediated within the cell rather than by a circulating kinase. Unfortunately, this finding contradicts the PLA data with IL-6, leaving the question of which outcome is more reliable. It can be challenging with PLA experiments to image representative areas, as there is often large variability even within the same well. They are also limited by a lack of suitable negative control for the phosphoserine antibody. The western blot is a more stable approach with measurable loading and phosphorylation controls. However, repeat experiments are necessary to confirm the result in figure 58, and enable statistical analysis.

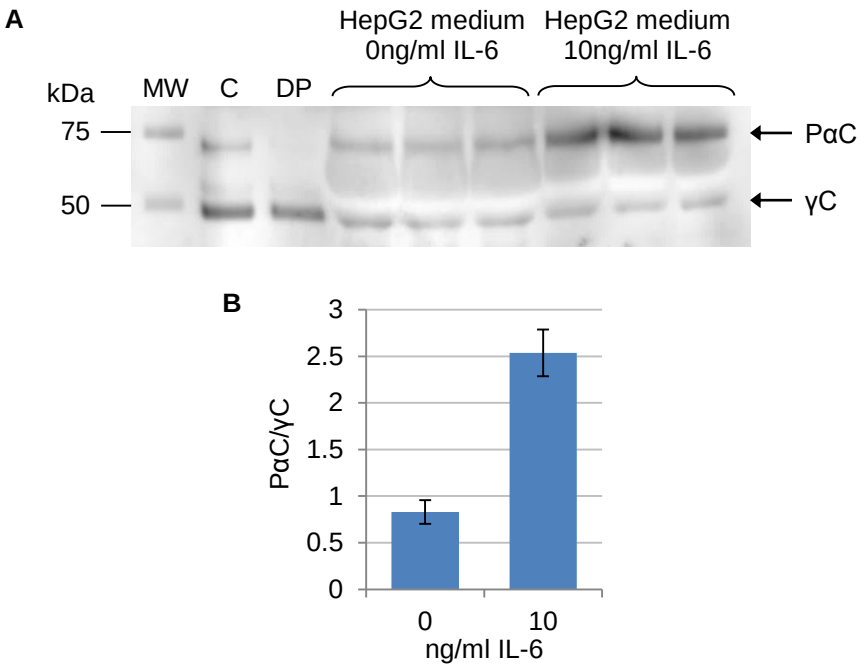

Figure 58. The effect of IL-6 on the degree of phosphorylated fibrinogen secreted by HepG2 cells. HepG2 cells were incubated ± 10 ng/ml IL-6 for 24 hours in triplicate. Conditioned medium was harvested and fibrinogen concentration determined by ELISA. A) Control AP-fibrinogen (C; 25% phosphorylation) and dephosphorylated (DP) fibrinogen (1 µg each), as well as samples of conditioned medium containing 1 µg fibrinogen, were separated by reducing SDS-PAGE. Western blots were probed with rabbit polyclonal anti-phosphoserine (1/100) and mouse monoclonal anti-fibrinogen γ chain (γC) (1/5000) antibodies. PαC: phosphorylated fibrinogen Aα chain; MW: molecular weight marker. B) Densitometry analysis of phosphorylated Aα chain bands normalised to the fibrinogen γ chain (PαC/γC). Averages of triplicate data from a single experiment (n=1) are displayed with error bars representing standard deviation.

3.3.7. The effect of kinase inhibitor STSP on the degree of fibrinogen phosphorylation in HepG2 cells

Having identified a dramatic increase in Fam20A expression in HepG2 cells incubated with IL-6, promiscuous kinase inhibitor STSP was enlisted to investigate whether fibrinogen is phosphorylated by the G-CK, which is uniquely insensitive to this inhibitor. Staurosporine induces apoptosis, therefore finding the right concentration was critical to achieve inhibition of kinases with minimal cell death. Initially, a concentration range of 0.5 to 10 µM STSP was tested by immunofluorescence, screening for cleaved caspase 3 as a marker of apoptosis. This method failed to detect any cleaved caspase 3 which most likely reflects a problem with the antibody and a need for optimisation, as 10 µM STSP should have been a more than adequate concentration to induce

apoptosis (Giuliano et al., 2004). Chosen concentrations were therefore based on observation of cell changes under the microscope. During culture, there was significant cell death above 1 µM, accompanied by apparent morphological changes during confocal microscopy, including minor changes at 500 nM. Proximity ligation was carried out after incubation of cells with 250 nM STSP. The results of the assay ± 250 nM STSP are displayed in figure 59A. There was significant detachment of cells from the slide during fixation, leaving few areas for imaging. Hence, the results could be slightly biased. Analysis of the mean number of spots per cell using ImageJ revealed a 60 % reduction from 13.0 to 5.2 spots per cell (figure 59B). This might indicate inhibition of the fibrinogen kinase by STSP, and that fibrinogen is not phosphorylated by the G-CK. However, this may also be an adverse effect of the toxicity of this concentration of STSP on the cells.

To avoid the various issues surrounding this method, secreted fibrinogen in conditioned medium was analysed by western blotting, rather than looking at intracellular fibrinogen. First, HepG2 cells were incubated with 0, 50, 100 and 200 nM STSP for 24 hours and the medium analysed by SDS-PAGE and western blotting with anti-phosphoserine and anti-fibrinogen γ chain antibodies. Due to concentration of the medium prior to loading, the blot image was not very clear, with background and bulging of the lanes around the fibrinogen (figure 59C). However, the Aα chain appeared to be present even up to 200 nM STSP. The experiment was repeated with 0 and 200 nM STSP and fibrinogen was immunoprecipitated before electrophoresis. This time, bands were much clearer but the phosphorylated fibrinogen Aα chain band was weaker with 200 nM STSP compared to control, supporting the PLA data. It could be concluded from these data that the G-CK is not responsible for fibrinogen phosphorylation. However, the data sets are inconsistent and the final method of western blot analysis with immunoprecipitation of fibrinogen should be repeated to confirm whether this is a genuine result.

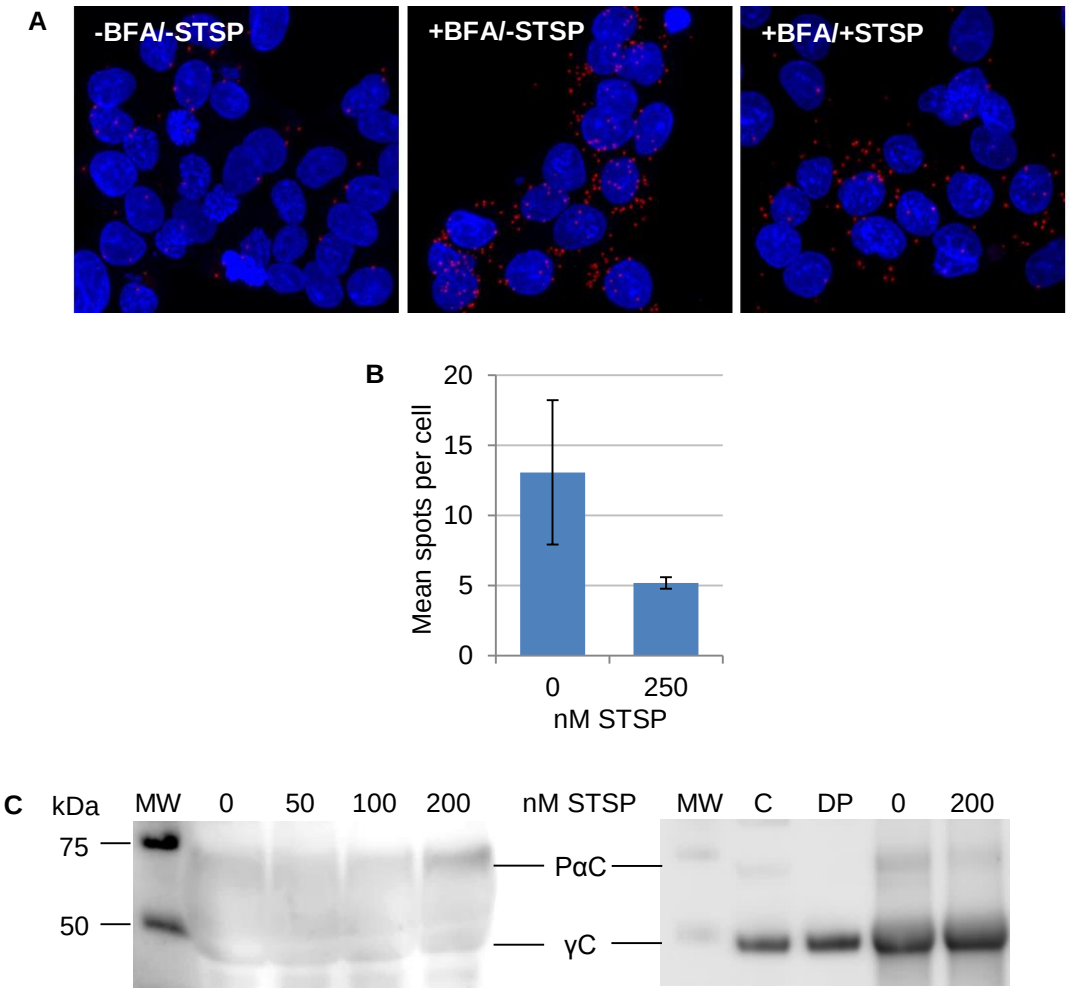

Figure 59. The effect of STSP on fibrinogen phosphorylation in HepG2 cells. A) HepG2 cells were incubated ± 250 nM STSP for 24 hours, including 8 hours with 20 µg/ml BFA. Cells were probed with mouse monoclonal anti-fibrinogen Aα chain (1.5 µg/ml) and rabbit polyclonal anti-phosphoserine (2.5 µg/ml) primary antibodies in a PLA to detect phosphorylated Aα chain (PαC; red). Nuclei (blue) were stained with DAPI. Images were captured by LSCM with a 60x oil-objective lens. B) Individual spots were counted using ImageJ software. The average number of spots from three wells within a single experiment (n=1) are displayed with error bars representing standard deviation. C) HepG2 cells were incubated with 0, 50, 100 and 200 nM STSP (left hand blot), or 0 and 200 nM STSP (right hand blot) for 24 hours. Conditioned medium containing 1 µg fibrinogen was analysed by reducing SDS-PAGE and western blotting with rabbit polyclonal anti-phosphoserine (1/100) and mouse monoclonal anti-fibrinogen γ chain (1/5000) antibodies (left hand blot). In a repeat experiment, fibrinogen was immunoprecipitated prior to analysis (right hand blot). MW: molecular weight marker; C: control AP-fibrinogen; DP: dephosphorylated fibrinogen; PαC: phosphorylated fibrinogen Aα chain; γC: fibrinogen γ chain.

3.3.8. Knockdown of Fam20A expression in HepG2 cells with siRNA

Expression of Fam20A is significantly elevated with IL-6 (section 3.3.6.2). To investigate whether Fam20A phosphorylates fibrinogen *in vivo*, HepG2 cells were transfected with siRNA to switch off expression of this kinase. For optimisation, the cells were transfected with a concentration range of Fam20A siRNA from 5 to 50 nM in 5 nM intervals. Cells were assayed by real-time PCR 3 days post-transfection (figure 60A). The siRNA transfection was successful at the lowest concentration (5 nM) which caused an 86 % reduction in Fam20A expression. Subsequently, the transfection was repeated with the optimal siRNA concentration for Fam20A siRNA and scrambled control siRNA. Again, RNA was extracted 3 days after transfection, and medium was also harvested for analysis of fibrinogen phosphorylation. A fibrinogen ELISA was carried out to measure the concentration of fibrinogen in each medium sample and unfortunately, even after concentration, the yields were too low for analysis by western blotting. Due to time constraints, one final experiment was performed with changes to the transfection protocol, including addition of IL-6 and medium change 12 hours post-transfection, in attempt to improve the yield of fibrinogen. Ribonucleic acid was extracted from cells after 3 days for real-time PCR (figure 60B). The real-time PCR data showed a 6-fold increase in Fam20A expression with IL-6, as expected. However, there was only a 53 % reduction in Fam20A expression after siRNA transfection, indicating that the changes had compromised transfection efficiency. Further optimisation is necessary to achieve substantial knockdown of Fam20A expression with sufficient yield of fibrinogen. As for the harvested fibrinogen, ELISA data confirmed a good yield which enabled analysis by SDS-PAGE and western blotting with an anti-phosphoserine antibody (figure 60C). Levels of phosphorylated fibrinogen Aα chain on the blot were very similar for each sample, with no apparent reduction in phosphorylation with the Fam20A siRNA. However, this outcome is inconclusive as the expression was only partially inhibited. This process should be repeated with an optimised siRNA transfection protocol to feasibly address the question of whether Fam20A phosphorylates fibrinogen.

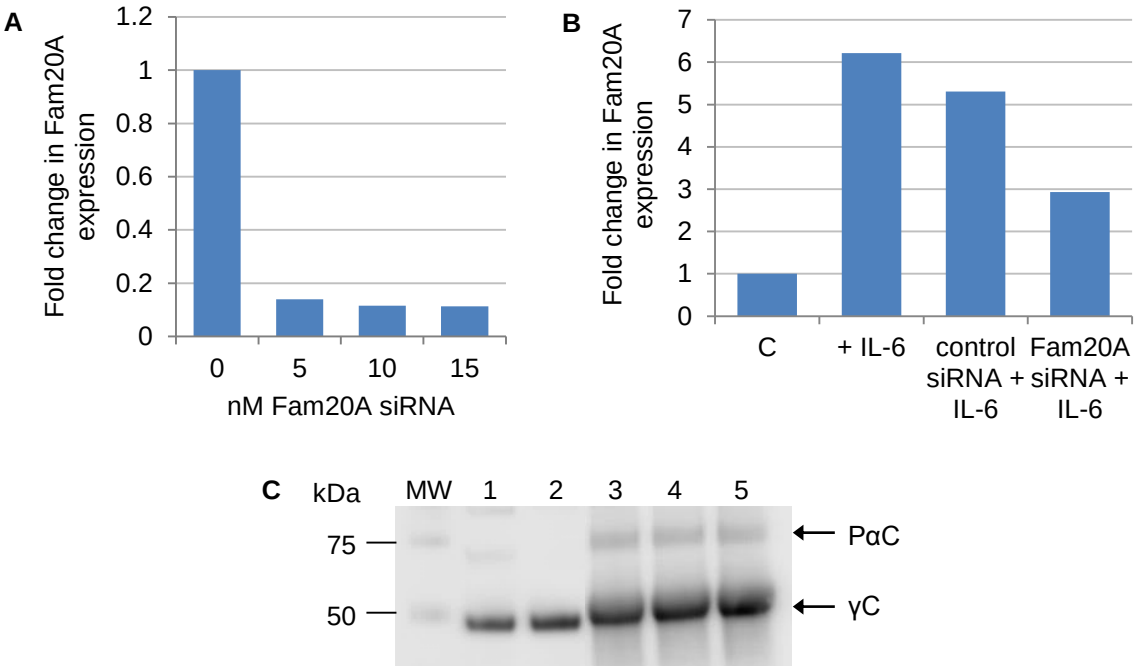

Figure 60. Optimisation of Fam20A siRNA transfection. A) HepG2 cells were transfected with 0-15 nM Fam20A siRNA and Fam20A mRNA levels in the cells were assayed by real-time PCR. Extracted RNA was reverse transcribed and amplified (100 ng) with Fam20A-specific primers [0.2 µM] for 40 cycles. The fold-change in Fam20A expression was calculated using a $2^{-\Delta\Delta Ct}$ calculation, normalising to 18S rRNA. The data are an average of triplicate wells from a single experiment (n=1). B) HepG2 cells were incubated with medium only (C), 10 ng/ml IL-6 (+IL-6), scrambled control siRNA and 10 ng/ml IL-6, or Fam20A siRNA and 10 ng/ml IL-6. Extracted RNA was analysed by real-time PCR in the same way as (A), to compare Fam20A expression. C) Fibrinogen in conditioned medium from cells in (B) was immunoprecipitated and analysed for phosphate content by reducing SDS-PAGE and western blotting with rabbit polyclonal anti-phosphoserine (1/100) and mouse monoclonal anti-fibrinogen γ chain (1/5000) antibodies. Lanes 1 and 2 contain purified fibrinogen controls; lanes 3-5 contain conditioned medium from HepG2 cells. Each lane has been loaded with 1 µg fibrinogen. Lane 1: control AP-fibrinogen; lane 2: dephosphorylated fibrinogen; lane 3: 10 ng/ml IL-6 only; lane 4: control siRNA and 10 ng/ml IL-6; lane 5: Fam20A siRNA and 10 ng/ml IL-6. MW: molecular weight marker; PαC: phosphorylated fibrinogen Aα chain; γC: fibrinogen γ chain.

Chapter 4

Discussion

In physiological circumstances, there is a delicate haemostatic balance between pro-coagulant and anti-coagulant activities, which permits crucial vessel repair in a carefully executed and self-limiting fashion, so as to avoid harmful bleeding or thrombus formation. Disruption of this balance can have devastating consequences. Fibrin(ogen) is at the heart of the clotting cascade. Abnormal or variant fibrinogens can affect clottability and produce different fibrin clot structures. Two common polymorphisms – AαThr312Ala and BβArg448Lys – affect clot stiffness, compactness, porosity and persistence (Standeven et al., 2003, Lim et al., 2003, Ajjan et al., 2008), while a higher than average proportion of γ' fibrinogen is associated with coronary artery disease and thrombosis, and produces clots with thinner fibres, increased branching and a weaker structure (Cooper et al., 2003, Allan et al., 2012). There are also many naturally-occurring and abnormal post-translational modifications of fibrinogen that lead to altered clot phenotypes, affecting fibre diameter and branching, as well as clot porosity, stiffness and resistance to lysis, as reviewed in section 1.4.

Fibrinogen is phosphorylated on its Aα chain at Ser3 in FpA and Ser345 in the αC region (Blomback et al., 1963, Blomback et al., 1966, Seydewitz et al., 1984, Wind et al., 2003), but the effects of this modification on the developing clot, or on fibrinolysis, are poorly understood. The effects of multiple kinases on the phosphorylation state of fibrinogen and fibrin clot structure *in vitro* have been characterised (Engstrom et al., 1980, Papanikolaou et al., 1982, Guasch et al., 1986, Itarte et al., 1983, Heldin et al., 1987a, Forsberg, 1989), but these studies produced varied and conflicting results and did not shed light on the situation *in vivo*. There is, however, an agreement that changes to clot architecture may have an inhibitory effect on fibrinolysis, as several studies have demonstrated that fibrinogen phosphorylation, both *in vitro* and *in vivo*, leads to increased resistance to plasmin digestion (Forsberg and Martin, 1990, Martin et al., 1991, Martin et al., 1992, Martin and Bjork, 1990).

Phosphorylation of Ser3 causes faster FpA cleavage and enhanced complex formation with thrombin (Maurer et al., 1998), but little is known about the role of Ser345 phosphorylation. This residue is thought to have a special function, as it is surrounded

by an extremely polar region with high sequence homology, including eight tandem repeats between residues 270 and 372 (Seydewitz et al., 1984, Rixon et al., 1983). Additionally, Ser345 is positioned between FXIII-a cross-linking acceptor sites (Gln328 and Gln366) and close to the FXIII-A2B2 binding region (Smith et al., 2011, Seydewitz et al., 1984, Cottrell et al., 1979). Hence, phosphorylation at this site might be implicated in the regulation of α chain cross-linking by FXIII and lateral growth of the fibrin network. It may also coordinate fibrinolysis as several key proteins which function within this system interact with the fibrinogen αC region (Tsurupa and Medved, 2001a, Tsurupa and Medved, 2001b, Ritchie et al., 2000, Kimura and Aoki, 1986a).

Over the last decade, research into the mechanism and effects of fibrinogen phosphorylation has been largely neglected. Such research may be of great significance, as there is a body of evidence linking the phosphorylation state of fibrinogen with the acute phase response and thrombotic diseases (Ogata et al., 2006, Seydewitz et al., 1987, Seydewitz and Witt, 1985, Haglund et al., 2000, Reganon et al., 1993, Suhre et al., 2011). Recently, two studies have flagged the importance of fibrinogen phosphorylation in terms of its potential biomarker or biopharmaceutical applications (Suhre et al., 2011, Nagel and Meyer, 2014). The ambiguity of previous *in vitro* work and difficulties with phosphorylation analysis, particularly for the Ser345 phosphorylation site, may explain the limited progress in establishing the contribution of fibrinogen phosphorylation to thrombosis.

A key aim of this investigation was to express fibrinogen Aα chain variants lacking the Ser3 and Ser345 phosphorylation sites, in order to assess their function. Initially, recombinant WT fibrinogen was expressed in CHO cells and purified by affinity chromatography, producing a good yield of fibrinogen with demonstrable clotting capability and susceptibility to FXIII-catalysed cross-linking of fibrin α and γ chains. Fibrinogen Aα chain constructs were mutated at Ser3 and Ser345 to non-phosphorylatable residues, but transfecting and expressing the variant fibrinogens using the CHO cell system was troublesome. Recombinant WT and S345N variant fibrinogens were both expressed using an alternative transient transfection system with Expi293F cells. Although the yield was insufficient, there is potential to optimise this system for a much faster approach to recombinant fibrinogen expression compared to current methods.

A novel phosphate capturing molecule – Phos-tag™ – was used to separate phosphorylated and non-phosphorylated plasma fibrinogen by affinity chromatography. Together with control and dephosphorylated fibrinogens, this produced four fibrinogen samples with varying degrees of phosphorylation for use in functional studies. In these

studies, the phosphorylation state of fibrinogen did not influence FXIII activity in the cross-linking of fibrin α and γ chains, α2-AP binding or covalent incorporation at Lys303, or plasminogen binding to fibrinogen. Plasmin digestion of fibrinogen was slightly reduced in samples with higher phosphate contents, which may indicate a protective effect of phosphorylation against clot lysis. Increased phosphorylation of fibrinogen also caused alterations to fibrin clot formation and structure, with notable reductions in clotting rate and fibre thickness, and an apparent increase in fibre branching.

Several methods have been developed to explore the cellular mechanism of fibrinogen phosphorylation. A proximity ligation assay enabled detection and quantification of phosphorylated fibrinogen Aα chains in HepG2 cells. Secretion inhibitor BFA caused a significant increase in the number of fibrinogen Aα chains per cell, demonstrating that the intracellular phosphorylation of fibrinogen occurs before the *trans*-Golgi, either in the ER or *cis/medial*-Golgi compartments. Methods were also developed for analysis of phosphorylation levels in secreted fibrinogen. The use of anti-phosphoserine antibodies and Phos-tag™ Biotin for detection and quantification of phosphorylated fibrinogen by ELISA were deemed unsuitable due to issues with poor affinity and non-specific binding. However, a western blotting protocol with an antiphosphoserine antibody was successfully optimised to give specific detection of phosphorylated fibrinogen Aα chain.

Real-time PCR and western blotting were used to compare fibrinogen expression and phosphorylation, as well as kinase expression, in the presence of acute phase-mediator IL-6. Incubation of HepG2 cells with IL-6 caused a 3.5-fold increase in fibrinogen Aα chain expression and a 3.1-fold increase in the degree of fibrinogen phosphorylation. This has demonstrated for the first time that the elevated phosphorylation of fibrinogen in acute phase conditions is associated with its biosynthesis, rather than modification in plasma. Interleukin-6 also caused a substantial increase in expression of Golgi casein kinase Fam20A, suggesting this kinase has an important function in the acute phase response and may phosphorylate fibrinogen *in vivo*. Further investigations with kinase inhibitor STSP and Fam20A siRNA are ongoing.

Overall, this work has indicated that elevated fibrinogen phosphorylation in acute phase conditions and thrombosis might be attributed to increased cellular kinase activity, and ultimately produces clots with different properties which may favour thrombosis.

4.1. Recombinant fibrinogen expression

4.1.1. Wild-type fibrinogen expression in CHO cells

An established in-house method of CHO cell transfection and protein expression was enlisted for the expression of recombinant WT and variant fibrinogen (Binnie et al., 1993). Chinese hamster ovary cells are commonly used for recombinant protein expression due to rapid cell growth and high protein production. Expression of WT fibrinogen in CHO cells and subsequent purification successfully produced a good yield of fibrinogen, despite some loss of protein during purification. As the IF-1 affinity chromatography was estimated to give approximately 80 % recovery of fibrinogen during optimisation prior to this investigation (data not shown), protein yield was most likely compromised during the ammonium sulphate precipitation step, or due to proteolytic degradation in the medium. Analysis of purified fibrinogen confirmed correct subunit structure and full functionality in terms of fibrin polymerisation and lysis, and fibrin Aα and γ chain cross-linking in the presence of FXIII. This supports data published by Gorkun et al. (1997), who reported that the fibrinopeptide release, polymerisation and FXIII cross-linking of recombinant fibrin(ogen) resembles that of plasma fibrin(ogen). Preliminary mass spectrometric analysis of fibrinogen expressed in CHO cells has also demonstrated phosphorylation at Aα Ser3 and Ser345 residues (Appendix 3), in support of findings by Binnie et al. (1993), who reported a 22 % degree of phosphorylation at Aα Ser3 in recombinant fibrinogen expressed in CHO cells, as determined by HPLC experiments. Based on these results, the use of CHO cells seems a suitable and viable choice for the large-scale production of recombinant WT fibrinogen and fibrinogen Aα chain variants.

4.1.2. Variant fibrinogen expression in CHO cells

Unfortunately, attempts to express variant fibrinogen in CHO cells were problematic. Mutated fibrinogen Aα cDNA constructs were transfected into CHO-Bβγ cells for expression of variant fibrinogen lacking the Ser3 and/or Ser345 phosphorylation sites. There was an unmitigated absence of fibrinogen-secreting clones when the medium was screened by ELISA, which was not rectified by mutation of serine phosphorylation sites to alternative residues – glutamic acid (phospho-mimetic) or alanine – indicating that the size and charge of the replacement residue was not responsible for the failed expression. This leaves a few possible explanations, the first being unsuccessful transfection of the fibrinogen Aα chain constructs. The success of transient transfection of the newly cloned pmC constructs into CHO cells by $CaPO_4$ precipitation was

inconsistent, and the method had to be repeated. Despite being an easy, cost-effective approach, the success of $CaPO_4$ precipitation is dependent on several variables, such as reagent concentration, order of addition and pH. Indeed, Wright (2009) has reported that deviation of just 0.05 pH units from the optimal range (pH 7.05-7.15) can significantly affect precipitate size, compromising transfection efficiency. Cationic lipids, such as Lipofectamine® (Life Technologies), are highly efficient in DNA transfection and, depending on the cell line, are between 5- and 100-fold more effective than $CaPO_4$ transfection (Felgner et al., 1987). This could therefore be a valuable replacement in the transfection of fibrinogen constructs into CHO cells.

However, as the pmC constructs created for variant fibrinogen expression in Expi293F cells were successfully transfected into CHO cells by $CaPO_4$ precipitation, as confirmed by western blotting, this is unlikely to explain the failure of each stable transfection. This suggests the problem may lie at the selection stage. Selection with L-histidinol was developed by Hartman and Mulligan (1988). During selection, L-histdinol inhibits protein synthesis via inhibition of histidyl-tRNA synthetase. The pMSVHis selection vector contains the *hisD* gene, which encodes histidinol dehydrogenase to catalyse the oxidation of L-histdinol to non-toxic L-histidine. Cells that have taken up the selection vector are therefore able to survive in selection medium containing L-histidinol. If the concentration of L-histidinol is inadequate, cells which have not taken up the vector may also survive and form colonies. The concentration of L-histidine in selection medium could therefore be re-optimised to prevent untransfected cells from surviving selection pressure.

Cell lysis, immunofluorescence and RT-PCR experiments were conducted to investigate the presence of intracellular variant Aα chain in transfected CHO cells. Cell lysis and western blotting had an encouraging outcome. Although faint, an Aα S345N band was detected in CHO cell lysate, suggesting the transfection had worked and the cells were able make this variant polypeptide chain, even if it was not secreted. On its own, this outcome indicates that either the expression was too low to obtain a measurable yield of secreted fibrinogen, or that variant fibrinogen could not be secreted, but instead was degraded inside the cell. Incubation of CHO cells with proteasome and lysosome inhibitors would address this possibility.

The results of immunofluorescence and RT-PCR experiments were not in agreement with the cell lysis findings. The fibrinogen Aα chain was not detected in CHO cells transfected with pMLP-Aα S3N, S345N, S3/345N, S3E, or S345E by immunofluorescence. Similarly, RT-PCR with RNA from transfected CHO cells failed to detect amplification of fibrinogen Aα S3N mRNA in any of the four clones that were

screened, while the bands corresponding to the Aα chain amplification product in S345N clones were very faint and may represent contamination. A better approach would be to use real-time PCR for quantitative comparison of Aα mRNA in each clone, as well as melting curve analysis to provide information on the source of each band. The reason for discrepancy between methods is unclear; however, the Aα chain band detected in S345N cell lysate is unlikely to be non-specific, given that it is at the correct molecular weight (66kDa). The key limitation of this work is the number of clones that were analysed. Healthy clones were selected at random for further analysis, but not all surviving clones would be expected to test positive for fibrinogen Aα chain expression. However, the results do collectively point to low (or absent) expression of variant fibrinogen Aα chain. Notably, a control transfection did result in one positive clone out of the six tested by fibrinogen ELISA, suggesting successful transfection of the WT Aα chain construct. This result implies that the problem is specific to variant fibrinogen expression and secretion in CHO cells, rather than the method used. However, when developing this method of recombinant fibrinogen expression, Lord et al. (1993) found that 23 out of 24 selected clones transfected with WT fibrinogen expression constructs were positive for fibrinogen secretion when screened by ELISA. Hence, the transfection efficiency was still low with the WT fibrinogen Aα chain construct.

If reduced expression in CHO cells is specific to the Aα chain variants, it suggests there may be a requirement for phosphate at Ser3 and Ser345 for normal progression of fibrinogen along its biosynthetic pathway and release into the extracellular environment. Secretory proteins are transported from the ER to Golgi, where they migrate from the *cis*-Golgi compartment to the *trans*-Golgi network. The Golgi complex is a common site of protein phosphorylation due to resident kinases and translocation of ATP into the lumen (Capasso et al., 1989). Phosphorylation of casein – a secretory protein containing multiple phosphorylation sites – takes place in both the *cis*-Golgi (α-casein) and *trans*-Golgi network (β and γ-casein) (Turner et al., 1993). The phosphorylation of secretory proteins can influence a phenomenon known as 'protein targeting', which refers to delivery of a protein to the correct subcellular location. For example, phosphorylation of furin by CK2 regulates its retrieval from the plasma membrane and localisation at the *trans*-Golgi network (Jones et al., 1995). In some cases, phosphorylation may regulate the sorting of proteins from the *trans*-Golgi network to secretory vesicles or lysosomes, possibly mediating a switch from one destination to the other in response to an extracellular stimulus. This is the case for aquaporin 2, whose secretion is dependent on phosphorylation at Ser256 in the Golgi apparatus; impaired constitutive phosphorylation of aquaporin 2 directs the protein to lysosomes for degradation (Procino et al., 2003). Similarly, indirectly increasing

phosphorylation of the amyloid precursor protein, by inhibiting phosphatases, leads to a rise in secretion, suggesting that non-phosphorylated molecules may be destined for proteolytic degradation (Caporaso et al., 1992). As well as protein targeting, phosphorylation may be important for correct protein folding. Misfolded proteins are recognised and retained in the ER by molecular chaperones prior to degradation. Intracellular phosphorylation can therefore prove fundamental for protein expression and secretion. This scenario would require all of the secretory protein in question to be phosphorylated inside the cell. If this were the case for fibrinogen, it would need to then be partially dephosphorylated either at a later stage of secretion, at the cell surface, or in the extracellular environment, to achieve the reported 20-25 % degree of phosphorylation in secreted fibrinogen (Binnie et al., 1993, Blomback et al., 1966). Indeed, dog fibrinogen is secreted into plasma in an almost entirely phosphorylated form (Kudryk et al., 1982). Furthermore, dephosphorylation of human fibrinogen in plasma is unlikely given that Binnie et al. (1993) have reported partial phosphorylation of FpA in recombinant human fibrinogen expressed in CHO cells. This finding suggests that the partial phosphorylation of fibrinogen occurs prior to secretion from the cell, unless fibrinogen is susceptible to secreted phosphatases in the conditioned medium.

One final option to consider is the order of transfection of individual constructs and the ratio of each expressed chain within the cell. Published accounts of recombinant fibrinogen expression in CHO cells describe three types of transfection: i) transfection of Bβ cDNA into a CHO-Aαγ cell line for expression of wild-type or variant fibrinogen (Binnie et al., 1993, Ajjan et al., 2008), ii) variant γ cDNA transfection into CHO-AαBβ cells (Okumura et al., 1997), and iii) in the case of an Aα chain variant, co-transfection of Aα and γ cDNA into CHO-Bβ cells (Park et al., 2013). There is no previous report of transfection of fibrinogen Aα cDNA into a CHO-Bβγ cell line. It has come to light during this investigation that other research groups have also had difficulties with expression of fibrinogen Aα chain variants when transfecting in this way. Given that other combinations have been successful, it is possible that expression of fibrinogen is affected by the ratio of each chain inside the cell, which may be dictated in part by their order of transfection. There are known cases, such as heteromeric ion channels, where a defined ratio of individual polypeptides comprising a multi-subunit protein is essential for maintaining expression levels (Eertmoed et al., 1998, Tretter et al., 2001). Normally, in HepG2 cells, surplus Aα and γ chains in the ER exist as Aα-γ complexes or free γ chains, owing to a faster rate of synthesis in comparison to Bβ chains and retention of Aα-γ complexes by lectin-like chaperones (Yu et al., 1984, Tamura et al., 2013, Xia and Redman, 2001). For the stepwise assembly of fibrinogen, pools of Aα and γ chains combine with rate-limiting Bβ chain during their co-translational translocation into the

ER and form Bβ-Aα and Bβ-γ complexes, which combine with additional Aα and γ chains to form fibrinogen half-molecules and dimers.

4.1.2.1. Co-transfection of Aα and γ chain constructs into CHO-Bβ cells

To investigate whether the order of transfection of each construct is important for expression, the process was repeated according to methods used by Park et al. (2013) for expression of a fibrinogen variant with mutated Aα chain cross-linking acceptor sites. A CHO-Bβ cell line was created by transfecting the Bβ chain construct into new, untransfected CHO cells and screening for the best clone by real-time PCR. Co-transfection of Aα and γ chain constructs into CHO-Bβ cells was then carried out for expression of fibrinogen. After transfection, cells were split and re-plated at varying dilutions in selection medium containing 200 µg/ml zeocin – a broad-spectrum antibiotic from *Streptomyces verticillus* which induces double-strand breaks in DNA (Chankova et al., 2007). Only one set of plates formed colonies, but ELISA data revealed that none of the selected clones secreted fibrinogen. Cells in all of the other dishes died in selection medium. This indicates that either the transfection hadn't worked, or the concentration of zeocin was too high. The concentration of zeocin was optimised and lowered slightly in a subsequent transfection, but this did not resolve the problem. As zeocin has previously been used successfully at concentrations of 100-500 µg/ml for stable CHO cell transfection (Oliva-Trastoy et al., 2005, Chung et al., 2014, Van Blokland et al., 2011, Trapani and Korn, 2003), this might suggest that uptake of DNA by the cells was unsuccessful. Due to time constraints, optimisation of this method was not completed and it remains to be seen whether the order of transfection of fibrinogen constructs does indeed affect the cells' ability to express and secrete fibrinogen.

4.1.3. Wild-type and variant fibrinogen expression in Expi293F cells

Due to difficulties with expression of variant fibrinogen in CHO cells, an alternative system was sought. Various cell lines and transgenic animals have been used for expression of biologically active recombinant fibrinogen, including COS-1, BHK, yeast Pichia pastoris, and the murine mammary gland (Roy et al., 1991, Huang et al., 1993b, Roy et al., 1995, Prunkard et al., 1996). Our division also uses an Expi293F cell line for recombinant protein expression. This cell line is derived from HEK293, from which cells were selected for viability in high density cultures and high yields of recombinant protein. According to the manufacturers (Life Technologies), transfection of Expi293F cells can yield up to 1 mg protein per ml of culture. Therefore, as an alternative to the CHO cell expression system, the three fibrinogen cDNA constructs were transiently transfected into an Expi293F cell line. An additional advantage over the CHO cell

system is the timing of this method, which can be completed in just one week. The CHO cell system, on the other hand, takes approximately 2 months to achieve stable expression, followed by 2-3 months of harvesting recombinant fibrinogen. With regards to fibrinogen expression, the cells were able to express and secrete both WT and S345N fibrinogen, raising the question of why biosynthesis could be achieved in Expi293F cells but not in CHO cells. This may corroborate a problem with the CHO cell transfection methodology. Additionally, the co-transfection of all three chains during Expi293F transfection may be more conducive for fibrinogen expression than the lone transfection of Aα chain cDNA into CHO-Bβγ cells.

It should be noted that the γ chain of S345N fibrinogen appeared to be of slightly higher molecular weight (approximately 50 kDa) than the WT fibrinogen γ chain (48 kDa) on an SDS-PAGE gel. A repeat transfection would therefore be beneficial to confirm whether this is a genuine effect. This is unlikely to have been caused by a problem with the γ chain construct or alternative splicing, given that the same construct was used for expression of both WT and S345N fibrinogen. Equally, the removal of the phosphorylation sites is unlikely to affect pre-translational events. The apparent shift in molecular weight may reflect additional PTM, such as glycosylation of the γ chain, possibly facilitated by the altered conformation of fibrinogen in the absence of phosphorylation. Indeed, Tagliabracci et al. (2014) have recently reported some cross-talk between phosphorylation and O-glycosylation of secretory proteins, revealing that phosphorylation of fibroblast growth factor 23 (FGF23) by Fam20C inhibits O-glycosylation of FGF23 and promotes its cleavage. However, this scenario also seems unlikely given that only 25 % of Ser3 and Ser345 phosphorylation sites are modified intracellularly (Binnie et al., 1993), and would therefore give rise to two bands on the gel. The reason for this difference remains unclear and could be investigated further by mass spectrometry to determine the size of the polypeptide and screen for any additional modifications.

Unfortunately, despite successful expression and secretion of WT and S345N fibrinogen in Expi293F cells, the yield was insufficient for purification and functional analyses, with only 300 µg and 480 µg from a 30 ml culture respectively. The transfection system could be scaled up to a much larger volume, using 500 ml or 1 L spinner flasks, but this would be a very costly approach for a small amount of fibrinogen. Hence, this method would be unsuitable for large-scale expression of recombinant fibrinogen variants. The most likely explanation for the low yield of fibrinogen from Expi293F cells is poor transfection efficiency, given that the cDNA for each fibrinogen chain was co-transfected in three separate plasmids. In terms of recombinant protein expression, achieving expression of a complex multi-subunit

protein is always more challenging than expression of a single polypeptide chain. Successful transfection is dependent upon integration of plasmid DNA into the genome by non-homologous recombination – an event which occurs with very low frequency (Murnane et al., 1990). Therefore, the probability of successful integration decreases with each additional plasmid transfected.

One way to increase fibrinogen expression levels in Expi293F cells would be to clone Aα, βB and γ chain cDNA into one construct. This can be achieved using multicistronic vectors, whereby genes are inserted into more than one multiple cloning site, typically separated by internal ribosome entry sites (IRES) for attachment of ribosomes to the mRNA transcript and production of separate polypeptide chains (Gurtu et al., 1996, Zhu et al., 1999). However, the widely used IRES sequence has two important limitations: i) its large size (>500 nucleotides), and ii) reduced transfection efficiency of genes after the IRES sequence, leading to differential expression of each gene (de Felipe, 2002). An alternative is the use of 2A viral peptides, which provide a 'ribosomal-skip' site for release of individual polypeptides (Szymczak et al., 2004). These peptides yield a more even stoichiometry than IRES, but do leave a 2A tag at the end of the expressed protein. Both of these methods can also be very time consuming. A novel cloning strategy – site-specific recombinational cloning – is becoming more popular due to ease of use and high efficiency. An example of a recombinational cloning system is the Multisite Gateway® Technology (Cheo et al., 2004). This system exploits integrase-mediated recombination between two attachment sites and enables parallel transfer of multiple cDNA molecules into the same vector, whilst maintaining their correct orientation and reading frame (Hartley et al., 2000, Park and Labaer, 2006). This approach could be applied to expression of recombinant fibrinogen variants, making for an easier, more effective expression system regardless of the cell line of choice.

4.2. The functional effects of fibrinogen phosphorylation

4.2.1. Chromatographic enrichment of phosphorylated fibrinogen

4.2.1.1. Anion exchange chromatography

As an alternative to expression of recombinant fibrinogen variants, commercial plasma fibrinogen (25 % phosphorylated) was subjected to chromatographic procedures to produce fibrinogen samples with varying degrees of phosphorylation. Separation of phosphorylated and non-phosphorylated proteins by anion exchange chromatography

can be heavily influenced by the pH of the equilibration buffer, which should be as close as possible to the pI of the protein, without risking precipitation. This would result in a weaker affinity between the non-phosphorylated protein and the column, enabling earlier elution and better separation. Despite optimisation of the equilibration buffer pH, as well as gradient time and flow rate, the enrichment of fibrinogen phosphorylation was still small (from 25 % to 36 %) and peaks were not resolved. It may not be possible to achieve adequate separation of phosphorylated and non-phosphorylated fibrinogen using this method if the degree of phosphorylation does not cause a large enough shift in pI. Egg white-constituent ovalbumin has two phosphorylation sites and can be separated into three peaks by strong anion exchange chromatography. Different grades of ovalbumin with a phosphate/protein mole ratio ranging from 0.37 to 1.64 have been compared using this technique (Kornfeld et al., 2009). Interestingly, ratios of 1.14 mol phosphate/mol ovalbumin and below resulted in poor resolution of peaks. As fibrinogen molecules have only 0.8-1.0 mol phosphate, this may explain the inadequate separation. Furthermore, if phosphorylated fibrinogen molecules are not all fully phosphorylated (4 mol phosphate/mol fibrinogen), but instead represent a mixture of 1, 2, 3 or 4 mol phosphate/mol fibrinogen, the change in pI would be smaller and separation would be more difficult.

4.2.1.2. Phos-tag™ affinity chromatography

Due to the poor separation of phosphorylated and non-phosphorylated fibrinogen by anion exchange chromatography, another method was sourced. Phos-tag™ is an alkoxide-bridged dinuclear zinc(II) complex which recognises phosphate monoester dianions (Kinoshita et al., 2004). Phos-tag™ Agarose can be used for enrichment of phosphorylated proteins by affinity chromatography. The ideal enrichment of fibrinogen phosphorylation would have been from 25 % to between 50 and 70 % to mimic the phosphorylation levels in acute phase conditions. Although not as effective as hoped, Phos-tag™ chromatography did produce two fibrinogen samples with a much greater difference in phosphorylation (13 % and 33 %) compared to those from anion exchange chromatography (24 % and 36 %). In fact, the difference in phosphorylation between the two fractions was similar to the difference between control fibrinogen (25 % phosphorylation) and acute phase fibrinogen (50-70 % phosphorylation). Therefore, this method was successful in generating fibrinogen samples that could be used to investigate the function of phosphorylation.

However, the limited enrichment of phosphorylated fibrinogen (from 25 % to 33 %) suggests there may be poor affinity of Phos-tag™ for fibrinogen. Kinoshita et al. (2005) have described the use of a Phos-tag™ Agarose affinity chromatography column for

retrieval of phosphorylated ovalbumin, α_{S1}-casein and β-casein, which have two, eight and five phosphorylated serine residues respectively. Each phosphoprotein was retained by the column and eluted with phosphate buffer, with ovalbumin appearing first due to its lesser degree of phosphorylation. The specificity of the method was confirmed using dephosphorylated samples of each protein. Prior to optimisation, this same method was followed for the separation of phosphorylated and non-phosphorylated fibrinogen, but was unsuccessful under these conditions. This may reflect differences in protein characteristics, such as structure and conformation, or differences in the number of phosphorylated residues per protein molecule.

Another important consideration in assessing the efficacy of this method is the distribution of the 25 % of phosphorylated sites between fibrinogen molecules. For example, the presence of one to two phosphorylation sites out of four possible phosphorylation sites per molecule (two per Aα chain) would convey a 25-50% degree of phosphorylation, yet close to 100 % of molecules could potentially contain at least one phosphoserine capable of interacting with the column. This could well be the case, as Nagel and Meyer (2014) found a 1:1:1 ratio of non-, mono- and di-phosphorylated fibrinogen Aα chains, with a 55-71 % proportion of mono- or di-phosphorylated Aα chains, in healthy patient samples by liquid chromatography-mass spectrometry. In other words, approximately only one third of fibrinogen Aα chains were non-phosphorylated. However, they did report large variation in the percentage of non- and di-phosphorylated fibrinogen Aα chains between patients. On the other hand, given that 67 % of fibrinogen phosphorylation sites in the elution fraction were non-phosphorylated, this might indicate interaction of non-phosphorylated fibrinogen with the column. This could be explained by an affinity of Phos-tag™ for other anionic residues within fibrinogen, which would also provide competition for specific binding. Furthermore, this would support findings from the Phos-tag™ western blotting and ELISA experiments (sections 3.3.4.2 and 3.3.4.3), which failed to detect phosphorylated fibrinogen and also highlighted non-specific interaction between Phos-tag™ and fibrinogen.

Phosphoserine antibodies exhibit notoriously poor sensitivity and specificity. Unlike phosphotyrosine antibodies, which are highly selective, phosphoserine and phosphotyrosine antibodies are dependent on the surrounding amino acid sequence as well as the phosphorylated side chain itself (Dhein, 2005, Vogel, 2008). This means that these antibodies bind a limited range of phosphorylated sites, and can cross-react with similar sequences in the absence of phosphorylation. The low specificity of anti-phosphoserine and anti-phosphothreonine antibodies undermines the use of immunoaffinity chromatography for the enrichment of phosphorylated proteins, but

there are additional affinity chromatography procedures that might be fitting for this purpose. Phosphoproteins can be enriched by immobilised metal affinity chromatography (IMAC), in which positively charged metal ions, such as Fe^{3+}, Ga^{3+}, Al^{3+} and Zr^{4+}, are coupled to a stationary phase and interact with negatively charged phosphate groups. Phosphoproteins are then eluted with EDTA, phosphate buffer or a buffer with alkaline pH (Thingholm and Jensen, 2009). Similarly, metal oxide/hydroxide affinity chromatography (MOAC) relies on the affinity of phosphate for metal oxides (i.e. titanium dioxide) or hydroxides (i.e. aluminium hydroxide), which have a positively charged surface at acidic pH; this is currently the most common technique used prior to analysis of protein phosphorylation by mass spectrometry (Wolschin et al., 2005, Dunn et al., 2010). However, both methods have their drawbacks. One limitation is the non-specific binding of acidic protein residues such as glutamic or aspartic acid. In addition, proteins with multiple phosphorylation sites bind with high affinity to MOAC columns, making elution difficult (Batalha et al., 2012). This would make IMAC a more promising option for enrichment of phosphorylated fibrinogen.

Fibrinogen samples separated by Phos-tag™ affinity chromatography were 13 % and 33 % phosphorylated. The 2.5-fold increase between the highest and least phosphorylated samples is similar to the difference between normal and acute phase levels *in vivo* (from 20-25 % to 50-70 %), but any comparisons would be based on the assumption of a linear relationship between the degree of phosphorylation and its functional effect. Price et al. (1994) have reported a hyperbolic (i.e. linear until saturation) dependence of phosphoprotein activity on kinase activity if only one serine is phosphorylated. With two phosphoserines, the relationship becomes sigmoidal, meaning the change in phosphoprotein activity would be larger than that of kinase activity. If phosphorylated fibrinogen isoforms exist with less than 4 mol phosphate, it is possible that the effect of increasing phosphorylation from 20-25 % to 50-70 % might be greater than that observed here between the 13 % and 33 % samples, due to fewer mono-phosphorylated Aα chains. This scenario is unlikely, however, as both phosphorylation sites would need to have the same function in order to exhibit this cooperative activity. Although the function of Ser345 has yet to be confirmed, it is unlikely to be the same as Ser3 in facilitating interaction with thrombin.

4.2.2. The effect of fibrinogen phosphorylation on interactions with other plasma components

4.2.2.1. FXIII-A activity

Phosphorylated fibrinogen isoforms separated by Phos-tag™ affinity chromatography were compared in a variety of assays to determine whether the phosphorylation sites promote or inhibit the interaction of fibrinogen with other plasma components, including FXIII, α2-antiplasmin and plasmin(ogen). In addressing the question of whether phosphorylation alters FXIII cross-linking and stabilisation of fibrin clots, two glutamine cross-linking acceptor residues located either side of the Ser345 phosphorylation site – Gln328 and Gln366 – are of particular interest. Additional glutamine acceptor sites Gln221 and Gln237 may also be affected, as well as several lysine donor residues: Lys539, Lys556, Lys580, Lys601 (Matsuka et al., 1996). The results of the biotin pentylamine incorporation FXIII-A activity assay showed no difference between samples, suggesting that phosphorylation of Ser345 does not affect the FXIII-A-mediated cross-linking of adjacent fibrin α and γ chains to glutamine acceptor residues in the fibrin α chain. However, this does not rule out a potential effect of phosphorylation on the availability of fibrin α chain lysine donor residues, which could be investigated in a similar assay using a biotin-TVQQEL-OH glutamine donor substrate, as described by Smith et al. (2013).

Moreover, the result of the biotin pentylamine incorporation FXIII-A activity assay does not dismiss an effect of fibrinogen phosphorylation on the cross-linking of fibrin α and γ chains by FXIII-A2B2. Smith et al. (2011) have demonstrated that both FXIII-A and FXIII-A2B2 bind to the αC region of fibrinogen in close proximity to Ser345, at residues 389-403 and 371-425 respectively. There is evidence to suggest that the B subunits of FXIII-A2B2 are important in the binding of this transglutaminase to fibrin(ogen). Firstly, the surface of the A subunits of FXIII-A2B2 are largely covered by the B subunits for protection from proteolytic digestion (Souri et al., 2008). In addition, FXIII-A has relatively low affinity for the αC region of fibrinogen (K_d of ~2.35 ± 0.09 μM), in contrast to the high affinity interaction between FXIII-A2B2 and the αC region of fibrinogen (K_d of < 35 nM) (Smith et al., 2011). Therefore, under physiological conditions, phosphorylation of fibrinogen may affect the nearby anchoring of the B subunits of FXIII-A2B2 to residues 371-425 of the fibrinogen αC region, thereby affecting cross-linking activity.

The dissociation of the A and B subunits of FXIII-A2B2 is a two-step process, requiring initial proteolytic activation by thrombin, followed by full dissociation in the presence of

Ca^{2+} ions. Credo et al. (1981) have shown that the presence of fibrinogen during this dissociation significantly lowers the Ca^{2+} requirement from 10 mM to 1.5 mM, and reported that residues 242-424 are important for this Ca^{2+}-modulating function of fibrinogen in FXIII activation. Three high affinity calcium binding sites are present in fibrinogen – two in fragment D between γ311 and γ336 (Lindsey et al., 1978, Dang et al., 1985b), and one in the N-terminal disulphide knot in the central domain (Nieuwenhuizen et al., 1982, Nieuwenhuizen et al., 1983). Sialic acid residues on fibrinogen function as additional low affinity calcium binding sites (Marguerie et al., 1977, Dang et al., 1989). Similarly, phosphate groups on proteins can also act as carriers of Ca^{2+} ions, such as those on casein and other proteins phosphorylated by the G-CK that are involved in biomineralisation processes (Tagliabracci et al., 2012, West, 1986). Hence, phosphorylation of fibrinogen may also affect the rate of dissociation of the A and B subunits of FXIII-A2B2 through altered Ca^{2+} binding, either directly with phosphorylated Ser345, or by conformational change leading to exposure of Ca^{2+} binding sites in fibrinogen.

4.2.2.2. Binding and cross-linking of α2-AP

In addition to cross-linking of fibrin α and γ chains, the effect of fibrinogen phosphorylation on the binding and cross-linking of α2-AP to fibrin was investigated by means of an α2-AP incorporation assay and a plasmin generation assay. Recombinant FXIII-A was included in each assay for covalent incorporation of α2-AP, as well as binding. Alpha-2-antiplasmin is cross-linked to the fibrin(ogen) αC region at Lys303 (Kimura and Aoki, 1986a). More recently, high affinity binding of α2-AP to fibrin(ogen) fragments D1 and D-D, as well as the αC region and αC domain of fibrin(ogen), has also been characterised, with a proposed function of providing the proper orientation of cross-linking sites (Tsurupa et al., 2010). Tsurupa et al. (2010) demonstrated that these binding sites are cryptic in fibrinogen but available in fibrin, or adsorbed fibrinogen. In both assays, fibrinogen was converted to fibrin by addition of thrombin and Ca^{2+}, permitting interaction with α2-AP.

The α2-AP incorporation assay and plasmin generation assay both produced identical graphical trends for each fibrinogen sample, regardless of the degree of phosphorylation. This suggests phosphorylation of fibrinogen does not influence its interaction with α2-AP for inhibition of fibrinolysis. Although plasmin generation was delayed in the presence of its inhibitor α2-AP, phosphorylation of fibrinogen does not appear to regulate this inhibition. Furthermore, these findings support the result of the FXIII-A activity assay, providing no evidence for a change in FXIII-A activity with the different phosphorylation isoforms. Any effect of fibrinogen phosphorylation on FXIII

activity, via altered binding affinity for fibrinogen or FXIII-A2B2 subunit dissociation, would be expected to indirectly influence α2-AP incorporation at Lys303, which was not observed in these experiments. This is of particular importance given that α2-AP incorporation, rather than cross-linking of fibrin α and γ chains by FXIII, is the principal determinant of resistance to fibrinolysis (Fraser et al., 2011). Plasminogen activator inhibitor-2 is also cross-linked in proximity to Ser345, at Lys413 and Lys457 (Ritchie et al., 2000, Ritchie et al., 2001). The plasmin generation assay could therefore be repeated in the presence and absence of this inhibitor to see whether phosphorylation facilitates this interaction.

4.2.2.3. Interaction with plasmin(ogen)

It has previously been reported that elevated *in vivo* fibrinogen phosphorylation leads to increased resistance to plasmin digestion (Martin et al., 1992), an effect which is irreversible. Interestingly, phosphorylation of fibrinogen *in vitro* has the same effect, irrespective of the conflicting effects of the kinases in question on fibre thickness (Martin et al., 1991). This suggests that the principal mechanism of phosphorylation-induced resistance to fibrinolysis is independent of changes to clot architecture, and may result from impaired interactions with fibrinolytic proteins. In this thesis, phosphorylation of fibrinogen did not affect incorporation of α2-AP. Therefore, the reported increased resistance to plasmin digestion most likely relates directly to the interaction of plasmin(ogen) with fibrinogen, either by altered binding, or by protection of plasmin cleavage sites due to a phosphorylation-induced conformational change. These possibilities are discussed in more detail below.

4.2.2.3.1. Plasminogen binding to fibrinogen

Plasminogen binds to the αC region of fibrin with high affinity (K_d of 32 nM) (Tsurupa and Medved, 2001a, Tsurupa and Medved, 2001b), and to additional sites in fibrinogen D and E fragments (Varadi and Patthy, 1983, Varadi and Patthy, 1984, Lucas et al., 1983). As with α2-AP binding sites on fibrinogen, plasminogen binding sites in fragments D and E, as well as in the αC region, are cryptic in fibrinogen but exposed in fibrin (Tsurupa and Medved, 2001a, Varadi and Patthy, 1983). However, while α2-AP does not bind soluble fibrinogen, Tsurupa et al. (2010) demonstrated that binding does occur in adsorbed fibrinogen. The process of immobilising fibrinogen affects its conformation and can expose sites that would otherwise be hidden and unavailable for interaction. This has also been demonstrated for the N-terminal fibrinogen Aα chain platelet-binding RGD sequence (Ugarova et al., 1993). Therefore, cryptic plasminogen binding sites are likely to also be exposed upon adsorption of fibrinogen to a 96-well

plate. An ELISA was performed to investigate the binding of plasminogen to adsorbed fibrinogen. There was no difference in the amount of bound plasminogen between the phosphorylation isoforms, suggesting phosphorylation does not hinder this interaction. Surface plasmon resonance (SPR) would enable determination of the K_d for plasminogen and immobilised full-length fibrinogen, for further characterisation of binding affinity. Both ELISA and SPR could also be used to investigate the effect of phosphorylation on the activation of fibrinolysis by the binding of tPA to the αC region. However, there was no evidence from the plasmin generation assay of a phosphorylation-dependent alteration of plasmin activity by any means, including an effect on tPA, which was added to activate plasmin and initiate lysis.

4.2.2.3.2. Plasmin digestion of fibrinogen

With regards to conformational change, Martin and Bjork (1990) have reported that phosphorylation alters the conformation of fibrinogen. Phosphorylation of fibrinogen by PKC or CK2 caused alterations to the secondary structure, while phosphorylation with PKA or CK1 showed no such change. Similarly, phosphorylation with PKA or PKC caused changes in the tertiary structure of fibrinogen around tryptophan residues, but this was not the case after phosphorylation with CK1 or CK2. This study by Martin and Bjork highlights that phosphorylation-induced changes to the secondary or tertiary structure of fibrinogen are kinase-specific. Furthermore, the observed conformational changes and decreased rate of proteolysis by plasmin after phosphorylation were both unaltered by removal of phosphate using alkaline phosphatase. This suggests that phosphorylation causes an irreversible conformational change, which in turn reduces susceptibility to proteolysis. The effect of *in vivo* fibrinogen phosphorylation on conformation has yet to be confirmed, but could be investigated in the same way, using nuclear magnetic resonance, x-ray crystallography or circular dichroism. This may provide reasoning for any observed effects of fibrinogen phosphorylation on resistance to fibrinolysis.

A plasmin digestion time course experiment was conducted to compare the rate of plasmin digestion of fibrinogen with increasing levels of phosphorylation. The levels of fibrinogen degradation products – fragment Y and fragment D1 – were measured over time. There was no difference seen in the intensity of fragment Y over time between the phosphorylation isoforms. For fragment D1, there was a slight difference between samples, with the 13 % phosphorylated fibrinogen sample exhibiting a faster rate of fragment D1 formation than the control 25 % sample, and the 33 % sample exhibiting a slower rate of fragment D1 formation compared to the control. This would suggest that phosphorylation has a protective effect over fibrinogen, promoting resistance to

fibrinolysis. Although the effect was marginal in this investigation, the reduced rate of fragment D1 formation with higher phosphate contents supports previous literature with *in vitro* and *in vivo*-phosphorylated fibrinogen, reporting that this modification protects fibrinogen from plasmin digestion (Martin et al., 1992, Martin et al., 1991, Martin and Bjork, 1990, Forsberg and Martin, 1990). This finding may reflect hindered interaction with plasmin due to conformational change, or as previously discussed, increased binding of Ca^{2+} ions to fibrinogen, which has been shown to protect fibrinogen from degradation by plasmin (Dang et al., 1985a). Had the results demonstrated a significant trend, measurement of individual α chain fragments by densitometry could have been used as an indication of the particular cleavage site(s) affected by the presence of phosphate.

The removal of fibrinogen-bound phosphate with alkaline phosphatase, following incubation with kinases *in vitro*, has demonstrated an irreversible effect of fibrinogen phosphorylation on resistance to plasmin digestion (Martin et al., 1991, Martin and Bjork, 1990, Forsberg and Martin, 1990). Martin et al. (1992) have shown the same effect with fibrinogen taken from patients on days 0, 1 and 8 following hip-replacement surgery. Despite a return to normal phosphorylation levels on day 8, the susceptibility to plasmin digestion remained at 50 % of that on day 0. Based on this evidence, the expected result for dephosphorylated fibrinogen in this experiment would be to mimic control fibrinogen. Appearance of fragment D1 in the dephosphorylated sample was similar to the control, but unexpectedly was slightly slower. Hence, the trace of the DP fibrinogen sample may indicate some experimental error. Furthermore, cleavage of the α chain results in fragment X formation prior to fragment Y formation. Therefore, if phosphorylation was affecting α chain cleavage by plasmin, you would expect to see a difference in both fragment Y and fragment D1 between samples, which was not the case. However, this method may not have permitted detection of subtle differences in fragment Y formation as the bands were much darker, possibly approaching saturation. Fragment X would also be expected to follow the same trend but was not measured in this instance as it was not clearly distinct from the dark full-length fibrinogen band. For such reasons, densitometry analysis can be troublesome and somewhat subjective (Gassmann et al., 2009). It also may not be sensitive enough to highlight small differences in digestion rates.

Investigations into plasmin digestion of fibrinogen can provide clues as to whether phosphorylation of Ser3 and Ser345 causes a conformational change in fibrinogen, altering resistance to fibrinolysis. However, plasmin digestion of fibrinogen is not physiological, and any effect of fibrinogen phosphorylation on susceptibility to plasmin may be more pronounced in polymerised, cross-linked fibrin. This approach would also

take into account any phosphorylation-induced changes to clot structure. Turbidity analysis and SEM experiments from this investigation revealed thinner fibres and increased branching, suggestive of an increase in clot density. Hence, fibrinolysis is likely to be compromised. In addition, plasminogen binds to sites that are cryptic in fibrinogen but exposed in fibrin (Tsurupa and Medved, 2001a, Varadi and Patthy, 1983), and the rate of plasminogen activation by tPA is significantly enhanced in the presence of fibrin (Hoylaerts et al., 1982). Therefore, examination of the effect of phosphorylation on fibrin clot degradation would be a valuable addition to this work. To investigate this, turbidity and lysis analysis of fibrin clots could be used to monitor changes in lysis rate and $Lys50_{MA}$ over time. Laser scanning confocal microscopy of clots could also be used to calculate lysis front velocity by overlaying wells with plasminogen and tPA, and measuring the distance the lysis front moves within a particular time frame (Collet et al., 2000, Ajjan et al., 2008). However, these methods wouldn't reveal which of the plasmin cleavage sites on fibrinogen are affected by phosphorylation.

4.2.2.4. Additional interactions

So far, this work has demonstrated that the effect of elevated fibrinogen phosphorylation *in vivo* on resistance to fibrinolysis, as demonstrated by Martin et al. (1992), is not mediated by altered FXIII-, α2-AP- or plasminogen-fibrinogen interactions. The effects on tPA binding and PAI-2 cross-linking have yet to be determined, while plasmin digestion data reported here warrants further investigation. Aside from plasma proteins, it would also be interesting to look for any effect of fibrinogen phosphorylation on the binding of fibrinogen to cell surfaces. There is one integrin-binding RGD sequence at either end of the fibrinogen Aα chain (residues 95-97 and 572-574), as well as an additional AGDV attachment site in the γ chain C-terminus (residues 408-411) (Kloczewiak et al., 1984, Hawiger et al., 1989). It has been shown that the N-terminal RGD site of the fibrinogen Aα chain is not readily available for interaction as it is buried within the coiled-coil domain (Doolittle et al., 1978, Ugarova et al., 1993). The C-terminal RGD sequence, on the other hand, is both accessible and important for the initial binding of fibrinogen to the $\alpha_V\beta_3$ integrin on the surface of endothelial cells (Cheresh et al., 1989). This initial ligand-receptor interaction can induce a conformational change, exposing the Aα 95-97 RGD site (Ugarova et al., 1993).

Binding of proteins to human vascular endothelial cells can be analysed by ELISA, by culturing the cells on a gelatinised 96-well plate and fixing with 1 % paraformaldehyde (Collard et al., 1999). To investigate whether Ser3 phosphorylation alters the

availability of Aα 95-97, or whether Ser345 phosphorylation enhances binding of Aα 572-574 to $\alpha_V\beta_3$, an ELISA could be performed by coating a 96-well plate with human vascular endothelial cells, incubating with DP, 13 %, 25 % or 33 % phosphorylated fibrinogen, and detecting bound fibrinogen with an anti-fibrinogen HRP antibody. With regards to platelet binding, only the fibrinogen γ chain AGDV domain is needed for interaction with activated GPIIbIIIa (Cheresh et al., 1989, Liu et al., 1997); hence the Aα chain RGD sites are less likely to be regulated by phosphorylation at Ser3 or Ser345 for this particular purpose. Yet there are still many options to explore, and preliminary data to expand, to decipher potential contributions of fibrinogen phosphorylation in the co-ordination of coagulation.

4.2.3. The effect of fibrinogen phosphorylation on fibrin clot formation

4.2.3.1. Fibre diameter

The structure of fibrin clots formed from fibrinogen with varying degrees of phosphorylation was investigated by turbidity analysis and SEM. Turbidity assays revealed that phosphorylation causes a significant reduction in fibre thickness, as represented by a lower MaxAbs. Measurement of fibre diameter in electron micrographs of fibrin clots supported data from the turbidity analyses. Although the measurements are not an accurate representation of diameter due to sample dehydration, the trend of relative fibre thickness mimicked that of the turbidity data, providing convincing evidence of an inverse relationship between the percentage of phosphorylation and fibre thickness.

In vitro, phosphorylation of fibrinogen with PKA and PKC generates fibres with smaller diameters (Heldin et al., 1987a, Martin et al., 1991, Forsberg, 1989), while phosphorylation with CK1 and CK2 produces thicker fibrin fibres (Heldin, 1987, Martin et al., 1991). It could be argued that the observation of thinner fibres with increasing phosphorylation in this study indicates that phosphorylation of fibrinogen by PKA or PKC is more likely than phosphorylation by CK1 or CK2. However, subsequent characterisation of phosphorylation sites with PKC and CK2 did not identify phosphorylation at Ser3 or Ser345. Protein kinase C was found to phosphorylate Ser557, Ser558, Ser559 and Ser599, as well as additional sites in the central portion of the polypeptide chain (Heldin and Humble, 1987). Casein kinase 2, on the other hand, phosphorylated Ser523 and Ser590, plus other undefined serine and threonine residues between amino acids 259 and 268 (Heldin, 1987). Hence, the results here cannot be related to the effects of kinases in previous studies, as kinases exhibit altered specificity *in vitro* (Olsen et al., 2006). Furthermore, fibrinogen may not be

phosphorylated by any of these enzymes *in vivo*. The effect of elevated fibrinogen phosphorylation on fibre diameter has previously been reported by Martin et al. (1992), using fibrinogen taken from patients before and after hip-replacement surgery. The phosphate content of fibrinogen doubled 24 hours after surgery, with a similar increase in fibrin fibre thickness, disagreeing with the data from this investigation. This may reflect discrepancies in methodology. The fibrinogen used in this thesis investigation was plasma purified, but had not been exposed to acute phase conditions, unlike that used by Martin et al. (1992). There may be other factors or modifications to fibrinogen that occur *in vivo* during the acute phase response, such as phosphorylation at additional sites in circulation, that could influence fibre diameter. Despite these differences, the results of this investigation are specific to Ser3 and Ser345, and demonstrate for the first time that an increased degree of phosphorylation at these residues leads to thinner fibres in the resulting clot.

4.2.3.2. Fibre branching

Clot structures also exhibited increased branching of fibres with higher levels of phosphorylation, based on qualitative assessment of SEM images. Fibre branching could be analysed quantitatively using software that allows 3D-reconstruction of scanning electron micrographs and rotation in the *x*-, *y*- and *z*-directions, in order to mark and count fibre branching points, as detailed by Collet et al. (2005b) and Ryan et al. (1999). The increased branching may be related to the reduced fibre diameter, as Ryan et al. (1999) report a relationship between the two, with large fibres only occurring when branching is minimal. Branching can occur during end-to-end binding of fibrin monomers (protofibril extension) or by divergence of protofibrils during lateral aggregation. The former is a two-step binding process; interference from a third fibrin molecule between these two steps creates a branch. This type of branch formation is dependent on monomer supply rate (Fogelson and Keener, 2010). Phosphorylation of fibrinogen Aα Ser3 has been demonstrated to enhance complex formation between fibrinogen and thrombin, leading to faster cleavage of FpA and fibrin monomer formation (Maurer et al., 1998). Furthermore, Blomback et al. (1989) describe a clot structure with thinner fibres and smaller pores with higher thrombin concentrations. Although the thrombin concentration was kept constant here, the greater substrate specificity of thrombin for phosphorylated FpA may produce a similar effect. It is therefore likely that phosphorylation of FpA contributes to the reduced fibre diameter and increased branching that coincide with higher degrees of fibrinogen phosphorylation. However, the effect of phosphorylation on FpA cleavage and protofibril formation could not be deduced from the turbidity data as lag times were too

short. This could be verified by repeating the assays with a lower thrombin concentration to extend lag times.

4.2.3.3. Clotting rate

In addition to the observed structural changes, the turbidity analysis also revealed an inverse relationship between the degree of fibrinogen phosphorylation and the rate of clot formation. Although the effect appeared small, statistical analysis confirmed significant differences. To the best of my knowledge, this is the first report of *in vivo* fibrinogen phosphorylation leading to a reduction in clotting rate. Interestingly, it has previously been reported that phosphorylation of Ser3 promotes complex formation with thrombin and facilitates FpA cleavage (Maurer et al., 1998). The findings by Maurer et al. coupled with this current observation therefore suggest distinct roles of Ser3 and Ser345 in clot formation, with phosphorylation of Ser3 enhancing protofibril formation (the 'lag' period), and phosphorylation of Ser345 interfering with lateral aggregation of protofibrils, leading to a slower clotting rate beyond the initial lag period. As mentioned above, lag times were too short in these experiments to be accurately determined. For this reason, this may not be the most suitable method for comparison of clotting rates, as calculation of this variable is also dependent on lag times. Again, further investigations with lower thrombin concentrations and extended lag times would be beneficial to clarify the effects of Ser3 and Ser345 phosphorylation on protofibril formation and clotting rate.

4.2.3.4. Clinical implications

The findings from this thesis suggest that elevated fibrinogen phosphorylation produces clots with structural changes that may alter thrombotic potential. In particular, the observed clot structure is comparable to that of diabetic patients. Subjects with diabetes or metabolic syndrome, who are at greater cardiovascular risk, generate clots that are denser and less porous, owing to thinner fibres and more branch points. Importantly, these structural changes make the clot more resistant to fibrinolysis (Dunn et al., 2005, Carter et al., 2007). It would therefore be interesting to quantify the degree of fibrinogen phosphorylation in diabetic patients. This could be done on a small scale by malachite green assay, but as this requires plasma-purified fibrinogen, an ELISA with phospho-specific antibodies would be the ideal method to screen large sample numbers. Clots of patients with other cardiovascular complications, including AMI, stroke, PAD and VTE, tend to form thicker fibres compared to healthy controls, but all exhibit reduced permeability and prolonged lysis times (Bhasin et al., 2009, Undas et al., 2009b, Undas et al., 2008, Undas et al., 2009a). Despite the thinner fibres, the

increased branching in clots composed of 33 % phosphorylated fibrinogen is likely to raise clot density and lower porosity – properties which antagonise the infiltration of fibrinolytic agents. Clot density could be measured by LCSM of fibrin clots and analysis using an ImageJ macro to count the number of times the fibres cross a set of gridlines, as an estimate of fibre number within the frame. This does not work well with SEM images due to insufficient contrast between fibres and background (Greenhalgh, 2013). Permeability could also be compared by measuring the flow rate of buffer through the fibrin clots and calculating the permeation coefficient, K_S, as previously described (Ariens et al., 2000). In addition to the observed structural changes, Martin et al. (1992) have demonstrated that a doubling of fibrinogen phosphate content *in vivo* leads to a concurrent reduction in susceptibility to plasmin digestion. With all of this in mind, it would be reasonable to conclude that elevated fibrinogen phosphorylation yields a pro-thrombotic clot structure, and therefore deserves attention in the quest to develop new therapeutic strategies.

4.3. Characterisation of intracellular fibrinogen phosphorylation

To complement the functional characterisation of fibrinogen phosphorylation, intracellular studies were conducted to investigate the regulatory processes underlying this modification, including the subcellular location of phosphorylation, as well as changes to kinase expression and the degree of fibrinogen phosphorylation that occur in response to acute phase cytokine IL-6. A range of methods were employed to determine the effect of cellular fibrinogen phosphorylation levels in the presence of IL-6, kinase inhibitor staurosporine and Fam20A siRNA.

4.3.1. Developing methods for the detection of phosphorylated fibrinogen

4.3.1.1. Detection and quantification of intracellular phosphorylated fibrinogen Aα chain by PLA

A proximity ligation assay was developed to visualise and quantify phosphorylated fibrinogen Aα chains in CHO and HepG2 cells. Antibodies to the fibrinogen Aα chain, PDI (ER marker) and TGN46 (*trans*-Golgi marker) were optimised first by standard immunofluorescence. Fibrinogen Aα chain staining co-localised with the ER marker in both cell lines, with little or no co-localisation with TGN46 in the *trans*-Golgi. This agrees with recent findings by Tamura et al. (2013) who have also conducted immunofluorescent analysis of fibrinogen in HepG2 cells. They too observed co-localisation with an ER marker but not a *cis*-Golgi marker, and report that the

majority of fibrinogen molecules are confined to this early secretory compartment. The detection of fibrinogen Aα chains in the ER likely represents the pools of Aα chains that have previously been described (Yu et al., 1984, Huang et al., 1993b, Huang et al., 1996, Xia and Redman, 2001).

Optimal antibody concentrations were used for subsequent PLA experiments. Initially, PLA was performed using CHO cells, so that the signal in CHO-WT cells could be compared to CHO-Bβγ cells as a negative control for the anti-fibrinogen Aα chain antibody. Previous studies have used liquid chromatography-electrospray ionisation-tandem mass spectrometry to demonstrate that fibrinogen phosphorylation occurs exclusively on the Aα chain (Wind et al., 2003, Nagel and Meyer, 2014). Given that phosphoserine antibodies are prone to non-specific binding, and have indeed demonstrated non-specific binding to the fibrinogen β chain in a western blot (figure 52), this assay would benefit from a suitable control for the non-specific binding of anti-phosphoserine to fibrinogen. This would require each chain of fibrinogen to be present but not phosphorylated, hence the ideal negative control would be the S3/345N variant lacking both of the Aα chain phosphorylation sites. Unfortunately, this was not achieved as part of this investigation due to problems with expression of fibrinogen variants in CHO cells.

In the first PLA experiment, a concentration range of anti-phosphoserine antibody was optimised to give adequate signal with minimal background. Subsequent assays using HepG2 cells included ER and Golgi markers to investigate the intracellular location of phosphorylated fibrinogen Aα chains. The signal was low and randomly distributed throughout the cell, with no detectable co-localisation of phosphorylated fibrinogen with the ER or trans-Golgi. This implies that the intracellular pools of fibrinogen Aα chain, as demonstrated previously and by immunofluorescence in this investigation, are non-phosphorylated (Yu et al., 1984, Huang et al., 1993b, Huang et al., 1996, Xia and Redman, 2001). Therefore, phosphorylation is likely to occur only in fully assembled fibrinogen. Tamura et al. (2013) have demonstrated that lectin chaperones retain fibrinogen intermediate complexes in the ER so that only fully assembled fibrinogen is transported out of the cell for secretion. Hence, phosphorylated fibrinogen does not appear to accumulate in the cell. The low signal in PLA images, despite abundant detection of intracellular fibrinogen Aα chains by immunofluorescence, also suggests that the assay is specific to *phosphorylated* fibrinogen Aα chains.

4.3.1.1.1. The subcellular location of fibrinogen phosphorylation

To further investigate the subcellular location of fibrinogen phosphorylation, and to increase the PLA signal, HepG2 cells were incubated with secretion inhibitor BFA. Brefeldin A blocks the transit of proteins beyond the ER and redistributes *cis*- and *medial*-Golgi compartments back to the ER (Lippincott-Schwartz et al., 1989). The average number of PLA spots, representing individual phosphorylated fibrinogen Aα chains, was counted per cell using an ImageJ macro. The signal was found to increase from an average of 5.0 to 16.8 spots per cell in the presence of BFA. Pre-incubation of HepG2 cells with BFA is therefore a useful tool to obtain sufficient signal for comparison of phosphorylation levels. The build-up of phosphorylated fibrinogen in the presence of BFA also indicates that fibrinogen is phosphorylated before it reaches the *trans*-Golgi network, either in earlier Golgi compartments or in the ER. Consequently, these data still permit the possibility of phosphorylation by the two suspected fibrinogen kinases: i) the G-CK, which has been shown to reside in the lumen of the *cis*-Golgi (Tagliabracci et al., 2012), and ii) CK2, which is predominantly active in the ER in hepatocytes (Lasa et al., 1997).

4.3.1.1.2. Limitations of PLA

It should be noted that there are some limitations to the PLA method used in these investigations to measure fibrinogen phosphorylation in HepG2 cells. Firstly, HepG2 cells have a tendency to grow in clumps. This was minimised by passing cells through a needle during passage, but could not be completely avoided. Imaging was therefore restricted to monolayer areas. Secondly, there was significant cell-to-cell variation in signal, making it difficult to choose representative areas. Another point to note is the potential for additional phosphorylation sites inside the cell that have not been characterised; analysis of fibrinogen phosphorylation sites has only been performed on fibrinogen from an extracellular environment. Matrix assisted laser desorption ionisation-TOF/TOF mass spectrometry could be used to confirm or identify phosphorylation sites on fibrinogen from HepG2 cells before and after secretion; this technique was used to confirm phosphorylation of Ser3 and Ser345 in recombinant fibrinogen expressed in CHO cells (Appendix 3). Finally, it is important to consider that fibrinogen Aα chains might represent a mixture of mono- and di-phosphorylated polypeptides. In fact, this has recently been demonstrated for the first time by Nagel and Meyer (2014), and presents a significant limitation for comparing the degree of phosphorylation, as only one site can be detected per Aα chain molecule by PLA. Taking all of this into account, together with the lack of negative control, PLA does not seem to be the most reliable approach for quantification of intracellular fibrinogen

phosphorylation. Therefore additional methods were sought, which focused on comparing phosphorylation levels of fibrinogen secreted by HepG2 cells into conditioned medium. The use of secreted fibrinogen circumvented any additional intracellular modification which may occur, and provided a larger yield of fibrinogen for analysis than cell lysis.

4.3.1.2. Phos-tag™ applications for detection of phosphorylated fibrinogen

Phos-tag™ – a novel molecule which is able to bind phosphate groups with high affinity – was employed in several methods for the detection of phosphorylation in secreted fibrinogen. Phos-tag™ affinity SDS-PAGE using pre-cast gels from the manufacturer did not result in separation of phosphorylated and non-phosphorylated fibrinogen, with bands appearing at the same position for control (25 % phosphorylated) and dephosphorylated fibrinogen. This outcome most likely indicates inadequate affinity of Phos-tag™ for phosphorylated fibrinogen, possibly reflecting a low number of phosphorylated residues per molecule. Loading of phosphorylated and dephosphorylated β-casein, which is more heavily phosphorylated (5 mol phosphate/mol protein), for comparison would be useful to ascertain whether the Phos-tag™ agarose is able to capture phosphoproteins and slow their migration under the given experimental conditions, thus indicating whether the problem is methodological or due to insufficient phosphate on fibrinogen. An ELISA using Phos-tag™ Biotin and streptavidin alkaline phosphatase revealed non-specific binding of Phos-tag™ Biotin to the plate, as indicated by high absorbance values in blank wells without fibrinogen, perhaps due to a large molar excess of Phos-tag™ Biotin. In addition, development times were slow and specific detection of phosphorylated fibrinogen was minimal. Finally, western blotting with Phos-tag™ Biotin and streptavidin HRP was unsuccessful due to non-specific binding of streptavidin HRP to the Aα and Bβ chains of fibrinogen, as confirmed with a streptavidin-HRP-only control. The results of the SDS-PAGE and ELISA suggest that Phos-tag™ has poor affinity for phosphorylated fibrinogen, perhaps because fibrinogen is not phosphorylated heavily enough to permit sufficient Phos-tag™-fibrinogen interaction. However, Phos-tag™ has been used for enrichment of phosphorylated fibrinogen by affinity chromatography, as previously discussed, and therefore does exhibit some affinity for phosphorylated fibrinogen.

4.3.1.3. Detection of phosphorylated fibrinogen using anti-phosphoserine antibodies

Similar problems were encountered using anti-phosphoserine antibodies, which are renowned for exhibiting poor sensitivity and specificity for their phosphorylated substrates. For ELISA, conditions were optimised to minimise non-specific interaction between the antibodies and fibrinogen, but non-specific binding to the wells or coating antibody was still high. Using dephosphorylated fibrinogen as a negative control, there was some specific detection of phosphoserine, but the change in absorbance was too small to enable comparison of phosphorylation levels. Despite some initial non-specific binding to the Bβ chain and high background, a western blotting protocol was successfully optimised for specific detection of phosphorylated fibrinogen. The optimised protocol abrogated non-specific binding of anti-phosphoserine to dephosphorylated fibrinogen, the Bβ chain, and the PVDF membrane. It also demonstrated the change in phosphorylation levels between samples separated by Phos-tag™ chromatography, supporting the results of the malachite green assay. The limitation of this method is the requirement for a relatively large mass (1-2 µg) of fibrinogen in the well due to poor antibody sensitivity – approximately 20-40 times more than would be needed for detection of fibrinogen using an anti-fibrinogen antibody, which presented a challenge for harvesting sufficient fibrinogen from HepG2 culture. However, this method was successfully used to compare the degree of fibrinogen phosphorylation in subsequent experiments with samples of harvested medium.

4.3.2. The effect of IL-6 on fibrinogen expression and phosphorylation in HepG2 cells

Having established a suitable method for the specific detection of phosphorylation in secreted fibrinogen, HepG2 cells were incubated with several reagents to monitor changes in phosphorylation levels in acute phase conditions or with kinase inhibitors. Interleukin-6 was added to the cells to mimic the acute phase response. While other cytokines, notably interleukin-1 and TNF-α, also induce acute phase protein expression, IL-6 is the principal mediator of this response (Yudkin et al., 2000). The concentration of IL-6 was optimised to 10 ng/ml, resulting in a 3.5-fold increase in fibrinogen expression, as determined by real-time PCR. This is similar to previous reports by Faber et al. (2012) and Igaz et al. (1998), who both found a 4.5-fold increase in fibrinogen expression in HepG2 cells incubated with 10 ng/ml IL-6. Increased fibrinogen expression in response to IL-6 is well characterised, and is regulated at the transcriptional level via IL-6 response elements in fibrinogen genes (Ray, 2000, Fuller

and Zhang, 2001). The effect of IL-6 on fibrinogen phosphorylation was first of all examined by PLA. In the presence of IL-6, the mean number of spots per cell increased 4.0-fold, from 2.1 to 8.3. This increase is only slightly higher than the 3.5-fold increase in expression, which would suggest almost the same proportion of fibrinogen molecules are phosphorylated, and therefore the elevated phosphorylation that occurs during the acute phase response is mediated in circulation rather than intracellularly. Several studies have indeed suggested that fibrinogen can be phosphorylated in circulation by kinases released from activated platelets (Krust et al., 1983, Lerer et al., 1991, Ekdahl et al., 1997, Zahedi et al., 2008). However, as discussed previously, the PLA results should be interpreted with caution due to difficulties with analysis and the limitation of only being able to detect one phosphate molecule per Aα chain.

For more accurate analysis, conditioned medium was harvested from HepG2 cells after a 24 hour incubation period with IL-6. Fibrinogen phosphorylation was compared in medium samples in the presence and absence of IL-6 by western blotting with an anti-phosphoserine antibody, normalising to the fibrinogen γ chain using an anti-fibrinogen γ chain antibody. The results showed a clear increase in phosphorylation of the Aα chain after incubation with IL-6. Further analysis by densitometry revealed a 3.1-fold increase – equivalent to a rise from 25 % to 78 % – which is only slightly higher than the values reported for acute phase conditions *in vivo* (Seydewitz and Witt, 1985, Reganon et al., 1993, Martin et al., 1992). The significant increase in phosphorylation of fibrinogen from HepG2 cells incubated with IL-6 suggests that fibrinogen is partially phosphorylated when secreted. Otherwise, if fibrinogen molecules were fully phosphorylated when secreted from HepG2 cells, there would be no observable increase in phosphorylation levels in the presence of IL-6. The exception would be if additional sites, other than Ser3 and Ser345, are phosphorylated in the presence of IL-6. Although fibrinogen can be phosphorylated in circulation by platelet kinases (Krust et al., 1983, Zahedi et al., 2008, Ekdahl et al., 1997), these results demonstrate for the first time that the mechanism responsible for increased phosphorylation of fibrinogen in acute phase conditions occurs at the cellular level rather than in circulation. However, this conclusion is based on the assumption that phosphorylation levels are not altered in the medium by secreted kinases or phosphatases. This is a reasonable assumption as there would be very little phosphate bound to fibrinogen after a 24 hour incubation period if fibrinogen was susceptible to secreted phosphatases. An intracellular increase in phosphorylation also seems logical given that extracellular ATP concentrations are typically very low, with a basal plasma concentration of 2 nM, meaning that phosphorylation of fibrinogen in plasma is unlikely to occur without release of ATP and kinases from activated platelets (Zhong and Wright, 2013, Ekdahl and Nilsson, 1995).

4.3.3. The effect of IL-6 on kinase expression in HepG2 cells

Having observed an increase in cellular phosphorylation of fibrinogen in the presence of IL-6, the next step was to investigate whether there is altered expression of relevant fibrinogen kinases, including CK2 and the G-CK. First, HepG2 cells were screened for expression of each kinase under control conditions by real-time PCR. Previously, Nalbant et al. (2005) have demonstrated by RNA extraction and RT-PCR that Fam20B and Fam20C are expressed in a wide variety of tissues, while the Fam20A expression pattern was relatively limited. Expression of all three proteins was detected in the liver, with highest expression of Fam20C, followed by Fam20A and finally Fam20B. In agreement, expression of Fam20A, Fam20B and Fam20C were all detected in HepG2 cells in this investigation, as well as CK2, but late Ct values indicated low expression of Fam198A and Fam198B. These kinases were therefore excluded from the following experiments. Second, real-time PCR was repeated using RNA from HepG2 cells incubated in the presence and absence of IL-6, to determine the fold-change in expression. Interestingly, expression of CK2, Fam20B and Fam20C did not change, but there was a significant 6-fold increase in expression of Fam20A. This remarkable increase in Fam20A expression indicates that this kinase plays a role in the hepatocellular response to acute phase conditions. Fam20A has previously been implicated in biomineralisation processes, with mutations in the Fam20A gene leading to severe Amelogenesis Imperfecta and Enamel-Renal Syndrome (Vogel et al., 2012, Wang et al., 2013), but there are no reports of altered coagulation in these cases. A recent study by Kiliszek et al. (2012) has also implicated Fam20A in the acute phase response, revealing significant up-regulation of Fam20A expression in leukocytes from AMI patients. The reason for this increased expression is unknown, although Fam20A does play a role in haematopoiesis, which is stimulated by cytokines during the acute phase response (Nalbant et al., 2005, Trey and Kushner, 1995). To the best of my knowledge, however, this is the first time that increased Fam20A expression has been demonstrated in HepG2 cells in response to IL-6. This may similarly be linked to the hematopoietic function of the liver (Seki et al., 2000), but also highlights a potential function of Fam20A in phosphorylating fibrinogen and/or other acute phase proteins. In support of this, Szymanski and Farrell (1982) have demonstrated phosphorylation of FpA *in vitro* by a casein kinase isolated from the Golgi apparatus of bovine mammary glands.

It has been suggested by Salvi et al. (2010) that the G-CK has a prominent role in generating the human plasma phosphoproteome, with the majority of plasma phosphorylation sites satisfying its consensus sequence: S-X-E. The list of plasma phosphoproteins also displays a similar profile to that of the G-CK substrates, but

distinct from that of CK2 substrates. There are several other acute phase proteins secreted by hepatocytes that contain S-X-E motifs, including kininogen, α1-antitrypsin, fetuin A, apolipoprotein E, insulin-like growth factor binding proteins (IGFBP) 1 and 3, complement C3, plasminogen, plasminogen-related protein B2, fibronectin I, proprotein convertase subtilisin/kexin type 9 (PCSK9), kallikrein-6, FV, FIX and serum albumin (Tagliabracci et al., 2012). Tagliabracci et al. (2012) have demonstrated phosphorylation of kininogen, complement C3, FV and serum albumin by Fam20C *in vitro*. Fibrinogen, on the other hand, was not phosphorylated by Fam20C. It is not yet clear whether Fam20C phosphorylates these substrates *in vivo*, or whether there is some cross-over between substrates for the different Fam20 proteins. However, there must be additional specificity determinants if secretory proteins are phosphorylated by other Fam20 kinases. Phosphorylation of FIX, complement C3 and PCSK9 has been shown to promote or diminish the protein's susceptibility to proteolysis (Dewpura et al., 2008, Nilsson Ekdahl and Nilsson, 1999, Atoda et al., 2006), as is the case with fibrinogen phosphorylation and plasmin digestion (Martin et al., 1992, Martin et al., 1991, Martin and Bjork, 1990, Forsberg and Martin, 1990). Phosphorylation can also increase the affinity of protein-protein interactions. For example, phosphorylation of IGFBP-1 leads to increased binding, and therefore reduced bioavailability, of its substrate insulin-like growth factor-1 – a negative acute phase protein (Jones et al., 1991); the significance of this is yet to be characterised. Hence, increased phosphorylation of acute phase proteins in hepatocytes may alter their function in circulation, possibly to promote coagulation and facilitate wound repair.

In support of fibrinogen phosphorylation by the G-CK, there are in fact many similarities between fibrinogen and κ-casein – a G-CK substrate. Interestingly, Vorbach et al. (2006) have postulated that the mammary gland evolved from the innate immune system, and, based on structural and sequence similarities, that κ-casein may have evolved from fibrinogen. Approximately 80 % of the κ-casein sequence has counterparts in the fibrinogen γ chain sequence, with 31-42 % of amino acids at identical positions (Jolles et al., 1978). Additionally, as with fibrinogen, κ-casein contains two well-established phosphorylation sites at Ser149 and Ser127 (Hernandez-Hernandez et al., 2011). The similarities of κ-casein and fibrinogen extend further to their regulation and function. The mechanism underlying increased fibrinogen expression in response to IL-6 in hepatocytes is similar to the transcriptional regulation of casein induced by prolactin in mammary epithelial cells, including similarities in response factors and activation of the Janus kinase/signal transducers and activators of transcription (JAK-STAT) pathway for downstream effects (Standke et al., 1994, Vorbach et al., 2006). In terms of function, κ-casein triggers the process of milk clotting

(Brinkhuis and Payens, 1985). Micelles are stabilised by transglutaminase activity and casein is degraded by a plasmin-like enzyme that acts on lysine residues (Ferranti et al., 2004, Smiddy et al., 2006). In addition, fibrinogen and κ-casein exhibit similar behaviour in terms of platelet aggregation (Jolles et al., 1986). It is also worth noting that the cross-linking of casein is influenced by its phosphorylation status (Aoki et al., 1992). Given that casein is phosphorylated by the G-CK, these studies provide convincing evidence for a similar mechanism of fibrinogen phosphorylation *in vivo*.

4.3.4. The effects of kinase inhibitor STSP and Fam20A siRNA on fibrinogen phosphorylation in HepG2 cells

To test the hypothesis that fibrinogen is phosphorylated by Fam20A, HepG2 cells were incubated with kinase inhibitor STSP. Staurosporine inhibits the majority of kinases and is especially effective for PKC inhibition, but is unable to bind Fam20 proteins due to the unique structure of their active site (Xiao et al., 2013, Meggio et al., 1995). In the first instance, the effect of STSP on fibrinogen phosphorylation in HepG2 cells was investigated by PLA. There was a 60 % reduction in the mean number of spots per cell, suggesting that fibrinogen is not phosphorylated by the G-CK. However, STSP is known to induce apoptosis in HepG2 cells (Giuliano et al., 2004), which were showing visible signs of apoptosis at the concentration used. Many cells detached from the wells during fixation which meant there were few areas to image, leading to difficulty in finding representative areas. In light of these difficulties, phosphorylation of secreted fibrinogen was also analysed by western blotting with an anti-phosphoserine antibody. As Fallon and Danaher (1992) have reported half-maximal STSP-induced up-regulation of a carbohydrate-binding lectin with only 30 nM STSP, a lower concentration range of STSP (0-200 nM) was used for these experiments to minimise apoptosis. In the first attempt, the phosphorylated Aα chain band persisted with increasing concentrations of STSP up to 200 nM, suggesting that fibrinogen is phosphorylated by the G-CK. To improve clarity of the blot, fibrinogen was immunoprecipitated from the medium prior to electrophoresis for the second experiment. Immunoprecipitation was successful, as clear fibrinogen bands were detected on the blot. This time, however, the phosphorylated Aα chain band appeared weaker with 200 nM STSP compared to control, indicating that a kinase other than the G-CK phosphorylates fibrinogen in HepG2 cells. The difference between the two results may reflect minor loading errors or non-specific binding of the phosphoserine antibody to the highly concentrated samples of conditioned medium in the absence of prior immunoprecipitation.

To provide a more conclusive answer as to whether Fam20A phosphorylates fibrinogen *in vivo,* Fam20A siRNA was transfected into HepG2 cells to knock down expression of this kinase. The protocol was successfully optimised, achieving an 86 % reduction in Fam20A expression. However, methodological changes to increase the yield of fibrinogen for analysis led to a decrease in efficiency of Fam20A knockdown by siRNA (53 %) and no visible difference in Aα chain phosphorylation by western blotting. Unfortunately, the question remains whether Fam20A phosphorylates fibrinogen *in vivo*. If this is the case, the significant rise in Fam20A expression in acute phase conditions may highlight an important role of Fam20A, not only in fibrinogen phosphorylation, but in facilitating elevated phosphorylation of a plethora of acute phase proteins. It would therefore be interesting to compare the degree of phosphorylation of other proteins with the S-X-E motif in the presence and absence of IL-6. This scenario would make Fam20A a valuable therapeutic target.

In a review article, Cohen (2002) has proposed that protein kinases may be the major drug target of the 21st century owing to recent advances in the field, with the development of orally active ATP-competitive kinase inhibitors. The first drug to target a protein kinase was developed in 2001, named Gleevec. Gleevec inhibits the Abelson, c-KIT and platelet derived growth factor receptor tyrosine kinases, and is used in the treatment of chronic myelogenous leukaemia and gastrointestinal stromal tumours (Buchdunger et al., 2000, Druker et al., 1996, Joensuu et al., 2001). Many more kinase inhibitors are undergoing clinical trials, and Cohen (2002) reports that this therapeutic category is now the second largest after G protein-coupled receptor inhibitors. It would therefore be valuable to establish the specific role(s) of Fam20A in hepatocytes, as well as its increased expression in acute phase conditions and how this affects the numerous acute phase proteins that are secreted.

4.4. Summary

Phosphorylation of fibrinogen is associated with the acute phase response and thrombotic disorders, but the mechanism and functional role of this modification *in vivo* is not yet known. Work from this thesis aimed to advance understanding of this important regulatory process. Despite problems with variant fibrinogen expression, phosphorylation isoforms were separated by affinity chromatography for functional analyses. These studies revealed that fibrinogen phosphorylation does not affect FXIII cross-linking activity of fibrin α and γ chains, plasminogen binding to fibrinogen, or incorporation of α2-AP, but did highlight a potential effect of phosphorylation on protection from plasmin digestion. With regards to clot structure, increasing

phosphorylation levels caused reductions in fibre thickness and increased branching, which may represent a pro-thrombotic structure. Clotting rate was also significantly reduced with higher phosphate contents. Finally, intracellular studies demonstrated an increase in fibrinogen phosphorylation with acute phase cytokine IL-6, showing for the first time that the rise in phosphorylation during the acute phase response occurs inside the cell rather than in circulation. In support of this, there was a significant increase in expression of Golgi casein kinase Fam20A with IL-6, highlighting a potential role for this kinase in the hepatocellular acute phase response, including phosphorylation of fibrinogen. Further investigations are underway to determine whether Fam20A does indeed phosphorylate fibrinogen *in vivo*.

4.5. Future direction

In recalling one of the original aims of this thesis, expression of fibrinogen with mutations at Ser3 and Ser345 would be highly advantageous in deciphering the role of each individual phosphorylation site in fibrin clot formation and interactions. If the yield could be improved, perhaps by multicistronic cloning, recombinant WT and variant fibrinogen could be expressed using the Expi293™ system. Similarly, more efficient chromatographic procedures, such as IMAC or MOAC, could be tested for greater separation of phosphorylated and non-phosphorylated fibrinogen for functional analyses. The functional investigations presented in this thesis could be expanded to study the effect of fibrinogen phosphorylation on resistance to fibrinolysis, FXIII cross-linking at lysine acceptor residues in fibrinogen, the rate of FXIII subunit dissociation and activation, incorporation of PAI-2, tPA binding to fibrinogen, and the interaction of fibrinogen with platelets and endothelial cells. It would also be valuable to further clarify the regulation of fibrinogen phosphorylation *in vivo*, including identification of the relevant kinase. This work would greatly benefit from the use of phospho-specific antibodies targeted to the fibrinogen phosphorylation sites, to detect and quantify changes in the degree of phosphorylation. Preliminary investigations with Fam20A siRNA should be continued to establish whether this kinase phosphorylates fibrinogen in HepG2 cells. Other kinase inhibitors, such as STSP and a CK2 inhibitor could also be employed to facilitate identification of the fibrinogen kinase.

There are many additional questions surrounding fibrinogen phosphorylation to be addressed in the future. Phospho-specific antibodies could be used to investigate whether the degree of Ser3 and Ser345 phosphorylation is altered in other pathologies, such as bleeding disorders and diabetes. This could potentially highlight fibrinogen phosphorylation as a biomarker for a range of disease states, and further testify to the

importance of understanding the regulation and function of this modification at the molecular level. One particular aspect which has not been covered during this investigation is the phosphorylation of fibrinogen in circulation by platelet kinases, which occurs at sites other than Ser3 and Ser345 in resting human platelets (Zahedi et al., 2008). Increased phosphorylation of fibrinogen is associated with platelet activation (Krust et al., 1983, Ekdahl et al., 1997). Identification of additional phosphorylation sites on circulating fibrinogen could be investigated by MALDI-TOF/TOF after incubation of fibrinogen with activated platelets. This would enable functional characterisation of additional modifications to fibrinogen that are likely to be important in stemming bleeding or in contributing to undesired, pathological coagulation. Furthermore, this would help decipher a complex but important regulatory aspect of fibrinogen, altering its function according to the corresponding stimulus and location.

Appendix 1

Buffer and Media Compositions

Recombinant fibrinogen expression

Growth medium (CHO cells)

500 ml	Dulbecco's Modified Eagle Medium:Nutrient Mixture F-12	Invitrogen
25 ml	Newborn bovine calf serum	Fisher Scientific
25 ml	Nu-Serum IV	VWR
5 ml	100X Antibiotic Antimycotic Solution	Sigma-Aldrich

Stored at +4°C.

1X PBS pH 7.4

2.7 mM	Potassium chloride (KCl)
1.5 mM	Potassium di hydrogen orthophosphate (KH_2PO_4)
137 mM	NaCl
8 mM	Di-sodium hydrogen orthophosphate dihydrate ($Na_2HPO_4.2H_2O$)

Dissolved in dH_2O and autoclaved.

ITS medium

500 ml	Dulbecco's Modified Eagle Medium:Nutrient Mixture F-12	
5 ml	100X Antibiotic Antimycotic Solution	
1 ml	5 mg/ml ITS Supplement	Roche
1 ml	2 mg/ml Aprotinin	Sigma-Aldrich

Stored at +4°C.

Fibrinogen ELISA

Buffer A pH 7.2

2.5 mM $NaH_2PO_4.2H_2O$

7.5 mM $Na_2HPO_4.2H_2O$

145 mM NaCl

Dissolved in dH_2O.

Buffer B pH 7.2

0.2 % v/v Tween 20

355 mM NaCl

Dissolved in Buffer A.

Ammonium sulphate precipitation of fibrinogen

Protease inhibitor cocktail

Per 1 L medium:

656 mg	ε-Amino-caproic acid	
785 mg	Benzamidine hydrochloride hydrate	Sigma-Aldrich
130 µl	8 mM Pepstatin A	Sigma-Aldrich
260 µl	4 mM Leupeptin	Sigma-Aldrich
1040 µl	100 mM PMSF	Sigma-Aldrich
30 ml	700 mM MES buffer pH 5.6	

Pellet cocktail

66 mg	ε-Amino-caproic acid	
79 mg	Benzamidine	
63 µl	8 mM Pepstatin A	
125 µl	4 mM Leupeptin	
100 µl	100 mM PMSF	
17 µl	58594 U/ml Soybean Trypsin Inhibitor	Sigma-Aldrich
200 µl	500 mM EDTA	
6 ml	5 M NaCl	
20 ml	1 M Tris pH 7.4	

Made up to 100 ml with dH_2O.

IF-1 affinity chromatography

IF-1 equilibration buffer pH 7.4

20 mM Tris base

300 mM NaCl

1 mM $CaCl_2$

Dissolved in dH_2O.

Filtered through a 0.22 µm filter and degassed.

IF-1 wash buffer I pH 7.4

20 mM Tris base

1 M NaCl

1 mM $CaCl_2$

Dissolved in dH_2O.

Filtered through a 0.22 µm filter and degassed.

IF-1 wash buffer II pH 6.0

50 mM Sodium acetate ($NaCH_3COO$)

300 mM NaCl

1 mM $CaCl_2$

Dissolved in dH_2O.

Filtered through a 0.22 µm filter and degassed.

IF-1 elution buffer pH 7.4

20 mM Tris base

300 mM NaCl

50 mM EGTA

Dissolved in dH_2O.

Filtered through a 0.22 µm filter and degassed.

TBS buffers

Buffer	Tris (mM)	NaCl (mM)	% Tween (v/v)	pH
TBS-1	50	100	–	7.4
TBS-2	40	140	–	7.4
TBS-2-Tween 20	40	140	0.05	7.4
TBS-3	40	140	–	8.3
TBS-3-Tween 20	40	140	0.05	8.3
TBS-4	10	100	–	7.4
TBS-4-Tween 20	10	100	0.1	7.4
TBS-5-Tween 20	40	1000	0.05	7.4
TBS-6-Tween 20	40	75	0.01	7.4

Reagents were dissolved in dH_2O and adjusted to the appropriate pH.

Recombinant GST-FXIII-A expression

Terrific broth

24 g Tryptone

48 g Yeast extract

8 ml Glycerol

Made up to 1800 ml with dH_2O and autoclaved.

Added 200 ml phosphate buffer before use.

Phosphate buffer

170 mM KH_2PO_4

720 mM Di potassium hydrogen phosphate trihydrate ($K_2HPO_4.3H_2O$)

Dissolved in dH_2O and autoclaved.

Stored at +4°C.

***E. Coli* wash buffer**

20 ml 1 M Tris pH 8.0

10 ml 5 M NaCl

Dissolved in dH_2O and stored at +4°C.

1X PBS pH 7.4

137 mM NaCl

2.7 mM KCl

10 mM $Na_2HPO_4.2H_2O$

2 mM KH_2PO_4

Dissolved in dH_2O and autoclaved.

GST affinity chromatography

GST equilibration buffer (1X PBS) pH 7.4

15 % v/v Glycerol

Dissolved in 1X PBS and autoclaved.

GST wash buffer pH 7.4 (1X PBS with 0.2 % (v/v) Triton X-100)

15 % v/v Glycerol

0.2 % v/v Triton X-100

Dissolved in 1X PBS and autoclaved.

GST elution buffer pH 8.0

50 mM Tris base

Dissolved in dH_2O and adjusted to pH 8.0 with HCl.

Added 0.92 g Glutathione to 150 ml elution buffer before use.

Western blotting

1X TBS-Tween 20 pH 7.4

40 mM Tris base

140 mM NaCl

0.05 % v/v Tween 20

Dissolved in dH_2O.

Transfer buffer pH 8.1-8.4

25 mM Tris base

192 mM Glycine

20 % v/v Methanol

Dissolved in dH_2O and stored at +4°C.

Molecular cloning

Lysogeny broth (LB)

10 g NaCl

10 g Tryptone

5 g Yeast extract

Dissolved in 1 L dH_2O and autoclaved.

LB agar pH 7.0

5 g NaCl

5 g Tryptone

2.5 g Yeast extract

10 g Agar

Dissolved in 500 ml dH_2O and autoclaved.

TAE buffer pH 8.0

40 mM Tris base

20 mM Glacial acetic acid

1 mM EDTA

Dissolved in dH_2O and autoclaved.

6X DNA loading buffer

0.05 g Bromophenol blue

3 g Ficoll 400

Dissolved in 20 ml dH_2O.

Calcium phosphate transfection

2X HeBS pH 7.05

280 mM NaCl

50 mM Hepes

1.2 mM Na_2HPO_4

Dissolved in dH_2O.

CHO cell lysis

1X PBS pH 7.4

2.7mM KCl

1.5mM KH_2PO_4

137mM NaCl

8 mM $Na_2HPO_4.2H_2O$

1.8 mM $CaCl_2.2H_2O$

1 mM $MgCl_2.6H_2O$

Dissolved in dH_2O and filtered through a 0.22 µm filter.

HepG2 cell culture

Growth medium

500 ml	Minimum Essential Eagle Medium	Sigma-Aldrich
50 ml	Fetal Bovine Serum	Fisher Scientific
5 ml	100X Antibiotic Antimycotic Solution	
5 ml	200 mM L-glutamine solution	Sigma-Aldrich

Stored at +4°C.

Phos-tag™ affinity chromatography

Phos-tag™ storage buffer pH 7.4

20 mM Tris base

20 % v/v Propan-2-ol

Dissolved in dH_2O and adjusted to pH 7.4 with glacial acetic acid.

Filtered through a 0.22 µm filter and degassed.

Phos-tag™ wash buffer pH 7.4

100 mM Tris base

Dissolved in dH_2O and adjusted to pH 7.4 with glacial acetic acid.

Filtered through a 0.22 µm filter and degassed.

Phos-tag™ equilibration buffer pH 7.4

100 mM Tris base

1 M $NaCH_3COO$

100 µM Zinc acetate ($ZnCH_3COO$)

Dissolved in dH_2O and adjusted to pH 7.4 with glacial acetic acid.

Filtered through a 0.22 µm filter and degassed.

Phos-tag™ binding buffer pH 7.4

100 mM Tris base

1 M $NaCH_3COO$

Dissolved in dH_2O and adjusted to pH 7.4 with glacial acetic acid.

Filtered through a 0.22 µm filter and degassed.

Phos-tag™ elution buffer pH 7.4

50 mM EDTA

100 mM Tris base

1 M NaCl

Dissolved in dH_2O.

<u>Immunofluorescence/PLA</u>

1X PBS pH 7.4

2.7 mM KCl

1.5 mM KH_2PO_4

137 mM NaCl

8 mM $Na_2HPO_4.2H_2O$

Dissolved in dH_2O and filtered through a 0.22 µm filter.

PLA wash buffer A

10 mM Tris base

150 mM NaCl

0.05 % v/v Tween 20

Dissolved in dH_2O and filtered through a 0.22 µm filter.

Immunoprecipitation

1X PBS-Tween 20 pH 7.4

2.7 mM KCl

1.5 mM KH_2PO_4

137 mM NaCl

8 mM $Na_2HPO_4.2H_2O$

0.02 % v/v Tween 20

Dissolved in dH_2O.

Appendix 2

Sequencing Data

Sequencing of variant fibrinogen Aα chain open reading frames (pMLP-Aα)

Sequencing data were compared to the nucleotide sequence of the original pMLP-Aα open reading frame to identify base changes. Altered codons of interest are highlighted in blue. Nucleotide sequences were translated into protein sequences and BLAST was used to identify differences between query (WT sequence) and subject (variant sequence) by generating a consensus sequence (middle). For each variant, the only differences found were at position 3 and/or 345 (highlighted in red), indicating that these residues were successfully changed from serine to asparagine/glutamic acid/alanine.

Aα S3N

Original nucleotide sequence (Ser3): ACT GCA GAT **AGT** GGT GAA GGT
Mutated nucleotide sequence (Asn3): ACT GCA GAT **AAT** GGT GAA GGT

Protein sequence BLAST:

```
Query1    MFSMRIVCLVLSVVGTAWTADSGEGDFLAEGGGVRGPRVVERHQSACKDSDWPFCSDEDW
          MFSMRIVCLVLSVVGTAWTAD+GEGDFLAEGGGVRGPRVVERHQSACKDSDWPFCSDEDW
Sbjct1    MFSMRIVCLVLSVVGTAWTADNGEGDFLAEGGGVRGPRVVERHQSACKDSDWPFCSDEDW
                              ↑
                             S3N
```

Aα S345N

Original nucleotide sequence (Ser345): AAT CCT GGC **AGC** TCT GAA CGC
Mutated nucleotide sequence (Asn345): AAT CCT GGC **AAC** TCT GAA CGC

Protein sequence BLAST:

```
Query361  NPGSSERGSAGHWTSESSVSGSTGQWHSESGSFRPDSPGSGNARPNNPDWGTFEEVSGNV
          NPG+SERGSAGHWTSESSVSGSTGQWHSESGSFRPDSPGSGNARPNNPDWGTFEEVSGNV
Sbjct361  NPGNSERGSAGHWTSESSVSGSTGQWHSESGSFRPDSPGSGNARPNNPDWGTFEEVSGNV
             ↑
          S345N
```

Aα S3/345N

Original nucleotide sequence (Ser3): ACT GCA GAT **AGT** GGT GAA GGT
Mutated nucleotide sequence (Asn3): ACT GCA GAT **AAT** GGT GAA GGT

Protein sequence BLAST:

```
Query1    MFSMRIVCLVLSVVGTAWTADSGEGDFLAEGGGVRGPRVVERHQSACKDSDWPFCSDEDW
          MFSMRIVCLVLSVVGTAWTAD+GEGDFLAEGGGVRGPRVVERHQSACKDSDWPFCSDEDW
Sbjct1    MFSMRIVCLVLSVVGTAWTADNGEGDFLAEGGGVRGPRVVERHQSACKDSDWPFCSDEDW
                                 ↑
                                S3N
```

Original nucleotide sequence (Ser345): AAT CCT GGC **AGC** TCT GAA CGC
Mutated nucleotide sequence (Asn345): AAT CCT GGC **AAC** TCT GAA CGC

Protein sequence BLAST:

```
Query361  NPGSSERGSAGHWTSESSVSGSTGQWHSESGSFRPDSPGSGNARPNNPDWGTFEEVSGNV
          NPG+SERGSAGHWTSESSVSGSTGQWHSESGSFRPDSPGSGNARPNNPDWGTFEEVSGNV
Sbjct361  NPGNSERGSAGHWTSESSVSGSTGQWHSESGSFRPDSPGSGNARPNNPDWGTFEEVSGNV
            ↑
          S345N
```

Aα S3E

Original nucleotide sequence (Ser3): ACT GCA GAT **AGT** GGT GAA GGT
Mutated nucleotide sequence (Glu3): ACT GCA GAT **GAG** GGT GAA GGT

Protein sequence BLAST:

```
Query1    MFSMRIVCLVLSVVGTAWTADSGEGDFLAEGGGVRGPRVVERHQSACKDSDWPFCSDEDW
          MFSMRIVCLVLSVVGTAWTAD+GEGDFLAEGGGVRGPRVVERHQSACKDSDWPFCSDEDW
Sbjct1    MFSMRIVCLVLSVVGTAWTADEGEGDFLAEGGGVRGPRVVERHQSACKDSDWPFCSDEDW
                                 ↑
                                S3E
```

Aα S345E

Original nucleotide sequence (Ser345): AAT CCT GGC **AGC** TCT GAA CGC
Mutated nucleotide sequence (Glu345): AAT CCT GGC **GAG** TCT GAA CGC

Protein sequence BLAST:

```
Query361  NPGSSERGSAGHWTSESSVSGSTGQWHSESGSFRPDSPGSGNARPNNPDWGTFEEVSGNV
          NPG+SERGSAGHWTSESSVSGSTGQWHSESGSFRPDSPGSGNARPNNPDWGTFEEVSGNV
Sbjct361  NPGESERGSAGHWTSESSVSGSTGQWHSESGSFRPDSPGSGNARPNNPDWGTFEEVSGNV
            ↑
          S345E
```

Aα S3/345E

Original nucleotide sequence (Ser3): ACT GCA GAT **AGT** GGT GAA GGT
Mutated nucleotide sequence (Glu3): ACT GCA GAT **GAG** GGT GAA GGT

Protein sequence BLAST:

```
Query1    MFSMRIVCLVLSVVGTAWTADSGEGDFLAEGGGVRGPRVVERHQSACKDSDWPFCSDEDW
          MFSMRIVCLVLSVVGTAWTAD+GEGDFLAEGGGVRGPRVVERHQSACKDSDWPFCSDEDW
Sbjct1    MFSMRIVCLVLSVVGTAWTADEGEGDFLAEGGGVRGPRVVERHQSACKDSDWPFCSDEDW
                                 ↑
                                S3E
```

Original nucleotide sequence (Ser345): AAT CCT GGC **AGC** TCT GAA CGC
Mutated nucleotide sequence (Glu345): AAT CCT GGC **GAG** TCT GAA CGC

Protein sequence BLAST:

```
Query361  NPGSSERGSAGHWTSESSVSGSTGQWHSESGSFRPDSPGSGNARPNNPDWGTFEEVSGNV
          NPG+SERGSAGHWTSESSVSGSTGQWHSESGSFRPDSPGSGNARPNNPDWGTFEEVSGNV
Sbjct361  NPGESERGSAGHWTSESSVSGSTGQWHSESGSFRPDSPGSGNARPNNPDWGTFEEVSGNV
            ↑
          S345E
```

Aα S345A

Original nucleotide sequence (Ser345): AAT CCT GGC **AGC** TCT GAA CGC
Mutated nucleotide sequence (Ala345): AAT CCT GGC **GCC** TCT GAA CGC

Protein sequence BLAST:

```
Query361  NPGSSERGSAGHWTSESSVSGSTGQWHSESGSFRPDSPGSGNARPNNPDWGTFEEVSGNV
          NPG+SERGSAGHWTSESSVSGSTGQWHSESGSFRPDSPGSGNARPNNPDWGTFEEVSGNV
Sbjct361  NPGASERGSAGHWTSESSVSGSTGQWHSESGSFRPDSPGSGNARPNNPDWGTFEEVSGNV
            ↑
          S345A
```

Whole construct sequencing of pMLP-Aα, -Bβ and -γ

Nucleotide sequences of the three fibrinogen expression constructs pMLP-Aα, -Bβ and –γ were determined from sequencing data. The sequence for each construct is displayed below with start/stop, Aα Ser3 and Aα Ser345 codons highlighted in yellow, blue and green respectively.

pMLP-Aα sequence

```
TCAGAATATACCTTATTTTGGATTGAAGCCAATATGATAATGAGGGGGTGGAGTTTGTGACGTGGCGCGG
GGCGTGGGAACGGGGCGGGTGACGTAGTAGTGTGGCGGAAGTGTGATGTTGCAAGTGTGGCGGAACACAT
GTAAGCGACGGATGTGGCAAAAGTGACGTTTTTGGTGTGCGCCGGTGTACACAGGAAGTGACAATTTTCG
CGCGGTTTTAGGCGGATGTTGTAGTAAATTTGGGCGTAACCGAGTAAGATTTGGCCATTTTCGCGGGAAA
ACTGAATAAGAGGAAGTGAAATCTGAATAATTTTGTGTTACTCATAGCGCGTAATATTTGTCTAGGGCCC
AAGCTTTTTGCAAAAGCCTAGGCCTCCAAAAAAGCCTCCTCACTACTTCTGGAATAGCTCAGAGGCCGAG
```

GCGGCCTCGGCCTCTGCATAAATAAAAAAAATTAGTCAGCCATGGGGCGGAGAATGGGCGGAACTGGGCG
GAGTTAGGGGCGGGATGGGCGGAGTTAGGGGCGGGACTATGGTTGCTGACTAATTGAGATGCATGCTTTG
CATACTTCTGCCTGCTGGGGAGCCTGGGGACTTTCCACACCTGGTTGCTGACTAATTGAGATGCATGCTT
TGCATACTTCTGCCTGCTGGGGAGCCTGGGGACTTTCCACACCCTAACTGACACACATTCCACAGCTGGT
TCTTTCCGCCTCAGAAGGTACCCGGTCCTCCTCGTATAGAAACTCGGACCACTCTGAGACGAAGGCTCGC
GTCCAGGCCAGCACGAAGGAGGCTAAGTGGGAGGGGTAGCGGTCGTTGTCCACTAGGGGGTCCACTCGCT
CCAGGGTGTGAAGACACATGTCGCCCTCTTCGGCATCAAGGAAGGTGATTGGTTTATAGGTGTAGGCCAC
GTGACCGGGTGTTCCTGAAGGGGGGCTATAAAAGGGGGTGGGGGCGCGTTCGTCCTCACTCTCTTCCGCA
TCGCTGTCTGCGAGGGCCAGCTGTTGGGCTCGCGGTTGAGGACAAACTCTTCGCGGTCTTTCCAGTACTC
TTGGATCGGAAACCCGTCGGCCTCCGAACGGTACTCCGCCACCGAGGGACCTGAGCGAGTCCGCATCGAC
CGGATCGGAAAACCTCTCGAGAAAGGCGTCTAACCAGTCACAGTCGCAAGGTAGGCTGAGCACCGTGGCG
GGCGGCAGCGGGTGGCGGTCGGGGTTGTTTCTGGCGGAGGTGCTGCTGATGATGTAATTAAAGTAGGCGG
TCTTGAGACGGCGGATGGTCGAGGTGAGGTGTGGCAGGCTTGAGATCTGGCCATACACTTGAGTGACAAT
GACATCCACTTTGCCTTTCTCTCCACAGGTGTCCACTCCCAGGTCCAACCTGATCAGAATTGCGCCGCTC
TCGAGTGAATTGTCGACCGCGGCCCCTGGAGTGCTCCTCAGGAGCCAGCCCCACCCTTAGAAAAG**ATG**TT
TTCCATGAGGATCGTCTGCCTGGTCCTAAGTGTGGTGGGCACAGCATGGACTGCAGAT**AGT**GGTGAAGGT
GACTTTCTAGCTGAAGGAGGAGGCGTGCGTGGCCCAAGGGTTGTGGAAAGACATCAATCTGCCTGCAAAG
ATTCAGACTGGCCCTTCTGCTCTGATGAAGACTGGAACTACAAATGCCCTTCTGGCTGCAGGATGAAAGG
GTTGATTGATGAAGTCAATCAAGATTTTACAAACAGAATAAATAAGCTCAAAAATTCACTATTTGAATAT
CAGAAGAACAATAAGGATTCTCATTCGTTGACCACTAATATAATGGAAATTTTGAGAGGCGATTTTTCCT
CAGCCAATAACCGTGATAATACCTACAACCGAGTGTCAGAGGATCTGAGAAGCAGAATTGAAGTCCTGAA
GCGCAAAGTCATAGAAAAAGTACAGCATATCCAGCTTCTGCAAAAAAATGTTAGGGCCCAGTTGGTTGAT
ATGAAACGACTGGAGGTGGACATTGATATTAAGATCCGATCTTGTCGAGGGTCATGCAGTAGGGCTTTAG
CTCGTGAAGTAGATCTGAAGGACTATGAAGATCAGCAGAAGCAACTTGAACAGGTCATTGCCAAAGACTT
ACTTCCCTCTAGAGATAGGCAACACTTACCACTGATAAAAATGAAACCAGTTCCAGACTTGGTTCCCGGA
AATTTTAAGAGCCAGCTTCAGAAGGTACCCCCAGAGTGGAAGGCATTAACAGACATGCCGCAGATGAGAA
TGGAGTTAGAGAGACCTGGTGGAAATGAGATTACTCGAGGAGGCTCCACCTCTTATGGAACCGGATCAGA
GACGGAAAGCCCCAGGAACCCTAGCAGTGCTGGAAGCTGGAACTCTGGGAGCTCTGGACCTGGAAGTACT
GGAAACCGAAACCCTGGGAGCTCTGGGACTGGAGGGACTGCAACCTGGAAACCTGGGAGCTCTGGACCTG
GAAGTGCTGGAAGCTGGAACTCTGGGAGCTCTGGAACTGGAAGTACTGGAAACCAAAACCCTGGGAGCCC
TAGACCTGGTAGTACCGGAACCTGGAATCCTGGC**AGC**TCTGAACGCGGAAGTGCTGGGCACTGGACCTCT
GAGAGCTCTGTATCTGGTAGTACTGGACAATGGCACTCTGAATCTGGAAGTTTTAGGCCAGATAGCCCAG
GCTCTGGGAACGCGAGGCCTAACAACCCAGACTGGGGCACATTTGAAGAGGTGTCAGGAAATGTAAGTCC
AGGGACAAGGAGAGAGTACCACACAGAAAAACTGGTCACTTCTAAAGGAGATAAAGAGCTCAGGACTGGT
AAAGAGAAGGTCACCTCTGGTAGCACAACCACCACGCGTCGTTCATGCTCTAAAACCGTTACTAAGACTG
TTATTGGTCCTGATGGTCACAAAGAAGTTACCAAAGAAGTGGTGACCTCCGAAGATGGTTCTGACTGTCC
CGAGGCAATGGATTTAGGCACATTGTCTGGCATAGGTACTCTGGATGGGTTCCGCCATAGGCACCCTGAT
GAAGCTGCCTTCTTCGACACTGCCTCAACTGGAAAAACATTCCCAGGTTTCTTCTCACCTATGTTAGGAG
AGTTTGTCAGTGAGACTGAGTCTAGGGGCTCAGAATCTGGCATCTTCACAAATACAAAGGAATCCAGTTC
TCATCACCCTGGGATAGCTGAATTCCCTTCCCGTGGTAAATCTTCAAGTTACAGCAAACAATTTACTAGT
AGCACGAGTTACAACAGAGGAGACTCCACATTTGAAAGCAAGAGCTATAAAATGGCAGATGAGGCCGGAA
GTGAAGCCGATCATGAAGGAACACATAGCACCAAGAGAGGCCATGCTAAATCTCGCCCTGTCAGAGGTAT
CCACACTTCTCCTTTGGGGAAGCCTTCCCTGTCCCCC**TAG**ACTAAGTTAAATGGGCGGCCGCAATTCTGA
TCATAATCAGCCATACCACATTTGTAGAGGTTTTACTTGCTTTAAAAAACCTCCCACACCTCCCCCTGAA
CCTGAAACATAAAATGAATGCAATTGTTGTTGTTAACTTGTTTATTGCAGCTTATAATGGTTACAAATAA
AGCAATAGCATCACAAATTTCACAAATAAAGCATTTTTTTCACTGCATTCTAGTTGTGGTTTGTCCAAAC
TCATCAATGTATCTTATCATGTCTGGATCCTCTACGCCGGACGCATCGTGGCCGGCATCACCGGCGCCAC
AGGTGCGGTTGCTGGCGCCTATATCGCCGACATCACCGATGGGGAAGATCGGGCTCGCCACTTCGGGCTC
ATGAGCGCTTGTTTCGGCGTGGGTATGGTGGCAGGCCCCGTGGCCGGGGGACTGTTGGGCGCCATCTCCT
TGCATGCACCATTCCTTGCGGCGGCGGTGCTCAACGGCCTCAACCTACTACTGGGCTGCTTCCTAATGCA
GGAGTCGCATAAGGGAGAGCGTCTAGACCGATGCCCTTGAGAGCCTTCAACCCAGTCAGCTCCTTCCGGT
GGGCGCGGGGCATGACTATCGTCGCCGCACTTATGACTGTCTTCTTTATCATGCAACTCGTAGGACAGGT
GCCGGCAGCGCTCTGGGTCATTTTCGGCGAGGACCGCTTTCGCTGGAGCGCGACGATGATCGGCCTGTCG
CTTGCGGTATTCGGAATCTTGCACGCCCTCGCTCAAGCCTTCGTCACTGGTCCCGCCACCAAACGTTTCG
GCGAGAAGCAGGCCATTATCGCCGGCATGGCGGCCGACGCGCTGGGCTACGTCTTGCTGGCGTTCGCGAC
GCGAGGCTGGATGGCCTTCCCCATTATGATTCTTCTCGCTTCCGGCGGCATCGGGATGCCCGCGTTGCAG
GCCATGCTGTCCAGGCAGGTAGATGACGACCATCAGGGACAGCTTCAAGGCCAGCAAAAGGCCAGGAACC
GTAAAAAGGCCGCGTTGCTGGCGTTTTTCCATAGGCTCCGCCCCCCTGACGAGCATCACAAAAATCGACG
CTCAAGTCAGAGGTGGCGAAACCCGACAGGACTATAAAGATACCAGGCGTTTCCCCCTGGAAGCTCCCTC
GTGCGCTCTCCTGTTCCGACCCTGCCGCTTACCGGATACCTGTCCGCCTTTCTCCCTTCGGGAAGCGTGG
CGCTTTCTCATAGCTCACGCTGTAGGTATCTCAGTTCGGTGTAGGTCGTTCGCTCCAAGCTGGGCTGTGT
GCACGAACCCCCCGTTCAGCCCGACCGCTGCGCCTTATCCGGTAACTATCGTCTTGAGTCCAACCCGGTA
AGACACGACTTATCGCCACTGGCAGCAGCCACTGGTAACAGGATTAGCAGAGCGAGGTATGTAGGCGGTG

CTACAGAGTTCTTGAAGTGGTGGCCTAACTACGGCTACACTAGAAGGACAGTATTTGGTATCTGCGCTCT
GCTGAAGCCAGTTACCTTCGGAAAAAGAGTTGGTAGCTCTTGATCCGGCAAACAAACCACCGCTGGTAGC
GGTGGTTTTTTTGTTTGCAAGCAGCAGATTACGCGCAGAAAAAAAGGATCTCAAGAAGATCCTTTGATCT
TTTCTACGGGGTCTGACGCTCAGTGGAACGAAAACTCACGTTAAGGGATTTTGGTCATGAGATTATCAAA
AAGGATCTTCACCTAGATCCTTTTAAATTAAAAATGAAGTTTTAAATCAATCTAAAGTATATATGAGTAA
ACTTGGTCTGACAGTTACCAATGCTTAATCAGTGAGGCACCTATCTCAGCGATCTGTCTATTTCGTTCAT
CCATAGTTGCCTGACTCCCCGTCGTGTAGATAACTACGATACGGGAGGGCTTACCATCTGGCCCCAGTGC
TGCAATGATACCGCGAGACCCACGCTCACCGGCTCCAGATTTATCAGCAATAAACCAGCCAGCCGGAAGG
GCCGAGCGCAGAAGTGGTCCTGCAACTTTATCCGCCTCCATCCAGTCTATTAATTGTTGCCGGGAAGCTA
GAGTAAGTAGTTCGCCAGTTAATAGTTTGCGCAACGTTGTTGCCATTGCTGCAGGCATCGTGGTGTCACG
CTCGTCGTTTGGTATGGCTTCATTCAGCTCCGGTTCCCAACGATCAAGGCGAGTTACATGATCCCCCATG
TTGTGCAAAAAAGCGGTTAGCTCCTTCGGTCCTCCGATCGTTGTCAGAAGTAAGTTGGCCGCAGTGTTAT
CACTCATGGTTATGGCAGCACTGCATAATTCTCTTACTGTCATGCCATCCGTAAGATGCTTTTCTGTGAC
TGGTGAGTACTCAACCAAGTCATTCTGAGAATAGTGTATGCGGCGACCGAGTTGCTCTTGCCCGGCGTCA
ACACGGGATAATACCGCGCCACATAGCAGAACTTTAAAAGTGCTCATCATTGGAAAACGTTCTTCGGGGC
GAAAACTCTCAAGGATCTTACCGCTGTTGAGATCCAGTTCGATGTAACCCACTCGTGCACCCAACTGATC
TTCAGCATCTTTTACTTTCACCAGCGTTTCTGGGTGAGCAAAAACAGGAAGGCAAAATGCCGCAAAAAAG
GGAATAAGGGCGACACGGAAATGTTGAATACTCATACTCTTCCTTTTTCAATATTATTGAAGCATTTATC
AGGGTTATTGTCTCATGAGCGGATACATATTTGAATGTATTTAGAAAAATAAACAAATAGGGGTTCCGCG
CACATTTCCCCGAAAAGTGCCACCTGACGTCTAAGAAACCATTATTATCATGACATTAACCTATAAAAAT
AGGCGTATCACGAGGCCCTTTCGTCTTCCTGA

Start/stop codon Ser3 codon Ser345 codon

pMLP-Bβ sequence

TCAGAATATACCTTATTTTGGATTGAAGCCAATATGATAATGAGGGGGTGGAGTTTGTGACGTGGCGCGG
GGCGTGGGAACGGGGCGGGTGACGTAGTAGTGTGGCGGAAGTGTGATGTTGCAAGTGTGGCGGAACACAT
GTAAGCGACGGATGTGGCAAAAGTGACGTTTTTGGTGTGCGCCGGTGTACACAGGAAGTGACAATTTTCG
CGCGGTTTTAGGCGGATGTTGTAGTAAATTTGGGCGTAACCGAGTAAGATTTGGCCATTTTCGCGGGAAA
ACTGAATAAGAGGAAGTGAAATCTGAATAATTTTGTGTTACTCATAGCGCGTAATATTTGTCTAGGGCCC
AAGCTTTTTGCAAAAGCCTAGGCCTCCAAAAAAGCCTCCTCACTACTTCTGGAATAGCTCAGAGGCCGAG
GCGGCCTCGGCCTCTGCATAAATAAAAAAAATTAGTCAGCCATGGGGCGGAGAATGGGCGGAACTGGGCG
GAGTTAGGGGCGGGATGGGCGGAGTTAGGGGCGGGACTATGGTTGCTGACTAATTGAGATGCATGCTTTG
CATACTTCTGCCTGCTGGGGAGCCTGGGGACTTTCCACACCTGGTTGCTGACTAATTGAGATGCATGCTT
TGCATACTTCTGCCTGCTGGGGAGCCTGGGGACTTTCCACACCCTAACTGACACACATTCCACAGCTGGT
TCTTTCCGCCTCAGAAGGTACCCGGTCCTCCTCGTATAGAAACTCGGACCACTCTGAGACGAAGGCTCGC
GTCCAGGCCAGCACGAAGGAGGCTAAGTGGGAGGGGTAGCGGTCGTTGTCCACTAGGGGGTCCACTCGCT
CCAGGGTGTGAAGACACATGTCGCCCTCTTCGGCATCAAGGAAGGTGATTGGTTTATAGGTGTAGGCCAC
GTGACCGGGTGTTCCTGAAGGGGGGCTATAAAAGGGGGTGGGGGCGCGTTCGTCCTCACTCTCTTCCGCA
TCGCTGTCTGCGAGGGCCAGCTGTTGGGCTCGCGGTTGAGGACAAACTCTTCGCGGTCTTTCCAGTACTC
TTGGATCGGAAACCCGTCGGCCTCCGAACGGTACTCCGCCACCGAGGGACCTGAGCGAGTCCGCATCGAC
CGGATCGGAAAACCTCTCGAGAAAGGCGTCTAACCAGTCACAGTCGCAAGGTAGGCTGAGCACCGTGGCG
GGCGGCAGCGGGTGGCGGTCGGGGTTGTTTCTGGCGGAGGTGCTGCTGATGATGTAATTAAAGTAGGCGG
TCTTGAGACGGCGGATGGTCGAGGTGAGGTGTGGCAGGCTTGAGATCTGGCCATACACTTGAGTGACAAT
GACATCCACTTTGCCTTTCTCTCCACAGGTGTCCACTCCCAGGTCCAACCTGATCAGAATTGCGCCGCTC
TCGAGTGAATTGTCGAC**ATG**AAAAGAATGGTTTCGTGGAGCTTCCACAAACTTAAAACCATGAAACACCT
ATTATTGCTACTATTGTGTGTTTTTCTAGTTAAGTCCCAAGGTGTCAACGACAATGAGGAGGGTTTCTTC
AGTGCCCGTGGTCATCGACCCCTTGACAAGAAGAGAGAAGAGGCTCCCAGCCTGAGGCCTGCCCCACCGC
CCATCAGTGGAGGTGGCTATCGGGCTCGTCCAGCCAAAGCAGCTGCCACTCAAAAGAAAGTAGAAAGAAA
AGCCCCTGATGCTGGAGGCTGTCTTCACGCTGACCCAGACCTGGGGGTGTTGTGTCCTACAGGATGTCAG
TTGCAAGAGGCTTTGCTACAACAGGAAAGGCCAATCAGAAATAGTGTTGATGAGTTAAATAACAATGTGG
AAGCTGTTTCCCAGACCTCCTCTTCTTCCTTTCAGTACATGTATTTGCTGAAAGACCTGTGGCAAAAGAG
GCAGAAGCAAGTAAAAGATAATGAAAATGTAGTCAATGAGTACTCCTCAGAACTGGAAAAGCACCAATTA
TATATAGATGAGACTGTGAATAGCAATATCGCAACTAACCTTCGTGTGCTTCGTTCAATCCTGGAAAACC
TGAGAAGCAAAATACAAAAGTTAGAATCTGATGTCTCAGCTCAAATGGAATATTGTCGCACCCCATGCAC
TGTCAGTTGCAATATTCCTGTGGTGTCTGGCAAAGAATGTGAGGAAATTATCAGGAAAGGAGGTGAAACA
TCTGAAATGTATCTCATTCAACCTGACAGTTCTGTCAAACCGTATAGAGTATACTGTGACATGAATACAG
AAAATGGAGGATGGACAGTGATTCAGAACCGTCAAGACGGTAGTGTTGACTTTGGCAGGAAATGGGATCC
ATATAAACAGGGATTTGGAAATGTTGCAACCAACACAGATGGGAAGAATTACTGTGGCCTACCAGGTGAA
TATTGGCTTGGAAATGATAAAATTAGCCAGCTTACCAGGATGGGACCCACAGAACTTTTGATAGAAATGG

AGGACTGGAAAGGAGACAAAGTAAAGGCTCACTATGGAGGATTCACTGTACAGAATGAAGCCAACAAATA
CCAGATCTCAGTGAACAAATACAGAGGAACAGCCGGTAATGCCCTCATGGATGGAGCATCTCAGCTGATG
GGAGAAAACAGGACCATGACCATTCACAACGGCATGTTCTTCAGCACGTATGACAGAGACAATGACGGCT
GGTTAACATCAGATCCCAGAAAACAGTGTTCTAAAGAAGACGGTGGTGGATGGTGGTATAATAGATGTCA
TGCAGCCAATCCAAACGGCAGATACTACTGGGGTGGACAGTACACCTGGGACATGGCAAAGCATGGCACA
GATGATGGTGTAGTATGGATGAATTGGAAGGGGTCATGGTACTCAATGAGGAAGATGAGTATGAAGATCA
GGCCCTTCTTCCCACAGCAA**TAG**TCCCCAATACGGGCGGCCGCAATTCTGATCATAATCAGCCATACCAC
ATTTGTAGAGGTTTTACTTGCTTTAAAAAACCTCCCACACCTCCCCCTGAACCTGAAACATAAAATGAAT
GCAATTGTTGTTGTTAACTTGTTTATTGCAGCTTATAATGGTTACAAATAAAGCAATAGCATCACAAATT
TCACAAATAAAGCATTTTTTTCACTGCATTCTAGTTGTGGTTTGTCCAAACTCATCAATGTATCTTATCA
TGTCTGGATCCTCTACGCCGGACGCATCGTGGCCGGCATCACCGGCGCCACAGGTGCGGTTGCTGGCGCC
TATATCGCCGACATCACCGATGGGGAAGATCGGGCTCGCCACTTCGGGCTCATGAGCGCTTGTTTCGGCG
TGGGTATGGTGGCAGGCCCCGTGGCCGGGGGACTGTTGGGCGCCATCTCCTTGCATGCACCATTCCTTGC
GGCGGCGGTGCTCAACGGCCTCAACCTACTACTGGGCTGCTTCCTAATGCAGGAGTCGCATAAGGGAGAG
CGTCTAGACCGATGCCCTTGAGAGCCTTCAACCCAGTCAGCTCCTTCCGGTGGGCGCGGGGCATGACTAT
CGTCGCCGCACTTATGACTGTCTTCTTTATCATGCAACTCGTAGGACAGGTGCCGGCAGCGCTCTGGGTC
ATTTTCGGCGAGGACCGCTTTCGCTGGAGCGCGACGATGATCGGCCTGTCGCTTGCGGTATTCGGAATCT
TGCACGCCCTCGCTCAAGCCTTCGTCACTGGTCCCGCCACCAAACGTTTCGGCGAGAAGCAGGCCATTAT
CGCCGGCATGGCGGCCGACGCGCTGGGCTACGTCTTGCTGGCGTTCGCGACGCGAGGCTGGATGGCCTTC
CCCATTATGATTCTTCTCGCTTCCGGCGGCATCGGGATGCCCGCGTTGCAGGCCATGCTGTCCAGGCAGG
TAGATGACGACCATCAGGGACAGCTTCAAGGCCAGCAAAAGGCCAGGAACCGTAAAAAGGCCGCGTTGCT
GGCGTTTTTCCATAGGCTCCGCCCCCCTGACGAGCATCACAAAAATCGACGCTCAAGTCAGAGGTGGCGA
AACCCGACAGGACTATAAAGATACCAGGCGTTTCCCCCTGGAAGCTCCCTCGTGCGCTCTCCTGTTCCGA
CCCTGCCGCTTACCGGATACCTGTCCGCCTTTCTCCCTTCGGGAAGCGTGGCGCTTTCTCATAGCTCACG
CTGTAGGTATCTCAGTTCGGTGTAGGTCGTTCGCTCCAAGCTGGGCTGTGTGCACGAACCCCCCGTTCAG
CCCGACCGCTGCGCCTTATCCGGTAACTATCGTCTTGAGTCCAACCCGGTAAGACACGACTTATCGCCAC
TGGCAGCAGCCACTGGTAACAGGATTAGCAGAGCGAGGTATGTAGGCGGTGCTACAGAGTTCTTGAAGTG
GTGGCCTAACTACGGCTACACTAGAAGGACAGTATTTGGTATCTGCGCTCTGCTGAAGCCAGTTACCTTC
GGAAAAAGAGTTGGTAGCTCTTGATCCGGCAAACAAACCACCGCTGGTAGCGGTGGTTTTTTTGTTTGCA
AGCAGCAGATTACGCGCAGAAAAAAAGGATCTCAAGAAGATCCTTTGATCTTTTCTACGGGGTCTGACGC
TCAGTGGAACGAAAACTCACGTTAAGGGATTTTGGTCATGAGATTATCAAAAAGGATCTTCACCTAGATC
CTTTTAAATTAAAAATGAAGTTTTAAATCAATCTAAAGTATATATGAGTAAACTTGGTCTGACAGTTACC
AATGCTTAATCAGTGAGGCACCTATCTCAGCGATCTGTCTATTTCGTTCATCCATAGTTGCCTGACTCCC
CGTCGTGTAGATAACTACGATACGGGAGGGCTTACCATCTGGCCCCAGTGCTGCAATGATACCGCGAGAC
CCACGCTCACCGGCTCCAGATTTATCAGCAATAAACCAGCCAGCCGGAAGGGCCGAGCGCAGAAGTGGTC
CTGCAACTTTATCCGCCTCCATCCAGTCTATTAATTGTTGCCGGGAAGCTAGAGTAAGTAGTTCGCCAGT
TAATAGTTTGCGCAACGTTGTTGCCATTGCTGCAGGCATCGTGGTGTCACGCTCGTCGTTTGGTATGGCT
TCATTCAGCTCCGGTTCCCAACGATCAAGGCGAGTTACATGATCCCCCATGTTGTGCAAAAAAGCGGTTA
GCTCCTTCGGTCCTCCGATCGTTGTCAGAAGTAAGTTGGCCGCAGTGTTATCACTCATGGTTATGGCAGC
ACTGCATAATTCTCTTACTGTCATGCCATCCGTAAGATGCTTTTCTGTGACTGGTGAGTACTCAACCAAG
TCATTCTGAGAATAGTGTATGCGGCGACCGAGTTGCTCTTGCCCGGCGTCAACACGGGATAATACCGCGC
CACATAGCAGAACTTTAAAAGTGCTCATCATTGGAAAACGTTCTTCGGGGCGAAAACTCTCAAGGATCTT
ACCGCTGTTGAGATCCAGTTCGATGTAACCCACTCGTGCACCCAACTGATCTTCAGCATCTTTTACTTTC
ACCAGCGTTTCTGGGTGAGCAAAAACAGGAAGGCAAAATGCCGCAAAAAAGGGAATAAGGGCGACACGGA
AATGTTGAATACTCATACTCTTCCTTTTTCAATATTATTGAAGCATTTATCAGGGTTATTGTCTCATGAG
CGGATACATATTTGAATGTATTTAGAAAAATAAACAAATAGGGGTTCCGCGCACATTTCCCCGAAAAGTG
CCACCTGACGTCTAAGAAACCATTATTATCATGACATTAACCTATAAAAATAGGCGTATCACGAGGCCCT
TTCGTCTTCCTGA

Start/stop codon

pMLP-γ sequence

TCAGAATATACCTTATTTTGGATTGAAGCCAATATGATAATGAGGGGGTGGAGTTTGTGACGTGGCGCGG
GGCGTGGGAACGGGGCGGGTGACGTAGTAGTGTGGCGGAAGTGTGATGTTGCAAGTGTGGCGGAACACAT
GTAAGCGACGGATGTGGCAAAAGTGACGTTTTTGGTGTGCGCCGGTGTACACAGGAAGTGACAATTTTCG
CGCGGTTTTAGGCGGATGTTGTAGTAAATTTGGGCGTAACCGAGTAAGATTTGGCCATTTTCGCGGGAAA
ACTGAATAAGAGGAAGTGAAATCTGAATAATTTTGTGTTACTCATAGCGCGTAATATTTGTCTAGGGCCC
AAGCTTTTTGCAAAAGCCTAGGCCTCCAAAAAAGCCTCCTCACTACTTCTGGAATAGCTCAGAGGCCGAG
GCGGCCTCGGCCTCTGCATAAATAAAAAAAATTAGTCAGCCATGGGGCGGAGAATGGGCGGAACTGGGCG
GAGTTAGGGGCGGGATGGGCGGAGTTAGGGGCGGGACTATGGTTGCTGACTAATTGAGATGCATGCTTTG

CATACTTCTGCCTGCTGGGGAGCCTGGGGACTTTCCACACCTGGTTGCTGACTAATTGAGATGCATGCTT
TGCATACTTCTGCCTGCTGGGGAGCCTGGGGACTTTCCACACCCTAACTGACACACATTCCACAGCTGGT
TCTTTCCGCCTCAGAAGGTACCCGGTCCTCCTCGTATAGAAACTCGGACCACTCTGAGACGAAGGCTCGC
GTCCAGGCCAGCACGAAGGAGGCTAAGTGGGAGGGGTAGCGGTCGTTGTCCACTAGGGGGTCCACTCGCT
CCAGGGTGTGAAGACACATGTCGCCCTCTTCGGCATCAAGGAAGGTGATTGGTTTATAGGTGTAGGCCAC
GTGACCGGGTGTTCCTGAAGGGGGGCTATAAAAGGGGGTGGGGGCGCGTTCGTCCTCACTCTCTTCCGCA
TCGCTGTCTGCGAGGGCCAGCTGTTGGGCTCGCGGTTGAGGACAAACTCTTCGCGGTCTTTCCAGTACTC
TTGGATCGGAAACCCGTCGGCCTCCGAACGGTACTCCGCCACCGAGGGACCTGAGCGAGTCCGCATCGAC
CGGATCGGAAAACCTCTCGAGAAAGGCGTCTAACCAGTCACAGTCGCAAGGTAGGCTGAGCACCGTGGCG
GGCGGCAGCGGGTGGCGGTCGGGGTTGTTTCTGGCGGAGGTGCTGCTGATGATGTAATTAAAGTAGGCGG
TCTTGAGACGGCGGATGGTCGAGGTGAGGTGTGGCAGGCTTGAGATCTGGCCATACACTTGAGTGACAAT
GACATCCACTTTGCCTTTCTCTCCACAGGTGTCCACTCCCAGGTCCAACCTGATCAGAATTGCGCCGCTC
TCGAGTGAATTGTCGACCGCGGCCCGGGCACTCAGACATC**ATG**AGTTGGTCCTTGCACCCCCGGAATTTA
ATTCTCTACTTCTATGCTCTTTTATTTCTCTCTTCAACATGTGTAGCATATGTTGCTACCAGAGACAACT
GCTGCATCTTAGATGAAAGATTCGGTAGTTATTGTCCAACTACCTGTGGCATTGCAGATTTCCTGTCTAC
TTATCAAACCAAAGTAGACAAGGATCTACAGTCTTTGGAAGACATCTTACATCAAGTTGAAAACAAAACA
TCAGAAGTCAAACAGCTGATAAAAGCAATCCAACTCACTTATAATCCTGATGAATCATCAAAACCAAATA
TGATAGACGCTGCTACTTTGAAGTCCAGGAAAATGTTAGAAGAAATTATGAAATATGAAGCATCGATTTT
AACACATGACTCAAGTATTCGATATTTGCAGGAAATATATAATTCAAATAATCAAAAGATTGTTAACCTG
AAAGAGAAGGTAGCCCAGCTTGAAGCACAGTGCCAGGAACCTTGCAAAGACACGGTGCAAATCCATGATA
TCACTGGGAAAGATTGTCAAGACATTGCCAATAAGGGAGCTAAACAGAGCGGGCTTTACTTTATTAAACC
TCTGAAAGCTAACCAGCAATTCTTAGTCTACTGTGAAATCGATGGGTCTGGAAATGGATGGACTGTGTTT
CAGAAGAGACTTGATGGCAGTGTAGATTTCAAGAAAAACTGGATTCAATATAAAGAAGGATTTGGACATC
TGTCTCCTACTGGCACAACAGAATTTTGGCTGGGAAATGAGAAGATTCATTTGATAAGCACACAGTCTGC
CATCCCATATGCATTAAGAGTGGAACTGGAAGACTGGAATGGCAGAACCAGTACTGCAGACTATGCCATG
TTCAAGGTGGGACCTGAAGCTGACAAGTACCGCCTAACATATGCCTACTTCGCTGGTGGGGATGCTGGAG
ATGCCTTTGATGGCTTTGATTTTGGCGATGATCCTAGTGACAAGTTTTTCACATCCCATAATGGCATGCA
GTTCAGTACCTGGGACAATGACAATGATAAGTTTGAAGGCAACTGTGCTGAACAGGATGGATCTGGTTGG
TGGATGAACAAGTGTCACGCTGGCCATCTCAATGGAGTTTATTACCAAGGTGGCACTTACTCAAAAGCAT
CTACTCCTAATGGTTATGATAATGGCATTATTTGGGCCACTTGGAAAACCCGGTGGTATTCCATGAAGAA
AACCACTATGAAGATAATCCCATTCAACAGACTCACAATTGGAGAAGGACAGCAACACCACCTGGGGGGA
GCCAAACAGGCTGGAGACGTT**TAA**AAGACCGTTTCAAAAGAGATTTACTTTTTTAAAGGACTTTATCTGA
ACAGAGAGATATAATGGGCGGCCGCAATTCTGATCATAATCAGCCATACCACATTTGTAGAGGTTTTACT
TGCTTTAAAAAACCTCCCACACCTCCCCCTGAACCTGAAACATAAAATGAATGCAATTGTTGTTGTTAAC
TTGTTTATTGCAGCTTATAATGGTTACAAATAAAGCAATAGCATCACAAATTTCACAAATAAAGCATTTT
TTTCACTGCATTCTAGTTGTGGTTTGTCCAAACTCATCAATGTATCTTATCATGTCTGGATCCTCTACGC
CGGACGCATCGTGGCCGGCATCACCGGCGCCACAGGTGCGGTTGCTGGCGCCTATATCGCCGACATCACC
GATGGGGAAGATCGGGCTCGCCACTTCGGGCTCATGAGCGCTTGTTTCGGCGTGGGTATGGTGGCAGGCC
CCGTGGCCGGGGGACTGTTGGGCGCCATCTCCTTGCATGCACCATTCCTTGCGGCGGCGGTGCTCAACGG
CCTCAACCTACTACTGGGCTGCTTCCTAATGCAGGAGTCGCATAAGGGAGAGCGTCTAGACCGATGCCCT
TGAGAGCCTTCAACCCAGTCAGCTCCTTCCGGTGGGCGCGGGGCATGACTATCGTCGCCGCACTTATGAC
TGTCTTCTTTATCATGCAACTCGTAGGACAGGTGCCGGCAGCGCTCTGGGTCATTTTCGGCGAGGACCGC
TTTCGCTGGAGCGCGACGATGATCGGCCTGTCGCTTGCGGTATTCGGAATCTTGCACGCCCTCGCTCAAG
CCTTCGTCACTGGTCCCGCCACCAAACGTTTCGGCGAGAAGCAGGCCATTATCGCCGGCATGGCGGCCGA
CGCGCTGGGCTACGTCTTGCTGGCGTTCGCGACGCGAGGCTGGATGGCCTTCCCCATTATGATTCTTCTC
GCTTCCGGCGGCATCGGGATGCCCGCGTTGCAGGCCATGCTGTCCAGGCAGGTAGATGACGACCATCAGG
GACAGCTTCAAGGCCAGCAAAAGGCCAGGAACCGTAAAAAGGCCGCGTTGCTGGCGTTTTTCCATAGGCT
CCGCCCCCCTGACGAGCATCACAAAAATCGACGCTCAAGTCAGAGGTGGCGAAACCCGACAGGACTATAA
AGATACCAGGCGTTTCCCCCTGGAAGCTCCCTCGTGCGCTCTCCTGTTCCGACCCTGCCGCTTACCGGAT
ACCTGTCCGCCTTTCTCCCTTCGGGAAGCGTGGCGCTTTCTCATAGCTCACGCTGTAGGTATCTCAGTTC
GGTGTAGGTCGTTCGCTCCAAGCTGGGCTGTGTGCACGAACCCCCCGTTCAGCCCGACCGCTGCGCCTTA
TCCGGTAACTATCGTCTTGAGTCCAACCCGGTAAGACACGACTTATCGCCACTGGCAGCAGCCACTGGTA
ACAGGATTAGCAGAGCGAGGTATGTAGGCGGTGCTACAGAGTTCTTGAAGTGGTGGCCTAACTACGGCTA
CACTAGAAGGACAGTATTTGGTATCTGCGCTCTGCTGAAGCCAGTTACCTTCGGAAAAAGAGTTGGTAGC
TCTTGATCCGGCAAACAAACCACCGCTGGTAGCGGTGGTTTTTTTGTTTGCAAGCAGCAGATTACGCGCA
GAAAAAAAGGATCTCAAGAAGATCCTTTGATCTTTTCTACGGGGTCTGACGCTCAGTGGAACGAAAACTC
ACGTTAAGGGATTTTGGTCATGAGATTATCAAAAAGGATCTTCACCTAGATCCTTTTAAATTAAAAATGA
AGTTTTAAATCAATCTAAAGTATATATGAGTAAACTTGGTCTGACAGTTACCAATGCTTAATCAGTGAGG
CACCTATCTCAGCGATCTGTCTATTTCGTTCATCCATAGTTGCCTGACTCCCCGTCGTGTAGATAACTAC
GATACGGGAGGGCTTACCATCTGGCCCCAGTGCTGCAATGATACCGCGAGACCCACGCTCACCGGCTCCA
GATTTATCAGCAATAAACCAGCCAGCCGGAAGGGCCGAGCGCAGAAGTGGTCCTGCAACTTTATCCGCCT
CCATCCAGTCTATTAATTGTTGCCGGGAAGCTAGAGTAAGTAGTTCGCCAGTTAATAGTTTGCGCAACGT
TGTTGCCATTGCTGCAGGCATCGTGGTGTCACGCTCGTCGTTTGGTATGGCTTCATTCAGCTCCGGTTCC

CAACGATCAAGGCGAGTTACATGATCCCCCATGTTGTGCAAAAAAGCGGTTAGCTCCTTCGGTCCTCCGA
TCGTTGTCAGAAGTAAGTTGGCCGCAGTGTTATCACTCATGGTTATGGCAGCACTGCATAATTCTCTTAC
TGTCATGCCATCCGTAAGATGCTTTTCTGTGACTGGTGAGTACTCAACCAAGTCATTCTGAGAATAGTGT
ATGCGGCGACCGAGTTGCTCTTGCCCGGCGTCAACACGGGATAATACCGCGCCACATAGCAGAACTTTAA
AAGTGCTCATCATTGGAAAACGTTCTTCGGGGCGAAAACTCTCAAGGATCTTACCGCTGTTGAGATCCAG
TTCGATGTAACCCACTCGTGCACCCAACTGATCTTCAGCATCTTTTACTTTCACCAGCGTTTCTGGGTGA
GCAAAAACAGGAAGGCAAAATGCCGCAAAAAAGGGAATAAGGGCGACACGGAAATGTTGAATACTCATAC
TCTTCCTTTTTCAATATTATTGAAGCATTTATCAGGGTTATTGTCTCATGAGCGGATACATATTTGAATG
TATTTAGAAAAATAAACAAATAGGGGTTCCGCGCACATTTCCCCGAAAAGTGCCACCTGACGTCTAAGAA
ACCATTATTATCATGACATTAACCTATAAAAATAGGCGTATCACGAGGCCCTTTCGTCTTCCTGA

Start/stop codon

Appendix 3

Mass Spectrometry Data

Recombinant WT fibrinogen expressed in CHO cells was analysed by mass spectrometry for detection of phosphorylation sites. Phosphopeptides were enriched using titanium oxide and analysed by MALDI-TOF/TOF using a Bruker Ultraflex-III mass spectrometer. Work was carried out by Adam Dowle, University of York.

Mass spectra were matched to the fibrinogen Aα chain by Mascot search against the IPI human database. Two phosphopeptides were matched at positions 20-35 and 354-367, corresponding to fibrinogen Aα chain Ser3 (ADS*GEGDFLAEGGGVR) and Ser345 (PGSTGTWNPGS*SER), respectively.

Ser3 phosphorylation site

Tandem mass spectrum of the Ser3 phoshopeptide:

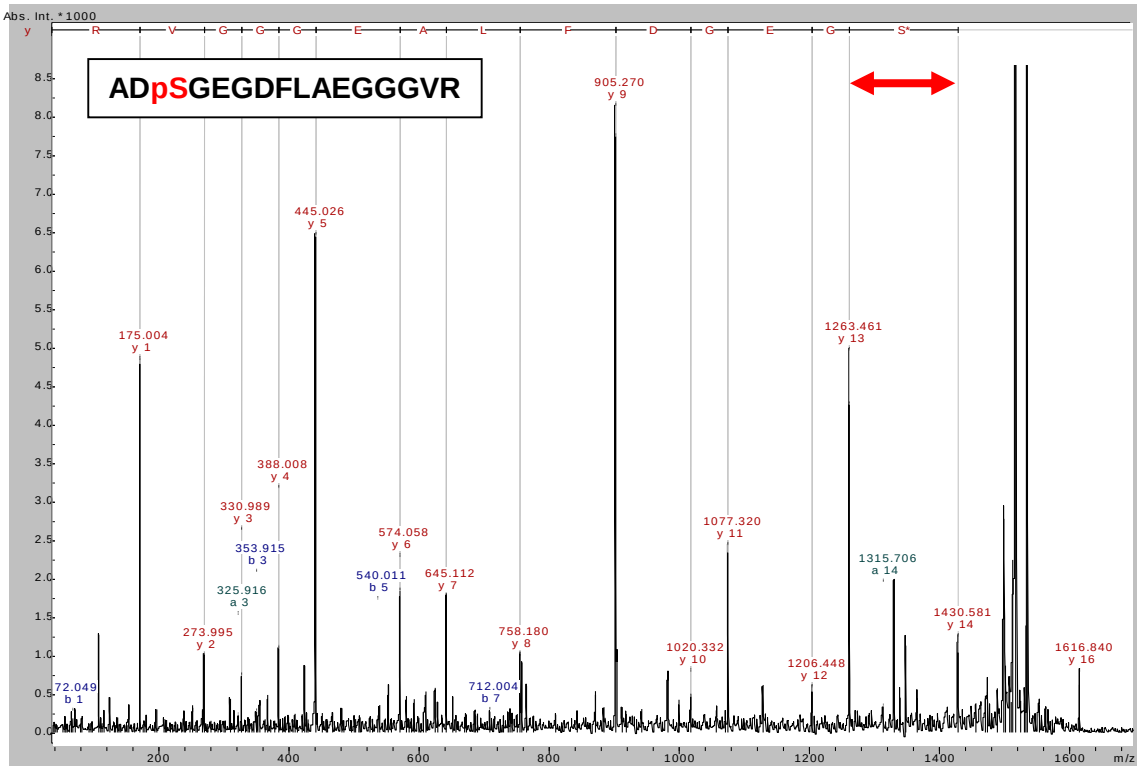

The presence of y13 and y14 (red arrow) identifies the phosphorylation site as Ser3.

Sequence overlay on the fragmentation spectrum for the Ser3 phosphopeptide:

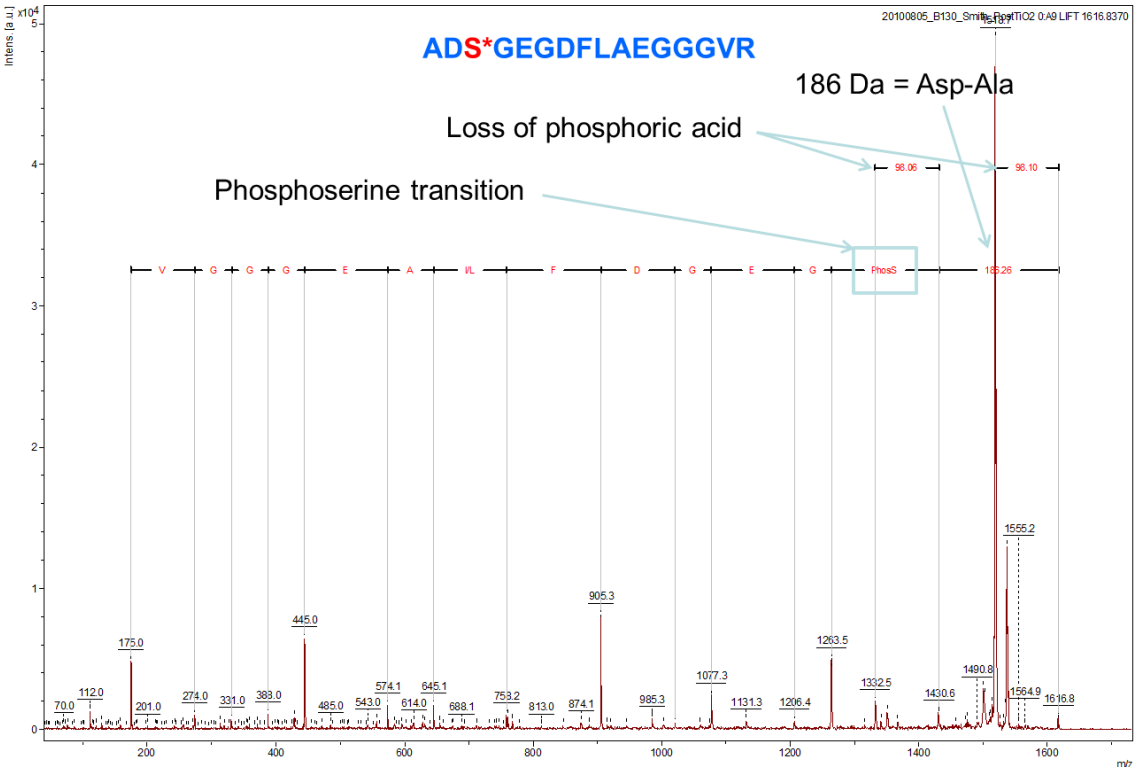

Ser345 phosphorylation site

Tandem mass spectrum of the Ser345 phoshopeptide:

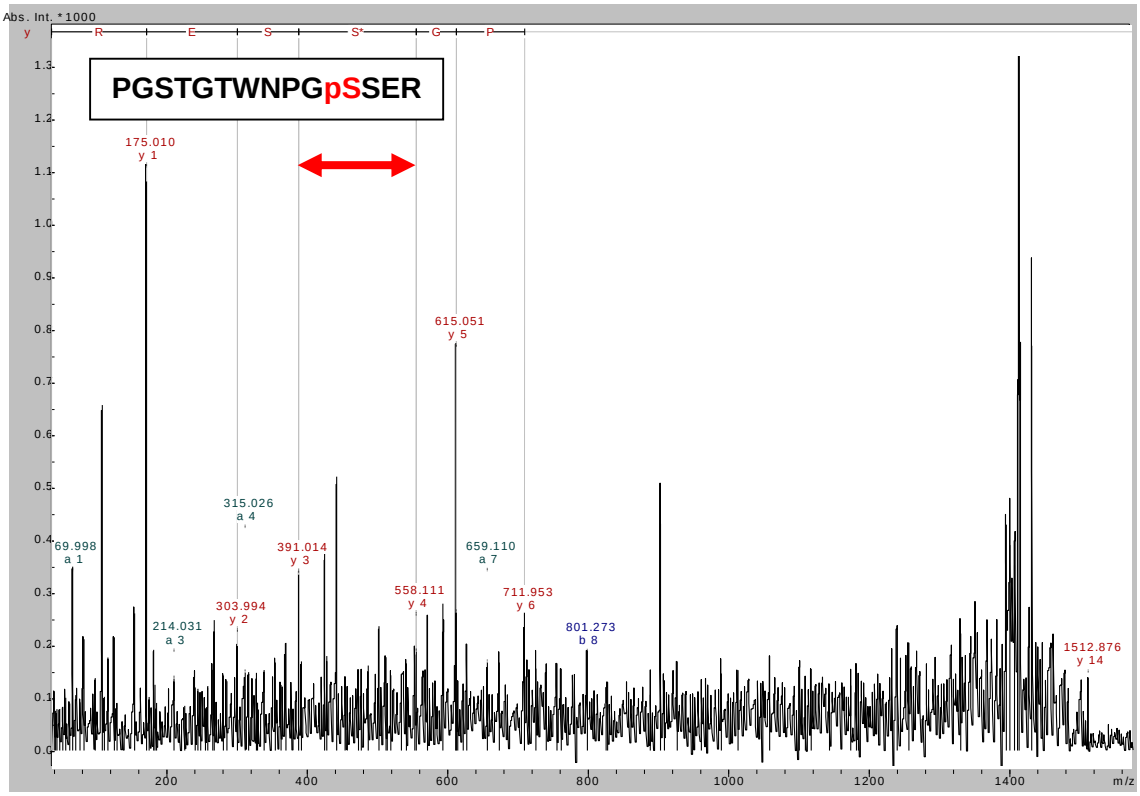

The presence of y3 and y4 (red arrow) identifies the phosphorylation site as Ser345.

Sequence overlay on the fragmentation spectrum for the Ser345 phosphopeptide:

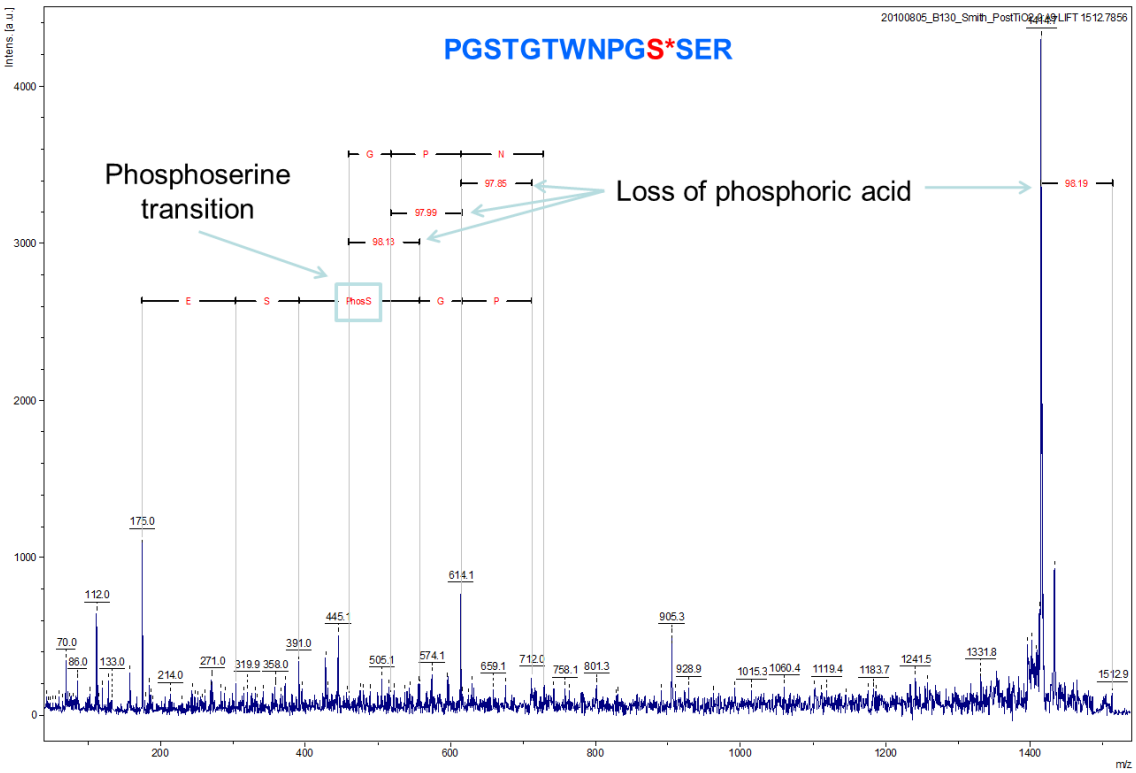

Publications and Presentations

Publications:

Smith, K.A., Pease, R.J., Avery, C.A., Brown, J.M., Adamson, P.J., **Cooke, E.J.**, Neergaard-Petersen, S., Cordell, P.A., Ariëns, R.A., Fishwick, C.W., Philippou, H., Grant, P.J. 2013. The activation peptide cleft exposed by thrombin cleavage of FXIII-A(2) contains a recognition site for the fibrinogen α chain. *Blood*, 121 (11), 2117-2126.

I was responsible for the expression and purification of recombinant fibrinogen. The other authors contributed to study design, laboratory work, data analysis and writing of the manuscript.

Poster presentations:

XXIV Congress of The International Society on Thrombosis and Haemostasis (ISTH), July 2013, Amsterdam, NL.

Title: Detection, localisation and quantification of intracellular phosphorylated human fibrinogen by proximity ligation: a novel approach for the characterisation of fibrinogen phosphorylation.

Authors: Cooke, E.J., Cordell, P.A., Pease, R.J., Grant, P.J., Smith, K.A.

Oral presentations:

Multidisciplinary Cardiovascular Research Centre retreat, March 2014, Leeds, UK.

Title: Characterisation of cellular fibrinogen phosphorylation.

Authors: Cooke, E.J., Cordell, P.A., Pease, R.J., Beckers, C.M.L., Simpson, K.R., Grant, P.J., Smith, K.A.

References

Adamczyk, B., Struwe, W. B., Ercan, A., Nigrovic, P. A. & Rudd, P. M. 2013. Characterization of fibrinogen glycosylation and its importance for serum/plasma N-glycome analysis. *J Proteome Res,* 12**,** 444-54.

Ajjan, R., Lim, B. C., Standeven, K. F., Harrand, R., Dolling, S., Phoenix, F., Greaves, R., Abou-Saleh, R. H., Connell, S., Smith, D. A., Weisel, J. W., Grant, P. J. & Ariens, R. A. 2008. Common variation in the C-terminal region of the fibrinogen beta-chain: effects on fibrin structure, fibrinolysis and clot rigidity. *Blood,* 111**,** 643-650.

Ajjan, R. A., Standeven, K. F., Khanbhai, M., Phoenix, F., Gersh, K. C., Weisel, J. W., Kearney, M. T., Ariens, R. A. & Grant, P. J. 2009. Effects of aspirin on clot structure and fibrinolysis using a novel in vitro cellular system. *Arterioscler Thromb Vasc Biol,* 29**,** 712-7.

Allan, P., Uitte de Willige, S., Abou-Saleh, R. H., Connell, S. D. & Ariens, R. A. 2012. Evidence that fibrinogen gamma' directly interferes with protofibril growth: implications for fibrin structure and clot stiffness. *J Thromb Haemost,* 10**,** 1072-80.

Alzahrani, S. H. & Ajjan, R. A. 2010. Coagulation and fibrinolysis in diabetes. *Diab Vasc Dis Res,* 7**,** 260-73.

Andrades, M. E., Lorenzi, R., Berger, M., Guimaraes, J. A., Moreira, J. C. & Dal-Pizzol, F. 2009. Glycolaldehyde induces fibrinogen post-translational modification, delay in clotting and resistance to enzymatic digestion. *Chem Biol Interact,* 180**,** 478-84.

Aoki, T., Umeda, T. & Kako, Y. 1992. The least number of phosphate groups for crosslinking of casein by colloidal calcium phosphate. *J Dairy Sci,* 75**,** 971-5.

Applegate, D., Haraga, L., Hertzberg, K. M., Steben, L. S., Zhang, J. Z., Redman, C. M. & Grieninger, G. 1998. The EC domains of human fibrinogen420 contain calcium binding sites but lack polymerization pockets. *Blood,* 92**,** 3669-74.

Ariens, R. A., Philippou, H., Nagaswami, C., Weisel, J. W., Lane, D. A. & Grant, P. J. 2000. The factor XIII V34L polymorphism accelerates thrombin activation of factor XIII and affects cross-linked fibrin structure. *Blood,* 96**,** 988-95.

Atoda, H., Yokota, E. & Morita, T. 2006. Characterization of a monoclonal antibody B1 that recognizes phosphorylated Ser-158 in the activation peptide region of human coagulation factor IX. *J Biol Chem,* 281**,** 9314-20.

Ayoubi, T. A. & Van De Ven, W. J. 1996. Regulation of gene expression by alternative promoters. *FASEB J,* 10**,** 453-60.

Bacon-Baguley, T., Ogilvie, M. L., Gartner, T. K. & Walz, D. A. 1990. Thrombospondin binding to specific sequences within the A alpha- and B beta-chains of fibrinogen. *J Biol Chem,* 265**,** 2317-23.

Baeuerle, P. A. & Huttner, W. B. 1987. Tyrosine sulfation is a trans-Golgi-specific protein modification. *J Cell Biol,* 105**,** 2655-64.

Bale, M. D., Janmey, P. A. & Ferry, J. D. 1982. Kinetics of formation of fibrin oligomers. II. Size distributions of ligated oligomers. *Biopolymers,* 21**,** 2265-77.

Baradet, T. C., Haselgrove, J. C. & Weisel, J. W. 1995. Three-dimensional reconstruction of fibrin clot networks from stereoscopic intermediate voltage electron microscope images and analysis of branching. *Biophys J,* 68**,** 1551-60.

Batalha, I. L., Lowe, C. R. & Roque, A. C. 2012. Platforms for enrichment of phosphorylated proteins and peptides in proteomics. *Trends Biotechnol,* 30**,** 100-10.

Baumann, R. E. & Henschen, A. H. 1993. Human fibrinogen polymorphic site analysis by restriction endonuclease digestion and allele-specific polymerase chain reaction amplification: identification of polymorphisms at positions A alpha 312 and B beta 448. *Blood,* 82**,** 2117-24.

Behague, I., Poirier, O., Nicaud, V., Evans, A., Arveiler, D., Luc, G., Cambou, J. P., Scarabin, P. Y., Bara, L., Green, F. & Cambien, F. 1996. Beta fibrinogen gene polymorphisms are associated with plasma fibrinogen and coronary artery disease in patients with myocardial infarction. The ECTIM Study. Etude Cas-Temoins sur l'Infarctus du Myocarde. *Circulation,* 93**,** 440-9.

Belisario, M. A., Di Domenico, C., Pelagalli, A., Della Morte, R. & Staiano, N. 1997. Metal-ion catalyzed oxidation affects fibrinogen activity on platelet aggregation and adhesion. *Biochimie,* 79**,** 449-55.

Bettelheim, F. R. 1954. Tyrosine O-sulfate in a peptide from fibrinogen. *J Am Chem Soc,* 76**,** 2838-2839.

Bhasin, N., Parry, D. J., Scott, D. J., Ariens, R. A., Grant, P. J. & West, R. M. 2009. Regarding "Altered fibrin clot structure and function in individuals with intermittent claudication". *J Vasc Surg,* 49**,** 1088-9.

Bierhaus, A., Hofmann, M. A., Ziegler, R. & Nawroth, P. P. 1998. AGEs and their interaction with AGE-receptors in vascular disease and diabetes mellitus. I. The AGE concept. *Cardiovasc Res,* 37**,** 586-600.

Binnie, C. G., Hettasch, J. M., Strickland, E. & Lord, S. T. 1993. Characterization of purified recombinant fibrinogen: partial phosphorylation of fibrinopeptide A. *Biochemistry,* 32**,** 107-113.

Bjoern, S., Foster, D. C., Thim, L., Wiberg, F. C., Christensen, M., Komiyama, Y., Pedersen, A. H. & Kisiel, W. 1991. Human plasma and recombinant factor VII. Characterization of O-glycosylations at serine residues 52 and 60 and effects of site-directed mutagenesis of serine 52 to alanine. *J Biol Chem,* 266**,** 11051-7.

Bjork, I., Jackson, C. M., Jornvall, H., Lavine, K. K., Nordling, K. & Salsgiver, W. J. 1982. The active site of antithrombin. Release of the same proteolytically cleaved form of the inhibitor from complexes with factor IXa, factor Xa, and thrombin. *J Biol Chem,* 257**,** 2406-11.

Blasi, F. 1993. Urokinase and urokinase receptor: a paracrine/autocrine system regulating cell migration and invasiveness. *Bioessays,* 15**,** 105-11.

Blomback, B. & Blomback, M. 1972. Molecular-Structure of Fibrinogen. *Ann N Y Acad Sci,* 202**,** 77-97.

Blomback, B., Blomback, M., Edman, P. & Hessel, B. 1962. Amino-acid sequence and the occurrence of phosphorus in human fibrinopeptides. *Nature,* 193**,** 833-834.

Blomback, B., Blomback, M., Edman, P. & Hessel, B. 1966. Human fibrinopeptides. Isolation, characterization and structure. *Biochim.Biophys.Acta,* 115**,** 371-396.

Blomback, B., Blomback, M., Hessel, B. & Iwanaga, S. 1967. Structure of N-terminal fragments of fibrinogen and specificity of thrombin. *Nature,* 215**,** 1445-8.

Blomback, B., Blomback, M. & Searle, J. 1963. On the occurrence of phosphorus in fibrinogen. *Biochim.Biophys.Acta,* 74**,** 148-151.

Blomback, B., Carlsson, K., Hessel, B., Liljeborg, A., Procyk, R. & Aslund, N. 1989. Native fibrin gel networks observed by 3D microscopy, permeation and turbidity. *Biochim Biophys Acta,* 997**,** 96-110.

Blomback, B., Hessel, B. & Hogg, D. 1976. Disulfide bridges in nh2 -terminal part of human fibrinogen. *Thromb.Res.,* 8**,** 639-658.

Blomback, B., Hessel, B., Hogg, D. & Therkildsen, L. 1978. A two-step fibrinogen--fibrin transition in blood coagulation. *Nature,* 275**,** 501-505.

Blomback, B., Hessel, B., Iwanaga, S., Reuterby, J. & Blomback, M. 1972. Primary structure of human fibrinogen and fibrin. I. Clevage of fibrinogen with cyanogen bromide. Isolation and characterization of NH 2 -terminal fragments of the ("A") chain. *J.Biol.Chem.,* 247**,** 1496-1512.

Bogli, C., Hofer, A., Baudo, F., Redaelli, R. & Furlan, M. 1992. Fibrinogen Milano IV, another case of congenital dysfibrinogenemia with an abnormal fibrinopeptide A release (A alpha 16 Arg----His). *Haemostasis,* 22**,** 7-11.

Bouma, H., Takagi, T. & Doolittle, R. F. 1978. The arrangement of disulfide bonds in fragment D from human fibrinogen. *Thromb Res,* 13**,** 557-62.

Brandt, J. T. 1985. Current concepts of coagulation. *Clin.Obstet.Gynecol.,* 28**,** 3-14.

Brill-Edwards, P. & Lee, A. 1999. D-dimer testing in the diagnosis of acute venous thromboembolism. *Thromb Haemost,* 82**,** 688-94.

Brinkhuis, J. & Payens, T. A. 1985. The rennet-induced clotting of para-kappa-casein revisited: inhibition experiments with pepstatin A. *Biochim Biophys Acta,* 832**,** 331-6.

Broze, G. J., Jr. 1992a. Tissue factor pathway inhibitor and the revised hypothesis of blood coagulation. *Trends Cardiovasc Med,* 2**,** 72-7.

Broze, G. J., Jr. 1992b. Why do hemophiliacs bleed? *Hosp Pract (Off Ed),* 27**,** 71-4, 79-82, 85-6.

Broze, G. J., Jr., Girard, T. J. & Novotny, W. F. 1991. The lipoprotein-associated coagulation inhibitor. *Prog Hemost Thromb,* 10**,** 243-68.

Buchdunger, E., Cioffi, C. L., Law, N., Stover, D., Ohno-Jones, S., Druker, B. J. & Lydon, N. B. 2000. Abl protein-tyrosine kinase inhibitor STI571 inhibits in vitro signal

transduction mediated by c-kit and platelet-derived growth factor receptors. *J Pharmacol Exp Ther,* 295**,** 139-45.

Burton, R. A., Tsurupa, G., Hantgan, R. R., Tjandra, N. & Medved, L. 2007. NMR solution structure, stability, and interaction of the recombinant bovine fibrinogen alphaC-domain fragment. *Biochemistry,* 46**,** 8550-60.

Burton, R. A., Tsurupa, G., Medved, L. & Tjandra, N. 2006. Identification of an ordered compact structure within the recombinant bovine fibrinogen alphaC-domain fragment by NMR. *Biochemistry,* 45**,** 2257-66.

Butenas, S. & Mann, K. G. 2002. Blood coagulation. *Biochemistry (Mosc.),* 67**,** 3-12.

Cao, W., Carney, J. M., Duchon, A., Floyd, R. A. & Chevion, M. 1988. Oxygen free radical involvement in ischemia and reperfusion injury to brain. *Neurosci Lett,* 88**,** 233-8.

Capasso, J. M., Keenan, T. W., Abeijon, C. & Hirschberg, C. B. 1989. Mechanism of phosphorylation in the lumen of the Golgi apparatus. Translocation of adenosine 5'-triphosphate into Golgi vesicles from rat liver and mammary gland. *J Biol Chem,* 264**,** 5233-40.

Caporaso, G. L., Gandy, S. E., Buxbaum, J. D., Ramabhadran, T. V. & Greengard, P. 1992. Protein phosphorylation regulates secretion of Alzheimer beta/A4 amyloid precursor protein. *Proc Natl Acad Sci U S A,* 89**,** 3055-9.

Carr, M. E. & Alving, B. M. 1995. Effect of fibrin structure on plasmin-mediated dissolution of plasma clots. *Blood Coagul Fibrinolysis,* 6**,** 567-73.

Carter, A. M., Catto, A. J., Bamford, J. M. & Grant, P. J. 1997. Gender-specific associations of the fibrinogen B beta 448 polymorphism, fibrinogen levels, and acute cerebrovascular disease. *Arterioscler Thromb Vasc Biol,* 17**,** 589-94.

Carter, A. M., Catto, A. J., Kohler, H. P., Ariens, R. A., Stickland, M. H. & Grant, P. J. 2000. alpha-fibrinogen Thr312Ala polymorphism and venous thromboembolism. *Blood,* 96**,** 1177-9.

Carter, A. M., Cymbalista, C. M., Spector, T. D. & Grant, P. J. 2007. Heritability of clot formation, morphology, and lysis: the EuroCLOT study. *Arterioscler Thromb Vasc Biol,* 27**,** 2783-9.

Cervera, R., Khamashta, M. A., Font, J., Sebastiani, G. D., Gil, A., Lavilla, P., Mejia, J. C., Aydintug, A. O., Chwalinska-Sadowska, H., de Ramon, E., Fernandez-Nebro, A., Galeazzi, M., Valen, M., Mathieu, A., Houssiau, F., Caro, N., Alba, P., Ramos-Casals, M., Ingelmo, M. & Hughes, G. R. 2003. Morbidity and mortality in systemic lupus erythematosus during a 10-year period: a comparison of early and late manifestations in a cohort of 1,000 patients. *Medicine (Baltimore),* 82**,** 299-308.

Cesarman-Maus, G. & Hajjar, K. A. 2005. Molecular mechanisms of fibrinolysis. *Br J Haematol,* 129**,** 307-21.

Chankova, S. G., Dimova, E., Dimitrova, M. & Bryant, P. E. 2007. Induction of DNA double-strand breaks by zeocin in Chlamydomonas reinhardtii and the role of increased DNA double-strand breaks rejoining in the formation of an adaptive response. *Radiat Environ Biophys,* 46**,** 409-16.

Cheo, D. L., Titus, S. A., Byrd, D. R., Hartley, J. L., Temple, G. F. & Brasch, M. A. 2004. Concerted assembly and cloning of multiple DNA segments using in vitro site-specific recombination: functional analysis of multi-segment expression clones. *Genome Res,* 14**,** 2111-20.

Cheresh, D. A. 1987. Human endothelial cells synthesize and express an Arg-Gly-Asp-directed adhesion receptor involved in attachment to fibrinogen and von Willebrand factor. *Proc Natl Acad Sci U S A,* 84**,** 6471-5.

Cheresh, D. A., Berliner, S. A., Vicente, V. & Ruggeri, Z. M. 1989. Recognition of distinct adhesive sites on fibrinogen by related integrins on platelets and endothelial cells. *Cell,* 58**,** 945-53.

Christensen, B., Refsum, H., Vintermyr, O. & Ueland, P. M. 1991. Homocysteine export from cells cultured in the presence of physiological or superfluous levels of methionine: methionine loading of non-transformed, transformed, proliferating, and quiescent cells in culture. *J Cell Physiol,* 146**,** 52-62.

Chung, D. W. & Davie, E. W. 1984. gamma and gamma' chains of human fibrinogen are produced by alternative mRNA processing. *Biochemistry,* 23**,** 4232-6.

Chung, D. W., Harris, J. E. & Davie, E. W. 1990. Nucleotide sequences of the three genes coding for human fibrinogen. *Adv Exp Med Biol,* 281**,** 39-48.

Chung, D. W., MacGillivray, R. T. & Davie, E. W. 1980. The biosynthesis of bovine fibrinogen, prothrombin, and albumin in a cell-free system. *Ann N Y Acad Sci,* 343**,** 210-7.

Chung, D. W., Que, B. G., Rixon, M. W., Mace, M., Jr. & Davie, E. W. 1983. Characterization of complementary deoxyribonucleic acid and genomic deoxyribonucleic acid for the beta chain of human fibrinogen. *Biochemistry,* 22**,** 3244-50.

Chung, N. P., Matthews, K., Kim, H. J., Ketas, T. J., Golabek, M., de Los Reyes, K., Korzun, J., Yasmeen, A., Sanders, R. W., Klasse, P. J., Wilson, I. A., Ward, A. B., Marozsan, A. J., Moore, J. P. & Cupo, A. 2014. Stable 293 T and CHO cell lines expressing cleaved, stable HIV-1 envelope glycoprotein trimers for structural and vaccine studies. *Retrovirology,* 11**,** 33.

Cierniewski, C. & Krajewski, T. 1974. Phosphorus-rich Aalpha polypeptide chains of pig and sheep fibrinogen. *Biochim Biophys Acta,* 351**,** 372-8.

Cohen, M. V. 1989. Free radicals in ischemic and reperfusion myocardial injury: is this the time for clinical trials? *Ann Intern Med,* 111**,** 918-31.

Cohen, P. 2002. Protein kinases--the major drug targets of the twenty-first century? *Nat Rev Drug Discov,* 1**,** 309-15.

Cohn, E. J., Strong, L. E. & et al. 1946. Preparation and properties of serum and plasma proteins; a system for the separation into fractions of the protein and lipoprotein components of biological tissues and fluids. *J Am Chem Soc,* 68**,** 459-75.

Collard, C. D., Agah, A., Reenstra, W., Buras, J. & Stahl, G. L. 1999. Endothelial nuclear factor-kappaB translocation and vascular cell adhesion molecule-1 induction by complement: inhibition with anti-human C5 therapy or cGMP analogues. *Arterioscler Thromb Vasc Biol,* 19**,** 2623-9.

Collet, J. P., Allali, Y., Lesty, C., Tanguy, M. L., Silvain, J., Ankri, A., Blanchet, B., Dumaine, R., Gianetti, J., Payot, L., Weisel, J. W. & Montalescot, G. 2006. Altered fibrin architecture is associated with hypofibrinolysis and premature coronary atherothrombosis. *Arterioscler Thromb Vasc Biol,* 26**,** 2567-73.

Collet, J. P., Moen, J. L., Veklich, Y. I., Gorkun, O. V., Lord, S. T., Montalescot, G. & Weisel, J. W. 2005a. The alphaC domains of fibrinogen affect the structure of the fibrin clot, its physical properties, and its susceptibility to fibrinolysis. *Blood,* 106**,** 3824-30.

Collet, J. P., Park, D., Lesty, C., Soria, J., Soria, C., Montalescot, G. & Weisel, J. W. 2000. Influence of fibrin network conformation and fibrin fiber diameter on fibrinolysis speed: dynamic and structural approaches by confocal microscopy. *Arterioscler Thromb Vasc Biol,* 20**,** 1354-61.

Collet, J. P., Shuman, H., Ledger, R. E., Lee, S. & Weisel, J. W. 2005b. The elasticity of an individual fibrin fiber in a clot. *Proc Natl Acad Sci U S A,* 102**,** 9133-7.

Collet, J. P., Woodhead, J. L., Soria, J., Soria, C., Mirshahi, M., Caen, J. P. & Weisel, J. W. 1996. Fibrinogen Dusart: electron microscopy of molecules, fibers and clots, and viscoelastic properties of clots. *Biophys J,* 70**,** 500-10.

Comp, P. C., Jacocks, R. M., Ferrell, G. L. & Esmon, C. T. 1982. Activation of protein C in vivo. *J Clin Invest,* 70**,** 127-34.

Cooper, A. V., Standeven, K. F. & Ariens, R. A. 2003. Fibrinogen gamma-chain splice variant gamma' alters fibrin formation and structure. *Blood,* 102**,** 535-40.

Cottrell, B. A., Strong, D. D., Watt, K. W. & Doolittle, R. F. 1979. Amino acid sequence studies on the alpha chain of human fibrinogen. Exact location of cross-linking acceptor sites. *Biochemistry,* 18**,** 5405-5410.

Crabtree, G. R., Comeau, C. M., Fowlkes, D. M., Fornace, A. J., Jr., Malley, J. D. & Kant, J. A. 1985. Evolution and structure of the fibrinogen genes. Random insertion of introns or selective loss? *J Mol Biol,* 185**,** 1-19.

Credo, R. B., Curtis, C. G. & Lorand, L. 1981. Alpha-chain domain of fibrinogen controls generation of fibrinoligase (coagulation factor XIIIa). Calcium ion regulatory aspects. *Biochemistry,* 20**,** 3770-8.

D'Angelo, A. & Selhub, J. 1997. Homocysteine and thrombotic disease. *Blood,* 90**,** 1-11.

Dalmon, J., Laurent, M. & Courtois, G. 1993. The human beta fibrinogen promoter contains a hepatocyte nuclear factor 1-dependent interleukin-6-responsive element. *Mol Cell Biol,* 13**,** 1183-93.

Damus, P. S., Hicks, M. & Rosenberg, R. D. 1973. Anticoagulant action of heparin. *Nature,* 246**,** 355-7.

Dang, C. V., Bell, W. R., Ebert, R. F. & Starksen, N. F. 1985a. Protective effect of divalent cations in the plasmin degradation of fibrinogen. *Arch Biochem Biophys,* 238**,** 452-7.

Dang, C. V., Ebert, R. F. & Bell, W. R. 1985b. Localization of a fibrinogen calcium binding site between gamma-subunit positions 311 and 336 by terbium fluorescence. *J Biol Chem,* 260**,** 9713-9.

Dang, C. V., Shin, C. K., Bell, W. R., Nagaswami, C. & Weisel, J. W. 1989. Fibrinogen sialic acid residues are low affinity calcium-binding sites that influence fibrin assembly. *J Biol Chem,* 264**,** 15104-8.

Davie, E. W. & Ratnoff, O. D. 1964. Waterfall Sequence for Intrinsic Blood Clotting. *Science,* 145**,** 1310-2.

de Felipe, P. 2002. Polycistronic viral vectors. *Curr Gene Ther,* 2**,** 355-78.

Dewpura, T., Raymond, A., Hamelin, J., Seidah, N. G., Mbikay, M., Chretien, M. & Mayne, J. 2008. PCSK9 is phosphorylated by a Golgi casein kinase-like kinase ex vivo and circulates as a phosphoprotein in humans. *FEBS J,* 275**,** 3480-93.

Dhein, S., Mohr, F.W., Delmar, M. 2005. *Practical Methods in Cardiovascular Research,* Germany, Springer.

Doolittle, R. F. 1973. Structural aspects of the fibrinogen to fibrin conversion. *Adv Protein Chem,* 27**,** 1-109.

Doolittle, R. F., Cottrell, B. A., Strong, D. & Watt, K. W. 1979. Preliminary report on the amino acid sequence of the alpha-chain of human fibrinogen. *Thromb Res,* 14**,** 787-92.

Doolittle, R. F., Goldbaum, D. M. & Doolittle, L. R. 1978. Designation of sequences involved in the "coiled-coil" interdomainal connections in fibrinogen: constructions of an atomic scale model. *J Mol Biol,* 120**,** 311-25.

Druker, B. J., Tamura, S., Buchdunger, E., Ohno, S., Segal, G. M., Fanning, S., Zimmermann, J. & Lydon, N. B. 1996. Effects of a selective inhibitor of the Abl tyrosine kinase on the growth of Bcr-Abl positive cells. *Nat Med,* 2**,** 561-6.

Duckert, P., Brunak, S. & Blom, N. 2004. Prediction of proprotein convertase cleavage sites. *Protein Eng Des Sel,* 17**,** 107-12.

Dunn, E. J., Ariens, R. A. & Grant, P. J. 2005. The influence of type 2 diabetes on fibrin structure and function. *Diabetologia,* 48**,** 1198-206.

Dunn, J. D., Reid, G. E. & Bruening, M. L. 2010. Techniques for phosphopeptide enrichment prior to analysis by mass spectrometry. *Mass Spectrom Rev,* 29**,** 29-54.

Duval, C., Allan, P., Connell, S. D., Ridger, V. C., Philippou, H. & Ariens, R. A. 2014. Roles of fibrin alpha- and gamma-chain specific cross-linking by FXIIIa in fibrin structure and function. *Thromb Haemost,* 111**,** 842-50.

Dyr, J. E., Blomback, B., Hessel, B. & Kornalik, F. 1989. Conversion of fibrinogen to fibrin induced by preferential release of fibrinopeptide B. *Biochim Biophys Acta,* 990**,** 18-24.

Eertmoed, A. L., Vallejo, Y. F. & Green, W. N. 1998. Transient expression of heteromeric ion channels. *Methods Enzymol,* 293**,** 564-85.

Ekdahl, K. N. & Nilsson, B. 1995. Phosphorylation of complement component C3 and C3 fragments by a human platelet protein kinase. Inhibition of factor I-mediated cleavage of C3b. *J Immunol,* 154**,** 6502-10.

Ekdahl, K. N., Ronnblom, L., Sturfelt, G. & Nilsson, B. 1997. Increased phosphate content in complement component C3, fibrinogen, vitronectin, and other plasma

proteins in systemic lupus erythematosus: covariation with platelet activation and possible association with thrombosis. *Arthritis Rheum,* 40**,** 2178-86.

Engstrom, L., Edlund, B., Ragnarsson, U., Dahlqvist-Edberg, U. & Humble, E. 1980. Phosphorylation of human fibrinogen in vitro with cyclic 3',5'-AMP-stimulated protein kinase and (32P)ATP. *Biochem.Biophys.Res.Commun.,* 96**,** 1503-1507.

Faber, D. R., Kalkhoven, E., Westerink, J., Bouwman, J. J., Monajemi, H. M. & Visseren, F. L. 2012. Conditioned media from (pre)adipocytes stimulate fibrinogen and PAI-1 production by HepG2 hepatoma cells. *Nutr Diabetes,* 2**,** e52.

Fallon, R. J. & Danaher, M. 1992. The effect of staurosporine, a protein kinase inhibitor, on asialoglycoprotein receptor endocytosis. *Exp Cell Res,* 203**,** 420-6.

Fantone, J. C. & Ward, P. A. 1982. Role of oxygen-derived free radicals and metabolites in leukocyte-dependent inflammatory reactions. *Am J Pathol,* 107**,** 395-418.

Farrell, D. H. 2012. gamma' Fibrinogen as a novel marker of thrombotic disease. *Clin Chem Lab Med,* 50**,** 1903-9.

Farrell, D. H., Huang, S. & Davie, E. W. 1993. Processing of the carboxyl 15-amino acid extension in the alpha-chain of fibrinogen. *J Biol Chem,* 268**,** 10351-5.

Felgner, P. L., Gadek, T. R., Holm, M., Roman, R., Chan, H. W., Wenz, M., Northrop, J. P., Ringold, G. M. & Danielsen, M. 1987. Lipofection: a highly efficient, lipid-mediated DNA-transfection procedure. *Proc Natl Acad Sci U S A,* 84**,** 7413-7.

Ferguson, E. W., Fretto, L. J. & McKee, P. A. 1975. A re-examination of the cleavage of fibrinogen and fibrin by plasmin. *J Biol Chem,* 250**,** 7210-8.

Ferranti, P., Traisci, M. V., Picariello, G., Nasi, A., Boschi, V., Siervo, M., Falconi, C., Chianese, L. & Addeo, F. 2004. Casein proteolysis in human milk: tracing the pattern of casein breakdown and the formation of potential bioactive peptides. *J Dairy Res,* 71**,** 74-87.

Fogelson, A. L. & Keener, J. P. 2010. Toward an understanding of fibrin branching structure. *Phys Rev E Stat Nonlin Soft Matter Phys,* 81**,** 051922.

Forman, W. B. & Barnhart, M. I. 1964. Cellular Site for Fibrinogen Synthesis. *JAMA,* 187**,** 128-32.

Forsberg, P. O. 1989. Dephosphorylation of human fibrinogen, previously phosphorylated in vitro by protein kinase C, by whole blood or intestinal alkaline phosphatase. Effects on thrombin-induced gelation of in vitro dephosphorylated human fibrinogen. *Thromb.Res.,* 53**,** 1-9.

Forsberg, P. O. & Martin, S. C. 1990. Plasmin digestion of human fibrinogen previously phosphorylated by protein kinase C or dephosphorylated by alkaline phosphatase in vitro. *Thromb.Res.,* 58**,** 119-127.

Francis, C. W., Marder, V. J. & Martin, S. E. 1980. Demonstration of a large molecular weight variant of the gamma chain of normal human plasma fibrinogen. *J Biol Chem,* 255**,** 5599-604.

Fraser, S. R., Booth, N. A. & Mutch, N. J. 2011. The antifibrinolytic function of factor XIII is exclusively expressed through alpha-antiplasmin cross-linking. *Blood,* 117**,** 6371-6374.

Fredriksson, S., Gullberg, M., Jarvius, J., Olsson, C., Pietras, K., Gustafsdottir, S. M., Ostman, A. & Landegren, U. 2002. Protein detection using proximity-dependent DNA ligation assays. *Nat Biotechnol,* 20**,** 473-7.

Fu, Y. & Grieninger, G. 1994. Fib420: a normal human variant of fibrinogen with two extended alpha chains. *Proc Natl Acad Sci U S A,* 91**,** 2625-8.

Fuller, G. M. & Zhang, Z. 2001. Transcriptional control mechanism of fibrinogen gene expression. *Ann N Y Acad Sci,* 936**,** 469-79.

Gabriel, D. A., Muga, K. & Boothroyd, E. M. 1992. The effect of fibrin structure on fibrinolysis. *J Biol Chem,* 267**,** 24259-63.

Gaffney, P. J. 1980. Breakdown products of fibrin and fibrinogen: molecular mechanisms and clinical implications. *J Clin Pathol Suppl (R Coll Pathol),* 14**,** 10-7.

Gailani, D. & Broze, G. J., Jr. 1991. Factor XI activation in a revised model of blood coagulation. *Science,* 253**,** 909-12.

Gailani, D. & Broze, G. J., Jr. 1993. Factor XI activation by thrombin and factor XIa. *Semin Thromb Hemost,* 19**,** 396-404.

Galanakis, D. K., Martinez, J., Mcdevitt, C. & Miller, F. 1983. Human-Fetal Fibrinogen - Its Characteristics of Delayed Fibrin Formation, High Sialic-Acid and Ap Peptide Content Are More Marked in Preterm Than in Term Samples. *Ann N Y Acad Sci,* 408**,** 640-643.

Gassmann, M., Grenacher, B., Rohde, B. & Vogel, J. 2009. Quantifying Western blots: pitfalls of densitometry. *Electrophoresis,* 30**,** 1845-55.

Gervois, P., Vu-Dac, N., Kleemann, R., Kockx, M., Dubois, G., Laine, B., Kosykh, V., Fruchart, J. C., Kooistra, T. & Staels, B. 2001. Negative regulation of human fibrinogen gene expression by peroxisome proliferator-activated receptor alpha agonists via inhibition of CCAAT box/enhancer-binding protein beta. *J Biol Chem,* 276**,** 33471-7.

Giuliano, M., Bellavia, G., Lauricella, M., D'Anneo, A., Vassallo, B., Vento, R. & Tesoriere, G. 2004. Staurosporine-induced apoptosis in Chang liver cells is associated with down-regulation of Bcl-2 and Bcl-XL. *Int J Mol Med,* 13**,** 565-71.

Gong, Y., Kim, S. O., Felez, J., Grella, D. K., Castellino, F. J. & Miles, L. A. 2001. Conversion of Glu-plasminogen to Lys-plasminogen is necessary for optimal stimulation of plasminogen activation on the endothelial cell surface. *J Biol Chem,* 276**,** 19078-83.

Gorkun, O. V., Veklich, Y. I., Medved, L. V., Henschen, A. H. & Weisel, J. W. 1994. Role of the alpha C domains of fibrin in clot formation. *Biochemistry,* 33**,** 6986-6997.

Gorkun, O. V., Veklich, Y. I., Weisel, J. W. & Lord, S. T. 1997. The conversion of fibrinogen to fibrin: recombinant fibrinogen typifies plasma fibrinogen. *Blood,* 89**,** 4407-14.

Greenhalgh, K. A. 2013. *Mechanistic studies on human fibrinogen polymorphisms that influence blood clot formation and lysis.* PhD Thesis, University of Leeds.

Grieninger, G., Plant, P. W., Liang, T. J., Kalb, R. G., Amrani, D., Mosesson, M. W., Hertzberg, K. M. & Pindyck, J. 1983. Hormonal regulation of fibrinogen synthesis in cultured hepatocytes. *Ann N Y Acad Sci,* 408**,** 469-89.

Guasch, M. D., Plana, M., Pena, J. M. & Itarte, E. 1986. Phosphorylation of fibrinogen by casein kinase 2. *Biochem.J.,* 234**,** 523-526.

Gullberg, M., Goransson, C. & Fredriksson, S. 2011. Duolink-[ldquo]In-cell Co-IP[rdquo] for visualization of protein interactions in situ. *Nat Meth,* 8.

Gurtu, V., Yan, G. & Zhang, G. 1996. IRES bicistronic expression vectors for efficient creation of stable mammalian cell lines. *Biochem Biophys Res Commun,* 229**,** 295-8.

Haglund, A. C., Ronquist, G., Frithz, G. & Ek, P. 2000. Alteration of the fibrinogen molecule and its phosphorylation state in myocardial infarction patients undergoing thrombolytic treatment. *Thromb.Res.,* 98**,** 147-156.

Haidaris, P. J., Francis, C. W., Sporn, L. A., Arvan, D. S., Collichio, F. A. & Marder, V. J. 1989. Megakaryocyte and hepatocyte origins of human fibrinogen biosynthesis exhibit hepatocyte-specific expression of gamma chain-variant polypeptides. *Blood,* 74**,** 743-50.

Hall, C. E. & Slayter, H. S. 1959. The fibrinogen molecule: its size, shape, and mode of polymerization. *J Biophys Biochem Cytol,* 5**,** 11-6.

Hammer, M. R., John, P. N., Flynn, M. D., Bellingham, A. J. & Leslie, R. D. 1989. Glycated fibrinogen: a new index of short-term diabetic control. *Ann Clin Biochem,* 26 (Pt 1)**,** 58-62.

Hanna, L. S., Scheraga, H. A., Francis, C. W. & Marder, V. J. 1984. Comparison of structures of various human fibrinogens and a derivative thereof by a study of the kinetics of release of fibrinopeptides. *Biochemistry,* 23**,** 4681-4687.

Hartley, J. L., Temple, G. F. & Brasch, M. A. 2000. DNA cloning using in vitro site-specific recombination. *Genome Res,* 10**,** 1788-95.

Hartman, S. C. & Mulligan, R. C. 1988. Two dominant-acting selectable markers for gene transfer studies in mammalian cells. *Proc Natl Acad Sci U S A,* 85**,** 8047-51.

Hartwig, R. & Danishefsky, K. J. 1991. Studies on the assembly and secretion of fibrinogen. *J Biol Chem,* 266**,** 6578-85.

Hawiger, J., Kloczewiak, M., Bednarek, M. A. & Timmons, S. 1989. Platelet receptor recognition domains on the alpha chain of human fibrinogen: structure-function analysis. *Biochemistry,* 28**,** 2909-14.

He, S., Blomback, M., Yoo, G., Sinha, R. & Henschen-Edman, A. H. 2001. Modified clotting properties of fibrinogen in the presence of acetylsalicylic acid in a purified system. *Fibrinogen,* 936**,** 531-535.

Heldin, P. 1987. Phosphorylation in vitro of human fibrinogen with casein kinase TS and characterization of phosphorylated sites. *Arch Biochem Biophys,* 257**,** 269-75.

Heldin, P., Hessel, B., Humble, E., Blomback, B. & Engstrom, L. 1987a. Effect of phosphorylation in vitro of human fibrinogen with protein kinase C on thrombin-induced gelation. *Thromb Res,* 47**,** 93-9.

Heldin, P., Hessel, B., Humble, E., Blomback, B. & Engstrom, L. 1987b. Effect of phosphorylation in vitro of human fibrinogen with protein kinase C on thrombin-induced gelation. *Thromb.Res.,* 47**,** 93-99.

Heldin, P. & Humble, E. 1987. Phosphorylation of human fibrinogen in vitro with protein kinase C: characterization of the phosphorylated sites. *Arch Biochem Biophys,* 252**,** 49-59.

Henry, I., Uzan, G., Weil, D., Nicolas, H., Kaplan, J. C., Marguerie, C., Kahn, A. & Junien, C. 1984. The genes coding for A alpha-, B beta-, and gamma-chains of fibrinogen map to 4q2. *Am.J.Hum.Genet.,* 36**,** 760-768.

Henschen, A. 1964. Number + Reactivity of Disulfide Bonds in Fibrinogen + Fibrin. *Arkiv for Kemi,* 22**,** 355-&.

Henschen, A. 1978. Disulfide Bridges in Middle Part of Human Fibrinogen. *Hoppe-Seylers Zeitschrift Fur Physiologische Chemie,* 359**,** 1757-1770.

Henschen, A., Lottspeich, F., Kehl, M. & Southan, C. 1983. Covalent structure of fibrinogen. *Ann.N.Y.Acad.Sci.,* 408**,** 28-43.

Henschen, A. H., Theodor, I. & Prikle, H. 1991. Hydroxyproline - a Posttranslational Modification of Proline, Is a Constituent of Human Fibrinogen. *Thromb Haemost,* 65**,** 821-821.

Henschen-Edman, A. H. 2001. Fibrinogen non-inherited heterogeneity and its relationship to function in health and disease. *Ann N Y Acad Sci,* 936**,** 580-93.

Hernandez-Hernandez, O., Lebron-Aguilar, R., Quintanilla-Lopez, J. E., Sanz, M. L. & Moreno, F. J. 2011. Detection of two minor phosphorylation sites for bovine kappa-casein macropeptide by reversed-phase liquid chromatography-tandem mass spectrometry. *J Agric Food Chem,* 59**,** 10848-53.

Higgins, D. L., Lewis, S. D. & Shafer, J. A. 1983. Steady state kinetic parameters for the thrombin-catalyzed conversion of human fibrinogen to fibrin. *J Biol Chem,* 258**,** 9276-82.

Hoffman, M. & Monroe, D. M., III 2001. A cell-based model of hemostasis. *Thromb.Haemost.,* 85**,** 958-965.

Holm, B., Nilsen, D. W., Kierulf, P. & Godal, H. C. 1985. Purification and characterization of 3 fibrinogens with different molecular weights obtained from normal human plasma. *Thromb Res,* 37**,** 165-76.

Hornyak, T. J. & Shafer, J. A. 1991. Role of calcium ion in the generation of factor XIII activity. *Biochemistry,* 30**,** 6175-82.

Hortin, G. L. 1989. Sulfation of a gamma-chain variant of human fibrinogen. *Biochem Int,* 19**,** 1355-62.

Hoylaerts, M., Rijken, D. C., Lijnen, H. R. & Collen, D. 1982. Kinetics of the activation of plasminogen by human tissue plasminogen activator. Role of fibrin. *J Biol Chem,* 257**,** 2912-9.

Huang, S., Cao, Z., Chung, D. W. & Davie, E. W. 1996. The role of betagamma and alphagamma complexes in the assembly of human fibrinogen. *J Biol Chem,* 271**,** 27942-7.

Huang, S., Cao, Z. & Davie, E. W. 1993a. The role of amino-terminal disulfide bonds in the structure and assembly of human fibrinogen. *Biochem Biophys Res Commun,* 190**,** 488-95.

Huang, S., Mulvihill, E. R., Farrell, D. H., Chung, D. W. & Davie, E. W. 1993b. Biosynthesis of human fibrinogen. Subunit interactions and potential intermediates in the assembly. *J Biol Chem,* 268**,** 8919-26.

Hubbard, M. J. & Cohen, P. 1993. On target with a new mechanism for the regulation of protein phosphorylation. *Trends Biochem Sci,* 18**,** 172-7.

Hunter, T. 1994. 1001 protein kinases redux--towards 2000. *Semin Cell Biol,* 5**,** 367-76.

Igaz, P., Toth, S., Rose-John, S., Madurka, I., Fejer, G., Szalai, C. & Falus, A. 1998. Soluble interleukin 6 (IL-6) receptor influences the expression of the protooncogene junB and the production of fibrinogen in the HepG2 human hepatoma cell line and primary rat hepatocytes. *Cytokine,* 10**,** 620-6.

International Human Genome Sequencing Consortium, 2004. Finishing the euchromatic sequence of the human genome. *Nature,* 431**,** 931-45.

Itarte, E., Plana, M., Guasch, M. D. & Martos, C. 1983. Phosphorylation of fibrinogen by casein kinase 1. *Biochem.Biophys.Res.Commun.,* 117**,** 631-636.

Jensen, O. N. 2004. Modification-specific proteomics: characterization of post-translational modifications by mass spectrometry. *Curr Opin Chem Biol,* 8**,** 33-41.

Joensuu, H., Roberts, P. J., Sarlomo-Rikala, M., Andersson, L. C., Tervahartiala, P., Tuveson, D., Silberman, S., Capdeville, R., Dimitrijevic, S., Druker, B. & Demetri, G. D. 2001. Effect of the tyrosine kinase inhibitor STI571 in a patient with a metastatic gastrointestinal stromal tumor. *N Engl J Med,* 344**,** 1052-6.

Jolles, P., Levy-Toledano, S., Fiat, A. M., Soria, C., Gillessen, D., Thomaidis, A., Dunn, F. W. & Caen, J. P. 1986. Analogy between fibrinogen and casein. Effect of an undecapeptide isolated from kappa-casein on platelet function. *Eur J Biochem,* 158**,** 379-82.

Jolles, P., Loucheux-Lefebvre, M. H. & Henschen, A. 1978. Structural relatedness of kappa-casein and fibrinogen gamma-chain. *J Mol Evol,* 11**,** 271-7.

Jones, B. G., Thomas, L., Molloy, S. S., Thulin, C. D., Fry, M. D., Walsh, K. A. & Thomas, G. 1995. Intracellular trafficking of furin is modulated by the phosphorylation state of a casein kinase II site in its cytoplasmic tail. *EMBO J,* 14**,** 5869-83.

Jones, J. I., D'Ercole, A. J., Camacho-Hubner, C. & Clemmons, D. R. 1991. Phosphorylation of insulin-like growth factor (IGF)-binding protein 1 in cell culture and in vivo: effects on affinity for IGF-I. *Proc Natl Acad Sci U S A,* 88**,** 7481-5.

Kaijzel, E. L., Koolwijk, P., van Erck, M. G., van Hinsbergh, V. W. & de Maat, M. P. 2006. Molecular weight fibrinogen variants determine angiogenesis rate in a fibrin matrix in vitro and in vivo. *J Thromb Haemost,* 4**,** 1975-81.

Kant, J. A., Fornace, A. J., Jr., Saxe, D., Simon, M. I., McBride, O. W. & Crabtree, G. R. 1985. Evolution and organization of the fibrinogen locus on chromosome 4: gene duplication accompanied by transposition and inversion. *Proc Natl Acad Sci U S A,* 82**,** 2344-8.

Kawamoto, Y. & Kaibara, M. 1990. Procoagulant activity of collagen. Effect of difference in type and structure of collagen. *Biochim Biophys Acta,* 1035**,** 361-8.

Kiliszek, M., Burzynska, B., Michalak, M., Gora, M., Winkler, A., Maciejak, A., Leszczynska, A., Gajda, E., Kochanowski, J. & Opolski, G. 2012. Altered gene expression pattern in peripheral blood mononuclear cells in patients with acute myocardial infarction. *PLoS One,* 7**,** e50054.

Kimura, S. & Aoki, N. 1986a. Cross-linking site in fibrinogen for alpha 2-plasmin inhibitor. *J.Biol.Chem.,* 261**,** 15591-15595.

Kimura, S. & Aoki, N. 1986b. Cross-linking site in fibrinogen for alpha 2-plasmin inhibitor. *J Biol Chem,* 261**,** 15591-5.

Kinoshita, E., Kinoshita-Kikuta, E. & Koike, T. 2009. Separation and detection of large phosphoproteins using Phos-tag SDS-PAGE. *Nat Protoc,* 4**,** 1513-21.

Kinoshita, E., Takahashi, M., Takeda, H., Shiro, M. & Koike, T. 2004. Recognition of phosphate monoester dianion by an alkoxide-bridged dinuclear zinc(II) complex. *Dalton Trans***,** 1189-93.

Kinoshita, E., Yamada, A., Takeda, H., Kinoshita-Kikuta, E. & Koike, T. 2005. Novel immobilized zinc(II) affinity chromatography for phosphopeptides and phosphorylated proteins. *J Sep Sci,* 28**,** 155-62.

Kloczewiak, M., Timmons, S., Lukas, T. J. & Hawiger, J. 1984. Platelet receptor recognition site on human fibrinogen. Synthesis and structure-function relationship of peptides corresponding to the carboxy-terminal segment of the gamma chain. *Biochemistry,* 23**,** 1767-74.

Kollman, J. M., Pandi, L., Sawaya, M. R., Riley, M. & Doolittle, R. F. 2009. Crystal structure of human fibrinogen. *Biochemistry,* 48**,** 3877-3886.

Koopman, J., Haverkate, F., Grimbergen, J., Lord, S. T., Mosesson, M. W., DiOrio, J. P., Siebenlist, K. S., Legrand, C., Soria, J., Soria, C. & et al. 1993. Molecular basis for fibrinogen Dusart (A alpha 554 Arg-->Cys) and its association with abnormal fibrin polymerization and thrombophilia. *J Clin Invest,* 91**,** 1637-43.

Kornfeld, R. A., Perati, P. R., Hanko, V. P. & Rohrer, J. S. 2009. High-performance ion-exchange chromatography for determination of protein microheterogeneity. Available: http://www.dionex.com/en-us/webdocs/70912-lpn_2206-01-R2.pdf [Accessed 13 November 2014].

Krust, B., Galabru, J. & Hovanessian, A. G. 1983. Phosphorylation of the alpha-chain of fibrinogen by a platelet kinase activity enhanced by interferon. *Biochem.Biophys.Res.Commun.,* 117**,** 350-357.

Kudryk, B., Okada, M., Redman, C. M. & Blomback, B. 1982. Biosynthesis of dog fibrinogen. Characterization of nascent fibrinogen in the rough endoplasmic reticulum. *Eur J Biochem,* 125**,** 673-82.

Langer, B. G., Weisel, J. W., Dinauer, P. A., Nagaswami, C. & Bell, W. R. 1988. Deglycosylation of fibrinogen accelerates polymerization and increases lateral aggregation of fibrin fibers. *J Biol Chem,* 263**,** 15056-63.

Lasa, M., Marin, O. & Pinna, L. A. 1997. Rat liver Golgi apparatus contains a protein kinase similar to the casein kinase of lactating mammary gland. *Eur J Biochem,* 243**,** 719-25.

Lasa-Benito, M., Marin, O., Meggio, F. & Pinna, L. A. 1996. Golgi apparatus mammary gland casein kinase: monitoring by a specific peptide substrate and definition of specificity determinants. *FEBS Lett,* 382**,** 149-52.

Lauricella, A. M., Quintana, I., Castanon, M., Sassetti, B. & Kordich, L. 2006. Influence of homocysteine on fibrin network lysis. *Blood Coagulation & Fibrinolysis,* 17**,** 181-186.

Lawson, J. H., Butenas, S., Ribarik, N. & Mann, K. G. 1993. Complex-dependent inhibition of factor VIIa by antithrombin III and heparin. *J Biol Chem,* 268**,** 767-70.

Lee, K. N., Tae, W. C., Jackson, K. W., Kwon, S. H. & McKee, P. A. 1999. Characterization of wild-type and mutant alpha2-antiplasmins: fibrinolysis enhancement by reactive site mutant. *Blood,* 94**,** 164-71.

Lee, M. H., Kaczmarek, E., Chin, D. T., Oda, A., McIntosh, S., Bauer, K. A., Clyne, L. P. & McDonagh, J. 1991. Fibrinogen Ledyard (A alpha Arg16----Cys): biochemical and physiologic characterization. *Blood,* 78**,** 1744-52.

Leeksma, O. C., Meijer-Huizinga, F., Stoepman-van Dalen, E. A., van Ginkel, C. J., van Aken, W. G. & van Mourik, J. A. 1986. Fibrinopeptide A and the phosphate content of fibrinogen in venous thromboembolism and disseminated intravascular coagulation. *Blood,* 67**,** 1460-7.

Lerer, G. D., Saavedra, M. C., Falcoff, R., Maiztegui, J. I. & Molinas, F. C. 1991. Activity of a platelet protein kinase that phosphorylates fibrinogen and histone in Argentine hemorrhagic fever. *Acta Physiol Pharmacol Ther Latinoam,* 41**,** 377-86.

Lewis, S. D., Janus, T. J., Lorand, L. & Shafer, J. A. 1985. Regulation of formation of factor XIIIa by its fibrin substrates. *Biochemistry,* 24**,** 6772-7.

Lim, B. C., Ariens, R. A., Carter, A. M., Weisel, J. W. & Grant, P. J. 2003. Genetic regulation of fibrin structure and function: complex gene-environment interactions may modulate vascular risk. *Lancet,* 361**,** 1424-31.

Lindsey, G. G., Brown, G. & Purves, L. R. 1978. Calcium binding to human fibrinogen - localization of two calcium specific sites. *Thromb Res,* 13**,** 345-50.

Lipinski, B. & Lipinska, I. 2000. Effect of magnesium on fibrin formation from lower molecular weight (LMW) fibrinogen. *Magnes Res,* 13**,** 233-7.

Lippincott-Schwartz, J., Yuan, L. C., Bonifacino, J. S. & Klausner, R. D. 1989. Rapid redistribution of Golgi proteins into the ER in cells treated with brefeldin A: evidence for membrane cycling from Golgi to ER. *Cell,* 56**,** 801-13.

Litvinov, R. I., Yakovlev, S., Tsurupa, G., Gorkun, O. V., Medved, L. & Weisel, J. W. 2007. Direct evidence for specific interactions of the fibrinogen alphaC-domains with the central E region and with each other. *Biochemistry,* 46**,** 9133-9142.

Liu, Q., Matsueda, G., Brown, E. & Frojmovic, M. 1997. The AGDV residues on the gamma chain carboxyl terminus of platelet-bound fibrinogen are needed for platelet aggregation. *Biochim Biophys Acta,* 1343**,** 316-26.

Lorand, L., Jeong, J. M., Radek, J. T. & Wilson, J. 1993. Human plasma factor XIII: subunit interactions and activation of zymogen. *Methods Enzymol.,* 222**,** 22-35.

Lord, S. T., Binnie, C. G., Hettasch, J. M. & Strickland, E. 1993. Purification and characterization of recombinant human fibrinogen. *Blood Coagul Fibrinolysis,* 4**,** 55-9.

Love, P. E. & Santoro, S. A. 1990. Antiphospholipid antibodies: anticardiolipin and the lupus anticoagulant in systemic lupus erythematosus (SLE) and in non-SLE disorders. Prevalence and clinical significance. *Ann Intern Med,* 112**,** 682-98.

Lovely, R. S., Moaddel, M. & Farrell, D. H. 2003. Fibrinogen gamma' chain binds thrombin exosite II. *J Thromb Haemost,* 1**,** 124-31.

Lucas, M. A., Fretto, L. J. & McKee, P. A. 1983. The binding of human plasminogen to fibrin and fibrinogen. *J Biol Chem,* 258**,** 4249-56.

Macfarlane, R. G. 1964. An enzyme cascade in the blood clotting mechanism, and its function as a biochemical amplifier. *Nature,* 202**,** 498-499.

Madrazo, J., Brown, J. H., Litvinovich, S., Dominguez, R., Yakovlev, S., Medved, L. & Cohen, C. 2001. Crystal structure of the central region of bovine fibrinogen (E5 fragment) at 1.4-A resolution. *Proc Natl Acad Sci U S A,* 98**,** 11967-72.

Maekawa, H., Yamazumi, K., Muramatsu, S., Kaneko, M., Hirata, H., Takahashi, N., de Bosch, N. B., Carvajal, Z., Ojeda, A., Arocha-Pinango, C. L. & et al. 1991. An A alpha Ser-434 to N-glycosylated Asn substitution in a dysfibrinogen, fibrinogen Caracas II, characterized by impaired fibrin gel formation. *J Biol Chem,* 266**,** 11575-81.

Makogonenko, E., Tsurupa, G., Ingham, K. & Medved, L. 2002. Interaction of fibrin(ogen) with fibronectin: further characterization and localization of the fibronectin-binding site. *Biochemistry,* 41**,** 7907-13.

Mann, M., Ong, S. E., Gronborg, M., Steen, H., Jensen, O. N. & Pandey, A. 2002. Analysis of protein phosphorylation using mass spectrometry: deciphering the phosphoproteome. *Trends Biotechnol,* 20**,** 261-8.

Manning, G., Whyte, D. B., Martinez, R., Hunter, T. & Sudarsanam, S. 2002. The protein kinase complement of the human genome. *Science,* 298**,** 1912-34.

Marguerie, G., Chagniel, G. & Suscillon, M. 1977. The binding of calcium to bovine fibrinogen. *Biochim Biophys Acta,* 490**,** 94-103.

Marinkovic, S., Jahreis, G. P., Wong, G. G. & Baumann, H. 1989. IL-6 modulates the synthesis of a specific set of acute phase plasma proteins in vivo. *J Immunol,* 142**,** 808-12.

Martin, S. C. & Bjork, I. 1990. Conformational changes in human fibrinogen after in vitro phosphorylation and their relation to fibrinogen behaviour. *FEBS Lett,* 272**,** 103-5.

Martin, S. C., Ekman, P., Forsberg, P. O. & Ersmark, H. 1992. Increased phosphate content of fibrinogen in vivo correlates with alteration in fibrinogen behaviour. *Thromb.Res.,* 68**,** 467-473.

Martin, S. C., Forsberg, P. O. & Eriksson, S. D. 1991. The effects of in vitro phosphorylation and dephosphorylation on the thrombin-induced gelation and plasmin degradation of fibrinogen. *Thromb.Res.,* 61**,** 243-252.

Martinelli, R. A. & Scheraga, H. A. 1980. Steady-state kinetic study of the bovine thrombin-fibrinogen interaction. *Biochemistry,* 19**,** 2343-2350.

Martinez, J. & Barsigian, C. 1987. Carbohydrate Abnormalities of N-Linked Plasma Glycoproteins in Liver-Disease. *Laboratory Investigation,* 57**,** 240-257.

Matsuka, Y. V., Medved, L. V., Migliorini, M. M. & Ingham, K. C. 1996. Factor XIIIa-catalyzed cross-linking of recombinant alpha C fragments of human fibrinogen. *Biochemistry,* 35**,** 5810-6.

Maurer, M. C., Peng, J. L., An, S. S., Trosset, J. Y., Henschen-Edman, A. & Scheraga, H. A. 1998. Structural examination of the influence of phosphorylation on the binding of fibrinopeptide A to bovine thrombin. *Biochemistry,* 37**,** 5888-5902.

McKee, P. A., Mattock, P. & Hill, R. L. 1970. Subunit structure of human fibrinogen, soluble fibrin, and cross-linked insoluble fibrin. *Proc.Natl.Acad.Sci.U.S.A,* 66**,** 738-744.

Medved, L. & Weisel, J. W. 2009. Recommendations for nomenclature on fibrinogen and fibrin. *J.Thromb.Haemost.,* 7**,** 355-359.

Medved, L. V., Gorkun, O. V. & Privalov, P. L. 1983. Structural organization of C-terminal parts of fibrinogen A alpha-chains. *FEBS Lett,* 160**,** 291-5.

Meggio, F., Donella Deana, A., Ruzzene, M., Brunati, A. M., Cesaro, L., Guerra, B., Meyer, T., Mett, H., Fabbro, D., Furet, P. & et al. 1995. Different susceptibility of protein kinases to staurosporine inhibition. Kinetic studies and molecular bases for the resistance of protein kinase CK2. *Eur J Biochem,* 234**,** 317-22.

Meh, D. A., Siebenlist, K. R., Brennan, S. O., Holyst, T. & Mosesson, M. W. 2001. The amino acid sequence in fibrin responsible for high affinity thrombin binding. *Thromb Haemost,* 85**,** 470-4.

Meh, D. A., Siebenlist, K. R. & Mosesson, M. W. 1996. Identification and characterization of the thrombin binding sites on fibrin. *J Biol Chem,* 271**,** 23121-5.

Morrison, D. C. & Cochrane, C. G. 1974. Direct evidence for Hageman factor (factor XII) activation by bacterial lipopolysaccharides (endotoxins). *J Exp Med,* 140**,** 797-811.

Mosesson, M. W., DiOrio, J. P., Siebenlist, K. R., Wall, J. S. & Hainfeld, J. F. 1993. Evidence for a second type of fibril branch point in fibrin polymer networks, the trimolecular junction. *Blood,* 82**,** 1517-21.

Mosesson, M. W., Hainfeld, J., Wall, J. & Haschemeyer, R. H. 1981. Identification and mass analysis of human fibrinogen molecules and their domains by scanning transmission electron microscopy. *J Mol Biol,* 153**,** 695-718.

Mount, S. M. 1982. A catalogue of splice junction sequences. *Nucleic Acids Res,* 10**,** 459-72.

Murnane, J. P., Yezzi, M. J. & Young, B. R. 1990. Recombination events during integration of transfected DNA into normal human cells. *Nucleic Acids Res,* 18**,** 2733-8.

Nagel, T. & Meyer, B. 2014. Simultaneous characterization of sequence polymorphisms, glycosylation and phosphorylation of fibrinogen in a direct analysis by LC-MS. *Biochim Biophys Acta,* 1844**,** 2284-2289.

Nakashima, A., Sasaki, S., Miyazaki, K., Miyata, T. & Iwanaga, S. 1992. Human fibrinogen heterogeneity: the COOH-terminal residues of defective A alpha chains of fibrinogen II. *Blood Coagul Fibrinolysis,* 3**,** 361-70.

Nakata, K., Saitoh, R., Amano, J., Koshiyama, A., Ichibangase, T., Murao, N., Ohta, K., Aso, Y., Ishigai, M. & Imai, K. 2012. Alteration of intracellular secretory acute phase response proteins expressed in human hepatocyte induced by exposure with interleukin-6. *Cytokine,* 59**,** 317-23.

Nalbant, D., Youn, H., Nalbant, S. I., Sharma, S., Cobos, E., Beale, E. G., Du, Y. & Williams, S. C. 2005. FAM20: an evolutionarily conserved family of secreted proteins expressed in hematopoietic cells. *BMC Genomics,* 6**,** 11.

Nemerson, Y. & Repke, D. 1985. Tissue factor accelerates the activation of coagulation factor VII: the role of a bifunctional coagulation cofactor. *Thromb Res,* 40**,** 351-8.

Nesheim, M. E., Taswell, J. B. & Mann, K. G. 1979. The contribution of bovine Factor V and Factor Va to the activity of prothrombinase. *J.Biol.Chem.,* 254**,** 10952-10962.

Nickerson, J. M. & Fuller, G. M. 1981. In vitro synthesis of rat fibrinogen: identification of preA alpha, preB beta, and pre gamma polypeptides. *Proc Natl Acad Sci U S A,* 78**,** 303-7.

Nieuwenhuizen, W. 1994. Sites in fibrin involved in the acceleration of plasminogen activation by t-PA. Possible role of fibrin polymerisation. *Thromb Res,* 75**,** 343-7.

Nieuwenhuizen, W., Vermond, A. & Hermans, J. 1983. Evidence for the localization of a calcium-binding site in the amino-terminal disulphide knot of fibrin (ogen). *Thromb Res,* 31**,** 81-6.

Nieuwenhuizen, W., Voskuilen, M. & Hermans, J. 1982. Anticoagulant and calcium-binding properties of high molecular weight derivatives of human fibrinogen (plasmin fragments Y). *Biochim Biophys Acta,* 708**,** 313-6.

Nilsson Ekdahl, K. & Nilsson, B. 1999. Phosphorylation of plasma proteins with emphasis on complement component C3. *Mol Immunol,* 36**,** 233-9.

Nussenzweig, V., Seligmann, M., Pelmont, J. & Grabar, P. 1961. [The products of degradation of human fibrinogen by plasmin. I. Separation and physicochemical properties]. *Ann Inst Pasteur (Paris),* 100**,** 377-89.

Ogata, Y., Heppelmann, C. J., Charlesworth, M. C., Madden, B. J., Miller, M. N., Kalli, K. R., Cilby, W. A., Bergen, H. R., III, Saggese, D. A. & Muddiman, D. C. 2006. Elevated levels of phosphorylated fibrinogen-alpha-isoforms and differential expression of other post-translationally modified proteins in the plasma of ovarian cancer patients. *J.Proteome.Res.,* 5**,** 3318-3325.

Okumura, N., Gorkun, O. V. & Lord, S. T. 1997. Severely impaired polymerization of recombinant fibrinogen gamma-364 Asp --> His, the substitution discovered in a heterozygous individual. *J Biol Chem,* 272**,** 29596-601.

Oliva-Trastoy, M., Defais, M. & Larminat, F. 2005. Resistance to the antibiotic Zeocin by stable expression of the Sh ble gene does not fully suppress Zeocin-induced DNA cleavage in human cells. *Mutagenesis,* 20**,** 111-4.

Olsen, J. V., Blagoev, B., Gnad, F., Macek, B., Kumar, C., Mortensen, P. & Mann, M. 2006. Global, in vivo, and site-specific phosphorylation dynamics in signaling networks. *Cell,* 127**,** 635-648.

Osterud, B. & Rapaport, S. I. 1977. Activation of factor IX by the reaction product of tissue factor and factor VII: additional pathway for initiating blood coagulation. *Proc Natl Acad Sci U S A,* 74**,** 5260-4.

Papanikolaou, P., Humble, E. & Engstrom, L. 1982. Phosphorylation of human fibrinogen in vitro with calcium-activated phospholipid-dependent protein kinase and [32P]ATP. *FEBS Lett.,* 143**,** 199-204.

Parastatidis, I., Thomson, L., Burke, A., Chernysh, I., Nagaswami, C., Visser, J., Stamer, S., Liebler, D. C., Koliakos, G., Heijnen, H. F., Fitzgerald, G. A., Weisel, J. W. & Ischiropoulos, H. 2008. Fibrinogen beta-chain tyrosine nitration is a prothrombotic risk factor. *J Biol Chem,* 283**,** 33846-53.

Parise, L. V. & Phillips, D. R. 1985. Reconstitution of the purified platelet fibrinogen receptor. Fibrinogen binding properties of the glycoprotein IIb-IIIa complex. *J Biol Chem,* 260**,** 10698-707.

Park, J. & Labaer, J. 2006. Recombinational cloning. *Curr Protoc Mol Biol,* Chapter 3**,** Unit 3 20.

Park, R., Ping, L., Song, J., Seo, J. Y., Choi, T. Y., Choi, J. R., Gorkun, O. V. & Lord, S. T. 2013. An engineered fibrinogen variant AalphaQ328,366P does not polymerise normally, but retains the ability to form alpha cross-links. *Thromb Haemost,* 109**,** 199-206.

Pearson, R. B. & Kemp, B. E. 1991. Protein kinase phosphorylation site sequences and consensus specificity motifs: tabulations. *Methods Enzymol,* 200**,** 62-81.

Pechik, I., Yakovlev, S., Mosesson, M. W., Gilliland, G. L. & Medved, L. 2006. Structural basis for sequential cleavage of fibrinopeptides upon fibrin assembly. *Biochemistry,* 45**,** 3588-97.

Pieters, M., van Zyl, D. G., Rheeder, P., Jerling, J. C., Loots du, T., van der Westhuizen, F. H., Gottsche, L. T. & Weisel, J. W. 2007. Glycation of fibrinogen in uncontrolled diabetic patients and the effects of glycaemic control on fibrinogen glycation. *Thromb Res,* 120**,** 439-46.

Plant, P. W. & Grieninger, G. 1986. Noncoordinate synthesis of the fibrinogen subunits in hepatocytes cultured under hormone-deficient conditions. *J Biol Chem,* 261**,** 2331-6.

Price, P. A., Rice, J. S. & Williamson, M. K. 1994. Conserved phosphorylation of serines in the Ser-X-Glu/Ser(P) sequences of the vitamin K-dependent matrix Gla protein from shark, lamb, rat, cow, and human. *Protein Sci,* 3**,** 822-30.

Procino, G., Carmosino, M., Marin, O., Brunati, A. M., Contri, A., Pinna, L. A., Mannucci, R., Nielsen, S., Kwon, T. H., Svelto, M. & Valenti, G. 2003. Ser-256 phosphorylation dynamics of Aquaporin 2 during maturation from the ER to the vesicular compartment in renal cells. *FASEB J,* 17**,** 1886-8.

Protopopova, A. D., Barinov, N. A., Zavyalova, E. G., Kopylov, A. M., Sergienko, V. I. & Klinov, D. V. 2014. Visualization of fibrinogen alphaC regions and their arrangement during fibrin network formation by high-resolution AFM. *J Thromb Haemost*.

Prunkard, D., Cottingham, I., Garner, I., Bruce, S., Dalrymple, M., Lasser, G., Bishop, P. & Foster, D. 1996. High-level expression of recombinant human fibrinogen in the milk of transgenic mice. *Nat Biotechnol,* 14**,** 867-71.

Purves, L., Purves, M. & Brandt, W. 1987. Cleavage of fibrin-derived D-dimer into monomers by endopeptidase from puff adder venom (Bitis arietans) acting at cross-linked sites of the gamma-chain. Sequence of carboxy-terminal cyanogen bromide gamma-chain fragments. *Biochemistry,* 26**,** 4640-4646.

Radek, J. T., Jeong, J. M., Wilson, J. & Lorand, L. 1993. Association of the A subunits of recombinant placental factor XIII with the native carrier B subunits from human plasma. *Biochemistry,* 32**,** 3527-34.

Ramackers, W., Klose, J., Vondran, F. W., Schrem, H., Kaltenborn, A., Klempnauer, J. & Kleine, M. 2014. Species-specific regulation of fibrinogen synthesis with implications for porcine hepatocyte xenotransplantation. *Xenotransplantation,* 21**,** 444-53.

Rao, S. P., Poojary, M. D., Elliott, B. W., Jr., Melanson, L. A., Oriel, B. & Cohen, C. 1991. Fibrinogen structure in projection at 18 A resolution. Electron density by co-ordinated cryo-electron microscopy and X-ray crystallography. *J Mol Biol,* 222**,** 89-98.

Ray, A. 2000. A SAF binding site in the promoter region of human gamma-fibrinogen gene functions as an IL-6 response element. *J Immunol,* 165**,** 3411-7.

Reganon, E., Vila, V., Aznar, J., Lacueva, V., Martinez, V. & Ruano, M. 1993. Studies on the functionality of newly synthesized fibrinogen after treatment of acute myocardial infarction with streptokinase, increase in the rate of fibrinopeptide release. *Thromb.Haemost.,* 70**,** 978-983.

Renne, T., Pozgajova, M., Gruner, S., Schuh, K., Pauer, H. U., Burfeind, P., Gailani, D. & Nieswandt, B. 2005. Defective thrombus formation in mice lacking coagulation factor XII. *J Exp Med,* 202**,** 271-81.

Ritchie, H., Lawrie, L. C., Crombie, P. W., Mosesson, M. W. & Booth, N. A. 2000. Cross-linking of plasminogen activator inhibitor 2 and alpha 2-antiplasmin to fibrin(ogen). *J.Biol.Chem.,* 275**,** 24915-24920.

Ritchie, H., Lawrie, L. C., Mosesson, M. W. & Booth, N. A. 2001. Characterization of crosslinking sites in fibrinogen for plasminogen activator inhibitor 2 (PAI-2). *Ann N Y Acad Sci,* 936**,** 215-8.

Rixon, M. W., Chan, W. Y., Davie, E. W. & Chung, D. W. 1983. Characterization of a complementary deoxyribonucleic acid coding for the alpha chain of human fibrinogen. *Biochemistry,* 22**,** 3237-3244.

Robbins, K. C., Summaria, L., Hsieh, B. & Shah, R. J. 1967. The peptide chains of human plasmin. Mechanism of activation of human plasminogen to plasmin. *J Biol Chem,* 242**,** 2333-42.

Roberts, H. R., Monroe, D. M., Oliver, J. A., Chang, J. Y. & Hoffman, M. 1998. Newer concepts of blood coagulation. *Haemophilia.,* 4**,** 331-334.

Robinson, B. R., Houng, A. K. & Reed, G. L. 2000. Catalytic life of activated factor XIII in thrombi. Implications for fibrinolytic resistance and thrombus aging. *Circulation,* 102**,** 1151-7.

Rocco, M., Molteni, M., Ponassi, M., Giachi, G., Frediani, M., Koutsioubas, A., Profumo, A., Trevarin, D., Cardinali, B., Vachette, P., Ferri, F. & Perez, J. 2014. A comprehensive mechanism of fibrin network formation involving early branching and delayed single- to double-strand transition from coupled time-resolved X-ray/light-scattering detection. *J Am Chem Soc,* 136**,** 5376-84.

Rogers, L. D. & Overall, C. M. 2013. Proteolytic post-translational modification of proteins: proteomic tools and methodology. *Mol Cell Proteomics,* 12**,** 3532-42.

Rojas, A. M., Kordich, L. & Lauricella, A. M. 2009. Homocysteine modifies fibrin clot deformability: Another possible explanation of harm. *Biorheology,* 46**,** 379-387.

Roska, F. J. & Ferry, J. D. 1982. Studies of fibrin film. I. Stress relaxation and birefringence. *Biopolymers,* 21**,** 1811-32.

Roy, S., Yu, S., Banerjee, D., Overton, O., Mukhopadhyay, G., Oddoux, C., Grieninger, G. & Redman, C. 1992. Assembly and secretion of fibrinogen. Degradation of individual chains. *J Biol Chem,* 267**,** 23151-8.

Roy, S. N., Kudryk, B. & Redman, C. M. 1995. Secretion of biologically active recombinant fibrinogen by yeast. *J Biol Chem,* 270**,** 23761-7.

Roy, S. N., Procyk, R., Kudryk, B. J. & Redman, C. M. 1991. Assembly and secretion of recombinant human fibrinogen. *J Biol Chem,* 266**,** 4758-63.

Rudchenko, S., Trakht, I. & Sobel, J. H. 1996. Comparative structural and functional features of the human fibrinogen alpha C domain and the isolated alpha C fragment. Characterization using monoclonal antibodies to defined COOH-terminal A alpha chain regions. *J Biol Chem,* 271**,** 2523-30.

Ryan, E. A., Mockros, L. F., Weisel, J. W. & Lorand, L. 1999. Structural origins of fibrin clot rheology. *Biophys J,* 77**,** 2813-26.

Salvi, M., Cesaro, L., Tibaldi, E. & Pinna, L. A. 2010. Motif analysis of phosphosites discloses a potential prominent role of the Golgi casein kinase (GCK) in the generation of human plasma phospho-proteome. *J Proteome Res,* 9**,** 3335-8.

Sanchez, J., Elgue, G., Riesenfeld, J. & Olsson, P. 1998. Studies of adsorption, activation, and inhibition of factor XII on immobilized heparin. *Thromb Res,* 89**,** 41-50.

Sanders, N. L., Bajaj, S. P., Zivelin, A. & Rapaport, S. I. 1985. Inhibition of tissue factor/factor VIIa activity in plasma requires factor X and an additional plasma component. *Blood,* 66**,** 204-12.

Sauls, D. L., Warren, M. & Hoffman, M. 2011. Homocysteinylated fibrinogen forms disulfide-linked complexes with albumin. *Thromb Res,* 127**,** 576-581.

Schmaier, A. H., Schutsky, D., Farber, A., Silver, L. D., Bradford, H. N. & Colman, R. W. 1987. Determination of the bifunctional properties of high molecular weight kininogen by studies with monoclonal antibodies directed to each of its chains. *J Biol Chem,* 262**,** 1405-11.

Schwartz, M. L., Pizzo, S. V., Hill, R. L. & McKee, P. A. 1973. Human Factor XIII from plasma and platelets. Molecular weights, subunit structures, proteolytic activation, and cross-linking of fibrinogen and fibrin. *J.Biol.Chem.,* 248**,** 1395-1407.

Seki, S., Habu, Y., Kawamura, T., Takeda, K., Dobashi, H., Ohkawa, T. & Hiraide, H. 2000. The liver as a crucial organ in the first line of host defense: the roles of Kupffer cells, natural killer (NK) cells and NK1.1 Ag+ T cells in T helper 1 immune responses. *Immunol Rev,* 174**,** 35-46.

Seo, J. & Lee, K. J. 2004. Post-translational modifications and their biological functions: proteomic analysis and systematic approaches. *J Biochem Mol Biol,* 37**,** 35-44.

Seydewitz, H. H., Kaiser, C., Rothweiler, H. & Witt, I. 1984. The location of a second in vivo phosphorylation site in the A alpha-chain of human fibrinogen. *Thromb.Res.,* 33**,** 487-498.

Seydewitz, H. H., Matthias, F. R., Schondorf, T. H. & Witt, I. 1987. Increase in the degree of phosphorylation of circulating fibrinogen under thrombolytic therapy with urokinase. *Thromb.Res.,* 46**,** 437-445.

Seydewitz, H. H. & Witt, I. 1985. Increased phosphorylation of human fibrinopeptide A under acute phase conditions. *Thromb.Res.,* 40**,** 29-39.

Shacter, E., Williams, J. A. & Levine, R. L. 1995. Oxidative modification of fibrinogen inhibits thrombin-catalyzed clot formation. *Free Radic Biol Med,* 18**,** 815-21.

Shacter, E., Williams, J. A., Lim, M. & Levine, R. L. 1994. Differential susceptibility of plasma proteins to oxidative modification: examination by western blot immunoassay. *Free Radic Biol Med,* 17**,** 429-37.

Shieh, B. H. & Travis, J. 1987. The reactive site of human alpha 2-antiplasmin. *J Biol Chem,* 262**,** 6055-9.

Smiddy, M. A., Martin, J. E., Kelly, A. L., de Kruif, C. G. & Huppertz, T. 2006. Stability of casein micelles cross-linked by transglutaminase. *J Dairy Sci,* 89**,** 1906-14.

Smith, K. A., Adamson, P. J., Pease, R. J., Brown, J. M., Balmforth, A. J., Cordell, P. A., Ariens, R. A., Philippou, H. & Grant, P. J. 2011. Interactions between factor XIII and the alphaC region of fibrinogen. *Blood,* 117**,** 3460-3468.

Smith, K. A., Pease, R. J., Avery, C. A., Brown, J. M., Adamson, P. J., Cooke, E. J., Neergaard-Petersen, S., Cordell, P. A., Ariens, R. A., Fishwick, C. W., Philippou, H. & Grant, P. J. 2013. The activation peptide cleft exposed by thrombin cleavage of FXIII-A(2) contains a recognition site for the fibrinogen alpha chain. *Blood,* 121**,** 2117-26.

Smith, S. A., Mutch, N. J., Baskar, D., Rohloff, P., Docampo, R. & Morrissey, J. H. 2006. Polyphosphate modulates blood coagulation and fibrinolysis. *Proc Natl Acad Sci U S A,* 103**,** 903-8.

Smolarczyk, K., Boncela, J., Szymanski, J., Gils, A. & Cierniewski, C. S. 2005. Fibrinogen contains cryptic PAI-1 binding sites that are exposed on binding to solid surfaces or limited proteolysis. *Arterioscler Thromb Vasc Biol,* 25**,** 2679-84.

Sobel, J. H. & Gawinowicz, M. A. 1996. Identification of the alpha chain lysine donor sites involved in factor XIIIa fibrin cross-linking. *J.Biol.Chem.,* 271**,** 19288-19297.

Soria, J., Soria, C. & Caen, P. 1983. A new type of congenital dysfibrinogenaemia with defective fibrin lysis--Dusard syndrome: possible relation to thrombosis. *Br J Haematol,* 53**,** 575-86.

Souri, M., Kaetsu, H. & Ichinose, A. 2008. Sushi domains in the B subunit of factor XIII responsible for oligomer assembly. *Biochemistry,* 47**,** 8656-64.

Southan, C., Thompson, E., Panico, M., Etienne, T., Morris, H. R. & Lane, D. A. 1985. Characterization of peptides cleaved by plasmin from the C-terminal polymerization domain of human fibrinogen. *J Biol Chem,* 260**,** 13095-101.

Spraggon, G., Everse, S. J. & Doolittle, R. F. 1997. Crystal structures of fragment D from human fibrinogen and its crosslinked counterpart from fibrin. *Nature,* 389**,** 455-462.

Standeven, K. F., Carter, A. M., Grant, P. J., Weisel, J. W., Chernysh, I., Masova, L., Lord, S. T. & Ariens, R. A. 2007. Functional analysis of fibrin {gamma}-chain cross-linking by activated factor XIII: determination of a cross-linking pattern that maximizes clot stiffness. *Blood,* 110**,** 902-907.

Standeven, K. F., Grant, P. J., Carter, A. M., Scheiner, T., Weisel, J. W. & Ariens, R. A. 2003. Functional analysis of the fibrinogen Aalpha Thr312Ala polymorphism: effects on fibrin structure and function. *Circulation,* 107**,** 2326-30.

Standke, G. J., Meier, V. S. & Groner, B. 1994. Mammary gland factor activated by prolactin on mammary epithelial cells and acute-phase response factor activated by interleukin-6 in liver cells share DNA binding and transactivation potential. *Mol Endocrinol,* 8**,** 469-77.

Suhre, K., Shin, S. Y., Petersen, A. K., Mohney, R. P., Meredith, D., Wagele, B., Altmaier, E., Deloukas, P., Erdmann, J., Grundberg, E., Hammond, C. J., de Angelis, M. H., Kastenmuller, G., Kottgen, A., Kronenberg, F., Mangino, M., Meisinger, C., Meitinger, T., Mewes, H. W., Milburn, M. V., Prehn, C., Raffler, J., Ried, J. S., Romisch-Margl, W., Samani, N. J., Small, K. S., Wichmann, H. E., Zhai, G., Illig, T., Spector, T. D., Adamski, J., Soranzo, N., Gieger, C., Assimes, T. L., Holm, H., Kathiresan, S., Konig, I. R., McPherson, R., Reilly, M. P., Roberts, R., Schunkert, H. & Stewart, A. F. 2011. Human metabolic individuality in biomedical and pharmaceutical research. *Nature,* 477**,** 54-60.

Suk, K., Lee, J. Y. & Kim, S. H. 1997. Synergistic stimulation of fibrinogen gelation by casein kinase II and polycationic compounds. *Biochem.Mol.Biol.Int.,* 42**,** 487-495.

Suttie, J. W. & Jackson, C. M. 1977. Prothrombin structure, activation, and biosynthesis. *Physiol Rev.,* 57**,** 1-70.

Svensson, J., Bergman, A. C., Adamson, U., Blomback, M., Wallen, H. & Jorneskog, G. 2012. Acetylation and glycation of fibrinogen in vitro occur at specific lysine residues in a concentration dependent manner: a mass spectrometric and isotope labeling study. *Biochem Biophys Res Commun,* 421**,** 335-42.

Swain, P. S. & Siggia, E. D. 2002. The role of proofreading in signal transduction specificity. *Biophys J,* 82**,** 2928-33.

Szymanski, E. S. & Farrell, H. M., Jr. 1982. Isolation and solubilization of casein kinase from Golgi apparatus of bovine mammary gland and phosphorylation of peptides. *Biochim Biophys Acta,* 702**,** 163-72.

Szymczak, A. L., Workman, C. J., Wang, Y., Vignali, K. M., Dilioglou, S., Vanin, E. F. & Vignali, D. A. 2004. Correction of multi-gene deficiency in vivo using a single 'self-cleaving' 2A peptide-based retroviral vector. *Nat Biotechnol,* 22**,** 589-94.

Tagliabracci, V. S., Engel, J. L., Wen, J., Wiley, S. E., Worby, C. A., Kinch, L. N., Xiao, J., Grishin, N. V. & Dixon, J. E. 2012. Secreted kinase phosphorylates extracellular proteins that regulate biomineralization. *Science,* 336**,** 1150-3.

Tagliabracci, V. S., Engel, J. L., Wiley, S. E., Xiao, J., Gonzalez, D. J., Nidumanda Appaiah, H., Koller, A., Nizet, V., White, K. E. & Dixon, J. E. 2014. Dynamic regulation of FGF23 by Fam20C phosphorylation, GalNAc-T3 glycosylation, and furin proteolysis. *Proc Natl Acad Sci U S A,* 111**,** 5520-5.

Takagi, T. & Doolittle, R. F. 1974. Amino acid sequence studies on factor XIII and the peptide released during its activation by thrombin. *Biochemistry,* 13**,** 750-6.

Tamura, T., Arai, S., Nagaya, H., Mizuguchi, J. & Wada, I. 2013. Stepwise assembly of fibrinogen is assisted by the endoplasmic reticulum lectin-chaperone system in HepG2 cells. *PLoS One,* 8**,** e74580.

Tateo, S., Mereu, L., Salamano, S., Klersy, C., Barone, M., Spyropoulos, A. C. & Piovella, F. 2005. Ovarian cancer and venous thromboembolic risk. *Gynecol Oncol,* 99**,** 119-25.

Thingholm, T. E. & Jensen, O. N. 2009. Enrichment and characterization of phosphopeptides by immobilized metal affinity chromatography (IMAC) and mass spectrometry. *Methods Mol Biol,* 527**,** 47-56, xi.

Topfer-Peterson, E., Lottspeich, F. & Henschen, A. 1976. Carbohydrate linkage site in the beta-chain of human fibrin. *Hoppe Seylers Z Physiol Chem,* 357**,** 1509-13.

Trapani, J. G. & Korn, S. J. 2003. Control of ion channel expression for patch clamp recordings using an inducible expression system in mammalian cell lines. *BMC Neurosci,* 4**,** 15.

Travis, J. & Salvesen, G. S. 1983. Human plasma proteinase inhibitors. *Annu Rev Biochem,* 52**,** 655-709.

Tregouet, D. A., Heath, S., Saut, N., Biron-Andreani, C., Schved, J. F., Pernod, G., Galan, P., Drouet, L., Zelenika, D., Juhan-Vague, I., Alessi, M. C., Tiret, L., Lathrop, M., Emmerich, J. & Morange, P. E. 2009. Common susceptibility alleles are unlikely to contribute as strongly as the FV and ABO loci to VTE risk: results from a GWAS approach. *Blood,* 113**,** 5298-5303.

Tretter, V., Hauer, B., Nusser, Z., Mihalek, R. M., Hoger, H., Homanics, G. E., Somogyi, P. & Sieghart, W. 2001. Targeted disruption of the GABA(A) receptor delta subunit gene leads to an up-regulation of gamma 2 subunit-containing receptors in cerebellar granule cells. *J Biol Chem,* 276**,** 10532-8.

Trey, J. E. & Kushner, I. 1995. The acute phase response and the hematopoietic system: the role of cytokines. *Crit Rev Oncol Hematol,* 21**,** 1-18.

Tsurupa, G. & Medved, L. 2001a. Fibrinogen alpha C domains contain cryptic plasminogen and tPA binding sites. *Ann.N.Y.Acad.Sci.,* 936**,** 328-330.

Tsurupa, G. & Medved, L. 2001b. Identification and characterization of novel tPA- and plasminogen-binding sites within fibrin(ogen) alpha C-domains. *Biochemistry,* 40**,** 801-808.

Tsurupa, G., Tsonev, L. & Medved, L. 2002. Structural organization of the fibrin(ogen) alpha C-domain. *Biochemistry,* 41**,** 6449-59.

Tsurupa, G., Yakovlev, S., McKee, P. & Medved, L. 2010. Noncovalent interaction of alpha(2)-antiplasmin with fibrin(ogen): localization of alpha(2)-antiplasmin-binding sites. *Biochemistry,* 49**,** 7643-7651.

Turner, M. D., Handel, S. E., Wilde, C. J. & Burgoyne, R. D. 1993. Differential effect of brefeldin A on phosphorylation of the caseins in lactating mouse mammary epithelial cells. *J Cell Sci,* 106 (Pt 4)**,** 1221-6.

Ubersax, J. A. & Ferrell, J. E., Jr. 2007. Mechanisms of specificity in protein phosphorylation. *Nat Rev Mol Cell Biol,* 8**,** 530-41.

Ugarova, T. P., Budzynski, A. Z., Shattil, S. J., Ruggeri, Z. M., Ginsberg, M. H. & Plow, E. F. 1993. Conformational changes in fibrinogen elicited by its interaction with platelet membrane glycoprotein GPIIb-IIIa. *J Biol Chem,* 268**,** 21080-7.

Undas, A. & Ariens, R. A. 2011. Fibrin clot structure and function: a role in the pathophysiology of arterial and venous thromboembolic diseases. *Arterioscler Thromb Vasc Biol,* 31**,** e88-99.

Undas, A., Brozek, J., Jankowski, M., Siudak, Z., Szczeklik, A. & Jakubowski, H. 2006. Plasma homocysteine affects fibrin clot permeability and resistance to lysis in human subjects. *Arteriosclerosis Thrombosis and Vascular Biology,* 26**,** 1397-1404.

Undas, A., Podolec, P., Zawilska, K., Pieculewicz, M., Jedliński, I., Stepień, E., Konarska-Kuszewska, E., Weglarz, P., Duszyńska, M., Hanschke, E., Przewlocki, T. & Tracz, W. 2009a. Altered fibrin clot structure/function in patients with cryptogenic ischemic stroke. *Stroke,* 40**,** 1499-501.

Undas, A., Szułdrzynski, K., Stepien, E., Zalewski, J., Godlewski, J., Tracz, W., Pasowicz, M. & Zmudka, K. 2008. Reduced clot permeability and susceptibility to lysis in patients with acute coronary syndrome: effects of inflammation and oxidative stress. *Atherosclerosis,* 196**,** 551-7.

Undas, A., Zawilska, K., Ciesla-Dul, M., Lehmann-Kopydłowska, A., Skubiszak, A., Ciepłuch, K. & Tracz, W. 2009b. Altered fibrin clot structure/function in patients with idiopathic venous thromboembolism and in their relatives. *Blood,* 114**,** 4272-8.

Vadseth, C., Souza, J. M., Thomson, L., Seagraves, A., Nagaswami, C., Scheiner, T., Torbet, J., Vilaire, G., Bennett, J. S., Murciano, J. C., Muzykantov, V., Penn, M. S., Hazen, S. L., Weisel, J. W. & Ischiropoulos, H. 2004. Pro-thrombotic state induced by post-translational modification of fibrinogen by reactive nitrogen species. *J Biol Chem,* 279**,** 8820-6.

Valnickova, Z. & Enghild, J. J. 1998. Human procarboxypeptidase U, or thrombin-activable fibrinolysis inhibitor, is a substrate for transglutaminases. Evidence for transglutaminase-catalyzed cross-linking to fibrin. *J Biol Chem,* 273**,** 27220-4.

Van Blokland, H. J., Hoeksema, F., Siep, M., Otte, A. P. & Verhees, J. A. 2011. Methods to create a stringent selection system for mammalian cell lines. *Cytotechnology,* 63**,** 371-84.

Varadi, A. & Patthy, L. 1983. Location of plasminogen-binding sites in human fibrin(ogen). *Biochemistry,* 22**,** 2440-6.

Varadi, A. & Patthy, L. 1984. Beta(Leu121-Lys122) segment of fibrinogen is in a region essential for plasminogen binding by fibrin fragment E. *Biochemistry,* 23**,** 2108-12.

Vogel, H. G. 2008. *Drug Discovery and Evaluation: Pharmacological Assays, Volume 1,* Germany, Springer.

Vogel, P., Hansen, G. M., Read, R. W., Vance, R. B., Thiel, M., Liu, J., Wronski, T. J., Smith, D. D., Jeter-Jones, S. & Brommage, R. 2012. Amelogenesis imperfecta and other biomineralization defects in Fam20a and Fam20c null mice. *Vet Pathol,* 49**,** 998-1017.

Vorbach, C., Capecchi, M. R. & Penninger, J. M. 2006. Evolution of the mammary gland from the innate immune system? *Bioessays,* 28**,** 606-16.

Voskuilen, M., Vermond, A., Veeneman, G. H., van Boom, J. H., Klasen, E. A., Zegers, N. D. & Nieuwenhuizen, W. 1987. Fibrinogen lysine residue A alpha 157 plays a crucial role in the fibrin-induced acceleration of plasminogen activation, catalyzed by tissue-type plasminogen activator. *J Biol Chem,* 262**,** 5944-6.

Vu, D., Di Sanza, C., Caille, D., de Moerloose, P., Scheib, H., Meda, P. & Neerman-Arbez, M. 2005. Quality control of fibrinogen secretion in the molecular pathogenesis of congenital afibrinogenemia. *Hum Mol Genet,* 14**,** 3271-80.

Wagner, O. F., de Vries, C., Hohmann, C., Veerman, H. & Pannekoek, H. 1989. Interaction between plasminogen activator inhibitor type 1 (PAI-1) bound to fibrin and either tissue-type plasminogen activator (t-PA) or urokinase-type plasminogen activator (u-PA). Binding of t-PA/PAI-1 complexes to fibrin mediated by both the finger and the kringle-2 domain of t-PA. *J Clin Invest,* 84**,** 647-55.

Wang, S. K., Aref, P., Hu, Y., Milkovich, R. N., Simmer, J. P., El-Khateeb, M., Daggag, H., Baqain, Z. H. & Hu, J. C. 2013. FAM20A mutations can cause enamel-renal syndrome (ERS). *PLoS Genet,* 9**,** e1003302.

Wang, W., Boffa, M. B., Bajzar, L., Walker, J. B. & Nesheim, M. E. 1998. A study of the mechanism of inhibition of fibrinolysis by activated thrombin-activable fibrinolysis inhibitor. *J Biol Chem,* 273**,** 27176-81.

Weigandt, K. M., White, N., Chung, D., Ellingson, E., Wang, Y., Fu, X. & Pozzo, D. C. 2012. Fibrin clot structure and mechanics associated with specific oxidation of methionine residues in fibrinogen. *Biophys J,* 103**,** 2399-407.

Weisel, J. W. 2007. Structure of fibrin: impact on clot stability. *J Thromb Haemost,* 5 Suppl 1**,** 116-24.

Weisel, J. W., Phillips, G. N., Jr. & Cohen, C. 1981. A model from electron microscopy for the molecular structure of fibrinogen and fibrin. *Nature,* 289**,** 263-7.

Weisel, J. W., Stauffacher, C. V., Bullitt, E. & Cohen, C. 1985. A model for fibrinogen: domains and sequence. *Science,* 230**,** 1388-1391.

Weisel, J. W., Veklich, Y. & Gorkun, O. 1993. The sequence of cleavage of fibrinopeptides from fibrinogen is important for protofibril formation and enhancement of lateral aggregation in fibrin clots. *J.Mol.Biol.,* 232**,** 285-297.

Weitzman, S. A. & Gordon, L. I. 1990. Inflammation and cancer: role of phagocyte-generated oxidants in carcinogenesis. *Blood,* 76**,** 655-63.

West, D. W. 1986. Structure and function of the phosphorylated residues of casein. *J Dairy Res,* 53**,** 333-52.

Williams, R. C. 1981. Morphology of bovine fibrinogen monomers and fibrin oligomers. *J Mol Biol,* 150**,** 399-408.

Williams, S., Fatah, K., Hjemdahl, P. & Blomback, M. 1998. Better increase in fibrin gel porosity by low dose than intermediate dose acetylsalicylic acid. *Eur Heart J,* 19**,** 1666-1672.

Williamson, M. P. 1994. The structure and function of proline-rich regions in proteins. *Biochem J,* 297 (Pt 2)**,** 249-60.

Wind, M., Gosenca, D., Kubler, D. & Lehmann, W. D. 2003. Stable isotope phospho-profiling of fibrinogen and fetuin subunits by element mass spectrometry coupled to capillary liquid chromatography. *Anal.Biochem.,* 317**,** 26-33.

Wolfenstein-Todel, C. & Mosesson, M. W. 1980. Human plasma fibrinogen heterogeneity: evidence for an extended carboxyl-terminal sequence in a normal gamma chain variant (gamma'). *Proc Natl Acad Sci U S A,* 77**,** 5069-73.

Wolschin, F., Wienkoop, S. & Weckwerth, W. 2005. Enrichment of phosphorylated proteins and peptides from complex mixtures using metal oxide/hydroxide affinity chromatography (MOAC). *Proteomics,* 5**,** 4389-97.

Woodhead, J. L., Nagaswami, C., Matsuda, M., Arocha-Pinango, C. L. & Weisel, J. W. 1996. The ultrastructure of fibrinogen Caracas II molecules, fibers, and clots. *J Biol Chem,* 271**,** 4946-53.

Wright, J. F. 2009. Transient transfection methods for clinical adeno-associated viral vector production. *Hum Gene Ther,* 20**,** 698-706.

Xia, H. & Redman, C. 1999. The degradation of nascent fibrinogen chains is mediated by the ubiquitin proteasome pathway. *Biochem Biophys Res Commun,* 261**,** 590-7.

Xia, H. & Redman, C. M. 2001. Differential degradation of the three fibrinogen chains by proteasomes: involvement of Sec61p and cytosolic Hsp70. *Arch Biochem Biophys,* 390**,** 137-45.

Xiao, J., Tagliabracci, V. S., Wen, J., Kim, S. A. & Dixon, J. E. 2013. Crystal structure of the Golgi casein kinase. *Proc Natl Acad Sci U S A,* 110**,** 10574-9.

Yakovlev, S., Makogonenko, E., Kurochkina, N., Nieuwenhuizen, W., Ingham, K. & Medved, L. 2000. Conversion of fibrinogen to fibrin: mechanism of exposure of tPA- and plasminogen-binding sites. *Biochemistry,* 39**,** 15730-41.

Yang, Z., Mochalkin, I. & Doolittle, R. F. 2000a. A model of fibrin formation based on crystal structures of fibrinogen and fibrin fragments complexed with synthetic peptides. *Proc.Natl.Acad.Sci.U.S.A,* 97**,** 14156-14161.

Yang, Z., Mochalkin, I., Veerapandian, L., Riley, M. & Doolittle, R. F. 2000b. Crystal structure of native chicken fibrinogen at 5.5-A resolution. *Proc.Natl.Acad.Sci.U.S.A,* 97**,** 3907-3912.

Yee, V. C., Pratt, K. P., Cote, H. C., Trong, I. L., Chung, D. W., Davie, E. W., Stenkamp, R. E. & Teller, D. C. 1997. Crystal structure of a 30 kDa C-terminal fragment from the gamma chain of human fibrinogen. *Structure.,* 5**,** 125-138.

Yu, S., Redman, C. M., Goldstein, J. & Blomback, B. 1980. Biosynthesis of canine fibrinogen: in vitro synthesis of A alpha, B beta and gamma precursor chains. *Biochem Biophys Res Commun,* 96**,** 1032-8.

Yu, S., Sher, B., Kudryk, B. & Redman, C. M. 1984. Fibrinogen precursors. Order of assembly of fibrinogen chains. *J Biol Chem,* 259**,** 10574-81.

Yuan, X., Waterworth, D., Perry, J. R., Lim, N., Song, K., Chambers, J. C., Zhang, W., Vollenweider, P., Stirnadel, H., Johnson, T., Bergmann, S., Beckmann, N. D., Li, Y., Ferrucci, L., Melzer, D., Hernandez, D., Singleton, A., Scott, J., Elliott, P., Waeber, G., Cardon, L., Frayling, T. M., Kooner, J. S. & Mooser, V. 2008. Population-based genome-wide association studies reveal six loci influencing plasma levels of liver enzymes. *Am J Hum Genet,* 83**,** 520-8.

Yudkin, J. S., Kumari, M., Humphries, S. E. & Mohamed-Ali, V. 2000. Inflammation, obesity, stress and coronary heart disease: is interleukin-6 the link? *Atherosclerosis,* 148**,** 209-14.

Zahedi, R. P., Lewandrowski, U., Wiesner, J., Wortelkamp, S., Moebius, J., Schutz, C., Walter, U., Gambaryan, S. & Sickmann, A. 2008. Phosphoproteome of resting human platelets. *J.Proteome.Res.,* 7**,** 526-534.

Zauner, G., Hoffmann, M., Rapp, E., Koeleman, C. A., Dragan, I., Deelder, A. M., Wuhrer, M. & Hensbergen, P. J. 2012. Glycoproteomic analysis of human fibrinogen reveals novel regions of O-glycosylation. *J Proteome Res,* 11**,** 5804-14.

Zhang, J. Z. & Redman, C. 1996. Fibrinogen assembly and secretion. Role of intrachain disulfide loops. *J Biol Chem,* 271**,** 30083-8.

Zhang, J. Z. & Redman, C. M. 1994. Role of interchain disulfide bonds on the assembly and secretion of human fibrinogen. *J Biol Chem,* 269**,** 652-8.

Zhong, X. & Wright, J. F. 2013. Biological Insights into Therapeutic Protein Modifications throughout Trafficking and Their Biopharmaceutical Applications. *Int J Cell Biol,* 2013**,** 273086.

Zhu, J., Musco, M. L. & Grace, M. J. 1999. Three-color flow cytometry analysis of tricistronic expression of eBFP, eGFP, and eYFP using EMCV-IRES linkages. *Cytometry,* 37**,** 51-9.